Novel mechanisms and signaling pathways in angiogenesis

Forghany, Z.

Novel Mechanisms and Signaling Pathways in Angiogenesis

ZARY FORGHANY

Novel Mechanisms and Signaling Pathways in Angiogenesis

PhD thesis, Leiden University, Leiden, the Netherland

The research described in this thesis was carried out at the Department of Cell and Chemical biology of Leiden University Medical Center (LUMC), Leiden, The Netherlands. This work was financially supported by a grant from KWF (Kankerbestrijding/ Dutch Cancer Society Grant 30861) and Oncode Institute.

Cover design: Zary Forghany

Layout: Zary Forghany

Printing: Ridderprint, the Netherlands

ISBN: 978-94-6506-662-2

Financial support by the Dutch Heart Foundation for the publication of this thesis is gratefully acknowledged. Support from ChipSoft and ABN AMRO is also appreciated.

Novel Mechanisms and Signaling Pathways in Angiogenesis

Proefschrift

ter verkrijging van
de graad van doctor aan de Universiteit Leiden,
op gezag van rector magnificus prof.dr.ir. H. Bijl,
volgens besluit van het college voor promoties
te verdedigen op woensdag 18 december 2024
klokke 13:00 uur

door

Zary Forghany

Promotor
Prof. dr. P. ten Dijke

Co-promotor
Dr. D.A. Baker

Promotiecommissie:

Prof. dr. B.E. Snaar-Jagalska
Prof. dr. M. J. Goumans
Prof. dr. E. Danen
Dr. L. Hawinkels

TABLE OF CONTENTS

CHAPTER 1

General Introduction

1. Normal Angiogenesis

1.1 Basic biology of normal angiogenesis

The endothelium expands by the process of angiogenesis, during which the formation of new blood vessels occurs from pre-existing ones. Angiogenesis is a normal physiological process that plays a crucial role in wound healing, embryonic development, and regulation of organ function. Generally speaking, at the tissue level, angiogenesis involves the degradation of the extracellular matrix, migration, and proliferation of endothelial cells (ECs) to form new blood vessels. At the cellular level, the migration of ECs is driven by chemical signals such as growth factors and cytokines. These signals activate intracellular signaling pathways that regulate cellular functions such as proliferation, migration, and survival. At the molecular level, key players in angiogenesis include vascular endothelial growth factor (VEGF) and its receptors, NOTCH signaling as well as other signaling molecules such as integrins and matrix metalloproteinases (MMPs). Understanding the molecular mechanisms underlying angiogenesis is crucial for developing new treatments for various diseases that involve dysregulation of the process, such as cancer and cardiovascular diseases (La Mendola et al., 2022; Carmeliet et al., 2011; Eelen. et al., 2020).

1.2 Angiogenic process

Angiogenesis is a dynamic process related to the remodeling and maturation of the vasculature into a complex and branched network of blood vessels, which occurs continuously throughout life (Eelen et al., 2020; Adair et al., 2010). Beginning in utero and embryonic development, a primitive vascular network is established through vasculogenesis, in which angioblasts aggregate to form tube-like structures (Patel-Hett & D'Amore, 2011). Subsequent angiogenic expansion of the vascular system represents a thorough orchestration of cell proliferation, differentiation, migration, matrix remodeling, and intercellular signaling mechanisms (Eelen et al., 2020). Angiogenesis can be classified as either sprouting or intussusceptive angiogenesis; both are thought to occur in utero and adults (Adair & Montani, 2010). Sprouting angiogenesis occurs when new blood vessels form in previously non-vascularized tissue regions, a common occurrence during embryonic development and also in the tumor microenvironment (TME), which will be described later (Adair & Montani, 2010; Fang & Salven, 2011). More specifically, following stimulation by angiogenic factors, MMP activation occurs, leading to the basement membrane's

degradation (Quintero-Fabián et al., 2019). This leads to a transformation of leading edge ECs from quiescent to pathfinding tip cells, characterized by increased cell-matrix interactions, matrix remodeling, and high migratory potential (Mukwaya et al., 2021). Tip cells are the leading edge cells at the sprouting front of a growing blood vessel. Tip cells dynamically extend filopodia in order to sense and respond to proangiogenic signals, which guide the vessel's direction and ensure proper vessel formation (Adams & Alitalo, 2007). Stalk cells trail behind the tip cells. They provide sprout elongation and contribute to the lumen formation (Pardali et al., 2010). Stalk cells proliferate to elongate the vessel, maintaining its width and guiding the vessel's growth behind the tip cells. Figure 1 depicts six different steps of sprouting angiogenesis, from the breakdown of the basement membrane to lumen formation (Gerhardt et al., 2008; Davis et al., 2005 Horowitz and Simons 2008).

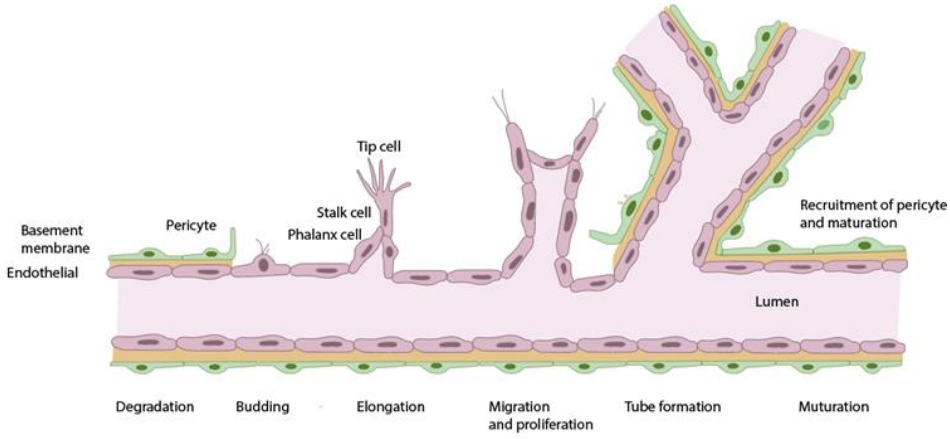

Figure 1. Angiogenesis steps.

- Matrix metalloproteinase (MMP) degradation - MMPs degrade extracellular matrix to create space for new blood vessel growth.
- Budding - Formation of small sprouts from existing blood vessels.
- Elongation - The sprouts grow and lengthen, forming new blood vessels.
- Migration and proliferation - Blood vessel cells move to the site of angiogenesis, multiply, and form a network of new vessels.
- Tube formation - Blood vessels form a lumen and become functional tubes.
- Maturation - Blood vessels mature, forming tight junctions and a functional vasculature (Dufraine et al., 2008; Aspriţoiu et al., 2021).

Intussusceptive angiogenesis is a different mechanism of forming new blood vessels. Instead of sprouting new vessels, this type of angiogenesis involves the splitting of existing blood vessels, creating a new lumen or cavity in a blood vessel. This type of angiogenesis is most commonly seen in tissues that experience rapid growth and increased oxygen demand, such as in the formation

of the placenta and in growing tumors. The process begins with the activation of mural cells, which form a barrier within the vessel, dividing it into two smaller vessels. This results in the formation of new, smaller vessels, which increases the total surface area available for blood flow (Burri et al., 2004; Kurz et al., 2003).
Quiescence, activation, and resolution of vessels are three sequential steps to form a sprouting vessel. It is worth mentioning that the maturation of blood vessels is a transition from an actively growing vascular to a quiescent, completely functional network. Establishing stable and mature blood vessels involves multiple processes, including stabilizing existing vascular tubes, suppressing EC sprouting, and protecting against proangiogenic signals such as VEGF. Cellular differentiation processes such as valve formation, fenestration, and apical-basal polarity are also part of vessel maturation (Pimanda et al., 2006; Cleaver & Melton, 2003).
The following sections will summarize the current knowledge of the known pathways orchestrating angiogenesis. Later, in the section describing pathological angiogenesis, we explore how an understanding of these processes may help find the best approaches to inhibit angiogenesis.

1.3 The role of NOTCH and VEGF signaling on coordination of angiogenesis

The interplay between NOTCH signaling and VEGF signaling in neighboring ECs influences the coordination of angiogenesis. These signaling pathways play a crucial role in regulating the formation and growth of new blood vessels during angiogenesis. The NOTCH signaling pathway is a highly conserved signaling pathway that is involved in a variety of cellular processes, including cell differentiation, proliferation, and survival in ECs and other cell types, including cancer cells (Akil et al., 2021)
The following section provides a brief introduction to the structure of NOTCH ligands and receptors, VEGF signaling, and their roles in tip and stalk cell formation.

1.3.1 The structure of the main components of the NOTCH signaling pathway

NOTCH receptors are classified as type I transmembrane receptors that pass once through the cellular membrane. These receptors are initially synthesized as single polypeptide chains and subsequently undergo proteolytic processing to form heterodimeric configurations displayed on the cell surface. All four NOTCH receptors (NOTCH1-4) in Homo sapiens comprise three distinct domains: (I) the NOTCH extracellular domain (NECD), (II) the transmembrane I domain, and (III) the NOTCH intracellular domain (NICD). The NECD of all NOTCH receptors contains 29-36 Epidermal Growth Factor (EGF) repeats, of which, EGF repeat 11-

12 mediate trans-interactions, whilst EGF repeats 24-29 mediate cis-interactions with NOTCH ligands (Below see trans and cis interactions). Additionally, a subset of the EGF repeats contains calcium-binding sites (Chillakuri et al., 2012; Kopan et al., 2009; Liu et al., 2014). The NICD consists of multiple domains: (I) the RBP association module (RAM) domain, (II) ankyrin (ANK) repeats forming the ANK domain, (III) the transactivation domain (TAD), and (IV) the proline/glutamic acid/serine/threonine (PEST) domain. The ANK domain is flanked by two nuclear localization signals (NLS) that target the NICD to the nucleus (Wang, M., 2011). While there are significant differences in size among various NOTCH family members, particularly compared to the C. elegans orthologs, several fundamental structural characteristics remain consistent across all members (Blaumueller et al., 1997; Logeat et al., 1998).

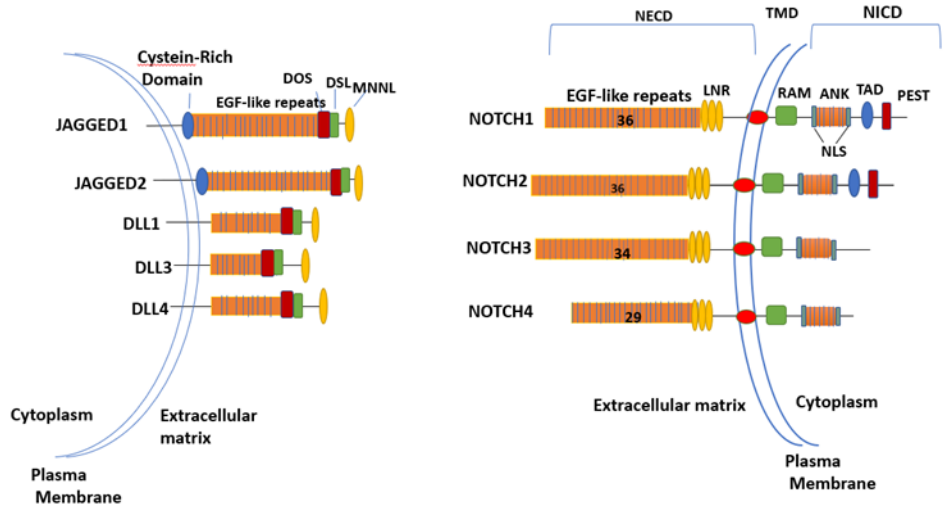

Figure 2. The structure of the NOTCH receptor family and its corresponding ligands**.** NOTCH1~4 consists of extracellular, intracellular and transmembrane domains. The five ligands present in mammals are categorized into two distinct groups: Delta-like (comprising DLLl1, DLL3, and DLL4) and Serrate-like (encompassing JAGGED1 and JAGGED2.

The NOTCH pathway is activated when a ligand binds to the single transmembrane NOTCH receptor on the cell's surface. Ligands are single pass transmembrane polypeptides on the cell surface, and their structure partially resembles that of the receptors (Phng & Gerhardt, 2009; D'Souza et al., 2008). The extracellular domain of the ligands contains multiple EGF-like repeats, which play a role in their interactions with their respective receptors.

For NOTCH canonical signaling responses to occur, ligands and receptors must be expressed on neighboring cells. In general, Notch-dependent signaling output in ECs depend on two central signaling mechanisms: trans-interactions, which

occur when ligands associate with receptors in adjacent cells, and cis-interactions, where ligands can inhibit NOTCH signaling within the same cell. Recently, a cis-activation process has also been identified, which occurs with multiple ligand-receptor pairs (Nandagopal et al., 2019).
The signaling outcomes of the NOTCH pathway and the varied results of specific cellular events rely on different combinations of NOTCH family ligands and receptors (Bigas et al., 2016).
Among the NOTCH ligands found in the vertebrate endothelium, only the absence of DLL4 or JAG1 leads to defects in the vascular system (Shah et al., 2017). Delta-like 4 (DLL4), as one of the key regulators of angiogenesis, is highly expressed in the endothelium of angiogenic blood vessels, as well as in quiescent arteries and capillaries throughout the tissues and organs of mammals (Lobov & Mikhailova, 2018). In addition, DLL4 and JAGGED1 play a crucial role in regulating the selection of tip cells and maintaining a delicate balance that coordinates the sprouting of ECs. Benedito et al. reported that these two ligands have opposing roles in the process of tip cell selection in ECs sprouting. Though Dll4 promotes Notch signaling, which typically inhibits tip cell formation, JAGGED1 plays a proangiogenic role by downregulating the DLL4-Notch signaling pathway (Benedito et al., 2009). Additionally, JAGGED1 has been reported to inhibit NOTCH signaling during embryonic pancreas development (Golson et al., 2009).
Studies have shown that DLL4, which effectively activates NOTCH1, displays a preference for activating NOTCH1 rather than NOTCH2, whereas DLL1, which in general has less affinity for NOTCH1 binding (Andrawes et al., 2013), can activate both NOTCH1 and NOTCH2 (Tveriakhina et al. 2018). It has also been demonstrated that DLL3 functions exclusively in cis-inhibition (Ladi et al., 2005; Chapman et al., 2011).

1.3.2 Intracellular VEGF signaling pathway

The other essential signaling pathway in EC sprouting is the intracellular VEGF signaling pathway (Hellström et al.,2007). VEGF-A is the best characterized and most studied VEGF factor in angiogenesis and acts by signaling through the receptor tyrosine kinase (RTKs) (VEGF receptor 1 [VEGFR1], -2, and- 3 [VEGFR3]) and coreceptors Neuropilin-1 (NP-1), and Neuropilin-2 (NP-2) (Otrock et al., 2007; Cross et al., 2001). While the VEGF165 isoform has been identified as crucial for vascular development (Grünewald, et al., 2010), it's noteworthy that various isoforms of VEGF-A exhibit specific interactions with VEGFR1 and VEGFR2. Among these interactions, the highest affinity is observed towards VEGFR1. However, despite this affinity, it is VEGFR2 that serves as the primary mediator of VEGF-A signaling during vessel branching (Takahashi & Shibuya, 2005; Olsson et al., 2006).

VEGFR-2 receptor consists of 1356 amino acids and comprises several distinct domains. The extracellular portion (amino asid 20-764) contains seven immunoglobulin (Ig)-like folds, with particular significance attributed to Ig domain three due to its role in determining ligand-binding specificity. Following this, there is a 21-amino acid transmembrane (TM) domain (amino acids 765-785), followed by the intracellular domain (amino acids 786-1356). Within the intracellular domain, there are two kinase domains (KD) separated by a kinase insert domain (KID) (Cross et al., 2001).

Under hypoxic conditions, increased transcription of VEGF occurs, leading to a VEGF gradient. The VEGF-A ligand binds to the extracellular Ig domains 2 and 3 on the VEGFR-2 receptor. This binding induces both homo- and heterodimerization of VEGFR-2 and activates the receptor's kinase activity, resulting in self-phosphorylation of the receptors. Subsequently, signaling molecules bind to the phosphorylated VEGFR-2, initiating MAPK (Mitogen activated protein kinase) signaling cascades, which, in turn, promote cell survival, proliferation, and migration of ECs (Olsson et al, 2006; Schweighofer et al., 2009; Kliche et al., 2012; Koch et al., 2012).

1.3.3 Overview of signaling in tip stalk cell formation

During angiogenic sprouting, it is well established that ECs compete dynamically for the tip cell position (Jakobsson et al., 2010). Tip cells are mobile cells that do not undergo proliferation. Instead, they perceive the angiogenic signal and invade the neighboring tissue by elongating multiple filopodia (Kamei et al., 2006; Gerhardt et al., 2003). Following tip cells are stalk cells (De Smet et al., 2009), which undergo proliferation, extend the sprouts, create lumens, and establish blood circulation under suitable conditions. The determination of tip and stalk cell selection relies on the differences in VEGFR levels between neighboring ECs, which are influenced by NOTCH/DLL4 signaling. (Hellström et al. 2007; Lobov et al. 2007; Siekmann and Lawson 2007; Suchting et al. 2007). In brief, the VEGFA ligand–receptor interaction induces dimerization of VEGFR-2 which, in turn, results in the up-regulation of DLL4 expression in leading tip cells. Elevated expression of DLL4 in tip cells leads to amplified NOTCH signaling in trailing stalk cells, which suppresses the tip cell phenotype resulting in decreased VEGFR2 expression within the stalk cells (Pardali et al., 2010) NOTCH activation reduces VEGFR-2 and VEGFR-3 expression in stalk cells, in contrast to tip cells that, upon lateral inhibition, exhibit low NOTCH signaling (Pardali et al. 2010). Besides that, the expression of DLL4 ligand, which is also a target gene regulated by the NOTCH signaling pathway, will be reduced (Uyttendaele et al., 1996; Sainson et al., 2005).

It's worth mentioning that the activity of VEGF-A, which acts through its endothelial receptor VEGFR-2, plays a crucial role in not only inducing tip cell

filopodia, EC migration and proliferation but also promoting EC survival and vascular permeability (Tomlins et al., 2005; Tomlins et al., 2006; Pimanda et al., 2006). As a result, upon VEGF signaling, activation of the intracellular MAPK cascade triggers the phosphorylation and activation of the ETS transcription factor ERG, which is necessary for DLL4 induction. As a consequence of the effect of ETS transcription factors on the *DLL4* promoter, a wave of DLL4 will be generated that mediates NOTCH signaling in the adjacent cells. Upon direct cell-cell interactions in neighboring ECs, a series of proteolytic cleavages of the NOTCH receptor causing the release of the NOTCH intracellular domain (NICD), which translocate to the nucleus where it directly interacts with the CSL transcription factor and thereby triggers the expression of NOTCH target genes such as HES and HEY family of basic helix-loop-helix (bHLH) transcription factors (Weinmaster, 1998; Mumm and Kopan 2000; Nakagawa et al., 2000; Davis and Turner, 2001; Iso et al., 2003) (Figure 3).

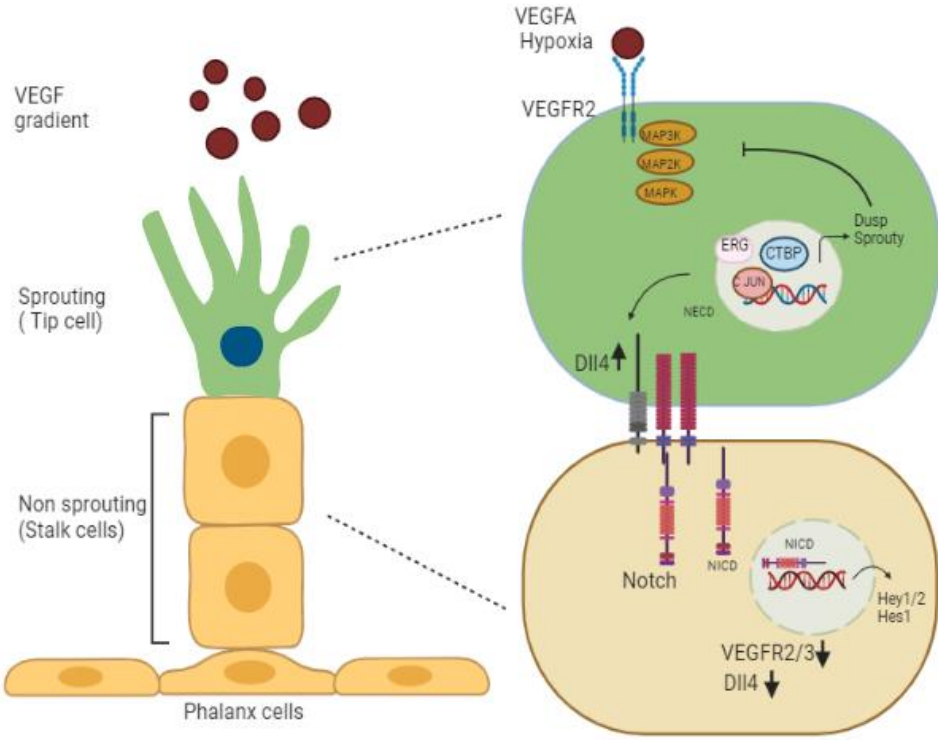

Figure 3. Formation of endothelial tip cells through two signaling pathways: VEGF/VEGFR and DLL4/NOTCH. The specification of tip and stalk cells within the vascular endothelium involves the intricate interplay of the VEGF and Notch signaling pathways. VEGF engages with VEGFR-2, which is expressed on the surface of quiescent ECs in vessels. Upon stimulation by VEGF and subsequent activation of the MAPK signaling pathway, coupled with the transcription factor CJUN, ERG and other transcriptional regulators, DLL4 expression is up-regulated, specifically in the tip cells.

< Figure 3 (continued). This up-regulation of DLL4 leads to the activation of the Notch signaling pathway in the neighboring stalk cells, thereby suppressing the tip cell phenotype. Activation of Notch signaling consequently diminishes the expression of VEGFR2 and orchestrates the expression of various Notch target genes, such as Hey and Hes (Blanco et al., 2013). Some parts of this image were created with Bio Render (https://www.biorender.com).

Among the first evidence of the necessity of the presence of ETS in DLL4 expression is our previous findings that showed in primary ECs, in response to VEGF and following the inactivation of a TEL/C-terminal Binding Protein (CtBP) complex from DLL4 promoter (which harbors a number of conserved consensus transcription factor ETS DNA-binding sites), a signature of genes would be up-regulated, including dual specificity phosphatase DUSP and receptor tyrosine kinase (RTK) antagonist SPROUTY4 as well as DLL4 (Roukens et al., 2010). Nonetheless, the precise mechanism by which SPROUTY proteins control RTK signaling is not fully understood.

In regards to DLL4 expression, *in vitro* studies also confirmed that VEGF-A stimulation consistently augments the expression of DLL4 protein on the surface of human umbilical vein ECs (HUVECs) (Ridgway et al., 2006). Consistent with this idea, there is evidence that shows hypoxic conditions highly induce VEGF-A expression, which, as a consequence, directly up-regulates the mRNA expression of DLL4 in ECs (Patel et al., 2005; Williams et al., 2006),

The NOTCH pathway is linked to other pathways, such as the WNT and HEDGEHOG pathways, through the involvement of ETS transcription factors (Bray, 2016) Briefly, ETS factors play a role in modulating the activity of NOTCH target genes and are involved in the regulation of angiogenesis. Knockdown studies in mice and zebrafish revealed the influence of ETS factors on the regulation of NOTCH signaling through the VEGF pathway. For example, ERG plays a role in maintaining the balance between NOTCH ligands by promoting the expression of DLL4 while inhibiting JAG1 expression (Shah et al., 2017).

Hence, the NOTCH/DLL4 and VEGF signaling pathways are critical players in the regulation of angiogenesis and are linked to other pathways through the involvement of ETS transcription factors. The intricate interplay between signaling pathways in the regulation of angiogenesis highlights the complex nature of this process and underscores the importance of understanding the underlying mechanisms of angiogenesis. In the following section, we elaborate on the function of the TFs ETS in the process of angiogenesis.

1.4 Role of ETS transcription factors in angiogenesis

ETS (E26 Transformation-Specific) transcription factors are a large and diverse protein family which are involved in various biological processes, including control of cellular proliferation, differentiation, hematopoiesis, and angiogenesis (Sementchenko and Watson 2000; Watson and Seth, 2000; Dittmer et al., 2003;

Oikawa et al., 2003). The ETS family is characterized by the presence of a highly conserved DNA-binding domain known as the ETS domain. The ETS domain allows these TFs to bind to specific DNA sequences and regulate the expression of target genes, including the expression of genes involved in the process of angiogenesis, such as NOTCH ligands DLL4 and JAG1, VEGF, and angiopoietin (Shah et al., 2017). It has been well documented that a number of target genes of ETS family transcription factor are expressed in ECs and are responsible for the regulation of angiogenesis. For example, MMP-1, MMP-3, MMP-9, and urokinase-type PA (u-PA) and VEGF and its receptors (Lelievre et al., 2000) (Figure 4).

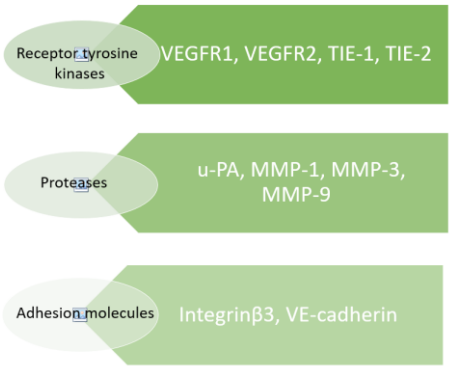

Figure 4. Target genes of ETS Family Transcription Factors in Endothelial cells

Among the members of the ETS family, it has been reported that transcription factors ETS-1, ERG, FLI-1, ELF-1, TEL, and NERF-2 are involved in the expression of proangiogenic genes and the regulation of vascular development (Sato, 2001). Among those, ERG is the most abundantly expressed in resting ECs and has been shown in *in vitro* studies to be essential for angiogenesis (Birdsey et al., 2012). *In vivo* studies in mouse retina showed that ERG orchestrates the NOTCH, and Wnt/β-catenin pathways to facilitate the maturation and stability of blood vessels (Shah,et al,. 2017). Research conducted in Xenopus, mouse, and zebrafish models has demonstrated that ERG, which is expressed in all ECs, plays a crucial role in the differentiation and vascular development of ECs (Baltzinger et al., 1999; Liu et al., 2008). Zebrafish studies have also shown that the highly homologous transcription factors FLI-1 and ERG have also been linked to the regulation of endothelial homeostasis and angiogenesis, as they play a role in the expression of genes defining the endothelial lineage (Liu & Patient, 2008). This aligns with our group's discovery that the disassembly of ETS transcription factor from the *DLL4* promoter can mediate sprouting by controlling DLL4 expression in ECs (Roukens et al., 2010).

Additionally, the transcription of von Willebrand factor is regulated by ERG (McLaughlin et al., 2001). Other functional studies demonstrated that FLI-1 disruption in mouse embryos results in aberrant hematopoiesis and hemorrhage of the animal (Schreiber et al., 2000).
Whereas several studies have investigated the role of FLI-1 in vascular development, Pham et al. took a comprehensive approach to explore the combinatorial function of four members of the ETS family (FLI1, FLI1b, ETS1, and ETSRP) in zebrafish vasculature through using morpholinos to target genes (Pham et al., 2007).
The current available data also shows that ETS proteins, including ETS-1 and ETS-2, have also been found to enhance angiogenesis by interaction with an ETS motif in the VEGFR promotor and via increasing vascular stability through the regulation of NOTCH signaling by ERG (Wei et al., 2009; Niu et al. 2018; Shah et al. 2017). Despite the presence of a conserved ETS binding site in the promoters of proangiogenic genes, the consequences of combining and manipulating these factors remain an area of limited knowledge (Oettgen, 2001). Further research is necessary to gain a deeper understanding of the mechanisms underlying the role of ETS in angiogenesis.
Of note, our group uncovered a new, previously overlooked pathway for the genetic control of angiogenesis. Our research demonstrated the direct role of the TEL (ETV6) in mediating angiogenesis (Roukens et al., 2010). Furthermore, we uncovered the crucial function of the TEL/CtBP transcription repressor complex in this process by bridging the two predominant angiogenic networks: the intracellular VEGF receptor signaling pathway and the intercellular NOTCH/DLL4 pathway, which will be elaborated in this thesis. Our findings suggest that there may be potential for inhibiting angiogenesis in cancer pathology by using inhibitors that target ETS activity (see Chapter 5).

1.5 Role of AP1 in angiogenesis

Activator Protein-1 (AP-1) is a dimeric transcription factor complex composed of the products of the JUN and FOS proto-oncogenes, which play a critical role in regulating various biological processes such as cell differentiation, proliferation, apoptosis, and angiogenesis.
Regarding angiogenesis, several members of the AP-1 family have been shown to differentially regulate genes associated with this process (Angel and Karin, 1991). For example, JUN and JUNB induce the expression of the proliferin gene, FOS induces VEGF-D, and FRA-1 induces urokinase-type plasminogen activator (uPA), uPA receptor (uPAR), and various MMPs (Kustikova et al., 1998; Belguise et al., 2005). Evidence also suggests that the transcription factor FRA-1 promotes vessel development (Schreiber et al., 2000). *In vivo* evidence suggests that the knockout of certain AP-1 family members contributes to the observed lethality

in animals. However, Fra-1-null embryos exhibit a deficiency in placental vascularization, which highlights the role of this factor in stimulating vessel development (Schreiber et al., 2000). In cancer biology, evidence has shown that JUND reduces tumor angiogenesis by protecting cells from oxidative stress (Gerald et al., 2004).
A recent study also demonstrated the impact of deoxy ribozymes targeting CJUN on solid tumor growth and angiogenesis. The findings showed that CJUN activation plays a significant role in the proliferation and angiogenesis of invasive breast cancer (Zhang et al., 2004). Additionally, Fosl1 (Fos-Like1; also known as Fra1) has been shown to play a crucial role in establishing normal placental vascularization in mice (Schreiber et al. 2000). Furthermore, Fra1 is involved in regulating the level of the αvβ3 intergin and the uPA-uPAR complexes on the surface of ECs, contributing to angiogenesis (Galvagni et al., 2013).
Previous studies in our lab have also revealed that DLL4 and JUN expression is highly responsive to VEGFR signaling in HUVECs (Roukens et al., 2010). We have also discovered that the interaction of DLL4 intracellular domain with JUN forms a feedback loop that causes VEGF-dependent changes in DLL4 expression and other angiogenesis-regulating genes (Forghany et al., 2018, Chapter 2) This regulation depends on ETS/AP-1 transcription factors and is controlled by the DLL4 intracellular domains.
Taken together, these findings provide evidence that the AP-1 transcription factor components may play a role in angiogenesis, though the precise mechanistic basis of this remains unclear.

2. Pathological Angiogenesis

2.1 Tumor angiogenesis is a hallmark of cancer, and vascular tumors are a model for deciphering novel mechanisms

Over the past 30 years, pioneering work, starting with the research of Folkman et al., has established that tumor development depends on angiogenesis. As stated before, angiogenesis is indispensable during tissue development and regeneration. Nevertheless, it also has implications in pathological conditions like cancer, termed tumor angiogenesis (Chambers et al., 2002). Tumor angiogenesis is one of the most prominent mechanisms driving tumor growth beyond a few cubic millimeters (Folkman, 1971). It is widely accepted that a critical stage known as the “angiogenic switch” occurs in the initial phase of tumor angiogenesis (De bock et al., 2011). Research on vascularization has a long tradition, with Rudolf Virchow describing tumor vascularization as a hallmark of cancer and a pivotal step in tumor growth in 1863. This phenomenon involves redirecting nearby blood vessels through angiogenesis, facilitated by the vast number of capillaries in the human body. Tumor cells that develop

spontaneously normally lack angiogenic characteristics in the beginning. The transition to angiogenesis typically takes place through a process where certain factors stimulate the formation of new capillaries, which subsequently align towards the tumor (Brossa et al., 2019; Ribatti et al.,2007). Therefore, what triggers vessel formation in both normal and tumor conditions is an essential topic of investigation.

Although a finely balanced equilibrium exists between proangiogenic and anti-angiogenic factors to maintain the homeostasis in physiological angiogenesis (Pollina et al., 2008), tumor growth requires disturbing this balance. Thus, triggering the angiogenic switch is crucial for cancer progression. This transition clearly entails more than just increasing angiogenic activity and is believed to result from a combination of positive and negative regulatory factors. Factors such as progenitor ECs, the interaction between angiogenic factors and their receptors, and the interplay between vasculogenesis and lymph angiogenesis may play a role in triggering this transition (Ribatti et al., 2007). For example, tumor ECs (TEC), shows elevated expression levels of proangiogenic genes like VEGFR, VEGF, platelet-derived growth factor (PDGF), and epidermal growth factor receptor (EGFR). Conversely, expression of endogenous inhibitors, such a tumstatin (Nyberg et al. 2005), thrombospondin-1 (TSP-1) or interferon, may be reduced. Therefore, the transition is not solely driven by increased angiogenic activity but is rather influenced by a complex interplay between positive and negative regulators (Ribatti et al., 2007).

Tumor vessels exhibit several distinct features compared to normal blood vessels. Abnormal structure, increased permeability, poor perfusion, uneven blood flow, and enhanced adaptation are some of the characteristics of tumor vessels that contribute to tumor progression, metastasis, and therapeutic resistance (Siemann et al., 2011). As an example of adaptation, recent studies have reported that TECs consist of heterogeneous populations with variable phenotypes, and they adapt their characteristics in reaction to the tumor microenvironment (TME), such as hypoxic conditions. Therefore, the importance of understanding of these characteristics of vascular tumors and deciphering their mechanisms provides intriguing discoveries that could be utilized to personalize existing cancer treatment (Siemann et al., 2011; Treps et al., 2022).

In many solid tumors, such as sarcomas and breast cancer, the level of angiogenesis and the subsequent vasculature determine the severity of the tumor’s malignancy (Dass and Choong, 2008). This could be viewed as cancer’s Achilles heel: cutting off the blood supply could lead to the failure of tumor development. Over the past years, many angiogenesis inhibitors have been approved by the FDA for cancer treatment, focusing on targeting molecules like VEGF, its receptor, or related factors. For instance, Bevacizumab, recognized as an inhibitor of VEGF's biological activity (Al-Abd et al., 2017), is combined with conventional chemotherapy. This combination, known as the first-line

therapeutic strategy for patients with non-small-cell lung cancer (NSCLC), represents one of the most promising angiogenesis inhibitors for cancer treatment (Sun et al., 2022).

Broadly speaking, the ultimate aim of anti-angiogenic therapy, particularly when combined with other conventional therapies, is to stop tumor growth by maintaining a balance between proliferation and apoptosis rates, thereby limiting the tumor size to just a few millimeters (Szeles et al., 2012). Unlike this conventional therapy, which can affect adjacent tissues, anti-angiogenic therapy targets ECs, thereby inhibiting only the formation of new blood vessels (Szeles et al., 2012). Although this approach may not completely eliminate the tumor, it could effectively stop its growth and maintains it at an early stage. Therefore, it is often used in combination with conventional approaches to achieve complete tumor elimination (Yazdjerdi et al., 2019). Overall, moderating the potential side effects associated with standard cancer treatments, lower the chance of developing drug resistance, and potentially converting cancer into chronic manageable disease would be the aim of utilizing anti-angiogenesis therapy (Ansari et al., 2022). Currently, cancer therapies have demonstrated limited clinical effectiveness due to issues like cytotoxicity and acquired resistance. Despite some progress, existing strategies have failed to fulfil the early promise and high expectations. Thus, it is imperative to expand the spectrum of potential targets for future anti-angiogenesis therapies. To achieve this, one must gain a thorough understanding of the pathways implicated in angiogenesis. By identifying new targets and elucidating the underlying mechanisms of angiogenesis, we can enhance the efficacy of current cancer therapies and ultimately improve patient outcomes. Recently, our lab uncovered a new, previously overlooked pathway for the genetic control of angiogenesis. Specifically, we showed that ETS transcription factors are an essential mediator of angiogenesis. As such, targeting the activity of these proteins through the production of small molecule inhibitors of its function represents an entirely novel approach to the problem of inhibiting illicit vascular development such as tumor angiogenesis. Our work suggests that inhibitors of the activity of ETS transcription factors could potentially inhibit tumor angiogenesis without the problems of acquired resistance and the strong side effects inherent in earlier strategies (see Chapter 5).

2.2 Role of ETS transcription factors in cancer

ETS factors are believed to play a fundamental role in the development and evolution of the majority of tumor types. Since the 1980s, multiple different alterations in ETS factor function have been identified in many different tumor types (reviewed in Sizemore et al., 2017). Activation and dysregulation of ETS TFs occur at both the transcriptional and post-transcriptional levels (Wei et al.,

2023). Such activations of ETS TFs are driven by several mechanisms that include (a) chromosomal rearrangement, which generates ETS gene fusions in Ewing's sarcoma, breast, gastric, head and neck, prostate, and thyroid cancers; (b) gene amplification in breast cancer and melanoma, (c) feed-forward loop signaling, (d) gain-of-function mechanisms, increased ETS factor activity and stability (Sizemore et al., 2017).

In the subsequent section, the involvement of ETS family members in various forms of human cancer is outlined.

For instance, overexpression of ETS-1 was observed in 80% of tumor tissues from esophageal squamous-cell carcinoma (ESCC) patients (Mukherjee et al., 2003). This excessive expression of ETS-1 often coincides with increased VEGF levels, known to trigger tumor angiogenesis (Hashim et al., 2010; Martins et al., 2013), and is strongly associated with lymph node metastasis. In addition, ETS-1 expression has been implicated in angiogenesis in endometrial uterine cancers (Fujimoto et al., 2002), and in ovarian cancers. This contributes to tumor growth and progression, partly through angiogenesis promotion. Moreover, elevated ETS-1 expression correlates strongly with increased microvessel density and VEGF expression in gastric cancer and colorectal carcinoma patients. Similarly, in various types of human brain cancer, ETS-1 expression significantly correlates with tumor grade, unlike in normal brain tissue where its expression is minimal (Kitange et al., 1999). Apart from angiogenesis, ETS factors play roles in DNA repair, genomic stability, and evasion of cell death (Knezevich et al., 1998; Seth and Watson 2005).

Recent findings have also revealed the impact of ETS factors on nucleotide, and steroid metabolism crucial for tumor cell survival. For example, ETS1 regulates genes encoding enzymes in glycolysis and lipid metabolism in ovarian and breast cancer (Verschoor et al. 2013). Additionally, in prostate cancer, TMPRSS2-ERG rearrangements deregulate fatty acid, sphingolipid, and polyamine signaling (Meller et al. 2016). Moreover, ETS factors influence the tumor microenvironment, particularly in extracellular matrix remodeling, angiogenesis, and inflammation (Knezevich et al., 1998; Findlay et al., 2013; Kar & Gutierrez-Hartmann, 2013).

A study by Huang et al. highlighted the critical role of ELF-1 in tumor angiogenesis development. High expression levels of ELF-1 correlate with TIE-2 expression in tumor blood vessels. Blocking ELF-1 using tailored membrane-permeable peptides inhibits ANG-1-mediated EC migration *in vitro* and reduces B16 melanoma tumor growth and tumor-associated angiogenesis in nude mice (Huang et al., 2006). Further studies on TIE-1, TIE-2, and the Ang-2 promoter suggest that ELF-1 acts as a transcriptional regulator of these genes during vascular development, emphasizing its essential role in regulating the ANG-TIE-2 pathway in tumor angiogenesis development (Dube et al. 2001; Hegen et al. 2004).

Overall, since the misregulation of ETS has been reported as a frequent feature in many different types of cancer, the prudent use of ETS inhibitors could selectively target tumor cells. It has been well documented that the ETS family also interacts with other transcription factor complexes, such as the FOS/JUN complex, to form more extensive transcriptional regulatory networks (Basuyaux et al., 1997). This highlights the importance of the ETS family in regulating gene expression and underscores the need for further study of these proteins in both normal and disease states.

2.3 Identification and characterization of novel angiogenesis/tumor cell Inhibitors

For decades, the development of targeted therapy for cancer has been a challenge that is being investigated by researchers around the world. The fundamental challenge of cancer research is the discovery of new treatments that eliminate tumors, are minimally toxic, and are not susceptible to acquired resistance. During the last two decades, the design of new cancer therapies can be broadly categorized into two approaches: those that have sought to target and inhibit tumor cell growth directly and those that target the tumor vasculature and tumor microenvironment.

Published surveys of all drugs approved in the last decade suggest little evidence of significant improvements in patient survival or quality of life. As mentioned before, angiogenesis is coordinated by NOTCH and VEGF signaling (Phng & Gerhardt, 2009). Several lines of evidence indicate that VEGF signaling acts upstream of the NOTCH pathway and impacts the control of the expression of different NOTCH components (Hashim et al. 2010; Mathis 1999; Stone et al. 1995; Lawson et al,.2002; Patel et al. 2005; Ridgway et al. 2006; Lobov et al. 2007). Current data suggests that combining anti-VEGF treatment with chemotherapy and radiation therapy results in greater antitumor effects than either treatment alone (Ziche & Morbidelli, 2004).

Although early results appeared promising regarding the efficacy of anti-VEGF therapy and DLL4/NOTCH targeting antibodies in inhibiting cancer cell growth or angiogenesis deregulation (Wu et al., 2010; Andersson & Lendahl, 2014) clinical studies have revealed that while anti-angiogenic drugs initially benefit patients, their efficacy diminishes over time, resulting in only modest disease-free survival rates. This primarily occurs because of redundancy resulting in the the activation of alternative angiogenic signaling pathways (Brossa et al., 2019). The widespread failure of conventional anti-tumor treatments can be attributed to the acquisition of resistance by tumor cells. This resistance is caused by the intra-tumor heterogeneity and the intrinsic redundancies in signal transduction pathways. When a pathway is inhibited or targeted, another functioning

pathway compensates for the loss of activity, allowing the tumor to evade the effects of treatment (Lei et al., 2023).
Broadly speaking, in the drug discovery process, one can look for potential targets within the "druggable genome." However, the number of possible targets is limited if it is assumed that only certain genes associated with diseases can be targeted by drugs. For example, a comparative analysis of antifungal targets in the yeast genome with human genes suggested that only a small portion of the human genome, about 2-5%, can be targeted by drugs. This translates to approximately 600-1,500 potential drug targets in humans, as indicated by Salami and Crews in 2017 (Figure 5).

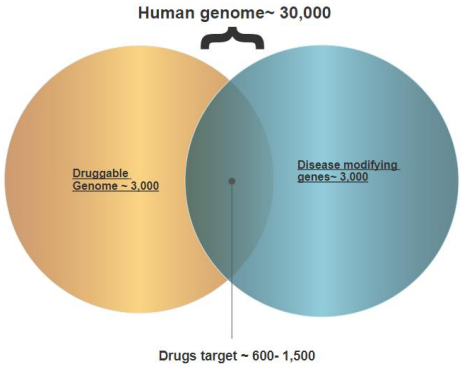

Figure 5. Susceptible drug targets within the human genome. Adapted from (Graham, 2022).

However, there are sound reasons to suppose that many other potential proteins that were previously considered to be undruggable may in fact represent valid targets. To address the issue, we proposed an entirely different methodology in this study: finding a new target beyond the druggable genome. Recently, instead of focusing on the upstream components of cell signaling networks (which were believed to be druggable), we have developed methods for identifying small molecule inhibitors of ETS transcription factors, which act downstream of these pathways. These transcription factors were previously considered "undruggable," but they play a crucial role in driving the behaviors of tumor cells. There are compelling reasons for considering the ETS family of transcription factors as an excellent target. The rationale for targeting ETS factors is simple: firstly, as ETS factors are located downstream of the major receptor signaling pathways, inhibiting this group of proteins could effectively suppress tumor cell growth and alleviate issues of redundancy and resistance (Oikawa et al.,2003). Secondly, because ETS factors are involved in blood vessel growth, selective inhibitors could simultaneously achieve two goals: they could prevent tumor cell proliferation and hinder tumor angiogenesis. Research has already shown that inhibiting ETS activity impedes tumor cell growth (Rahim et al., 2014; Huang et

al., 2021). Given that ETS function is misregulated in tumors, the controlled use of inhibitors might selectively target tumor cells, thereby reducing potential toxicity. In this light, in Chapter 5, we will consider potential approaches for therapeutically targeting oncogenic ETS factors.

3. A brief outline of the thesis

This dissertation has contributed novel perspectives to our comprehension of the mechanisms underlying angiogenesis. Additionally, it has introduced novel methodologies for targeting angiogenesis. **Chapter 1** provides a general introduction to both physiological and pathological angiogenesis, offering an exploration of these critical processes. **Chapter 2** introduces tube formation regulation in ECs through interactions between the intracellular domain of NOTCH ligands and the JUN proto-oncogene. **Chapter 3** presents a new model for controlling the intracellular cis-inhibition of NOTCH receptors by NOTCH ligand dimerization. In **Chapter 4**, we characterized the function of mutant FOS protein in the abnormal vessel growth of epithelioid hemangioma. We also showed through molecular and biochemical analysis how perturbation of normal FOS degradation could lead to this vascular neoplasm. **Chapter 5** builds upon our prior discovery, which identified TEL/CtBP as a promising new target for advancing anti-angiogenic therapies. In collaboration with the European Lead Factory, a consortium of leading academic institutions and pharmaceutical companies, we conducted screens and validated hit small molecules that can putatively inhibit ETS transcription factors by blocking their binding to specific DNA-binding sites and thereby inhibit tumor cell growth and angiogenic sprouting. Finally, **Chapter 6** summarizes the findings of this thesis within the context of contemporary scientific literature.

REFERENCES

1. Adair, T. H., and J. P. Montani. 2010. Angiogenesis (San Rafael (CA)).
2. Adams, R. H., and K. Alitalo. 2007. 'Molecular regulation of angiogenesis and lymphangiogenesis', Nat Rev Mol Cell Biol, 8: 464-78.
3. Al-Abd, A. M., A. J. Alamoudi, A. B. Abdel-Naim, T. A. Neamatallah, and O. M. Ashour. 2017. 'Anti-angiogenic agents for the treatment of solid tumors: Potential pathways, therapy and current strategies - A review', J Adv Res, 8: 591-605.
4. Akil, A., Gutiérrez-García, A. K., Guenter, R., Rose, J. B., Beck, A. W., Chen, H., & Ren, B. (2021). Notch Signaling in Vascular Endothelial Cells, Angiogenesis, and Tumor Progression: An Update and Prospective. Frontiers in cell and developmental biology, 9, 642352.
5. Andersson, ER, and U Lendahl. 2014. 'Therapeutic modulation of Notch signalling--are we there yet?', Nat Rev Drug Discov, 13: 357-78.
6. Andrawes MB, Xu X, Liu H, Ficarro SB, Marto JA, Aster JC, Blacklow SC. Intrinsic selectivity of notch 1 for Delta-like 4 over Delta-like 1(2013)
7. Angel, P, and M Karin. 1991 'The role of Jun, Fos and the AP-1 complex in cell-proliferation and transformation.', Biochim Biophys Acta, 1072: 129-57.
8. Ansari, M. J., D. Bokov, A. Markov, A. T. Jalil, M. N. Shalaby, W. Suksatan, S. Chupradit, H. S. Al-Ghamdi, N. Shomali, A. Zamani, A. Mohammadi, and M. Dadashpour. 2022. 'Cancer combination therapies by angiogenesis inhibitors; a comprehensive review', Cell Commun Signal, 20: 49.
9. Aspriţoiu VM, Stoica I, Bleotu C, Diaconu CC. Epigenetic Regulation of Angiogenesis in Development and Tumors Progression: Potential Implications for Cancer Treatment. Front Cell Dev Biol. 2021
10. Baltzinger, M, AM Mager-Heckel, and Remy P. 1999. 'Xl erg: expression pattern and overexpression during development plead for a role in endothelial cell differentiation', Dev Dyn, 216: 420-33.
11. Baluk, P, H Hashizume, and DM McDonald. 2005. 'Cellular abnormalities of blood vessels as targets in cancer', Curr Opin Genet Dev, 15: 102-11.
12. Basuyaux, J. P., Ferreira, E., Stéhelin, D., & Butticè, G. (1997). The Ets transcription factors interact with each other and with the c-Fos/c-Jun complex via distinct protein domains in a DNA-dependent and -independent manner. The Journal of biological chemistry, 272(42), 26188–26195
13. Belguise, K, N Kersual, F Galtier, and D Chalbos. 2005. 'FRA-1 expression level regulates proliferation and invasiveness of breast cancer cells', Oncogene, 24: 1434-44.
14. Bigas, A., Espinosa, L. Notch Signaling in Cell–Cell Communication Pathways. Curr Stem Cell Rep 2, 349–355 (2016).
15. Blanco, R., & Gerhardt, H. (2013). VEGF and Notch in tip and stalk cell selection. Cold Spring Harbor perspectives in medicine, 3 1, a006569.
16. Bray S. J. (2016). Notch signalling in context. Nature reviews. Molecular cell biology, 17(11), 722–735. https://doi.org/10.1038/nrm.2016.94
17. Brenner, J. C., F. Y. Feng, S. Han, S. Patel, S. V. Goyal, L. M. Bou-Maroun, M. Liu, R. Lonigro, J. R. Prensner, S. A. Tomlins, and A. M. Chinnaiyan. 2012. 'PARP-1 inhibition as a targeted strategy to treat Ewing's sarcoma', Cancer Res, 72: 1608-13.
18. Brossa A, Buono L, Fallo S, Fiorio Pla A, Munaron L, Bussolati B. Alternative Strategies to Inhibit Tumor Vascularization. Int J Mol Sci. 2019 Dec 7;20(24):618
19. Burri, P. H., R. Hlushchuk, and V. Djonov. 2004. 'Intussusceptive angiogenesis: its emergence, its characteristics, and its significance', Dev Dyn, 231: 474-88.
20. Carmeliet, P., and R. K. Jain. 2011. 'Molecular mechanisms and clinical applications of angiogenesis', Nature, 473: 298-307.
21. hapman, G., Sparrow, D. B., Kremmer, E., and Dunwoodie, S. L. (2011). Notch inhibition by the ligand DELTA-LIKE 3 defines the mechanism of abnormal vertebral segmentation in

Spondylocostal dysostosis. Hum. Mol. Genet. 20, 905–916.

22. Chambers, A. F., Groom, A. C., & MacDonald, I. C. (2002). Dissemination and growth of cancer cells in metastatic sites. Nature reviews. Cancer, 2(8), 563–572.

23. Chillakuri, Chandramouli R et al. “Notch receptor-ligand binding and activation: insights from molecular studies.” In: Seminars in cell & developmental biology 23.4 (2012), pp. 421–8.

24. Cleaver, O, and DA Melton. 2003. 'Endothelial signaling during development', Nat Med, 9: 661-8.

25. Cross, Michael J. and Claesson-Welsh, Lena. “FGF and VEGF function in angiogenesis: signalling pathways, biological responses and therapeutic inhibition”. In: TRENDS in Pharmacological Sciences 22.4 (2001).

26. Dass, C. R., and P. F. Choong. 2008. 'Cancer angiogenesis: targeting the heel of Achilles', J Drug Target, 16: 449-54.

27. Davis, RL, and DL Turner. 2001. 'Vertebrate hairy and Enhancer of split related proteins: transcriptional repressors regulating cellular differentiation and embryonic patterning', Oncogene, 20: 8342-57.

28. De Bock K., Cauwenberghs S., Carmeliet P. Vessel abnormalization: Another hallmark of cancer? Molecular mechanisms and therapeutic implications. Curr. Opin. Genet. Dev. 2011;21:73–79.

29. De Smet, F., Segura, I., De Bock, K., Hohensinner, P. J., & Carmeliet, P. (2009). Mechanisms of vessel branching: filopodia on endothelial tip cells lead the way. Arteriosclerosis, thrombosis, and vascular biology, 29(5), 639–649.

30. DiPietro, LA. 1997. 'Thrombospondin as a regulator of angiogenesis.' in, Regulation of Angiogenesis.

31. Dittmer, J. 2003. 'The biology of the Ets1 proto-oncogene', Mol Cancer: 2:29.

32. D’Souza, B, Miyamoto, a, and Weinmaster, G. “The many facets of Notch ligands.” In: Oncogene27.38 (2008), pp. 5148–67Dube, A, S Thai, J Gaspar, S Rudders, TA Libermann, L Iruela-Arispe, and P Oettgen. 2001. 'Elf-1 is a transcriptional regulator of the Tie2 gene during vascular development', Circ Res, 88: 237-44.

33. Dufraine, J., Y. Funahashi, and J. Kitajewski. 2008. 'Notch signaling regulates tumor angiogenesis by diverse mechanisms', Oncogene, 27: 5132-7.

34. Eelen, G., L. Treps, X. Li, and P. Carmeliet. 2020. 'Basic and Therapeutic Aspects of Angiogenesis Updated', Circ Res, 127: 310-29.

35. Fang, S., and P. Salven. 2011. 'Stem cells in tumor angiogenesis', J Mol Cell Cardiol, 50: 290-5.

36. Findlay, V. J., A. C. LaRue, D. P. Turner, P. M. Watson, and D. K. Watson. 2013. 'Understanding the role of ETS-mediated gene regulation in complex biological processes', Adv Cancer Res, 119: 1-61.

37. Fischetto, R., V. V. Palmieri, M. E. Tripaldi, A. Gaeta, A. Michelucci, M. Delvecchio, R. Francavilla, and P. Giordano. 2019. 'Alagille Syndrome: A Novel Mutation in JAG1 Gene', Front Pediatr, 7: 199.

38. Folkman, J. 1971. 'Tumor angiogenesis: therapeutic implications', N Engl J Med, 285: 1182-6.

39. Forghany, Z, F Robertson, A Lundby, JV Olsen, and Baker DA. 2018. 'Control of endothelial cell tube formation by Notch ligand intracellular domain interactions with activator protein 1 (AP-1)', J Biol Chem, 293: 1229-42.

40. Fujimoto, J., Aoki, I., Toyoki, H., Khatun, S., & Tamaya, T. (2002). Clinical implications of expression of ETS-1 related to angiogenesis in uterine endometrial cancers. Annals of oncology : official journal of the European Society for Medical Oncology, 13(10), 1605–1611. 4

41. Galvagni, F, M Orlandini, and S Oliviero. 2013. 'Role of the AP-1 transcription factor FOSL1 in endothelial cells adhesion and migration', Cell Adh Migr, 7: 408-11.

42. Gerald, D, E Berra, YM Frapart, DA Chan, AJ Giaccia, D Mansuy, J Pouysségur, M Yaniv, and F Mechta-Grigoriou. 2004. 'JunD reduces tumor angiogenesis by protecting cells from oxidative

stress', Cell, 118: 781-94.

43. Gerhardt, H, M Golding, M Fruttiger, C Ruhrberg, A Lundkvist, A Abramsson, M Jeltsch, C Mitchell, K Alitalo, D Shima, and C Betsholtz. 2003. 'VEGF guides angiogenic sprouting utilizing endothelial tip cell filopodia', J Cell Biol, 161: 1163-77.

44. Gerhardt, H. 2008. 'VEGF and endothelial guidance in angiogenic sprouting', Organogenesis, 4: 241-6.

45. Golson ML, Le Lay J, Gao N, Brämswig N, Loomes KM, Oakey R, May CL, White P, Kaestner KH. Jagged1 is a competitive inhibitor of notch signaling in the embryonic pancreas. Mechanisms of Development. 2009;126:687–699

46. Graham, H. 2022. 'The mechanism of action and clinical value of PROTACs: A graphical review', Cell Signal, 99: 110446.

47. Grünewald, F. S., Prota, A. E., Giese, A., & Ballmer-Hofer, K. (2010). Structure-function analysis of VEGF receptor activation and the role of coreceptors in angiogenic signaling. Biochimica et biophysica acta, 1804(3), 567–580.

48. Hashim, AF, AA Al-Janabi, LH Mahdi, KM Al-Toriahi, and AA Yasseen. 2010. 'Vascular endothelial growth factor (VEGF) receptor expression correlates with histologic grade and stage of colorectal cancer', Libyan J Med, 5.

49. Hegen, A, S Koidl, K Weindel, D Marmé, HG Augustin, and U Fiedler. 2004. 'Expression of angiopoietin-2 in endothelial cells is controlled by positive and negative regulatory promoter elements', Arterioscler Thromb Vasc Biol, 24: 1803-9.

50. Hellström, M1, LK Phng, JJ Hofmann, E Wallgard, L Coultas, P Lindblom, J Alva, AK Nilsson, L Karlsson, N Gaiano, K Yoon, J Rossant, ML Iruela-Arispe, M Kalén, H Gerhardt, and C Betsholtz. 2007. 'Dll4 signalling through Notch1 regulates formation of tip cells during angiogenesis', Nature, 445: 776-80.

51. Hellström, M., Phng, L. K., & Gerhardt, H. (2007). VEGF and Notch signaling: the yin and yang of angiogenic sprouting. Cell adhesion & migration, 1(3), 133–136.

52. Horowitz, A., and M. Simons. 2008. 'Branching morphogenesis', Circ Res, 103: 784-95.

53. Huang, L., Zhai, Y., La, J., Lui, J. W., Moore, S. P. G., Little, E. C., Xiao, S., Haresi, A. J., Brem, C., Bhawan, J., & Lang, D. (2021). Targeting Pan-ETS Factors Inhibits Melanoma Progression. Cancer research, 81(8), 2071–2085.

54. Huang, X, C Brown, W Ni, E Maynard, AC Rigby, and P Oettgen. 2006. 'Critical role for the Ets transcription factor ELF-1 in the development of tumor angiogenesis', Blood, 107: 3153–60.

55. Iso, T, L Kedes, and Y Hamamori. 2003. 'HES and HERP families: multiple effectors of the Notch signaling pathway', J Cell Physiol, 194: 237-55.

56. Jain, RK. 2005. 'Normalization of tumor vasculature: an emerging concept in antiangiogenic therapy', Science, 307: 58-62.

57. Jakobsson L, Franco CA, Bentley K, et al. Endothelial cells dynamically compete for the tip cell position during angiogenic sprouting. Nat Cell Biol. 2010;12(10):943-953.

58. Kamei, M., W. B. Saunders, K. J. Bayless, L. Dye, G. E. Davis, and B. M. Weinstein. 2006. 'Endothelial tubes assemble from intracellular vacuoles in vivo', Nature, 442: 453-6.

59. Kar, A., and A. Gutierrez-Hartmann. 2013. 'Molecular mechanisms of ETS transcription factor-mediated tumorigenesis', Crit Rev Biochem Mol Biol, 48: 522-43.

60. Keith, B, and MC Simon. 2014. 'Tumor Angiogenesis.' in J Mendelsohn, P Howley, M Israel, J Gray and C Thompson (eds.), The Molecular Basis of Cancer, (Fourth Edition).

61. Kitange, G., M. Kishikawa, T. Nakayama, S. Naito, M. Iseki, and S. Shibata. 1999. 'Expression of the Ets-1 proto-oncogene correlates with malignant potential in human astrocytic tumors', Mod Pathol, 12: 618-26.

62. Knezevich, S. R., D. E. McFadden, W. Tao, J. F. Lim, and P. H. Sorensen. 1998. 'A novel ETV6-NTRK3 gene fusion in congenital fibrosarcoma', Nat Genet, 18: 184-7.

63. Kliche, Stefanie and Waltenberger, Johannes. “Critical Review VEGF Receptor Signaling and Endothelial Function.” In: International Union of Biochemistry and Molecular Biology Life 52 (2001)

64. Koch, Sina and Claesson-Welsh, Lena. “Signal transduction by vascular endothelial growth factor receptors.” In: Cold Spring Harbor perspectives in medicine 2.7 (2012), a006502.

65. Konstantinidou, M, J Li, B Zhang, Z Wang, S Shaabani, F Ter Brake, K Essa, and A Dömling. 2019. 'PROTACs- a game-changing technology', Expert Opin Drug Discov, 14: 1255-68.

66. Kopan, Raphael and Ilagan, Maria Xenia G. “The canonical Notch signaling pathway: unfolding the activation mechanism.” In: Cell 137.2 (2009), pp. 216–33.

67. Kurz, H., P. H. Burri, and V. G. Djonov. 2003. 'Angiogenesis and vascular remodeling by intussusception: from form to function', News Physiol Sci, 18: 65-70.

68. Kustikova, O, D Kramerov, M Grigorian, V Berezin, E Bock, E Lukanidin, and E Tulchinsky. 1998. 'Fra-1 induces morphological transformation and increases in vitro invasiveness and motility of epithelioid adenocarcinoma cells', Mol Cell Biol, 18: 7095-105.

69. Lawson, ND, AM Vogel, and BM Weinstein. 2002. 'Sonic hedgehog and vascular endothelial growth factor act upstream of the Notch pathway during arterial endothelial differentiation', Dev Cell, 3: 127-36.

70. La Mendola, D., Trincavelli, M. L., & Martini, C. (2022). Angiogenesis in Disease. International journal of molecular sciences, 23(18), 10962. Lee M, Ellis. (2001). 'Tumor Angiogenesis.' in, Surgical Research.

71. Lelievre, E., V. Mattot, P. Huber, B. Vandenbunder, and F. Soncin. 2000. 'ETS1 lowers capillary endothelial cell density at confluence and induces the expression of VE-cadherin', Oncogene, 19: 2438-46.fbiologicaL

72. Lei, Z. N., Tian, Q., Teng, Q. X., Wurpel, J. N. D., Zeng, L., Pan, Y., & Chen, Z. S. (2023). Understanding and targeting resistance mechanisms in cancer. MedComm, 4(3), e265.Leslie, JD, L Ariza-McNaughton, AL Bermange, R McAdow, SL Johnson, and J Lewis. (2007). 'Endothelial signalling by the Notch ligand Delta-like 4 restricts angiogenesis', development, 134: 839-44.

73. Li, JL, RC Sainson, W Shi, R Leek, LS Harrington, M Preusser, S Biswas, H Turley, E Heikamp, JA Hainfellner, and AL Harris. 2007. 'Delta-like 4 Notch ligand regulates tumor angiogenesis, improves tumor vascular function, and promotes tumor growth in vivo', Cancer Res, 67: 11244-53.

74. Li, M., and C. Chen. 2022. 'Regulation of Metastasis in Ewing Sarcoma', Cancers (Basel), 14.

75. Lincoln, D. W., 2nd, P. G. Phillips, and K. Bove. 2003. 'Estrogen-induced Ets-1 promotes capillary formation in an in vitro tumor angiogenesis model', Breast Cancer Res Treat, 78: 167-78.

76. Liu, F, and R Patient. (2008). 'Genome-wide analysis of the zebrafish ETS family identifies three genes required for hemangioblast differentiation or angiogenesis', Circ Res, 103: 1147-54.

77. Liu, M., S. Xie, and J. Zhou. (2018). 'Use of animal models for the imaging and quantification of angiogenesis', Exp Anim, 67: 1-6.

78. Liu, Zhaoguo et al. “Dll4-Notch signaling in regulation of tumor angiogenesis”. In: Journal of Cancer Research and Clinical Oncology 140.4 (2014), pp. 525–536.

79. Liu, ZJ, T Shirakawa, Y Li, A Soma, M Oka, GP Dotto, RM Fairman, OC Velazquez, and M Herlyn. (2003). 'Regulation of Notch1 and Dll4 by vascular endothelial growth factor in arterial endothelial cells: implications for modulating arteriogenesis and angiogenesis', Mol Cell Biol, 23: 14-25.

80. Lobov, I, and N Mikhailova. 2018. 'The Role of Dll4/Notch Signaling in Normal and Pathological Ocular Angiogenesis: Dll4 Controls Blood Vessel Sprouting and Vessel Remodeling in Normal and Pathological Conditions', J Ophthalmol: 2018:3565292.

81. Lobov, IB, RA Renard, N Papadopoulos, NW Gale, G Thurston, GD Yancopoulos, and SJ Wiegand. (2007). 'Delta-like ligand 4 (Dll4) is induced by VEGF as a negative regulator of angiogenic sprouting', Proc Natl Acad Sci, 104: 3219-24.

82. Martins, SF, EA Garcia, MA Luz, F Pardal, M Rodrigues, and AL Filho. 2013. 'Clinicopathological correlation and prognostic significance of VEGF-A, VEGF-C, VEGFR-2 and VEGFR-3 expression in colorectal cancer', Cancer Genomics Proteomics, 10: 55-67.

83. Mathis, G. 1999. 'HTRF(R) Technology', J Biomol Screen, 4: 309-14McLaughlin, F, VJ Ludbrook, J Cox, I von Carlowitz, S Brown, and Randi AM. (2001). 'Combined genomic and antisense

analysis reveals that the transcription factor Erg is implicated in endothelial cell differentiation', Blood, 98: 3332-9.

84. Meller, S., H. A. Meyer, B. Bethan, D. Dietrich, S. G. Maldonado, M. Lein, M. Montani, R. Reszka, P. Schatz, E. Peter, C. Stephan, K. Jung, B. Kamlage, and G. Kristiansen. 2016. 'Integration of tissue metabolomics, transcriptomics and immunohistochemistry reveals ERG- and gleason score-specific metabolomic alterations in prostate cancer', Oncotarget, 7: 1421-38.

85. Mukherjee, T, A Kumar, M Mathur, TK Chattopadhyay, and R Ralhan. 2003. 'Ets-1 and VEGF expression correlates with tumor angiogenesis, lymph node metastasis, and patient survival in esophageal squamous cell carcinoma', J Cancer Res Clin Oncol, 129: 430-6.

86. Mukwaya, A., Jensen, L., & Lagali, N. (2021). Relapse of pathological angiogenesis: functional role of the basement membrane and potential treatment strategies. Experimental & molecular medicine, 53(2), 189–201. side in', Dev Biol, 228: 151-65.

87. Nakagawa, O, DG McFadden, M Nakagawa, H Yanagisawa, T Hu, D Srivastava, and EN Olson. 2000. 'Members of the HRT family of basic helix-loop-helix proteins act as transcriptional repressors downstream of Notch signaling', Proc Natl Acad Sci, 97: 13655-60.

88. Niu, N., C. Yu, L. Li, Q. Liu, W. Zhang, K. Liang, Y. Zhu, J. Li, X. Zhou, J. Tang, and J. Liu. (2018). 'Dihydroartemisinin enhances VEGFR1 expression through up-regulation of ETS-1 transcription factor', J Cancer, 9: 3366-72.

89. Noguera-Troise, I, C Daly, NJ Papadopoulos, S Coetzee, P Boland, NW Gale, HC Lin, GD Yancopoulos, and G Thurston. (2006). 'Blockade of Dll4 inhibits tumour growth by promoting non-productive angiogenesis', Nature, 444: 1032-7.

90. Nyberg, P, L Xie, and R Kalluri. 2005. 'Endogenous inhibitors of angiogenesis', Cancer Res, 65: 3967-79.

91. Oda, N., M. Abe, and Y. Sato. (1999). 'ETS-1 converts endothelial cells to the angiogenic phenotype by inducing the expression of matrix metalloproteinases and integrin beta3', J Cell Physiol, 178: 121-32.

92. Oettgen, P. 2001. 'Transcriptional regulation of vascular development', Circ Res, 89: 380-8.

93. Oikawa, T, and T Yamada. 2003. 'Molecular biology of the Ets family of transcription factors', Gene, 303: 11-34.

94. Olsson, AK, A Dimberg, J Kreuger, and L Claesson-Welsh. 2006. 'VEGF receptor signalling - in control of vascular function', Nat Rev Mol Cell Biol, 359-71

95. Otrock, Zaher K. et al. “Understanding the biology of angiogenesis: Review of the most important molecular mechanisms”. In: Blood Cells, Molecules, and Diseases 39.2 (2007), pp. 212–220.

96. Walker D M.,. Poczobutt J, Melissa S. Gonzales, Henrick Horita3 and Arthur Gutierrez-Hartmann Papakonstantinou, E., F. Bacopoulou, D. Brouzas, V. Megalooikonomou, D. D'Elia, E. Bongcam-Rudloff, and D. Vlachakis. (2010). ' SE-1 is Required to Maintain the Transformed Phenotype of MCF-7 and ZR-75-1 Human Breast Cancer Cells Open Cancer Journal, 2010

97. Pardali, E., M. J. Goumans, and P. ten Dijke. 2010. 'Signaling by members of the TGF-beta family in vascular morphogenesis and disease', Trends Cell Biol, 20: 556-67.

98. Patel-Hett, S., and P. A. D'Amore. 2011. 'Signal transduction in vasculogenesis and developmental angiogenesis', Int J Dev Biol, 55: 353-63.

99. Patel, NS, Li, JL, D Generali, R Poulsom, DW Cranston, and AL Harris. (2005). 'Up-regulation of delta-like 4 ligand in human tumor vasculature and the role of basal expression in endothelial cell function', Cancer Res, 65: 8690-7.

100. Pham, VN, ND Lawson, JW Mugford, L Dye, D Castranova, B Lo, and BM Weinstein. (2007). 'Combinatorial function of ETS transcription factors in the developing vasculature', Dev Biol, 303: 772-83.

101. Phng, LK, and H Gerhardt. 2009. 'Angiogenesis: a team effort coordinated by notch', Dev Cell, 16: 196-208.

102. Pimanda, JE, WY Chan, IJ Donaldson, M Bowen, AR Green, and B Göttgens. 2006 'Endoglin

expression in the endothelium is regulated by Fli-1, Erg, and Elf-1 acting on the promoter and a -8-kb enhancer', Blood.

103. Pollina, E. A., A. Legesse-Miller, E. M. Haley, T. Goodpaster, J. Randolph-Habecker, and H. A. Coller. (2008). 'Regulating the angiogenic balance in tissues', Cell Cycle, 7: 2056-70.

104. Quintero-Fabián, S., Arreola, R., Becerril-Villanueva, E., Torres-Romero, J. C., Arana-Argáez, V., Lara-Riegos, J., Ramírez-Camacho, M. A., & Alvarez-Sánchez, M. E. (2019). Role of Matrix Metalloproteinases in Angiogenesis and Cancer. Frontiers in oncology, 9, 1370. Ribatti, D., Nico, B., Crivellato, E., Roccaro, A. M., & Vacca, A. (2007). The history of the angiogenic switch concept. Leukemia, 21(1), 44–52.

105. Ribatti, D., Nico, B., Crivellato, E., & Vacca, A. (2007). The structure of the vascular network of tumors. Cancer letters, 248(1), 18–23.

106. Roukens, MG, M Alloul-Ramdhani, B Baan, K Kobayashi, J Peterson-Maduro, H van Dam, S Schulte-Merker, and DA Baker. 2010 'Control of endothelial sprouting by a Tel-CtBP complex', Nat Cell Biol, 12: 933-42.

107. Ruhrberg, C., H. Gerhardt, M. Golding, R. Watson, S. Ioannidou, H. Fujisawa, C. Betsholtz, and D. T. Shima. 2002. 'Spatially restricted patterning cues provided by heparin-binding VEGF-A control blood vessel branching morphogenesis', Genes Dev, 16: 2684-98.

108. Russo, A. E., D. Priolo, G. Antonelli, M. Libra, J. A. McCubrey, and F. Ferrau. (2017). 'Bevacizumab in the treatment of NSCLC: patient selection and perspectives', Lung Cancer (Auckl), 8: 259-69.

109. Sainson, RC, J Aoto, MN Nakatsu, M Holderfield, E Conn, E Koller, and CC Hughes. (2005). 'Cell-autonomous notch signaling regulates endothelial cell branching and proliferation during vascular tubulogenesis', FASEB J, 19: 1027-9.

110. Salami, J, and CM Crews. 2017. 'Waste disposal-An attractive strategy for cancer therapy', Science, 355: 1163-67.

111. Sato, Y. “Role of ETS family transcription factors in vascular development and angiogenesis.” Cell structure and function vol. 26,1 (2001): 19-24.

112. Schreiber, M, ZQ Wang, W Jochum, I Fetka, C Elliott, and EF Wagner. 2000. 'Placental vascularisation requires the AP-1 component fra1', development, 127: 4937-48.

113. Schweighofer, Bernhard et al. “The VEGF-induced transcriptional response comprises gene clusters at the crossroad of angiogenesis and inflammation”. In: Thrombosis and Haemostasis 102.3 (2009), pp. 544–554.

114. Seth, A., and D. K. Watson. (2005). 'ETS transcription factors and their emerging roles in human cancer', Eur J Cancer, 41: 2462-78.

115. Shah, A. V., G. M. Birdsey, C. Peghaire, M. E. Pitulescu, N. P. Dufton, Y. Yang, I. Weinberg, L. Osuna Almagro, L. Payne, J. C. Mason, H. Gerhardt, R. H. Adams, and A. M. Randi. (2017). 'The endothelial transcription factor ERG mediates Angiopoietin-1-dependent control of Notch signalling and vascular stability', Nat Commun, 8: 16002.

116. Siekmann, AF, and ND Lawson. (2007). 'Notch signalling limits angiogenic cell behaviour in developing zebrafish arteries', Nature, 445: 781-4.

117. Siemann DW. The unique characteristics of tumor vasculature and preclinical evidence for its selective disruption by Tumor-Vascular Disrupting Agents. Cancer Treat Rev. 2011 Feb;37(1):63-74

118. Sizemore, G. M., J. R. Pitarresi, S. Balakrishnan, and M. C. Ostrowski. 2017. 'The ETS family of oncogenic transcription factors in solid tumours', Nat Rev Cancer, 17: 337-51.

119. Smith, BE, SL Wang, S Jaime-Figueroa, A Harbin, J Wang, BD Hamman, and CM Crews. 2019. 'Differential PROTAC substrate specificity dictated by orientation of recruited E3 ligase', Nat Commun, 10: 131.

120. Stone, J, A Itin, T Alon, J Pe'er, H Gnessin, T Chan-Ling, and E Keshet. (1995). 'Development of retinal vasculature is mediated by hypoxia-induced vascular endothelial growth factor (VEGF) expression by neuroglia', J Neurosci, 15: 4738-47.

121. Suchting, S, C Freitas, F le Noble, R Benedito, C Bréant, A Duarte, and A Eichmann. 2007.

'The Notch ligand Delta-like 4 negatively regulates endothelial tip cell formation and vessel branching', Proc Natl Acad Sci, 104: 3225-30.

122. Szeles, J. Sápi, D.A. Drexler, I. Harmati, Z. Sápi, L. Kovács Model-based angiogenic inhibition of tumor growth using modern robust control method IFAC Proc., 45 (18) (2012), pp. 113-118,

123. Takahashi, H, and M Shibuya. 2005. 'The vascular endothelial growth factor (VEGF)/VEGF receptor system and its role under physiological and pathological conditions', Clin Sci (Lond), 109: 227-41.

124. Takahashi N, Hoshi H, Higa A, Hiyama G, Tamura H, Ogawa M, Takagi K, Goda K, Okabe N, Muto S, Suzuki H, Shimomura K, Watanabe S, Takagi M. An In Vitro System for Evaluating Molecular Targeted Drugs Using Lung Patient-Derived Tumor Organoids. Cells. 2019 May 20;8(5):481.

125. Tomlins, S. A., R. Mehra, D. R. Rhodes, L. R. Smith, D. Roulston, B. E. Helgeson, X. Cao, J. T. Wei, M. A. Rubin, R. B. Shah, and A. M. Chinnaiyan. 2006a. 'TMPRSS2:ETV4 gene fusions define a third molecular subtype of prostate cancer', Cancer Res, 66: 3396-400.

126. Treps, L., Ager, A., & Hida, K. (2022). Editorial: Tumor Vessels as Directors of the Tumor Microenvironment: New Findings, Current Challenges & Perspectives. Frontiers in cell and developmental biology, 10, 885670. https://doi.org/10.3389/fcell.2022.885670.

127. Tveriakhina, L., Schuster-Gossler, K., Jarrett, S. M., Andrawes, M. B., Rohrbach, M., Blacklow, S. C., & Gossler, A. (2018). The ectodomains determine ligand function in vivo and selectivity of DLL1 and DLL4 toward NOTCH1 and NOTCH2 in vitro. eLife, 7, e40045.

128. Uyttendaele, H, G Marazzi, G Wu, Q Yan, D Sassoon, and J Kitajewski. 1996. 'Notch4/int-3, a mammary proto-oncogene, is an endothelial cell-specific mammalian Notch gene', development, 122: 2251-9.

129. Verschoor, M. L., C. P. Verschoor, and G. Singh. 2013. 'Ets-1 global gene expression profile reveals associations with metabolism and oxidative stress in ovarian and breast cancers', Cancer Metab, 1: 17.

130. Wang, Michael M. “Notch signaling and Notch signaling modifiers.” In: The international journal of biochemistry & cell biology 43.11 (2011), pp. 1550–62.

131. Watson, DK, R Li, VI Sementchenko, G Mavrothalassitis, and A Seth. 2001. 'The ETS genes.' in JR Bertino (ed.), Encyclopedia of cancer (San Diego: Academic Press).

132. Watson, DK, and A Seth. 2000. 'Ets gene family.' in Reddy EP Jenkins J (ed.), Oncogene reviews (London: Nature Publishing Group).

133. Wei, Y., Han, S., Wen, J., Liao, J., Liang, J., Yu, J., Chen, X., Xiang, S., Huang, Z., & Zhang, B. (2023). E26 transformation-specific transcription variant 5 in development and cancer: modification, regulation and function. Journal of biomedical science, 30(1), 17.

134. Weinmaster, G. (1998). 'Notch signalling: Direct or what?', Curr Opin Genet Dev, 8: 436-42.

135. Williams, CK, JL Li, M Murga, AL Harris, and G Tosato. 2006. 'Up-regulation of the Notch ligand Delta-like 4 inhibits VEGF-induced endothelial cell function', Blood, 107: 931-9.

136. Wu, Y, C Cain-Hom, L Choy, TJ Hagenbeek, GP de Leon, Y Chen, D Finkle, R Venook, X Wu, J Ridgway, D Schahin-Reed, GJ Dow, A Shelton, S Stawicki, RJ Watts, J Zhang, R Choy, P Howard, L Kadyk, M Yan, J Zha, CA Callahan, and SG Hymowitz. (2010). 'Therapeutic antibody targeting of individual Notch receptors', Nature, 464: 1052-7.

137. Yazdjerdi, P., Meskin, N., Al-Naemi, M., Al Moustafa, A. E., & Kovács, L. (2019). Reinforcement learning-based control of tumor growth under anti-angiogenic therapy. Computer methods and programs in biomedicine, 173, 15–26.

138. Zhang, G, CR Dass, E Sumithran, N Di Girolamo, LQ Sun, and LM Khachigian. 2004. 'Effect of deoxyribozymes targeting c-Jun on solid tumor growth and angiogenesis in rodents', J Natl Cancer Inst, 96: 683-96.

139. Ziche, M, Donnini, S, and L Morbidelli. 2004. 'Development of new drugs in angiogenesis', Curr Drug Targets, 5: 485-93.

CHAPTER 2

Control of endothelial cell tube formation by Notch ligand intracellular domain interactions with activator protein 1 (AP-1)

J.Biol.Chem.(2017)292(52) 21282–21290

Zary Forghany[1]*, Francesca Robertson[1,4]*, Alicia Lundby[2,3], Jesper V. Olsen[2], David A. Baker

1. Leiden University Medical Center (LUMC), Department of Molecular Cell Biology, 2300 RC Leiden, The Netherlands.
2. Novo Nordisk Foundation Center for Protein Research, Faculty of Health and Medical Sciences, University of Copenhagen, Copenhagen, Denmark.
3. Department of Biomedical Sciences, Faculty of Health and Medical Sciences, University of Copenhagen, Copenhagen, Denmark.
4. University of Oxford, Department of Biochemistry, South Parks Rd, Oxford, OX1 3QU.

*Joint first authors

ABSTRACT

Notch signaling is a ubiquitous signal transduction pathway found in most if not all metazoan cell types characterized to date. It is indispensable for cell differentiation as well as tissue growth, tissue remodelling and apoptosis. Although the canonical Notch signaling pathway is well characterized, accumulating evidence points to the existence of multiple, less well-defined, layers of regulation. In this study, we have investigated the function of the intracellular domain (ICD) of the Notch ligand DLL4. We provide evidence that the DLL4 ICD is cleaved and interacts with the JUN proto-oncogene, which forms part of the activator protein 1 (AP-1) transcription factor complex. Mechanistically, the DLL4 ICD inhibits JUN binding to DNA and thereby controls the expression of JUN target genes, including DLL4. Our work demonstrates that JUN strongly stimulates endothelial sprouting and that DLL4 constrains this process. These data raise the possibility that Notch/DLL4 signaling is bi-directional and suggests that the DLL4 ICD could represent a point of cross-talk between Notch and RTK signaling.

INTRODUCTION

The generic Notch signaling network is a central regulator of cell fate (Kopan and Ilagan 2009; Guruharsha et al. 2012). This pathway is absolutely necessary for normal development and tissue homeostasis and corruption of it has been implicated in numerous diseases including the majority of solid tumors where it plays diverse oncogenic and tumor-suppressive roles (Aster et al. 2017; Braune et al. 2016; Ranganathan et al. 2011). In vertebrates, the Notch signaling system is composed of four single-pass cell surface receptors (Notch1-4) and five Type 1 transmembrane ligands: Jagged (JAG)1, JAG2, Delta-Like (DLL)1, DLL3, and DLL4 (Kopan and Ilagan 2009; Bray 2016; Ulla-Maj and Martinez Arias 2007). Operationally, the canonical Notch signaling pathway is relatively well characterized (Guruharsha et al. 2012; Bray 2016; Ulla-Maj and Martinez Arias 2007). It is activated by a trans interaction between a Notch receptor on one cell and a ligand expressed by a neighbouring cell. This triggers a cascade of proteolytic events terminating in the γ-secretase-mediated cleavage of the Notch intracellular domain which translocates to the nucleus whereupon it regulates expression of Notch target genes (Kopan and Ilagan 2009; Kitagawa 2016). By these means, the molecular and cellular asymmetries required for tissue maintenance and development are established across populations of cells. In recent years, studies have identified manifold, unique facets of Notch signaling (Bray 2006). These include cis receptor/ligand interactions (since each are expressed in the same cell (Del Alamo et al. 2011), ligand-independent signaling (Palmer and Deng 2015), endocytosis of Notch and Notch ligands as an essential mediator of signaling (Le Borgne et al. 2005; Nichols et al. 2007) and, in the case of DLL4, signaling at a distance through the incorporation of DLL4 into exosomes (Sheldon et al. 2010; Sharghi-Namini et al. 2014). Adding further to the complexity is the extensive crosstalk between the Notch pathway and other major signaling networks such as receptor tyrosine kinase (RTK) signaling (Doroquez and Rebay 2006), WNT, hedgehog and transforming growth factor (TGF) β signaling (Borggrefe et al. 2016) janus kinase (JAK)/ signal transducer and activator of transcription (STAT) signaling (Josten et al. 2004) and hypoxia signaling (Gustafsson et al. 2005). To understand these mechanisms in greater depth, new studies are beginning to elucidate the role of the Notch ligands in this process. The five ligands share a similar overall architecture: Module at the N-terminus of Notch Ligands (MNNL) domains, a Delta/Serrate/Lag-2 (DSL) domain, between 6-14 EGF-like repeats, a transmembrane segment, and an intracellular domain (ICD) 100-150 amino acids in length. The extracellular moiety is essential for establishing the direct contacts with the Notch receptor necessary for eliciting Notch signaling (Luca et al. 2015). Biochemical and genetic evidence has shown that the intracellular domain is clearly essential for normal functioning of the full length protein (Heuss et al. 2008; Pintar et al. 2007; Six et

al. 2004; Ascano et al. 2002). Ligand ICDs harbour putative PDZ domains that couple them to membrane-bound proteins required for the maintenance of cell-cell junctions and likely play a central role in assembling those complexes necessary for ligand trafficking (Dejana 2004; Lee and Zheng 2010). Consistent with this, in Drosophila (Sun and Artavanis-Tsakonas 1996) and in vertebrates (Chitnis et al. 1995), Delta (and Serrate) ligands lacking an intracellular domain behave as dominant negative mutants such that the phenotypes resemble Notch or Delta loss-of-function mutants. Likewise, corruption of the DLL1 C-terminus has been shown to provoke mislocalization of the ligand (Heuss et al. 2008).

In common with the Notch receptor, the DLL1 and JAG ligands can be sequentially processed by proteases. Both ADAM (A Disintegrin And Metalloprotease) Metalloendopeptidases (Dyczynska et al. 2007; Six et al. 2003) and matrix metalloproteinase (MMP)14 (in the case of DLL1) (Jin et al. 2011) mediate ectodomain shedding by cleavage of the ligand close to the transmembrane domain on the extracellular side. Subsequent intramembrane processing by γ-secretase liberates the ICD (Ikeuchi and Sisodia 2003; LaVoie and Selkoe 2003). A growing body of evidence suggests that these ICDs might participate in signaling and downstream transcription and ectopically expressed ICDs have been localized to the nucleus (Liebler et al. 2012). Moreover, it has been reported that both DLL1 (Jung et al. 2011) and JAG1 ICDs (Kim et al. 2011) are able to bind to and to disrupt the function of the Notch ICD, by mediating its degradation in the case of the JAG ICD. The DLL1 ICD has also been pinpointed as a modulator of TGF-β/Activin signaling through binding to SMAD proteins (Hiratochi et al. 2007). A number of studies have described the effects of ligand ICDs at the cellular level. Inhibition of Notch1 signaling by the JAG1 ICD was shown to regulate cardiac homeostasis in the postnatal heart (Metrich et al. 2015). When ectopically expressed in mesenchymal stromal cells, the JAG1 ICD regulated haematopoietic stem and progenitor cell proliferation (Duryagina et al. 2013). Finally, overexpression of the DLL1 ICD brought about the growth arrest of primary endothelial cells (Kolev et al. 2005).

Collectively, the mechanisms described above determine the strength, the direction, the specificity and the nature of the output of the Notch signaling pathway. The emerging evidence that ICDs are biologically active is thus important for fully understanding Notch signaling in both normal and disease contexts, not least because the Notch pathway in general (Andersson and Lendahl 2014) and the DLL4 ligand in particular (Kuhnert et al. 2011; Sainson and Harris 2007) has emerged as a potential target for novel therapeutic interventions in cancer. The DLL4 ligand is integral to the development and homeostasis of numerous tissues, most notably the endothelium where it plays a central role in angiogenesis (Adams and Alitalo 2007; Herbert and Stainier 2011; Carmeliet and Jain 2011; Chung and Ferrara 2011; Geudens and Gerhardt 2011), hematopoiesis (Ayllón et al. 2015) and the intestinal crypt where it regulates maintenance of the stem cell compartment (Clevers 2013). To date

little is known about the function of the DLL4 intracellular domain. Here we provide evidence that the DLL4 ICD is needed for appropriate DLL4 sub-cellular localization. We show that it encodes a functional PDZ-binding domain which is necessary for associating to the MUPP1 scaffold protein. We further show that the DLL4 ICD is cleaved. The liberated DLL4 (and DLL1) ICD could interact with the bZIP domain of the JUN proto-oncogene thereby blocking it's binding to the consensus AP1 DNA-binding site. We found that JUN strongly stimulated endothelial cell sprouting which was inhibited by the ICDs of both DLL4 and DLL1. These data highlight a previously unreported role for JUN as a potent pro-angiogenic signal and the DLL4 ICD as a potential regulator of Notch signaling. Our evidence suggests that the ICDs of DLL4 (and DLL1) could control angiogenic sprouting by linking Notch signaling to the action of the AP-1 transcription factor complex.

RESULTS

The intracellular domain of DLL4 is cleaved

The amino acid sequence of the intracellular domain of DLL4 (hereafter referred to as DLL4INTRA) has been highly conserved throughout vertebrate evolution (Fig 1A). The four C-terminal amino acids (ATEV) encode a putative PDZ-binding domain (De Biasio et al. 2008). PDZ-binding domains have been shown to mediate protein-protein interactions, cell adhesion, tight junction integrity and trafficking (Lee and Zheng 2010) and loss of DLL4INTRA led to a complete disruption of normal DLL4 localization in primary human endothelial cells (Fig 1B). DLL4INTRA harbours a number of additional motifs that suggest it is functionally important including GSK consensus phosphorylation sites (which are utilized- ZF and DAB unpublished), a sumoylation motif and putative ubiquitination sites. Moreover, ectopically expressed DLL4INTRA is strongly enriched in the nucleus (Fig 1B) indicating that it may play a role independently of ensuring appropriate DLL4 sub-cellular distribution. To explore the function of this domain, we raised custom-made antibodies directed against epitopes unique to the C-terminus of human DLL4. Fig 1C shows that these antibodies recognized full length endogenous DLL4 as well as a number of smaller DLL4 species (predominant forms with masses between approximately 25-35 kDa and a lower molecular weight form of approximately 12 KDa). Similar sized fragments could be detected by Western blotting of lysates prepared from cells ectopically expressing full length DLL4 fused to a C-terminal HA epitope tag (Fig 1C). Through mass spectrometry, we determined that these fragments constitute the C-terminus of DLL4 (Fig 1C).

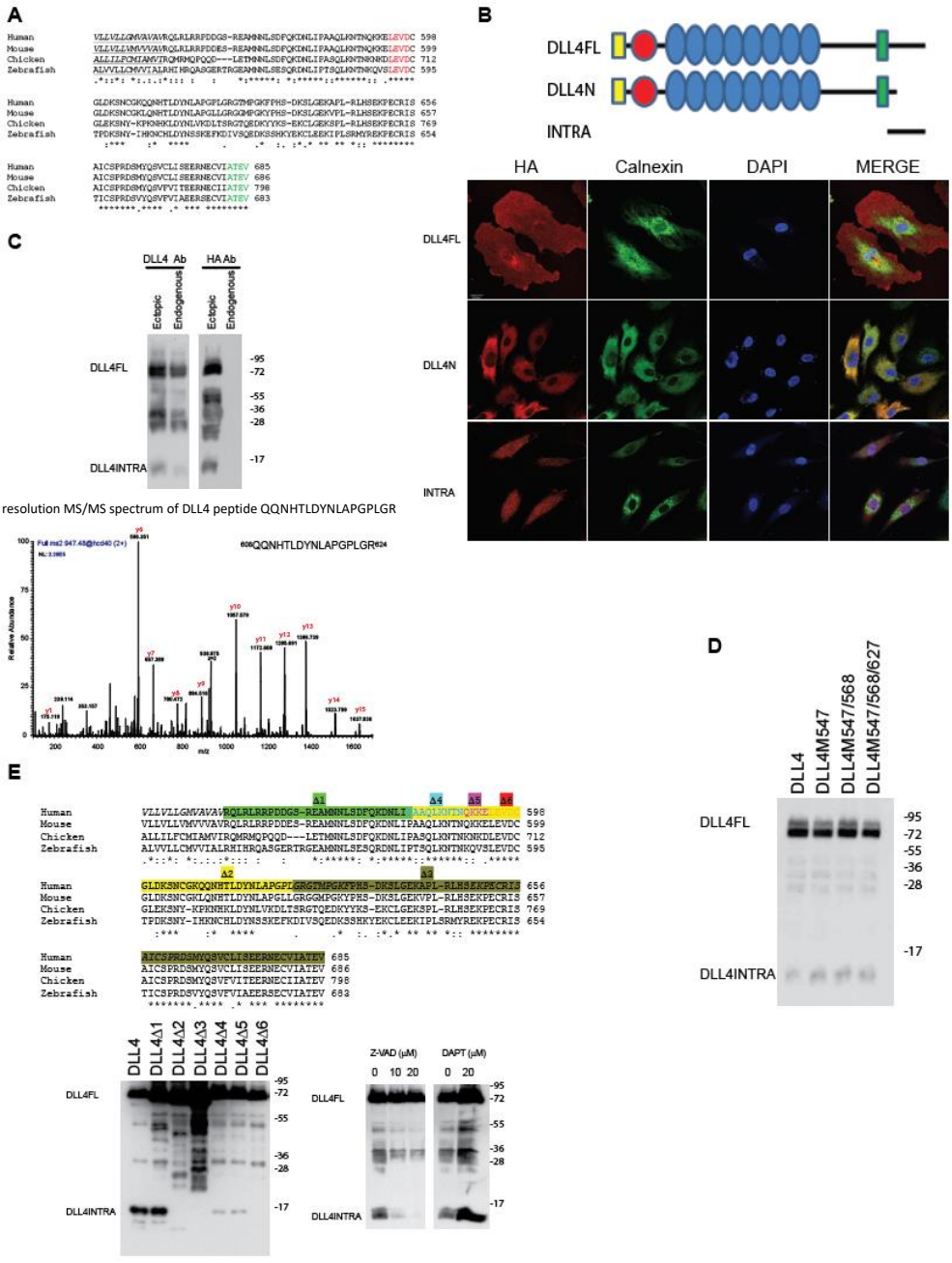

Figure 1. (A) The intracellular domain (ICD) of DLL4 is evolutionarily conserved. Highlighted are the transmembrane domain (underlined), a putative caspase cleavage site (red) and a PDZ-binding motif (green). (B) The DLL4 ICD is necessary for appropriate DLL4 sub-cellular localization and untethered DLL4INTRA is enriched in the nucleus. HUVECs were infected with lentiviruses for stably expressing the indicated HA epitope-tagged DLL4 constructs. DLL4N lacks the ICD and is otherwise identical to wild type DLL4. DLL4INTRA encompasses the ICD alone. The sub-cellular distribution of DLL4 was visualized by immunofluorescence using an HA antibody. Scale bar represents 20 μM.

< Figure 1 (continued). (C-E) The ICD of DLL4 is cleaved. (C) Mass spectrometry of cleaved DLL4 fragments. Endogenous DLL4 or DLL4 expressing a C-terminal HA epitope-tag were immunopurified from HUVECs. Samples were separated by SDS-PAGE and DLL4 ICDs were subjected to in-gel digestion with trypsin. Shown is an identified high resolution MS/MS spectrum of a recovered peptide corresponding to amino acids 608-624 of the DLL4 ICD. (D) The indicated ICD methionine residues of HA epitope tagged full length DLL4 were mutated to alanine. HA antibody Western blots were performed on lysates prepared from HUVECS stably expressing the indicated DLL4 ligands. (E) A conserved LEVD motif is required for cleavage of the DLL4 ICD. Left Panel: The indicated nested deletions of HA epitope tagged full length DLL4 were generated by site-directed mutagenesis. HA antibody Western blots were performed on lysates prepared from HUVECs stably expressing the indicated DLL4 ligands. Corresponding deletions are highlighted above. Right Panel: DLL4 ICD cleavage is blocked by the pan-caspase inhibitor, Z-VAD. Cells expressing wild type HA epitope tagged full length DLL4 were incubated overnight with or without the indicated concentrations of Z-VAD. DLL4 protein species were detected by HA antibody Western blotting.

The 25-35 KDa fragments are predicted to encompass the entire ICD, the transmembrane domain as well as sequences of the extracellular domain EGF repeats. The size of the shorter fragment indicates that it's composed uniquely of ICD sequences. Our evidence supports the view that this fragment is generated by post-translational proteolysis of the ICD distal to the transmembrane domain on the intracellular side. First, the molecular mass of the observed endogenous fragment precludes the possibility of it being generated by known mechanisms of alternative splicing alone. Second, mutation of the intracellular domain methionine residues failed to eliminate detection of the band in cells suggesting that it is not produced through use of internal initiation codons (Fig 1D). Third, a comprehensive deletion analysis mapped a putative cleavage site to the highly conserved LEVD motif (amino acids 594-597) (Fig 1E). LEVD closely resembles a consensus caspase cleavage site (Timmer and Salvesen 2007) and the pan-caspase inhibitor Z-VAD-FMK blocked the production of the DLL4ICD (Fig 1E). It has been reported that the closely related DLL1 ligand undergoes intramembrane processing mediated by γ-secretase to yield an intracellular fragment (Ikeuchi and Sisodia 2003; Six et al. 2003). Although we cannot formally rule out γ-secretase-dependent cleavage of DLL4, we found that release of the observed DLL4INTRA was not blocked by DAPT (data not shown). Together, these observations reveal two unique features of DLL4INTRA. They show that it is necessary for accurate ligand trafficking and also that it is proteolytically cleaved (and this proteolysis is caspase-dependent).

DLL4 interacts with the PDZ domain of MUPP1 and the bZIP domain of JUN

To investigate the potential molecular function(s) of the DLL4 intracellular domain, we performed yeast two-hybrid screens to identify partner proteins of DLL4INTRA. Three different DLL4 C-termini constructs were used as baits to independently screen a library prepared from primary HUVECs (Fig 2A).

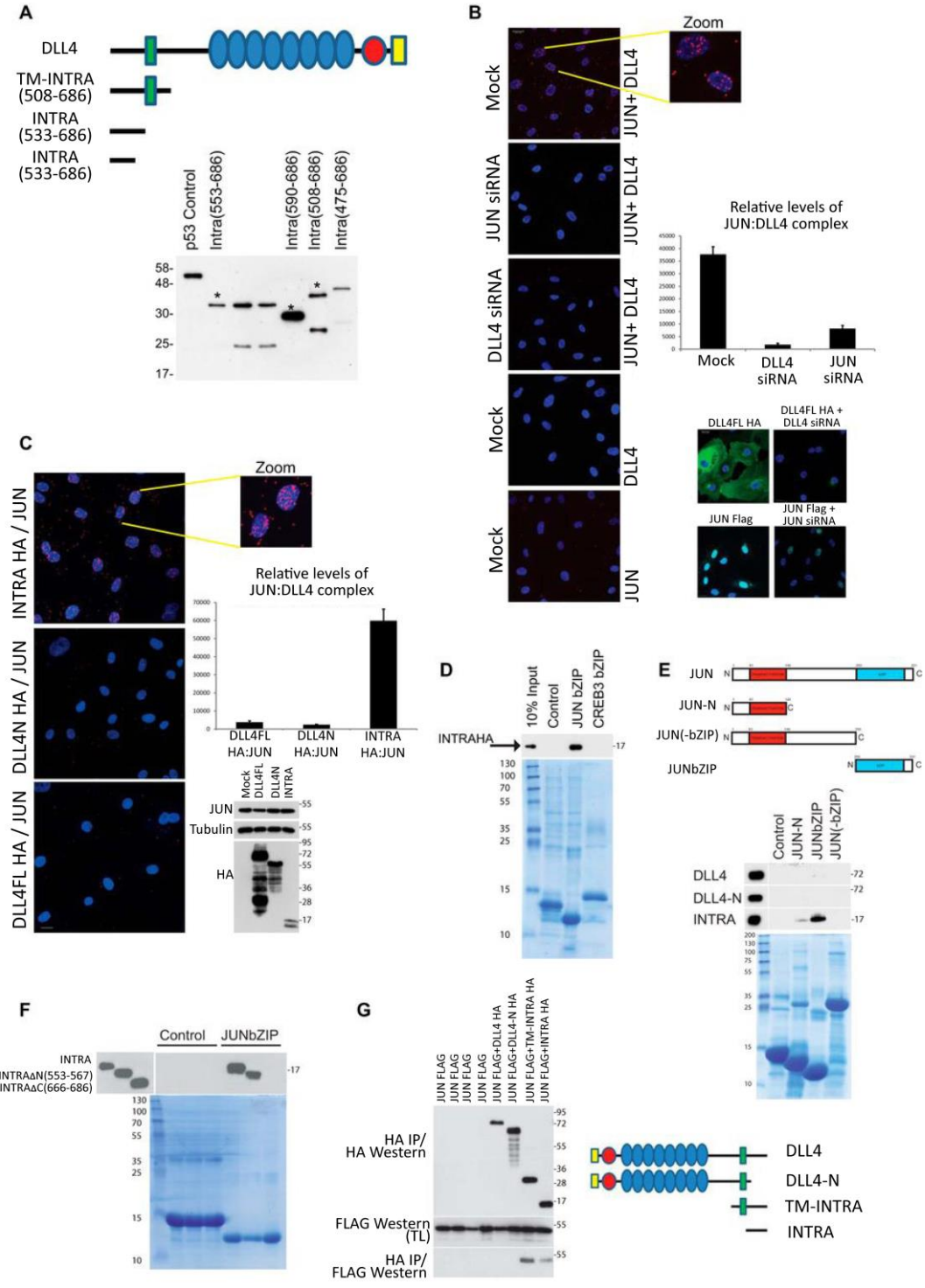
A
DLL4
TM-INTRA (508-686)
INTRA (533-686)
INTRA (533-686)
p53 Control
Intra(553-686)
Intra(590-686)
Intra(508-686)
Intra(475-686)
58-
48-
30-
25-
17-
B
Zoom
Mock
JUN+ DLL4
JUN siRNA
DLL4 siRNA
DLL4
JUN
Relative levels of JUN:DLL4 complex
Mock
DLL4 siRNA
JUN siRNA
DLL4FL HA
DLL4FL HA + DLL4 siRNA
JUN Flag
JUN Flag + JUN siRNA
C
Zoom
INTRA HA / JUN
DLL4N HA / JUN
DLL4FL HA / JUN
Relative levels of JUN:DLL4 complex
DLL4FL HA:JUN
DLL4N HA:JUN
INTRA HA:JUN
Mock
DLL4FL
DLL4N
INTRA
JUN
Tubulin
HA
D
10% Input
Control
JUN bZIP
CREB3 bZIP
INTRAHA
E
JUN
JUN-N
JUN(-bZIP)
JUNbZIP
Control
JUN-N
JUNbZIP
JUN(-bZIP)
DLL4
DLL4-N
INTRA
F
Control
JUNbZIP
INTRA
INTRAΔN(553-567)
INTRAΔC(666-686)
G
JUN FLAG
JUN FLAG
JUN FLAG
JUN FLAG
JUN FLAG+DLL4 HA
JUN FLAG+DLL4-N HA
JUN FLAG+TM-INTRA HA
JUN FLAG+INTRA HA
HA IP/ HA Western
FLAG Western (TL)
HA IP/ FLAG Western
DLL4
DLL4-N
TM-INTRA
INTRA

< Figure 2. **DLL4INTRA interacts with the bZIP domain of JUN.** (A) Yeast 2-hybrid baits were constructed by fusing DLL4 ICD fragments in-frame with a LexA DNA-binding domain either at the N- or the C-terminus of the ICD. Constructs were expressed in yeast to verify expression by Western blotting of lysates using a LexA antibody. A p53-LexA fusion is included as a control (Dualsystems Biotech). Predicted full length proteins of constructs used to screen a library prepared from HUVECs are marked with an asterisk. (B) A proximity ligation assay (PLA) revealed an endogenous DLL4:JUN complex. The graph shows relative complex formation per cell (right upper panel) that was abolished by ablation of either DLL4 or JUN (siRNA efficacies were demonstrated using cells ectopically expressing either DLL4 or JUN: see right lower panels). The endogenous DLL4:JUN complex was undetectable using single antibodies alone. Quantification was performed as described (see Methods) with an average of 100 cells scored. Scale bar represents 20 μM. (C) JUN specifically associated with the ICD of DLL4. PLA was performed on HUVECs ectopically expressing HA epitope tagged versions of either full length DLL4 (DLL4FL), the extracellular domain of DLL4, which lacks the ICD but retains the transmembrane domain (DLL4N) or the non-membrane tethered ICD of DLL4 (DLL4INTRA). Relative protein levels of DLL4 and endogenous JUN were determined by Western blotting with the indicated antibodies (right lower panel). The DLL4:JUN complex was detected using a combination of HA (for DLL4) and endogenous JUN antibodies. The graph shows relative complex formation per cell (right upper panel). Quantification was performed as described (see Methods) with an average of 100 cells scored. Scale bar represents 20 μM. (D and E) The ICD of DLL4 interacts biochemically with the bZIP domain of JUN. (D) Recombinant bZIP domains of JUN and CREB3 (and a control protein) were incubated with *in vitro* translated HA epitope-tagged DLL4INTRA. Recombinant proteins were visualized by Coomassie staining. Bound DLL4INTRA was detected by Western blotting. (E) Recombinant JUN domains (and a control protein) were incubated with *in vitro* translated HA epitope-tagged DLL4FL, DLL4N or DLL4INTRA. Recombinant proteins were visualized by Coomassie staining. Bound DLL4 was detected by Western blotting. (F) The C-terminus of DLL4INTRA is necessary for binding of DLL4INTRA to the JUN bZIP domain. Experiments were performed as in D and E. DLL4INTRAΔN lacks the N-terminal amino acids 553-567. DLL4INTRAΔC lacks the C-terminal amino acids 666-686. (G) The indicated constructs were stably expressed in HUVECs. JUN:DLL4 complexes were immunopurified from cell lysates using a rabbit HA polyclonal antibody and visualized by Western blotting with a Flag mouse monoclonal antibody. TM, transmembrane domain; IP, immunoprecipitation; TL, total lysate.

The PDZ domain-containing scaffold protein MUPP1 was obtained in all screens. It is involved in cell-cell junction integrity, including endothelial cell junctions, and protein trafficking (Balasubramanian et al. 2007; Dejana 2004). Immunoprecipitation studies in tissues culture cells corroborated the interaction between DLL4 and MUPP1 and its dependence on the extreme C-terminus (ATEV) of DLL4 lending substance to the view that DLL4INTRA has a bona fide PDZ-binding domain (Supplementary Fig 1; see Fig 1B). Less expected was the interaction with the bZIP-containing transcription factor JUN. We have previously established that JUN levels are dynamically balanced by VEGFR signaling in primary endothelial cells (Roukens et al. 2010) and several lines of evidence confirmed that DLL4INTRA and JUN can interact both *in vitro* and in cells. First, using a proximity ligation assay, we found that endogenous JUN and DLL4 associate (predominantly in the nucleus) in HUVECs (Fig 2B). By stably expressing engineered DLL4 mutants in HUVECs, we showed that DLL4INTRA was necessary and sufficient for this interaction (Fig 2C). Second, using purified

recombinant JUN protein domains and *in vitro* translated DLL4 proteins, we demonstrated that DLL4INTRA bound efficiently to the bZIP domain of JUN but not to the bZIP domain of CREB (Fig 2D). Third, Figs 2E and 2G substantiate our PLA findings (see Figs 2B and 2C) by showing that DLL4INTRA, but not the extracellular domain of DLL4 (DLL4N), is necessary for binding to JUN *in vitro* (Fig 2E) and in tissue culture cells (Fig 2G). Furthermore, the association between DLL4INTRA and JUN requires the bZIP domain of JUN (Fig 2E) as well as the highly conserved C-terminal twenty amino acids of DLL4, which are shared with the ICD of DLL1 (Fig 2F; See Supp. Fig 2), but not the PDZ-binding domain of DLL4INTRA (see Fig 3B). Collectively, these data highlight potentially a dual role for the DLL4ICD: it can interact with the bZIP domain of JUN and, in addition, it encodes a PDZ-binding domain that mediates a functional interaction with MUPP1.

DLL4INTRA blocks JUN binding to DNA

To determine the mechanistic consequences of DLL4INTRA:JUN binding, we established an *in vitro* assay to recapitulate JUN binding to DNA. For this, we employed a biotinylated consensus AP-1 DNA binding site and *in vitro* translated proteins. Fig 3A shows that JUN efficiently bound to the AP-1 site. As expected, JUN binding to the AP-1 site required the bZIP domain of JUN because a mutant lacking this domain, but not a mutant lacking amino acids C-terminal of this domain, was unable to bind the consensus sites, thus authenticating the specificity of the assay (Fig 3A). Compellingly, DLL4INTRA, but not DLL4N, impeded JUN associating to the AP-1 site (Fig 3B). Both the PDZ-binding motif of DLL4INTRA and sequences N-terminal of the LEVD motif were dispensable for this inhibition (Fig 3C). JUN represses or activates gene expression in a context-dependent fashion by docking on target promoters and through the differential recruitment of co-repressors and co-activators. To ascertain a more global view of regulation of JUN activity by DLL4INTRA, we performed transcriptome profiling of HUVECs ectopically expressing JUN in the presence or absence of DLL4INTRA or DLL4N. Ectopic expression of JUN is highly pro-angiogenic (see Fig 4) and leads to a dramatic alteration in the set of expressed genes (Fig 3D: compare Mock and JUN). Whereas co-expression of DLL4N had relatively more modest effects on the JUN-controlled transcriptome, DLLINTRA significantly altered the expression pattern of JUN-controlled genes (Fig 3D). These findings were verified by real time quantitative PCR (qPCR) of a subset of the genes, including DLL4 (Fig 3E). To test if these effects could have resulted from DLL4INTRA directly occluding JUN DNA-binding, we investigated JUN recruitment to the proximal promoter of DLL4. We have previously shown that DLL4 expression (and JUN expression) is highly attuned to VEGFR signaling in HUVECs (Roukens et al. 2010). Fig 3F shows that short-hairpin (sh) RNA-mediated loss of JUN in HUVECs abrogated the VEGF-stimulated wave of DLL4 expression signifying that DLL4 expression is governed by JUN.

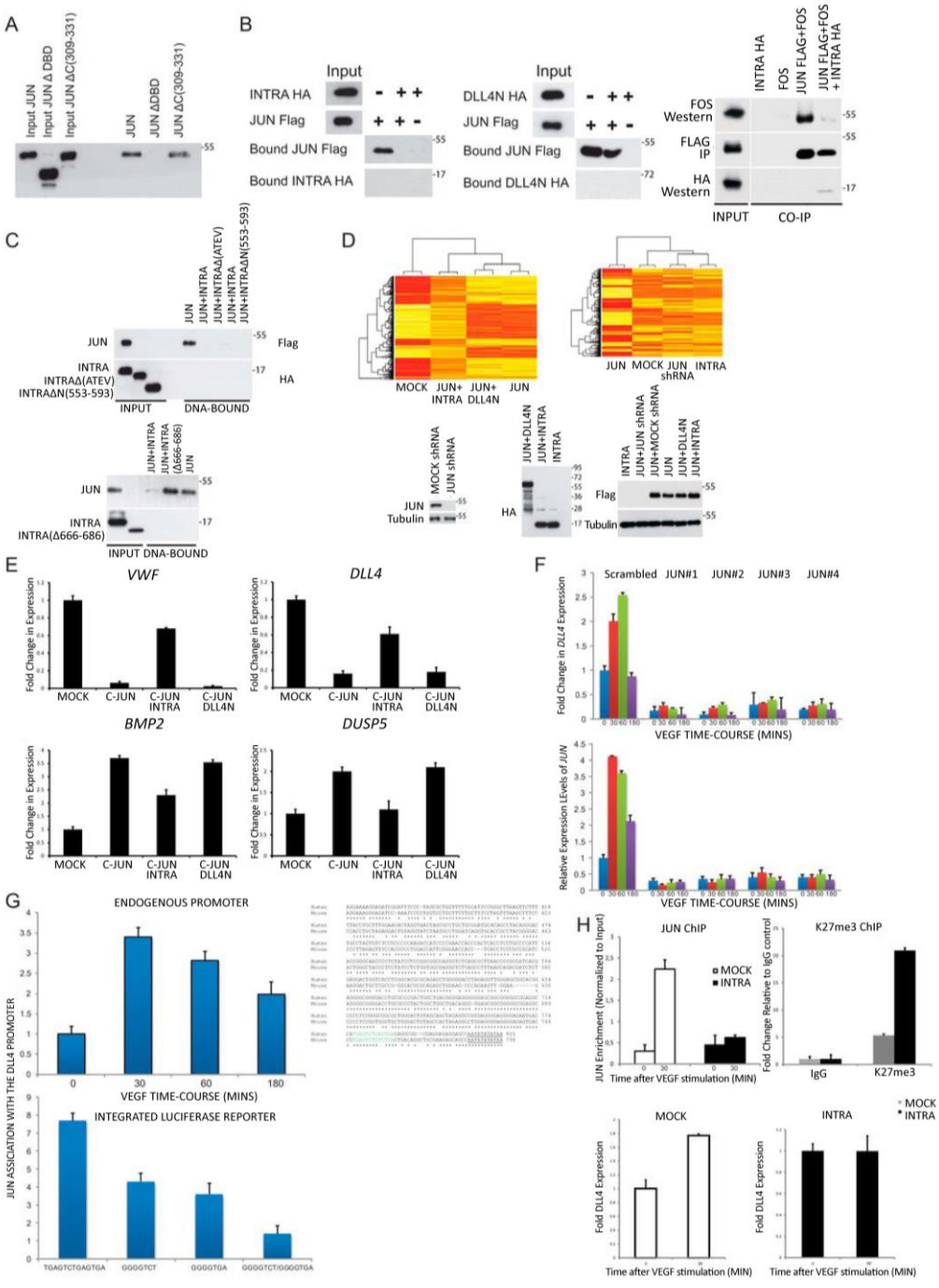
A
Input JUN
Input JUN Δ DBD
Input JUN ΔC(309-331)
JUN
JUN ΔDBD
JUN ΔC(309-331)
B
Input
INTRA HA
JUN Flag
Bound JUN Flag
Bound INTRA HA
DLL4N HA
FOS Western
FLAG IP
HA Western
INTRA HA
FOS
JUN FLAG+FOS
JUN FLAG+FOS + INTRA HA
INPUT
CO-IP
C
JUN
JUN+INTRA
JUN+INTRAΔ(ATEV)
JUN+INTRA ΔN(553-593)
INTRA
INTRAΔ(ATEV)
INTRAΔN(553-593)
Flag
HA
INPUT
DNA-BOUND
JUN+INTRA (Δ666-686)
INTRA(Δ666-686)
D
MOCK
JUN+ INTRA
JUN+ DLL4N
JUN
JUN MOCK JUN shRNA INTRA
MOCK shRNA
JUN shRNA
JUN
Tubulin
JUN+DLL4N
JUN+INTRA
INTRA
HA
INTRA
JUN+JUN shRNA
JUN+MOCK shRNA
JUN
JUN+DLL4N
JUN+INTRA
Flag
Tubulin
E
VWF
DLL4
BMP2
DUSP5
Fold Change in Expression
MOCK
C-JUN
C-JUN INTRA
C-JUN DLL4N
F
Scrambled
JUN#1
JUN#2
JUN#3
JUN#4
Fold Change in DLL4 Expression
VEGF TIME-COURSE (MINS)
Relative Expression LEvels of JUN
G
ENDOGENOUS PROMOTER
VEGF TIME-COURSE (MINS)
JUN ASSOCIATION WITH THE DLL4 PROMOTER
INTEGRATED LUCIFERASE REPORTER
TGAGTCTGAGTGA
GGGGTCT
GGGGTGA
GGGGTCTGGGGTGA
H
JUN ChIP
MOCK
INTRA
JUN Enrichment (Normalized to Input)
Time after VEGF stimulation (MIN)
K27me3 ChIP
Fold Change Relative to IgG control
IgG
K27me3
MOCK
INTRA
Fold DLL4 Expression
Time after VEGF stimulation (MIN)

< Figure 3. **DLL4INTRA antagonizes JUN DNA-binding.** (A) JUN binds to a consensus AP-1 DNA binding site *in vitro*. A biotinylated double-stranded oligonucleotide harboring three consensus AP-1 binding sites was incubated with the indicated Flag epitope tagged *in vitro* translated proteins. JUNΔDBD lacks the DNA-binding domain. JUNΔC(309-331) lacks the C-terminal amino acids abutting the DNA-binding domain. DNA-bound JUN was detected by Western blotting. (B) DLL4INTRA impedes JUN binding to DNA. As in (A), AP-1 DNA binding sites were incubated with the indicated *in vitro* translated proteins. DNA-bound JUN was detected by Western blotting. (C) The putative PDZ-binding motif of DLL4INTRA is dispensable for DLL4INTRA binding to JUN. As in (A and B), AP-1 DNA binding sites were incubated with the indicated *in vitro* translated proteins. INTRAΔ(ATEV) lacks the putative C-terminal PDZ-binding motif. INTRAΔN(553-593) lacks the highlighted N-terminal amino acids. DNA-bound JUN was detected by Western blotting. (D) DLL4INTRA alters the JUN-controlled transcriptome. A microarray analysis was performed on HUVECs stably expressing the indicated constructs. Protein levels were determined by Western blotting with the indicated antibodies (Lower panel). Heat maps show a comparison of global gene expression profiles (Upper panels). (E) Expression levels in HUVECs of the indicated transcripts were determined by real-time qPCR. All values were averaged relative to TATA binding protein (TBP), signal recognition particle receptor (SRPR) and calcium-activated neutral proteinase 1 (CAPNS1). Values were normalized against Mock treated cells. Values represent +/- the standard deviation (n = 3). (F) JUN controls DLL4 expression. Real time qPCR was performed on cDNA prepared from cells stably infected with one of four different JUN shRNA constructs and stimulated with or without VEGF for the shown time course (minutes). All values were averaged relative to TATA binding protein (TBP), signal recognition particle receptor (SRPR) and calcium-activated neutral proteinase 1 (CAPNS1). Values were normalized against the time 0 time point of Mock infected cells. Values represent +/- the standard deviation (n = 3). (G-H) JUN associates with the proximal promoter of human DLL4. (G) Upper panel: A ChIP analysis was performed on HUVECs incubated with or without 50 ng/ml VEGF for the indicated times. Three different primer sets centered on the illustrated promoter region were used and a single representative is shown (all three gave very similar results). Equivalent amounts of rabbit IgG were used as a control and results are presented as fold changes in recovery (as a fraction of input) relative to the 0 time point. Lower panel: Expression of a stably integrated luciferase reporter was placed under the control of the depicted wild type DLL4 proximal promoter or the same promoter in which the putative AP-1 sites have been singly or doubly mutated. The alignment of the human and mouse DLL4 promoter regions highlights the presumed transcription start site (underlined). Conserved consensus AP-1 DNA-binding sites are shown in green. A ChIP analysis was performed on reporter-expressing HUVECs incubated for 30 minutes with 50 ng/ml VEGF. Equivalent amounts of rabbit IgG were used as a control and results are presented as fold changes in recovery (as a fraction of input) relative to the control IgG. Two different primer sets were centered on the integrated luciferase gene. A single representative is shown (both gave comparable results). (H) Upper graphs: ChIP analyses were performed with the indicated antibodies (as described in G) on control HUVECs and HUVECs stably expressing DLL4INTRA. Lower graphs: DLL4 expression levels in control HUVECs and HUVECs stably expressing DLL4INTRA were determined by real-time qPCR. All values were averaged relative to TATA binding protein (TBP), signal recognition particle receptor (SRPR) and calcium-activated neutral proteinase 1 (CAPNS1). Values were normalized against Mock treated cells. Values represent +/- the standard deviation (n = 3). IP, immunoprecipitation; VWF, von Willebrand factor. Error bars represent S.D.

In support of this view, we found that endogenous JUN associated with the proximal promoter of DLL4 and, using an integrated luciferase reporter, loss of a consensus AP-1 site upstream of the DLL4 TATA box significantly diminished the detectable levels of promoter-bound JUN (Fig 3G). Accordantly, ectopic expression of DLLINTRA inhibited VEGF-dependent association of JUN with the

DLL4 promoter (Fig 3H, upper graph) and led to a concomitant inhibition of VEGF-stimulated DLL4 expression (Fig 3H, lower graphs). Consistent with these findings, stable expression of DLL4INTRA augmented the levels of the repressive H3K27me chromatin methylation mark found at the DLL4 proximal promoter (Fig 3H, upper graph). These data indicate that DLL4INTRA can negatively regulate JUN binding to DNA and, in consequence, control expression of genes required for endothelial sprouting.

DLL4INTRA attenuates JUN-mediated endothelial cell sprouting

To elucidate the biological consequences of DLL4INTRA binding to JUN, we used a 3D-matrigel sprouting assay. Figure 4A shows that enhanced JUN levels hugely increased endothelial sprouting (including filopodia formation), whereas loss of endogenous JUN abolished the ability of HUVECs to sprout. JUN-stimulated sprouting depended on the bZIP domain of JUN, and thus presumably relies on JUN binding to DNA, because a JUN mutant lacking this domain acted as a dominant negative resulting in strong inhibition of sprouting (Fig 4A). In this assay, wild type sprouting networks are relatively short-lived and collapse after approximately 24 hours. By contrast, endothelial cells ectopically expressing JUN were robustly sustained and continued to sprout for several weeks. Additionally, these JUN expressing cells could sprout efficiently in the absence of exogenous VEGF (ZF and DB, unpublished). In agreement with our prior findings that DLL4INTRA obstructs JUN DNA-binding (see Fig 3), Fig 4B shows co-expression of DLL4INTRA, but not DLL4N, restricted JUN-driven endothelial sprouting.
AP-1 transcription factors are characterized by the conserved bZIP domain, which mediates homo- and heterodimerization of AP-1 family members and DNA binding. This begs the question as to whether DLL4INTRA might also influence the activity of other AP-1 family members such as JUNB, which has an established role in vascular morphogenesis. Our experiments show that JUNB, like JUN, strongly stimulated endothelial tube formation (Fig. 5A), and DLL4INTRA could inhibit this process (Fig. 5B).

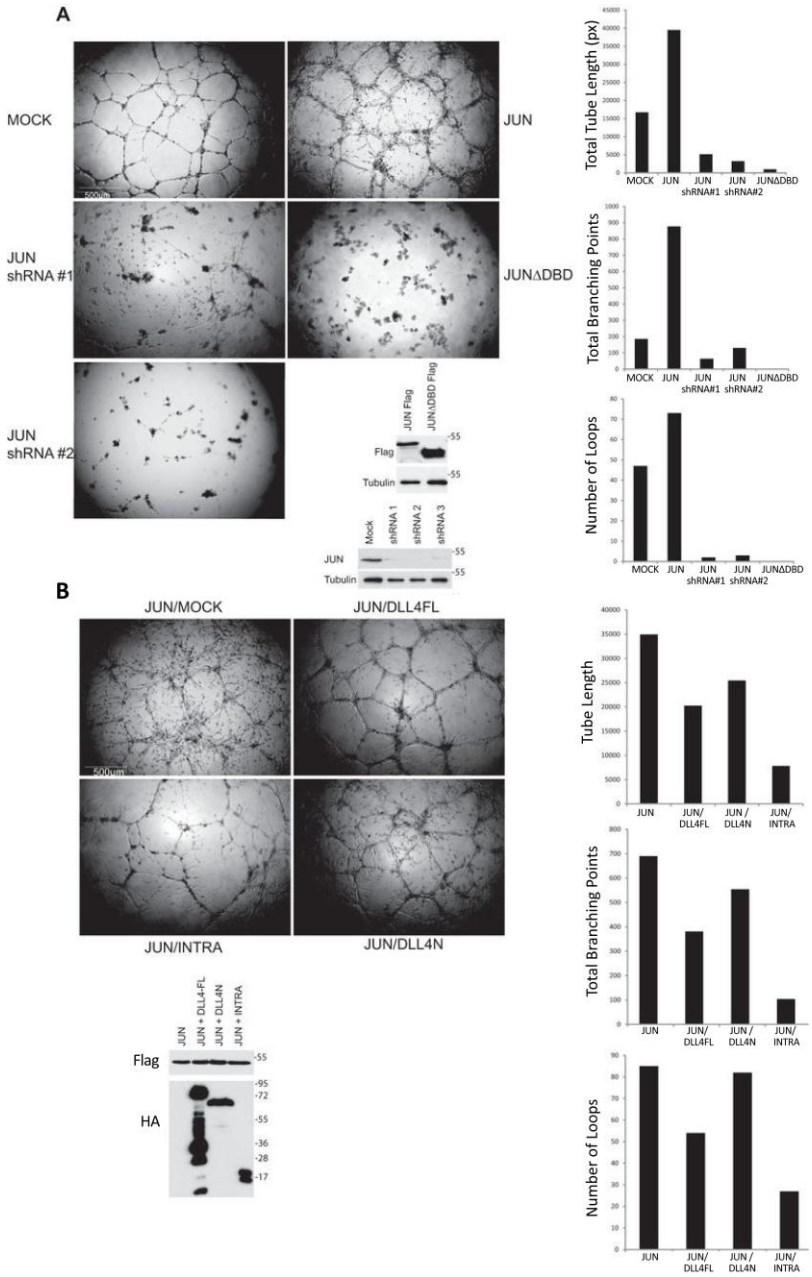

Figure 4. (A) JUN strongly stimulates endothelial cell tube formation/sprouting. HUVECs lacking endogenous JUN or ectopically expressing the indicated JUN proteins were cultured in Matrigel in the presence of 50 ng/ml VEGF. A representative of several independent experiments is shown. After 24 h, in-house computer software was used to quantify the total length of the sprouts, the number of branch points, and the number of loops. Protein levels were determined by Western blotting with the indicated antibodies. Scale bar, 500 µm. (B) DLL4INTRA attenuates JUN-mediated sprouting. HUVECs ectopically expressing the indicated proteins were cultured in Matrigel in the presence of 50 ng/ml VEGF. Experiments were conducted and quantified as in A. Scale bar,500 µm. DBD, DNA-binding domain; DLL4FL, full-length DLL4.

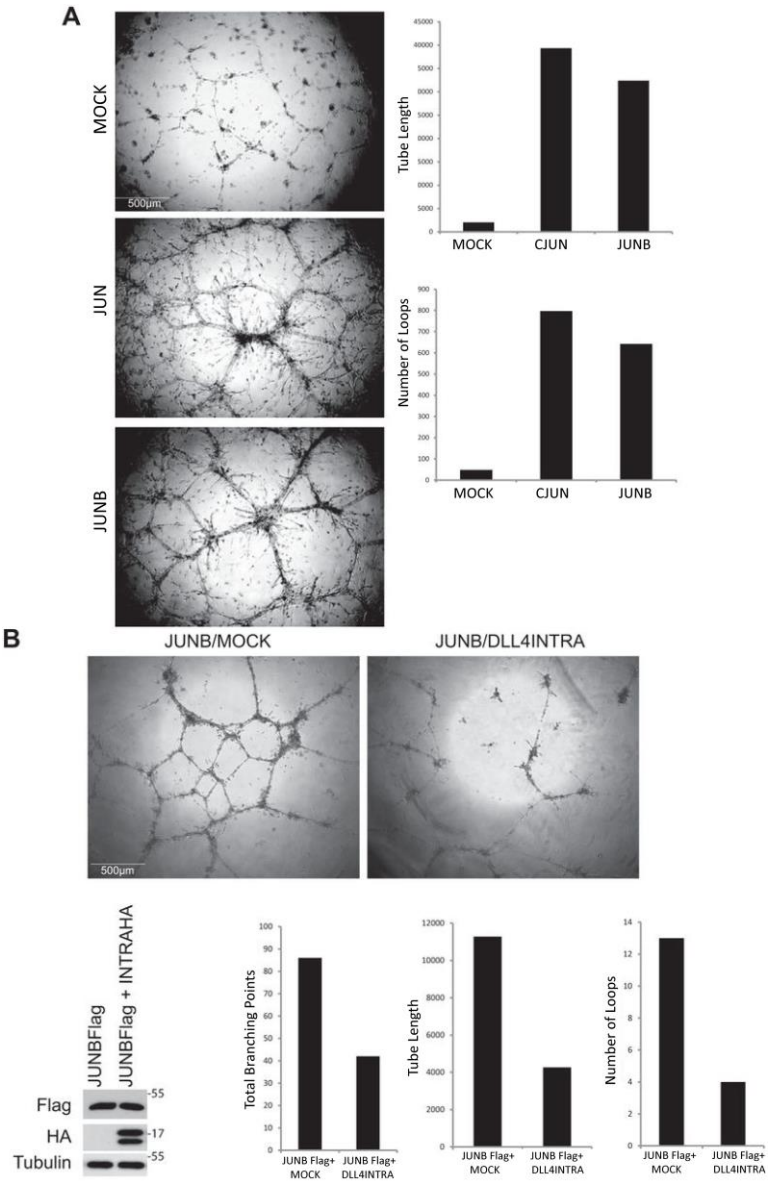

Figure 5. (A) JUNB strongly stimulates endothelial cell tube formation/sprouting. HUVECs ectopically expressing JUN or JUNB were cultured in Matrigel in the presence of 50 ng/ml VEGF. A representative of several independent experiments is shown. After 48 h, in-house computer software was used to quantify the total length of the sprouts, the number of branch points, and the number of loops. Protein levels were determined by Western blotting with the indicated antibodies. Scale bar, 500 m. B, DLL4INTRA attenuates JUNB-mediated sprouting. HUVECs ectopically expressing the indicated proteins were cultured in Matrigel in the presence of 50 ng/ml VEGF. A representative of several independent experiments is shown. After 24 h, in-house computer software was used to quantify the total length of the sprouts, the number of branch points, and the number of loops. Protein levels were determined by Western blotting with the indicated antibodies. Scale bar, 500 m.

DISCUSSION

In this study, we have presented evidence that the intracellular domain (ICD) of DLL4 (DLL4INTRA) could perform a dual function: it is essential for establishing normal DLL4 sub-cellular localization and, strikingly, the untethered ICD interacted with and inhibited the activity of the JUN transcription factor. By means of chemical inhibitors and targeted mutagenesis we demonstrated that one mechanism of ICD cleavage is caspase-dependent (see Fig 1). The pattern of cellular DLL4 protein species indicates that multiple DLL4 cleavage events could occur but their precise nature are yet to be delineated. What triggers the cleavage event(s), or if proteolysis is constitutive, is also currently unclear and will be important to establish. Certainly, DLL4INTRA is highly conserved and harbors a number of motifs that might control its function (see Introduction) and which could influence its fate. We found that endogenous DLL4INTRA accumulated following incubation of cells with VEGF (Supplementary Fig 2). Future work will determine if this simply reflects increased levels of DLL4 and/or specific signaling events. Related to this, unravelling the mechanism(s) of DLL4INTRA turnover could shed further light on its function. It has been noted that the DLL4 ICD contains an intrinsically disordered region (IDR) terminating in a structured C-terminal PDZ-binding domain (De Biasio et al. 2008). This conformation resembles the proto-oncogene FOS (Campbell et al. 2000; Gomard wt al. 2008; van Ijzendoorn et al) and other signaling proteins and transcription factors (Erales and Coffino 2014). We recently found that the C-terminus of FOS is composed of a comparable IDR/structured extreme C-terminus which controls intrinsic, rapid proteasomal degradation of FOS and a similar mechanism might control the activity of DLL4INTRA (van Ijzendoorn et al.). Indeed, we found that DLL4INTRA protein levels are strongly stabilized when the proteasome is blocked by MG132 indicating that DLL4INTRA is rapidly turned over (ZF and DAB, unpublished).

JUN is a member of the AP-1 family of transcription factors which plays a pivotal role in cell growth, differentiation and survival as well as the DNA damage response (Shaulian and Karin 2001; Shaulian and Karin 2002). These transcription factors are characterized by a conserved bZIP domain which begs the question as to whether DLL4INTRA might also influence the activity of other AP-1 family members such as JUNB which has an established role in vascular morphogenesis (Licht et al. 2006; Kanno et al. 2012; Schorpp-Kistner et al. 1999). Our experiments show that JUNB, like JUN, strongly stimulated endothelial cell sprouting (Supplementary Fig 3A) and DLL4INTRA could inhibit JUNB-driven endothelial cell sprouting (Supplementary Fig 3B). A related question is whether other Notch ligand ICDs can function similarly to DLL4INTRA. The DLL1 ligand shares a high degree of amino acid identity with DLL4 including approximately 40% of the ICD (see Supplementary Fig 4). Our results suggest that DLL1INTRA,

like DLL4INTRA, can bind to the bZIP domain of JUN (Supplementary Fig 4A) and block JUN binding to a consensus AP-1 DNA site (Supplementary Fig 4B). Interestingly, unlike DLL4INTRA, DLL1INTRA could also interact with the bZIP domain of CREB3 *in vitro* (see Supplementary Fig 4A) raising the possibility that they have specific as well as overlapping activities. At the cellular level, DLL1INTRA, in common with DLL4INTRA, inhibited JUN-driven endothelial cell sprouting (Supplementary Fig 4C). Collectively, these results highlight a potential link between untethered Notch ligand ICDs and the immediate-early gene, AP-1 transcription factor complex. Genome-wide screens have established the importance of ETS and AP-1 transcription factor cooperation by their associating to neighbouring AP-1 and ETS DNA-binding sites (Plotnik et al. 2014). Since ETS transcription factors are essential for angiogenesis (Roukens et al. 2010; Craig and Sumanas 2016; Randi et al. 2009) and have been reported to control DLL4 expression (Roukens et al. 2010; Shah et al. 2017) it is noteworthy that JUN potently stimulates endothelial sprouting and is required for normal expression of DLL4 (see Fig 3). JUN/DLL4INTRA interactions, therefore, could form part of a feedback loop whereby VEGF-dependent changes in DLL4 expression (as well as other angiogenesis-regulating genes) depend on ETS/AP-1 factors and are regulated by DLL ICDs.

In summary, our data lend support to the idea that biologically active Notch ligand ICDs could help establish appropriate endothelial cell responses through crosstalk with AP-1-dependent signal transduction pathways. They further highlight the possibility that corruption of this mechanism might play a role in disease processes such as tumor angiogenesis and developmental disorders. This is important because the Notch pathway has emerged as primary target for the design of novel therapeutic interventions in cancer (Andersson and Lendahl 2014). Also, it has recently been reported that heterozygous loss-of-function DLL4 mutations are a potential cause of Adams-Oliver syndrome, a rare congenital disorder characterized by multiple defects including vascular and cardiac anomalies (Meester et al. 2015). Two of the identified DLL4 mutations are nonsense mutations that would be predicted to lead to complete loss of the DLL4 ICD.

EXPREMENTAL PROCEDURE

Yeast Two-hybrid Screens

Screens were performed according to the manufacturer's protocol (Dualsystems Biotech). Bait and prey were rescued from yeast colonies and genuine interactions were confirmed through re-transfection of yeast. Protein-protein interactions were tested quantitatively using a LacZ reporter assay (Dualsystems Biotech).

Proximity Ligation Assay

Proximity Ligation Assay was performed using a Duolink in situ PLA kit (Sigma) according to the manufacturer's protocol. For each condition, an average of 100 cells were scored. Error bars show the standard error of the mean. Statistical analysis of fluorescent signal was performed by using Blobfinder (http://www.cb.uu.se/~amin/BlobFinder/).

Mass Spectrometry

Endogenous DLL4 or HA epitope tagged DLL4 were immunopurified from duplicate lysates each prepared by lysing HUVECS (20 x 15 cm and 10 x 15 cm dishes respectively) in ice-cold lysis buffer (50 mM Tris, pH 7.5, 1% NP40, 0.1% SDS, 0.5% Na-deoxycholate, 150 mM NaCl). Protein bands were excised from SDS-PAGE gels and subjected to in-gel trypsin digestion.

Cell culture, biochemistry and molecular biology

Primary HUVECs (Lonza) were cultured in EGM2 medium (Lonza). Human embryonic kidney 293T cells were cultured in DMEM (Gibco) supplemented with 10% fetal bovine serum (Gibco). 293T cells were typed using short tandem repeat analysis of the DNA and all cell lines were checked for mycoplasma with the MycoAlert kit (Lonza). Transfections, lentivirus production and cell infections, Western blotting and co-immunoprecipitations have been described previously (Roukens et al. 2008). All lysis buffers contained a cocktail of protease inhibitors (phenylmethylsulfonyl fluoride, trypsin inhibitor, pepstatin A, leupeptin, aprotinin).

Recombinant protein production/ *in vitro* protein:protein interaction

Domains for recombinant protein production were cloned into the pET 28a vector in-frame to an N-terminal 6x HIS epitope. His epitope–tagged proteins were manufactured in Escherichia coli BL21(DE3). Following sonication (Misonix Sonicator 3000) in 3 mls ice-cold buffer / 50 ml bacterial culture (150 mM NaCl, 2.7 mM KCl, Na2HPO4, KH2PO4, 20 mM imidazole, 10 mM □-mercaptoethanol), proteins were purified onto 50 ul of Nickel- agarose beads (Qiagen) by 3 hours rolling at 4C. Beads were washed in 10 x 1 ml of the same buffer. Protein yields were determined by Bradford assay (Bio-Rad) and relative protein integrity and purity was determined by SDS-PAGE and Colloidal Blue staining (Invitrogen). 5-10 µl of HIS beads (purified recombinant protein) in 1 ml of buffer were incubated for 2 hours at 4oC with *in vitro* translated DLL4 proteins made using the TNT-coupled reticulocyte *in vitro* translation system (Promega). Beads were washed x10 with 1 ml of buffer. Proteins were separated by SDS-PAGE and associated proteins were detected by Western blot.

Plasmid and shRNA construction

Unless otherwise stated, all cDNAs were fused in-frame with a Flag or an HA epitope tag and were cloned into the pLV lentiviral vector and pCS2 expression plasmid. The luciferase reporter was constructed by cloning 1 kb of the DLL4 proximal promoter downstream of the luciferase gene in the pLV lentiviral vector. All mutants were engineered by site-directed mutagenesis using Phusion High-Fidelity DNA polymerase (Thermofisher). All constructs were verified by Sanger sequencing (Macrogen). The following Mission shRNA library clones (Sigma) were used:

shRNA TRCN0000010366 JUN
shRNA TRCN0000039589 JUN
shRNA TRCN0000009845 JUN
shRNA TRCN0000039588 JUN
shRNA TRCN0000039590 JUN
shRNA TRCN0000039591 JUN
shRNA TRCN0000039592 JUN
shRNA TRCN0000033414 DLL4
shRNA TRCN0000033415 DLL4
shRNA TRCN0000033416 DLL4
shRNA TRCN0000033417 DLL4
shRNA TRCN0000033418 DLL4

The following siRNA duplexes (Thermo Scientific) were used (sense strands are shown):

DLL4 siRNA 1: GCUCCACUGCGAGAAGAAU
DLL4 siRNA 2: GCAUGGUGGCAGUGGCUGUUU
JUN siRNA 1: GGAUCAAGGCGGAGAGGAAUU
Scrambled: ON-TARGET plus Non-targeting siRNA (D-001810-01-05)

HUVECs cells were transfected with duplexes using DharmaFECT transfection reagent according to the manufacturer's recommendations (Thermo Scientific). Transfected cells were incubated for 72-hours prior to PLA assays. Efficient delivery of siRNA and subsequent silencing were tested by immunostaining and Western blotting.

Transcriptome Profiling
Total RNA was isolated using Trizol (Invitrogen) and further purified using RNeasy Minikit (Qiagen). Total RNA was labeled using Illumina RNA Amplification kit (Ambion). Duplicate samples from two independent experiments were tested. Gene profiles were determined by hybridization to Sentrix HumanHT-12 Expression Beadchips (ServiceXS). Microarray data has been posted on GEO database.

Analysis of mRNA expression
RNA isolation, first strand cDNA synthesis and analysis of expression of transcripts by quantitative PCR were performed as previously described 35. The following primer sets were used (5' to 3' orientation):
DLL4FOR ccctggcaatgtacttgtgat
DLL4REV tggtgggtgcagtagttgag
JUNFOR cgcctgataatccagtcca
JUNREV ttcttggggcacaggaact
DUSP5FOR caaatggatccctgtggaa
DUSP5REV ccctttccctgacacagtc
VWFFOR gtgcagacccaacttcacct
VWFREV gggtggggacactcttttg
BMP2FOR cagaccaccggttggaga
BMP2REV ccactcgtttctggtagttcttc

All qPCR values were averaged relative to the control gene, TATA binding protein (TBP), signal recognition particle receptor (SRPR) and calcium-activated neutral proteinase 1 (CAPNS1). For each data point, PCRs were performed in triplicate and error bars show standard deviations from the mean.

HUVEC sprouting assay
96-well plates were coated with 60 µl of Matrigel/well 30 minutes prior to seeding HUVECs. EGM-2 medium was supplemented with 50 ng/ml recombinant human VEGF 165 (R and D Systems). Images were taken at multiple timepoints. Analysis of the sprouting was performed with Stacks (In-house software: LUMC, MCB).

Immunofluorescence
Immunostaining was performed as previously described (Roukens et al. 2008) using Alexa Fluor 488 goat anti-mouse secondary antibodies (Thermo Fisher scientific). Imaging was performed with a Leica SP8 confocal microscope.

Protein-DNA interaction assays

In vitro translated protein was made using the TNT-coupled reticulocyte *in vitro* translation system (Promega). 50 pmol biotinylated double-stranded oligonucleotides harbouring three contiguous AP-1 DNA-binding sites were coupled to MyOne Streptavidin C1 beads (Invitrogen). Reactions were incubated at 4°C with vigorous shaking for 30 minutes in the presence of 1 µg poly (dI/dC), 4 mM Spermidine, 50 mM KCl, 10 mM HEPES (pH 7.6), 5 mM MgCl2, 10 mM Tris pH 8, 0.05 mM EDTA (pH 8), 0.05 mM, 0.1% Triton X-100 and 20% glycerol. Beads were successively washed three times with the aforementioned buffer. Associated proteins were eluted in Laemmli buffer and protein-DNA interactions were determined by Western blotting.

ChIP

Confluent 10 cm tissue culture dishes of HUVECs were cross-linked for 10 minutes with formaldehyde (final concentration = 1%). Glycine was added to a final concentration of 0.125 M and incubated for 5 minutes. Cells were washed 2x with PBS and subsequently lysed in ChIP Lysis Buffer (1%SDS,10 mM EDTA, 50mM Tris-HCL pH 8.1) supplemented with protease inhibitors. Chromatin was sheared by sonication (Bioruptor UCD-200 ultrasound sonicator: Diagenode), resulting in DNA fragments between 500 and 1000 bp in size. After centrifugation, 10% of the sample was kept as Input. Chromatin was diluted 10x in dilution buffer (1%Triton X-100, 2mM EDTA pH 8.0, 150 mM NaCl, 20 mM Tris-HCl pH 8.1 supplemented with protease inhibitors). For immunoprecipitation, 2 µg of test or control antibody was added to the diluted chromatin and incubated overnight at 4°C. Blocked protein A-Sepharose beads (10µg of sonicated herring sperm DNA) were added for 2 hrs. Beads were extensively washed (0.1 % SDS, 0.1% NaDOC, 1% TritonX-100, 0.15 M NaCl, 1mM EDTA, 0.5 mM EGTA, 20 mM HEPES) and complexes were eluted with elution buffer (1% SDS, 0.1 M NaH2CO3, 0.2 M NaCl) at 65oC overnight to reverse crosslinking. Associated DNA was purified by phenol/chloroform extraction and ethanol precipitation (in the presence of 15 µg/ml glycogen (Roche)). Realtime qPCR was used to determine recovery of specific DNA fragments. The following primers were used (5' to 3' orientation):

DLL4promFOR A ttctttttacctgctttggaaca
DLL4promREV A agtccctgtaggctgtgcat
DLL4promFOR B aatgaccatgagtctgagtgaca
DLL4promREV B cgccgctactgaaacctg
DLL4promFOR C gggtgggcactcataggtt
DLL4promREV C aaaccagcgctagggaaatc
DLL4promFOR D tcaggagagttcctccttgc
DLL4promREV D tgagtccagcttcagttcctg
DLL4promFOR E acgctcccaacctcttgtt

DLL4promREV E ccgagcatggtctgattttt
DLL4promFRO F tcatgaatgtcttttgatgctga
DLL4promREV F tcccagagatctagaaaggctct
DLL4promFOR G gaacacgaggccaagagc
DLL4promREV G cgcgtcttctgtctaatcctg
LuciferaseFOR 1 catgaccgagaaggagatcg
LuciferaseREV 1 cagcttcttggcggttgta
LuciferaseFOR 2 tgagtacttcgaaatgtccgttc
LuciferaseREV 2 gtattcagcccatatcgtttcat

Antibodies and drugs

Antibodies were obtained from the following sources: custom-made rabbit and goat polyclonals were generated by Eurogentec; Flag mouse M2 monoclonal (Sigma-Aldrich); anti-HA.11 mouse monoclonal (Covance); anti- Ha rabbit polyclonal (Abcam); anti-JUN rabbit (Cell Signaling Technology); anti-JUN mouse (Santa Cruz); anti-Flag rabbit (Sigma); anti-γTubulin (Sigma); H3K27me3 (Bethyl Laboratories). Z-VAD was purchased from Sigma.

ACKNOWLEDGMENTS

We thank members of the Departments of Molecular Cell Biology for helpful discussions, technical advice and support in particular Professor Peter ten Dijke. We are very grateful to Dr. Jan Oosting for the analyses of the microarray data and Annelies van der Laan for help with the confocal microscopy. We are indebted to Dr. Hans Vrolijk for designing computer software for quantifying sprouting assays. This work was supported by the Dutch Cancer Society to DAB (30861).

AUTHOR CONTRIBUTIONS

ZF and FR performed the majority of experiments assisted by DAB. AL and JVO performed mass spectrometry analyses. DAB supervised the study and wrote the paper. All authors read and approved the paper.

REFERENCES

1. Adams, R.H and Alitalo, K. (2007). Molecular regulation of angiogenesis and lymphangiogenesis. Nar Rev Mol Cell Biol 8(6), 464-78.

2. Andersson, AR and Lendahl, U. (2014). Therapeutic modulation of Notch signaling- are we there yet? Nature Rev. Drug Discovery 13, 357-378.

3. Ascano, JM; Beverly, LJ and Capobianco, AJ. (2002). The C-terminal PDZ-ligand of JAGGED1 is essential for cellular transformation. J Biol Chem. 278(10), 8771-9.

4. Aster, JC; Pear, WS and Blacklow SC. (2017). The varied roles of Notch in cancer. Annu. Rev. Pathol. Mech. Dis. 12, 245-75.

5. Ayllón, V; Bueno, C; Ramos-Mejía, V; Navarro-Montero, O; Prieto, C; Real, PJ; Romero, T; García-León, MJ; Toribio, ML; Bigas, A; and Menendez, P. (2015). The Notch ligand DLL4 specifically marks human hematoendothelial progenitors and regulates their hematopoietic fate. Leukemia 29, 1741-1753.

6. Balasubramanian, S; Fam, SR and Hall, RA. (2007). GABAB Receptor Association with the PDZ Scaffold Mupp1 Alters Receptor Stability and Function. J Biol Chem 282(6), 4162-4171.

7. Borggrefe, T; Lauth, M, Zwijsen, A; Huylebroeck, D; Oswald, F and Giaimo, BD. (2016). The Notch intracellular domain integrates signals from Wnt, Hedgehog, TGF/BMP and hypoxia pathways. BBA- Molecular Cell Research 1863 (2), 303-313.

8. Braune, EB and Lendahl, U. (2016) Notch- a Goldilocks signaling pathway in disease and cancer therapy. Discov Med 21(115), 189-196.

9. Bray, SJ. (2016) Notch Signaling in context. Nature Rev. Mol. Cell Biol. 17, 722-735.

10. Bray, SJ. (2006). Notch signaling: a simple pathway becomes complex. Nature Rev. Mol. Cell Biol. 7, 678-689.

11. Campbell, K.M; Terrell, A.R; Laybourn, P.J and Lumb K.J. (2000). Intrinsic structural disorder of the C-terminal activation domain from the bZIP transcription factor Fos. Biochemistry 39, 2708-2713.

12. Carmeliet, P and Jain, RK. (2011). Molecular mechanisms and clinical applications of angiogenesis. Nature 473, 298-307.

13. Chitnis, A; Henrique D; Lewis, J, Ish-Horowicz, D and Kintner, C. (1995). Primary neurogenesis in Xenopus embryos regulated by a homologue of the Drosophila neurogenic gene Delta. Nature 376, 761-766.

14. Chung, AS and Ferrara, N. (2011). Developmental and pathological angiogenesis. Annu. Rev. Cell Dev. Biol. 27, 563-584.

15. Clevers, H. (2013). The intestinal crypt, a prototype stem cell compartment. Cell 154(2), 274-284.

16. Craig, MP and Sumanas, S. (2016). ETS transcription factors in embryonic vascular development. Angiogenesis 19(3), 275-285.

17. De Biasio, A; Guarnaccia, C; Popovic, M; Uversky, AP and Pongor, S. (2008). Prevalence of intrinsic disorder in the intracellular region of human single-pass type I proteins: The case of the Notch ligand Delta-4. J. Proteome Research 7, 2496-2505.

18. Dejana, E. (2004). Endothelial cell-cell junctions: Happy together. Nature Reviews Molecular Cell Biology 5, 261-270.

19. Del Alamo, D; Rouault, H and Schweisguth, F. (2011). Mechanisms and significance of cis-inhibition in Notch signaling. Current Biology 21, R40-R47.

20. Doroquez, DB and Rebay, I. (2006). Signal integration during development: Mechanisms of EGFR and Notch pathway function and cross-talk. Crit. Rev. Biochem. and Mol. Biol. 41(6), 339-385.

21. Duryagina, R; Thieme, S; Anastassiadis, K; Werner, C; Schneider, S; Wobus, M; Brenner, S and Bornhauser, M. (2013). Overexpression of Jagged-1 and its intracellular domain in human mesenchymal stromal cells differentially affect the interaction with hematopoietic stem and progenitor cells. Stem Cells and Development 22 (20), 2736-2750.

22. Dyczynska, E; Sun, D; Yi, H; Sehara-Fujisawa, A; Blobel, CP and Zolkiewska, A. (2007).

Proteolytic processing of Delta-like 1 by ADAM proteases. The Journal of Biological Chemistry 282 (1), 436-444.

23. Erales, J and Coffino, P. (2014). Ubiquitin-independent proteosomal degradation. Biochem. Biophys. Acta 1843, 216-221.

24. Geudens, I and Gerhardt, H. (2011). Coordinating cell behavior during blood vessel formation. Development 138, 4569-4583.

25. Gomard, T; Jariel-Encontre, I; Basbous, J; Bossis, G; Moquet-Torcy, G and Piechaczyk, M. (2008). Fos family protein degradation by the proteasome. Biochemical Society Transactions 36, 858-863.

26. Guruharsha, KG; Kankel, MW and Artavanis-Tsakonas, S. (2012). The Notch signaling system: recent insights into the complexity of a conserved pathway. Nature Reviews Genetics 13, 654-666.

27. Gustafsson, MV; Zheng, X; Pereira, T; Gradin, K; Jin, S; Lundkvist, J; Ruas, JL; Poelinger, L; Lendahl, U and Bondesson, M. (2005). Hypoxia requires notch signaling to maintain the undifferentiated cell state. Dev. Cell 9(5), 617-628.

28. Herbert, SP and Stainier, DYR. (2011). Molecular control of endothelial cell behavior during blood vessel morphogenesis. Nature Reviews Molecular Cell Biology 12, 551-564.

29. Heuss, SF; Ndiaye-Lobry, D; Six, EM; Israel, A and Logeat, F. (2008). The intracellular region of Notch ligands Dll1 and Dll3 regulates their trafficking and signaling activity. PNAS 105, 11212-11217.

30. Hiratochi, M; Nagase, H; Kuramochi, Y; Koh, C-S; Ohkawara, T and Nakayama, K. (2007). The Delta intracellular domain mediates TGF-?/Activin signaling through binding to Smads and has an important bi-directional function in the Notch-Delta signaling pathway. Nucleic Acids Research 35 (3), 912-922.

31. Ikeuchi, T and Sisodia, SS. (2003). The Notch ligands, Delta1 and Jagged2, are substrates for presenelin-dependent γ-secretase cleavage. The Journal of Biological Chemistry 278 (10), 7751-7754.

32. Jin, G; Zhang, F; Chan, KM; Wong, HLX; Liu, B; Cheah, SE; Liu, X; Mauch, C, Liu, D and Zhou, Z. (2011). MT1-MMP cleaves Dll1 to negatively regulate Notch signaling to maintain normal B-cell development. EMBO J 30, 2281-2293.

33. Josten, F; Fuss, B; Felix, M; Meissner, T and Hoch, M. (2004). Cooperation of JAK/STAT and Notch signaling in the Drosophila foregut. Dev. Biol. 267(1), 181-189.

34. Jung, J; Mo, J-S; Kim, M-Y; Ann, E-J; Yoon, J-H and Park, H-S. (2011). Regulation of Notch1 signaling by Delta-like ligand 1 intracellular domain through physical interaction. Mol. Cells 32, 161-1665.

35. Kanno, T; Kamba, T; Yamasaki, T; Shibasaki, N; Saito, R; Terada, N; Toda, Y; Mikami, Y; Inoue, T; Kanematsu, A; Nishiyama, H; Ogawa, O and Nakamura, E. (2012). JunB promotes cell invasion and angiogenesis in VHL-defective renal cell carcinoma. Oncogene 31(25), 3098-110.

36. Kim, M-Y; Jung, J; Mo, J-S; Ann, E-J; Ahn, J-H; Yoon, J-H and Park, H-S. (2011). The intracellular domain of Jagged-1 interacts with Notch1 intracellular domain and promotes its degradation through Fbw7 E3 ligase. Experimental Cell Research 317, 2438-2446.

37. Kitagawa, M. (2016). Notch signaling in the nucleus: roles of Mastermind-like (MAML) transcriptional coactivators. J. Biochem. 159 (3), 287-294.

38. Kolev, V; Kacer, D; Trifonova, R; Small, D; Duarte, M; Soldi, R; Graziani, I; Sideleva, O; Larman, B; Maciag, T and Prudovsky, I. (2005). The intracellular domain of Notch ligand Delta1 induces cell growth arrest. FEBS Letters 579, 5798-5802.

39. Kopan, R and Ilagan, MXG. (2009). The canonical Notch signaling pathway: unfolding the activation. Cell 137(2), 216-233.

40. Kuhnert, F; Kirshner, JR and Thurston, G. (2011). Dll4-Notch signaling as a therapeutic target in tumor angiogenesis. Vascular Cell 3, 20.

41. LaVoie, MJ and Selkoe, DJ. (2003). The Notch ligands, Jagged and Delta, are sequentially processed by γ-secretase and presenelin/γ-secretase and release signaling fragments. Journal of

biological Chemistry 278 (36), 34427-34437.

42. Le Borgne, R; Bardin, A and Schweisguth, F. (2005). The roles of receptor and ligand endocytosis in regulating Notch signaling. Development 132(8), 1751-62.

43. Lee, H-J and Zheng, JJ. (2010). PDZ domains and their binding partners: structure, specificity and modification. Cell Comm. and Signaling 8, 8.

44. Licht, AH; Pein, OT; Florin, L; Hartenstein, B; Reuter, H; Arnold, B; Lichter, P; Angel, P and Schorpp-Kistner M. (2006). JunB is required for endothelial cell morphogenesis by regulating core-binding factor beta. J Cell Biol. 175(6), 981-91.

45. Liebler, SS; Feldner, A; Adam, MG; Korff, T, Augustin, HG and Fischer, A. (2012). No evidence for a functional role of bi-directional Notch signaling during angiogenesis. PLOS One 7 (12), e53074.

46. Luca, VC; Jude, KM; Pierce, NW; Nachury, MV; Fischer, S and Garcia, KC. (2015). Structural basis for Notch1 engagement of Delta-like 4. Science 347 (6224), 847-853.

47. Meester, JAN; Southgate, L; Stittrich, A-B; Venselaar, H; Beekmans, SJ; den Hollander, N; Bijlsma, EK; Helderman-van den Enden, A; Verheij, JB; Glusman, G; et al. (2015). Heterozygous loss-of-function nutations in DLL4 cause Adams-Oliver Syndrome. The American Journal of Human Genetics 97, 475-482.

48. Metrich, M; Pomey, AB; Berthonneche, C; Sarre, A; Nemir, M and Pedrazzini, T. (2015). Jagged1 intracellular domain-mediated inhibition of Notch1 siganalling regulates cardiac homeostasis in the postnatal heart. Cardiovascular Research 108: 74-86.

49. Nichols, JT; Miyamoto, A and Weinmaster G. (2007). Notch signaling--constantly on the move. Traffic 8(8), 959-69.

50. Palmer, WH and Deng, W-M. (2015). Ligand independent mechanisms of Notch activity. Trends in Cell Biology 25 (11), 697-707.

51. Pintar, A; DeBiasio, A; Popovic, M; Ivanova, N and Pongor, S. (2007). The intracellular region of Notch ligands: does the tail make the difference? Biology Direct 2, 19.

52. Plotnik, JP; Budka, JA; Ferris, MW and Hollenhorst, PC. (2014). ETS1 is a genome-wide effector of RAS/ERK signaling in epithelial cells. Nucleic Acid Res 42(19), 11928-11940.

53. Randi, AM; Sperone, A; Drydon, NH and Birdsey, GM. (2009). Regulation of angiogenesis by ETS transcription factors. Biochem Soc Trans 37, 1248-53.

54. Ranganathan, P; Weaver, KL and Capobianco, AJ. (2011). Notch signaling in solid tumours: a little bit of everything but not all the time. Nature Rev. Cancer 11, 338-351.

55. Roukens MG, Alloul-Ramdhani M, Baan B, kobayashi K, Peterson-Maduro J, van Dam H, Sculte-Merker S, Baker DA. (2010). Control of Endothelial Sprouting by a Tel:CtBP Complex. Nature Cell Biology 12(10), 933-942.

56. Roukens, M..G; Alloul-Ramdhani, M; Moghadasi, S; Op den Brouw, M and Baker, D.A. (2008). Downregulation of vertebrate Tel (ETV6) and Drosophila Yan is facilitated by an evolutionarily conserved mechanism of F-box-mediated ubiquitination. Mol. Cell Biol. 28, 4394–4406.

57. Roukens, M. G; Alloul-Ramdhani, M; Vertegaal, A.C; Anvarian, Z; Balog, C.I; Deelder, A.M; Hensbergen, P.J and Baker, D.A. (2008). Identification of a new site of sumoylation on Tel (ETV6) uncovers a PIAS-dependent mode of regulating Tel function. Mol. Cell Biol. 28, 2342–2357.

58. Sainson, RCA and Harris, AL. (2007). Anti-Dll4 therapy: can we block tumour growth by increasing angiogenesis. Trends in Molecular Medicine 13(9), 389-395.

59. Schorpp-Kistner, M; Wang, ZQ; Angel, P and Wagner, EF. (1999). JunB is essential for mammalian placentation. EMBO J. 18(4), 934-48.

60. Shah, AV; Birdsey, GM; Peghaire, C; Pitulescu, ME; Dufton, NP; Yang, Y; Weinberg, I; Osuna Almagro, L; Payne, L; Mason, JC; Gerhardt, H; Adams, RH and Randi, AM. (2017). The endothelial transcription factor ERG mediates Angiopoietin-1-dependent control of Notch signaling and vascular stability. Nat. Commun 8, 16002.

61. Sharghi-Namini, S; Tan, E; Sharon Ong, L-L; Ge, R and Asada, HH. (2014). DLL4-containing exosomes induce capillary sprout retraction in a 3D microenvironment. Science Reports 4, 4031.

62. Shaulian, E and Karin, M. (2001). AP-1 in cell proliferation and survival. Oncogene 20, 2390–

2400.

63. Shaulian, E and Karin, M. (2002). AP-1 as a regulator of cell life and death. Nature Cell Biology 4, 131-136.

64. Sheldon, H; Helkamp, E; Turley, H; Dragovic, R; Thomas, P; Oon, CE; Leek, R; Edelmann, M; Kessler, B; Sainson, RCA; Sargent, I; Li, J-L and Harris, AL. (2010). New mechanism of Notch signaling to endothelium at a distance by Delta-like 4 incorporation into exosomes. Blood 116 (13), 2385-2394.

65. Six, E; Ndiaye-Lobry, D; Laabi, Y; Brou, C; Gupta-Rossi, N; Israel, A and Logeat, F. (2003). The Notch ligand Delta1 is sequentially cleaved by an ADAM protease and γ-secretase. PNAS 100 (13), 7638-7643.

66. Six, EM; Ndiaye, D; Sauer, G; Laâbi, Y; Athman, R; Cumano, A; Brou, C; Israël, A and Logeat F. (2004). The notch ligand Delta1 recruits Dlg1 at cell-cell contacts and regulates cell migration. J Biol Chem. 279(53), 55818-26.

67. Sun, X and Artavanis-Tsakonas, S. (1996). The intracellular deletions of DELTA and SERRATE define dominant negative forms of the Drosophila Notch ligands. Development 122, 2465-2474.

68. Timmer, JC and Salvesen, GS. (2007). Caspase substrates. Cell Death and Differentiation 14, 66-72.

69. Ulla-Maj, F and Martinez Arias, A. (2007). Cell and molecular biology of Notch. Journal of Endocrinology 194, 459-474.

70.van Ijzendoorn, DGP; Forghany, Z; Liebelt, F; Vertegaal, AC; Jochemsen, AG; Bovée, JVMG; Szuhai, K and Baker, DA. Functional Analyses of Vascular

SUPPLEMENTARY FIGURES

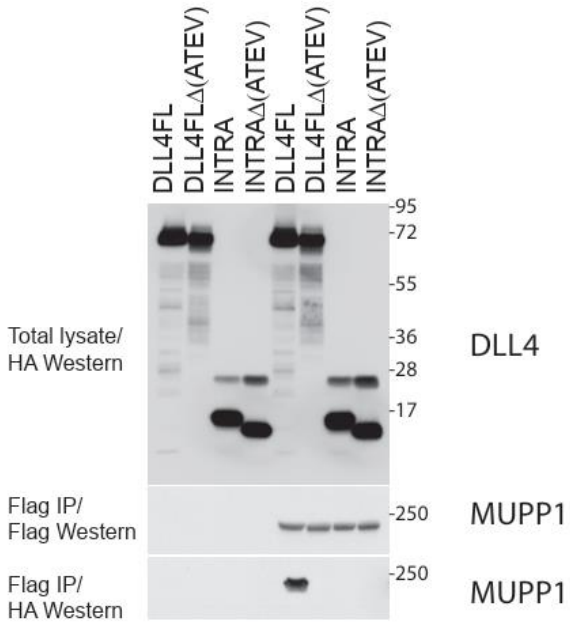

Supplementary Figure 1. MUPP1 interacts with the C-terminal PDZ-binding domain of DLL4. The indicated constructs were transfected into 293T cells. Flag epitope tagged MUPP1 was immunopurified from cell lysates using a Flag monoclonal antibody. Associated DLL4 proteins were visualized by Western blotting using an HA rabbit polyclonal antibody.

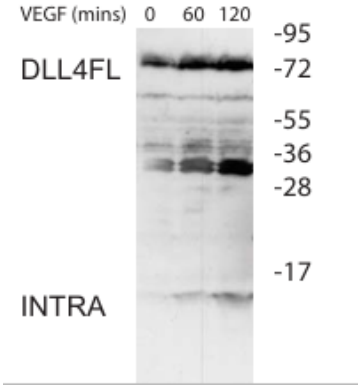

Supplementary Fig 2. HUVECs were treated with 50 ng/ml VEGF for the shown time periods. Endogenous DLL4 was immunopurified from the cells and visualized by Western blotting.

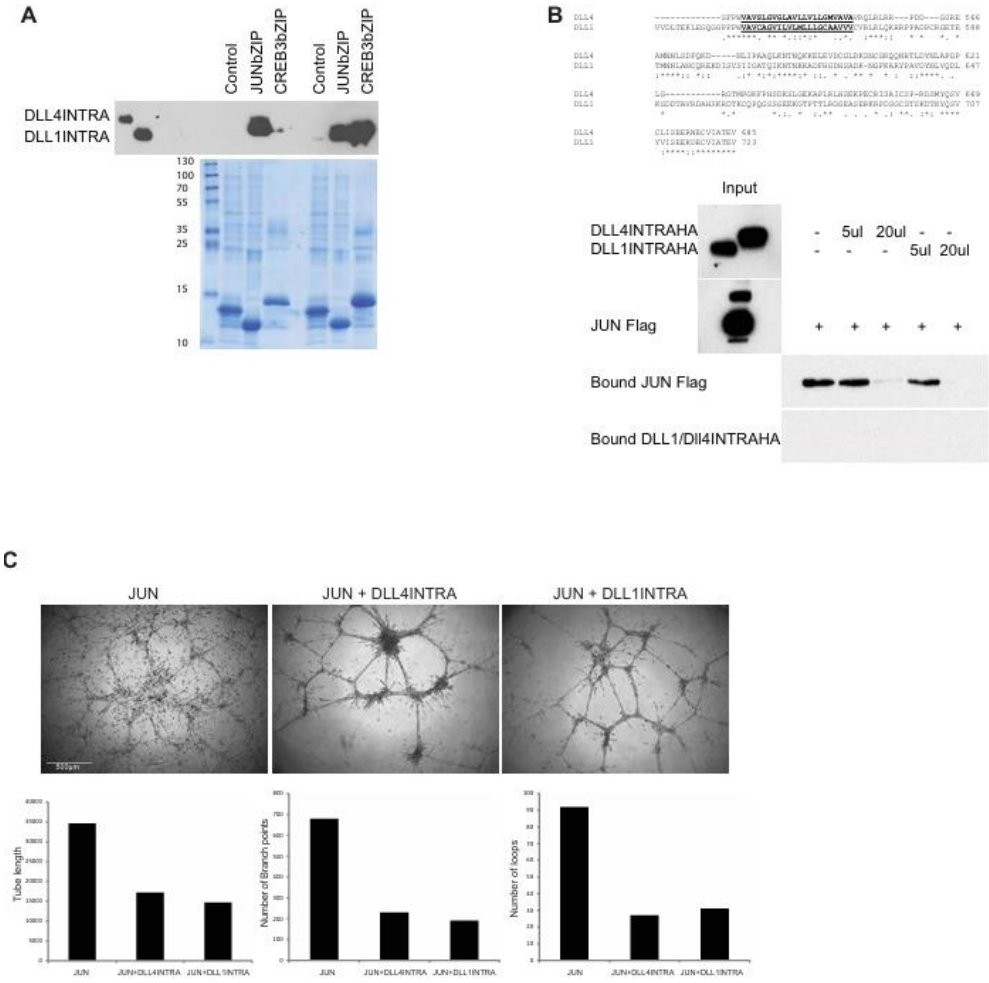

Supplementary Fig 3. (A) The ICD of DLL1 interacts biochemically with the bZIP domain of JUN. Recombinant bZIP domains of JUN and CREB3 (and a control protein) were incubated with *in vitro* translated HA epitope-tagged DLL4INTRA or DLL1INTRA. Recombinant proteins were visualized by Coomassie staining. Bound DLL4INTRA and DLL1INTRA were detected by Western blotting. **(B)** DLL1INTRA blocks JUN binding to DNA. Biotinylated AP-1 DNA binding sites were incubated with the indicated *in vitro* translated proteins. Associated JUN, DLL1 and DLL4 proteins were detected by Western blotting. **(C)** DLL1INTRA attenuates JUN-driven endothelial cell sprouting. HUVECs ectopically expressing the indicated proteins were cultured in Matrigel in the presence of 50 ng/ml VEGF. A representative of several independent experiments is shown. After 24 hours, in-house computer software was used to quantify the total length of the sprouts, the number of branch points and the number of loops. Scale bar represents 20 µM.

CHAPTER 3

A new model of Notch signalling: Control of Notch receptor cis-inhibition via Notch ligand dimers

PLoS Comput Biol 19, Jan 2023: e1010169

Daipeng Chen[2,3]*, **Zary Forghany[1*] ,** Xinxin LiuID[1‡] Haijiang WangID[1,4‡], Roeland M, H Merk[2,5#], David A.Baker[1#]

1. Leiden University Medical Center (LUMC), Department of Cell and Chemical Biology, Leiden
2. The Netherlands School of Mathematics and Statistics, Xi'an Jiaotong University, Xi'an China
3. Mathematical Institute, Leiden University, Leiden, The Netherlands
4. Department of General Surgery, The First Affiliated Hospital, Xi'an Jiaotong University, Xi'an, China
5. Institute of Biology Leiden, Leiden University, Leiden, The Netherlands

***Joint first authors**
‡ # Contributed equally

ABSTRACT

All tissue development and replenishment relies upon the breaking of symmetries leading to the morphological and operational differentiation of progenitor cells into more specialized cells. One of the main engines driving this process is the Notch signal transduction pathway, a ubiquitous signaling system found in the vast majority of metazoan cell types characterized to date. Broadly speaking, Notch receptor activity is governed by a balance between two processes: 1) intercellular Notch transactivation triggered via interactions between receptors and ligands expressed in neighbouring cells; 2) intracellular cis inhibition caused by ligands binding to receptors within the same cell. Additionally, recent reports have also unveiled evidence of cis activation. Whilst context-dependent Notch receptor clustering has been hypothesized, to date, Notch signaling has been assumed to involve an interplay between receptor and ligand monomers. In this study, we demonstrate biochemically, through a mutational analysis of DLL4, both *in vitro* and in tissue culture cells, that Notch ligands can efficiently self-associate. We found that the membrane proximal EGF-like repeat of DLL4 was necessary and sufficient to promote oligomerization/dimerization. Mechanistically, our experimental evidence supports the view that DLL4 ligand dimerization is specifically required for cis-inhibition of Notch receptor activity. To further substantiate these findings, we have adapted and extended existing ordinary differential equation-based models of Notch signaling to take account of the ligand dimerization-dependent cis-inhibition reported here. Our new model faithfully recapitulates our experimental data and improves predictions based upon published data. Collectively, our work favours a model in which net output following Notch receptor/ligand binding results from ligand monomer-driven Notch receptor transactivation (and cis activation) counterposed by ligand dimer-mediated cis-inhibition.

AUTHOR SUMMARY

The growth and maintenance of tissues is a fundamental characteristic of metazoan life, controlled by a highly conserved core of cell signal transduction networks. One such pathway, the Notch signalling system, plays a unique role in these phenomena by orchestrating the generation of the phenotypic and genetic asymmetries which underlie tissue development and remodeling. At the molecular level, it achieves this via two specific types of receptor/ligand interaction: intercellular binding of receptors and ligands expressed in neighbouring cells, which triggers receptor activation (trans activation); intracellular receptor/ligand binding within the same cell which blocks receptor activation (cis inhibition). Together, these counterposed mechanisms determine the strength, the direction and the specificity of Notch signalling output. Whilst, the basic mechanisms of receptor transactivation have been delineated in some detail, the precise nature of cis inhibition has remained enigmatic. Through a combination of experimental approaches and computational modelling, in this study, we present a new model of Notch signalling in which ligand monomers promote Notch receptor transactivation, whereas cis inhibition is induced via ligand dimers. This is the first model to include a concrete molecular distinction, in terms of ligand configuration, between the main branches of Notch signalling. Our model faithfully recapitulates both our presented experimental results as well as the recently published work of others, and provides a novel perspective for understanding Notch-regulated biological processes such as embryo development and angiogenesis.

INTRODUCTION

The ubiquitous Notch pathway is an ancient, highly conserved signalling system whose early appearance in evolution coincided with the emergence of multicellularity (1,2). It was the first cell receptor signal transduction pathway to be discovered, more than a century ago, and decades of research since then have established that it is a central regulator of cell fate (1,2) that underpins normal embryo development and tissue homeostasis, from controlling the fine-grain patterning of insect eyes and wings, to orchestrating vertebrate segmentation, neurogenesis, angiogenesis, and turnover and differentiation of the gastro-intestinal tract (3-8). Moreover, corruption of this network has been implicated in numerous pathologies including neurovascular diseases (CADASIL), multisystem disorders (ALAGILLE syndrome) (9) as well as the majority of solid tumors (10-12)**.** Whilst invertebrates such as *Drosophila* possess a single Notch receptor family member controlled by two cognate ligands, in vertebrates, the Notch pathway is composed of up to four distinct receptor types (Notch1-4) and five different Type 1 transmembrane ligands: Jagged (JAG)1, JAG2, Delta-Like (DLL)1, DLL3, and DLL4 (13,14). Operationally, the canonical Notch signaling pathway is relatively well characterized. It is activated in a juxtacrine manner through a *trans* interaction between single pass receptors expressed at the surface of one cell and ligands expressed by neighboring cells resulting in structural changes effected by biomechanical strain/pulling forces, which expose specific enzyme cleavage sites (15,16). Ultimately, a cascade of proteolytic events terminates in the γ-secretase-mediated cleavage of the Notch intracellular domain (17,18), which translocates to the nucleus whereupon it regulates expression of Notch target genes (19,20). In addition to transactivation, Notch is subject to another major regulatory mechanism termed cis-inhibition by which ligands block the activity of receptors expressed in the same cell (21,22). Collectively, these two counterposed processes (transactivation and cis-inhibition) are critical for determining the strength, the duration, the directionality and the specificity of Notch signalling.

In recent years, alongside cell, biochemical and genetic analyses, powerful mathematical approaches coupled to *in silico* modelling have become an important element of the toolkit needed to decipher the molecular details of Notch signalling and to understand the biological consequences of these processes (23-30). Collier et al. first proposed a mathematical description of lateral inhibition, an evolutionary conserved intercellular signalling mechanism that underlies symmetry breaking in tissues, in which Notch receptor (trans)activation in one cell via ligands expressed by neighbouring cells establishes the differential developmental cell fates necessary for patterning (23). Whereas this model can recapitulate essential features of transactivation, it was not until the work of Sprinzak et al., which has served as a common starting

point for subsequent refinements, that cis inhibition and transactivation were integrated into a single model (22,25). Latterly, Elowitz and co-workers have developed a new model which takes account of the recently reported phenomenon of cis-activation (31). Whilst these technical and conceptual advancements are beginning to unravel the deeper complexities of Notch signalling, arguably a significant impediment to obtaining a more complete picture of this vital pathway is the relative paucity of the architectural/molecular details of cis and trans receptor/ligand complexes. Quantitative measurements of Notch/ligand binding have been performed, and structural studies have sought to identify specific binding interfaces (16,32), however, these analyses have relied upon investigating isolated receptor and ligand domains owing to the currently unsurmounted technical difficulties associated with purifying, and structurally and biophysically characterizing full length proteins. One consequence of this, in the absence of available evidence, is that it has been generally assumed that cis and trans receptor/ligand interactions are essentially monomeric. There are, however, sound reasons to suppose that the true picture may be more complicated. Both receptors and ligands harbour multiple EGF-like repeats, which are known to mediate protein-protein interactions (33). Related to that, we here show biochemically that Notch ligands can efficiently self-associate. This begged the question: what are the potential molecular and biological consequences of Notch ligand oligomerization? Through a combination of experimental approaches and mathematical modelling, we propose a novel view of Notch signalling in which ligand monomer-driven receptor transactivation (and cis-activation) is counterbalanced by ligand dimer-mediated cis inhibition.

RESULTS

Notch ligands form dimers/oligomers

To date, it has been assumed that Notch ligands function as monomers. To formally explore this at the biochemical level, we first expressed epitope-tagged ligands in tissue culture cells and tested if the ligands could homo-oligomerize. Fig 1A shows that four different Notch ligands could efficiently self-associate. To further dissect the molecular basis of these interactions, we performed a detailed analysis of the DLL4 ligand. Fig 1B shows, in tissue culture cells, that the DLL4 extracellular domain is necessary and sufficient for homo-oligomerization and that plasma membrane anchorage is not required for this interaction. The DLL4 intracellular domain was found to be dispensable for DLL4-DLL4 binding (Fig 1B). We further demonstrate that whilst cis homo-oligomerization is very efficient (DLL4 molecules expressed in the same cell), trans oligomerization was not observed under the same conditions, though it cannot be ruled out that trans

interactions were beyond the detection limit of the experiment (Fig 1C). Collectively, these data show that Notch ligands can forms oligomers both in tissue culture cells and also *in vitro*.

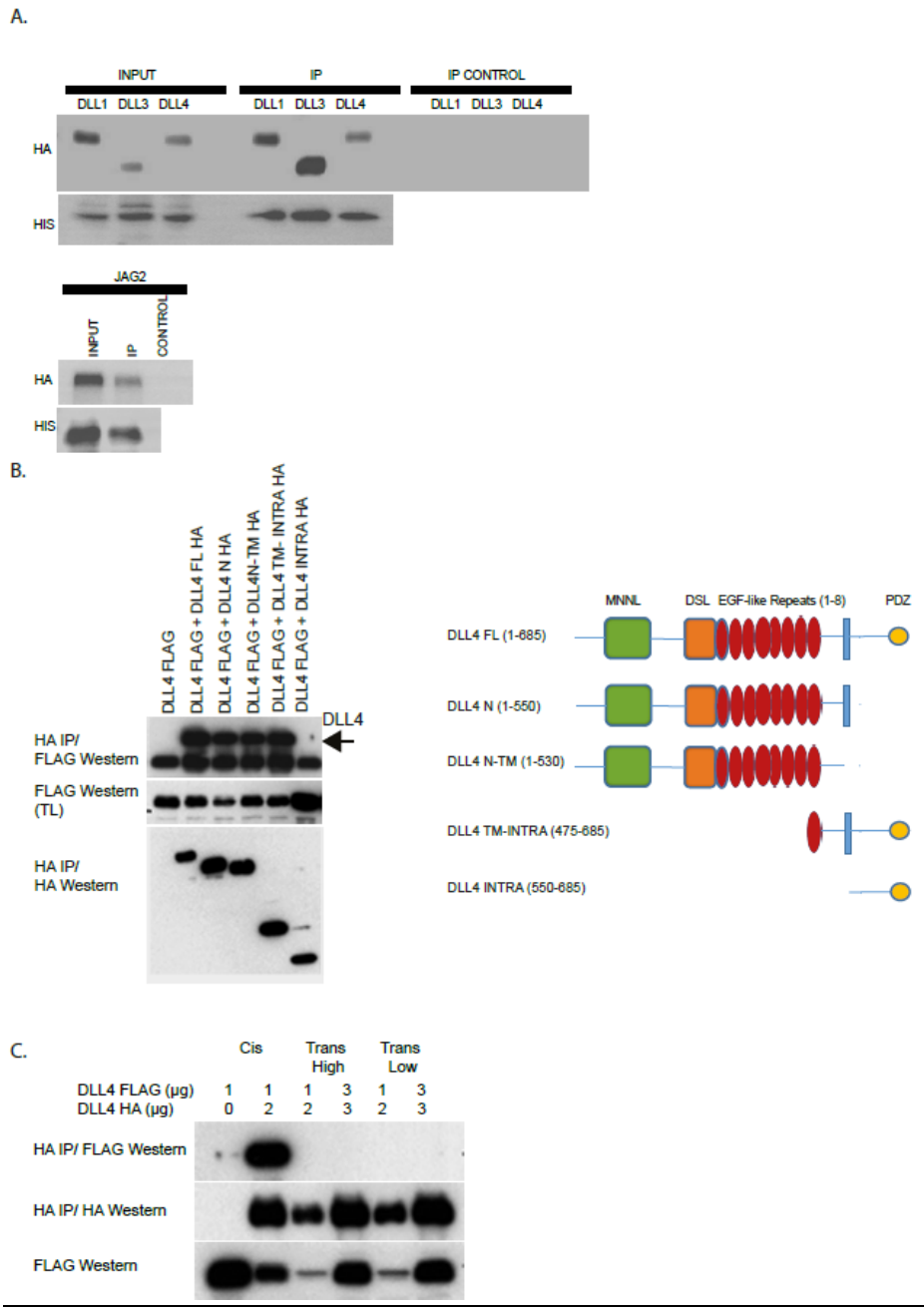

< Figure 1. Notch ligand homo-oligomerization. (A) HIS epitope-tagged Notch ligands were purified from tissue-culture cells and incubated with the indicated HA-epitope tagged proteins produced by *in vitro* translation. Ligand-ligand interactions were determined by Western blotting using the shown antibodies. (B) Left panel: The indicated constructs were transfected into tissue-culture cells. Complexes were resolved by immunoprecipitation and visualized with the shown antibodies. Right panel: schematic representation of the constructs used in the study. (C) The indicated constructs were transfected into tissue-culture cells in one of three ways: cis- ligands were co-expressed in the same cells sparsely plated to exclude trans interactions; trans (high)- differently tagged ligands were expressed individually in cells, which were subsequently mixed in confluent cell monolayers to enable trans interactions; trans (low)- as for trans (high) but cells were plated at low cell density. Complexes were resolved by immunoprecipitation and visualized using the shown antibodies.

The membrane proximal DLL4 (EGF-like repeat 8) and the MNNL domain bind to DLL4 *in vitro*

To identify the domains responsible for DLL4 oligomerization, we performed a comprehensive mapping analysis using purified proteins. By these means, we found that EGF-like repeat 8 but not EGF-like repeats 1-7, either as part of the DLL4 extracellular domain (see Fig 2A and 2B) or singularly (Fig 2C), binds to DLL4, consistent with the idea that this domain might underpin DLL4-DLL4 binding (see Fig 2). These experiments also highlighted the MNNL domain as binding efficiently to DLL4 (Fig 2B).

EGF-like repeat 8 mediates DLL4-DLL4 binding but is dispensable for DLL4 binding to the Notch receptor

To test the requirement of the EGF-like repeat 8 and the MNNL domain for DLL4 oligomerization, we expressed epitope-tagged wild type and mutant DLL4 ligands in tissue culture cells. Whereas the MNNL domain was found to be dispensable for DLL4-DLL4 binding under these conditions, loss of the EGF-like repeat 8 abrogated binding (Fig 3A). Moreover, deletion of EGF-like repeat 7 or EGF-like repeat 6 did not detectably inhibit ligand-ligand binding suggesting that the membrane proximal region encompassing EGF-like repeat 8 encodes a specific DLL4 oligomerization motif (Fig 3B) and that deletion of the EGF-like repeat did not non-specifically corrupt ligand-ligand binding. To determine the impact of deleting the EGF-like repeat 8 on ligand-receptor binding, we co-expressed wild type or mutant DLL4 ligands with Notch 2. Fig 3C shows that DLL4 mutants lacking either EGF-like repeat 8, EGF-like repeat 7, EGF-like repeat 6 or the MNNL domain, associated with Notch2 as efficiently as wild type DLL4. Together, these findings support the view that the DLL4 EGF-like repeat 8 specifically mediates DLL4-DLL4 binding but is not required for Notch receptor-DLL4 binding. Since mutant DLL4 harbouring a deletion of EGF-like repeat 8 presumably exists primarily as a monomer, these results suggest that ligand oligomerization is not a general pre-requisite for Notch receptor binding.

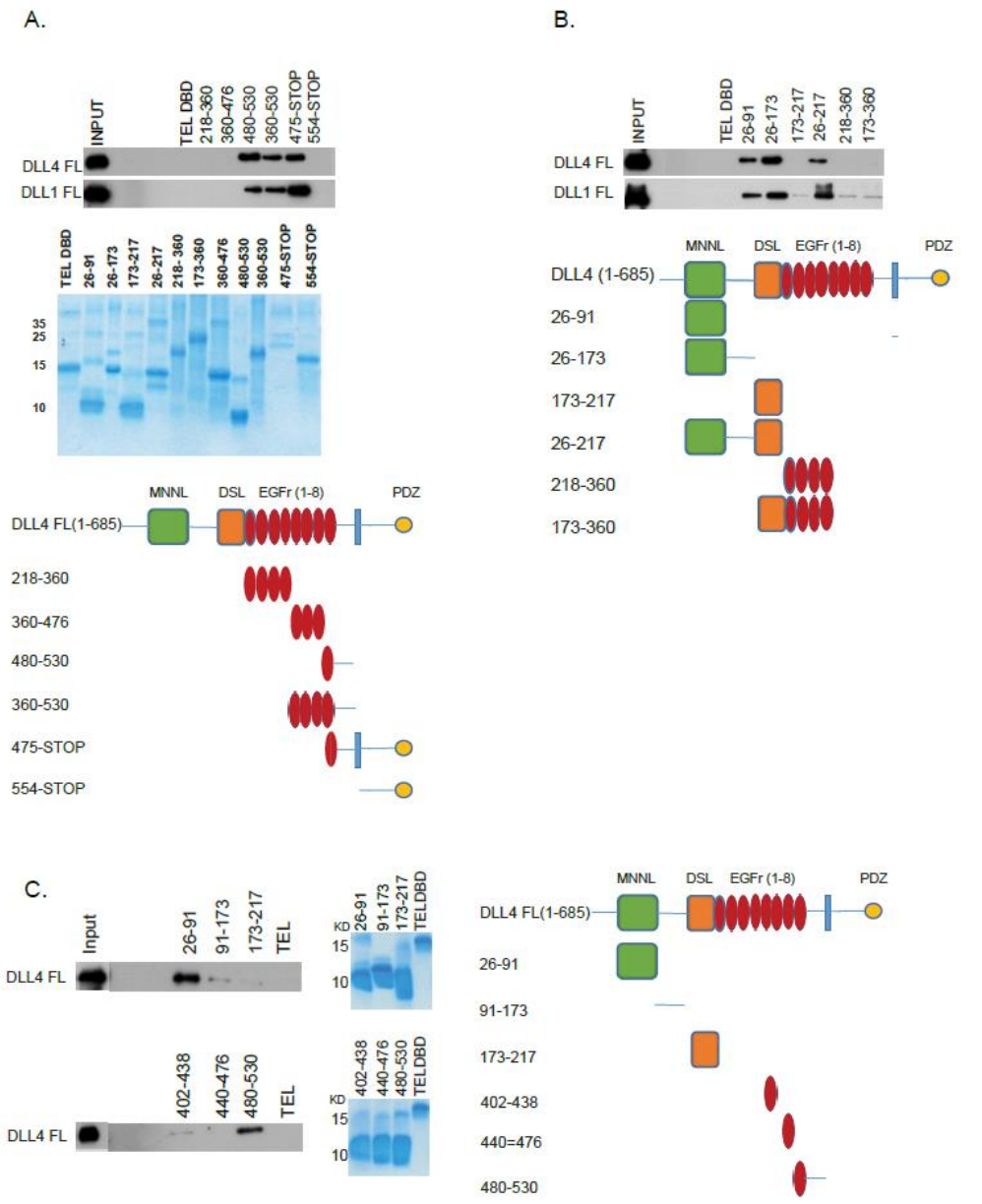

Figure 2. Biochemical mapping of DLL4 dimerization motifs. (A-C) The indicated HIS-epitope tagged proteins (a schematic representation of constructs is shown) were purified from E. coli (representative Coomassie-stained gels of protein preparations are shown) and incubated with full length DLL4 ligand manufactured by *in vitro* translation. Ligand-ligand Interactions were determined by Western blotting.

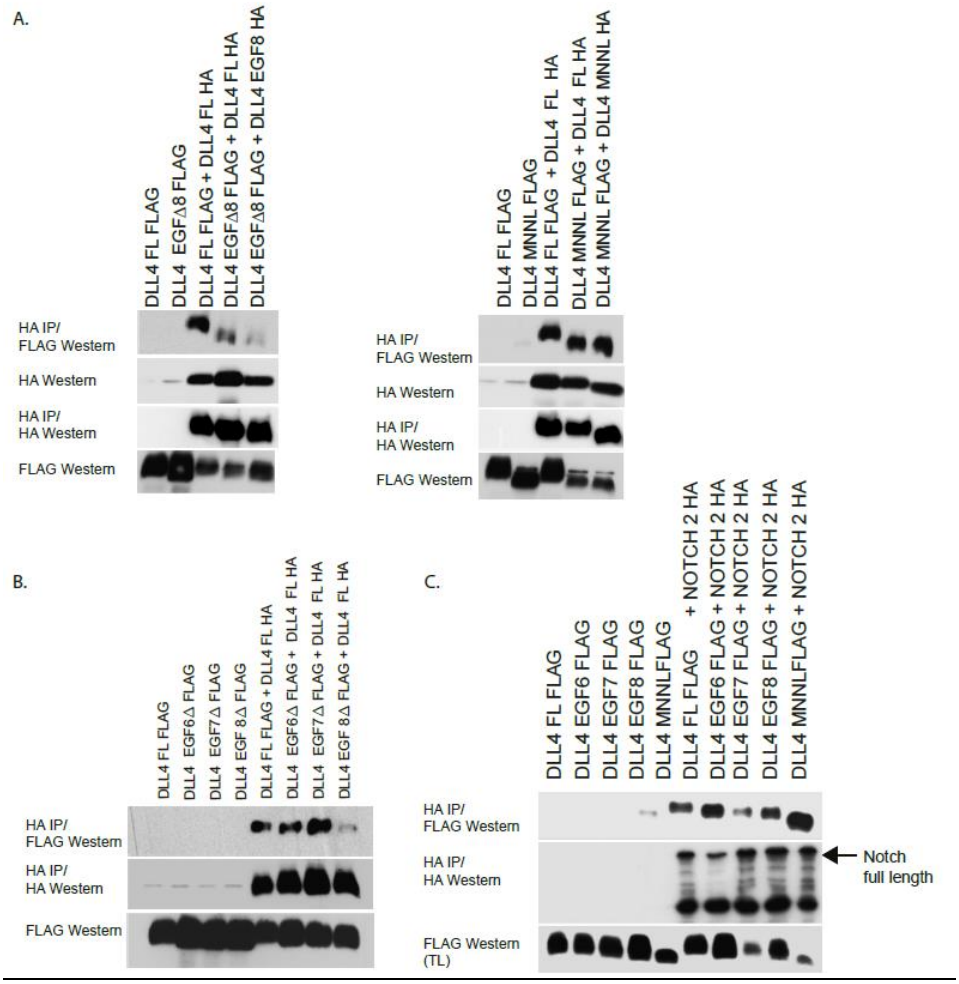

Figure 3. (A-C) The indicated constructs were transfected into tissue-culture cells. DLL4 EGF6, EFG7, EGF8, MNNL each have deletions of the named domain. Complexes were resolved by immunoprecipitation and visualized by Western blotting with the highlighted antibodies.

DLL4 oligomerization is required for cis-inhibition of the Notch receptor

To elucidate the mechanistic consequences of ligand oligomerization, we performed luciferase reporter assays to quantitatively measure Notch receptor activity. When expressed in the same cell as Notch2 receptors, wild type DLL4 or mutant DLL4 ligands lacking either EGF-like repeat 7 or EGF-like repeat 6, all of which can form oligomers, efficiently inhibited the activity of Notch2 in cis. By contrast, DLL4 ligands lacking EGF-like repeat 8, which thus act as monomers, failed to inhibit Notch2 activity when co-expressed in the same cell (Fig 4A). When Notch2 and wild type DLL4 (or mutant DLL4) were expressed in

neighboring cells, we found that Notch receptor transactivation was unaffected by deletions of EGF-like repeat 8, EGF-like repeat 7 or EGF-like repeat 6 (see Fig 4A). Fig 4B shows that deletion of EGF-like repeat 8 did not result in any overt change in the sub-cellular location of DLL4. Overall, these results favour a model in which cis-inhibition, but not transactivation, of Notch signalling specifically depends upon DLL4 ligand oligomerization.

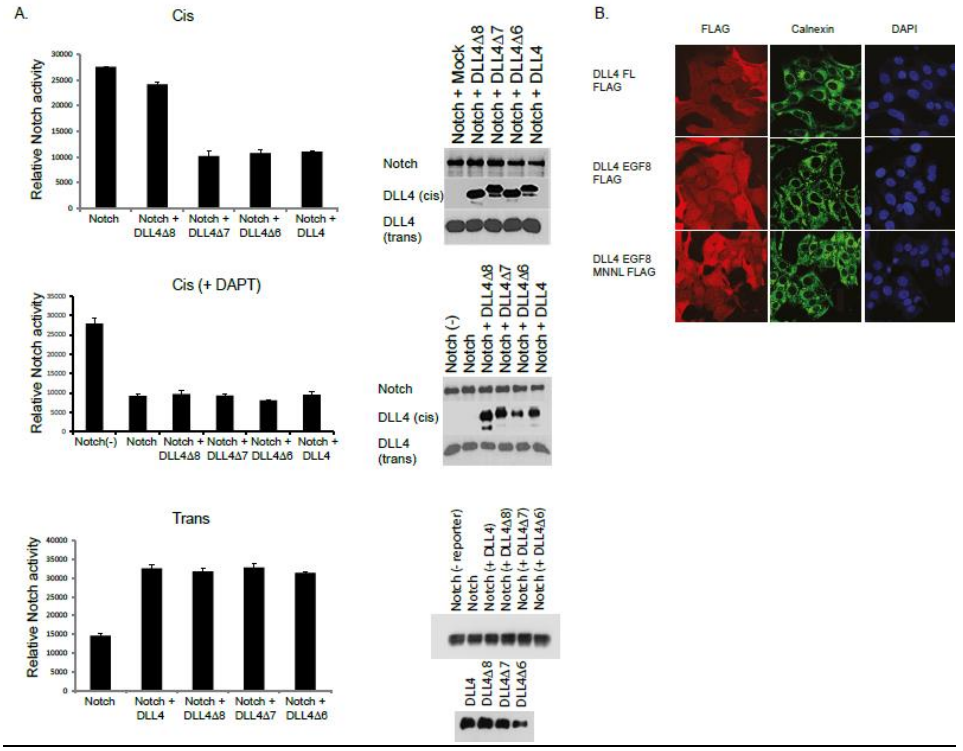

Figure 4. (A) Luciferase reporter assays were performed as described in the methods. Upper graph: U2OS cells co-expressing Notch activity luciferase reporter together with the indicated Notch2 and ligand constructs (cis cells) were co-cultured with cells stably expressing DLL4 (to enable transactivation). Middle panel: The same set-up as above, however, cells were cultured in the presence or absence of 10 μM DAPT. Lower panel: Cells expressing Notch2 and a Notch activity luciferase reporter were separately co-cultured with cells stably expressing the indicated DLL4 constructs. For each analysis, reporter activity was normalized using Renilla luciferase. Levels of ectopically expressed proteins were determined by Western blotting of cell lysates. Each condition in each experiment was performed in triplicate and error bars represent the standard deviation of the mean. Experiments were performed three times. Representative experiments are shown. (B) Immunofluorescence showing the sub-cellular distribution of wild type and mutant DLL4 ligands. The Golgi apparatus was visualized using a calnexin-specific antibody, to rule out aberrant accumulation of ligand.

A general mathematical model describing the potential roles of ligand monomers and dimers in Notch signalling

To further explore the potential biological mechanism of our biochemical findings presented above, we have adapted the mutual inactivation model recently proposed by Sprinzak et al. (22) to include ligand dimerization and cis-activation. Fig 5 schematically represents possible ligand and receptor interactions, which underlie these two models, the principal difference being that whereas cis-inhibition is driven via ligand monomers in the mutual inactivation model (Fig 5A), in our general model, cis-inhibition is driven via ligand monomers or dimers (Fig 5B).

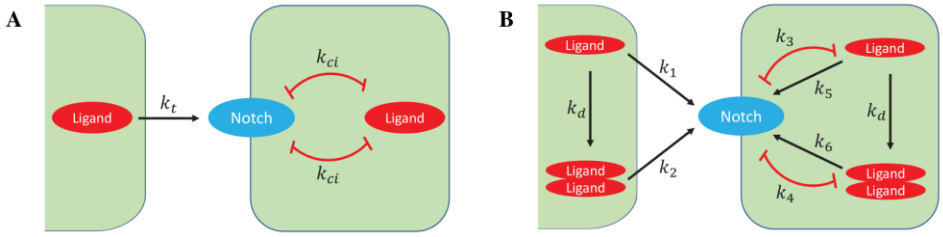

Figure 5. Diagrammatic representation of the mutual inactivation model and the general ligand dimerization model for Notch signaling. Black arrows indicate dimerization of ligand monomers, trans-activation and cis-activation of Notch; Red lines represent cis-inhibition.

The new general model is presented as Eq. (1), and encompasses the new terms L^*, indicating the amount of Notch ligand dimers, and k_d, representing the rate of ligand dimerization. In this model, Notch is trans-activated by ligand monomers (at rate k_1) or dimers (at rate k_2) expressed in neighboring cells, denoted by L_{ext} (ligand monomer) and L^*_{ext} (ligand dimer), and is cis-inhibited by ligand monomers, L, (at rate k_3) or dimers, L^*, (at rate k_4) co-expressed in the same cell. Thus, the general Eq 1, allows for monomer-dependent cis-inhibition, dimer-dependent cis-inhibition or a combination of both. Moreover, ligand monomers or dimers can trigger cis-activation of Notch in the same cell with rates k_5 and k_6, respectively. The amount of Notch receptors expressed in neighboring cells is denoted by, N_{ext}. These interactions in any given target cell are described mathematically by

$$\begin{cases} \frac{dL}{dt} = L_0 - \beta L - 2k_d L^2 - k_1 N_{ext} L - k_3 N L - k_5 N L, \\ \frac{dL^*}{dt} = k_d L^2 - \beta L^* - k_2 N_{ext} L^* - k_4 N L^* - k_6 N L^*, \\ \frac{dN}{dt} = N_0 - \beta N - (k_1 L_{ext} - k_2 L^*_{ext} - k_3 L - k_4 L^* - k_5 L - k_6 L^*) N, \\ \frac{dS}{dt} = (k_1 L_{ext} + k_2 L^*_{ext} + k_5 L + k_6 L^*) N - \beta_S S, \end{cases} \quad (1)$$

where L_0 and N_0 denote the production rates of Notch ligand (L) and Notch receptor (N), respectively. The proteins described in the model are assumed to be degraded at a constant rate given by β and β_S, which define the degradation rates of ligands and receptors, and the free Notch intracellular domain (S), respectively.

In summary, our general model enables us to consider, in an unbiased fashion, different Notch signalling scenarios. By example, in Eq. (1), setting $k_1 = k_t$ and $k_2 = 0$ means that transactivation of Notch is mediated by ligand monomers; $k_3 = 0$ and $k_4 = k_{ci}$ means that cis-inhibition of Notch is mediated specifically and exclusively by ligand dimers; and $k_5 = k_{ca}$ and $k_6 = 0$ means that cis-activation of Notch is mediated by ligand monomers. Alternative scenarios can be tested by varying the value of the corresponding parameters k_i $(i = 1,2,..,6)$. A comprehensive description of all parameters is detailed in Table 1.

To explore the potential roles of Notch ligand monomers and dimers in Notch signalling, we investigated a number of alternative scenarios in the context of cis-inhibition, trans-activation, and cis-activation. As a first step, we considered the currently accepted overall view of Notch signalling, namely ligand monomer-dependent cis-inhibition in the absence of ligand dimerization ($k_d = 0$) and cis-activation ($k_5 = k_6 = 0$). In this case, the general ligand dimerization model (Fig 5B) reduces to a mutual inactivation model (Fig 5A) with $k_1 = k_t$ and $k_3 = k_{ci}$ described mathematically by Eq. (2)

$$\begin{cases} \frac{dL}{dt} = L_0 - \beta L - k_t N_{ext} L - k_{ci} N L, \\ \frac{dN}{dt} = N_0 - \beta N - k_t L_{ext} N - k_{ci} L N, \\ \frac{dS}{dt} = k_t N L_{ext} - \beta_S S. \end{cases} \quad (2)$$

Eq. (2) can be analytically solved in the steady state ($\bar{L}$, $\bar{N}$, $\bar{S}$), leading to the following steady-state levels of Notch ligand and receptor:

$$\bar{L} = \frac{L_0 - N_0}{2\beta_1} - \frac{\beta_2}{2k_{ci}} + \sqrt{\left(\frac{L_0 - N_0}{2\beta_1} - \frac{\beta_2}{2k_{ci}}\right)^2 + \frac{\beta_2 L_0}{\beta_1 k_{ci}}}, \quad (3)$$

$$\bar{N} = \frac{\beta_1}{\beta_2}\bar{L} - \frac{L_0 - N_0}{\beta_2}, \quad (4)$$

where $\beta_1 = \beta + k_t N_{ext}$ and $\beta_2 = \beta + k_t L_{ext}$. When the production rate of ligand is bigger than the Notch receptor production rate ($L_0 > N_0$) and the affinity of cis-ligand for Notch receptor is high (e.g., $k_{ci} \gg 4L_0\beta_1\beta_2/(L_0 - N_0)^2$), it follows that Eq. (3-4) yields the following state:

$$\bar{L} \approx \frac{L_0 - N_0}{\beta_1}, \quad \bar{N} \approx 0 \quad (5)$$

Similarly, when the production rate of ligand is smaller than that of Notch receptor ($L_0 < N_0$), we find a different state given by:

$$\bar{L} \approx 0, \quad \bar{N} \approx \frac{N_0 - L_0}{\beta_2} \quad (6)$$

The mutual inactivation model (22) predicted that Notch receptor and Notch ligand levels are mutually exclusive in the same cell (Eq. 5-6). Consistently, the relative production rates of Notch ligand and receptor determine the output of cell signaling state.
In summary, by exclusively considering ligand monomer-driven cis inhibition, our general model essentially reduced to a mutual inactivation model, as defined by Sprinzak et al. (22). We next tested a number of alternative cases and compared these results to our experimental findings described in Fig 4.

Exploring the role of ligand monomers and ligand dimers in cis-inhibition and trans-activation

Fig 6A schematically depicts three alternative cases of cis-inhibition. Specifically, in Model C1, ligand dimers mediate cis-inhibition. In Model C2, ligand monomers mediate cis-inhibition of Notch signalling, which is similar to the mutual inactivation model (Fig 5A). In Model C3, cis-inhibition is mediated by both ligand monomers and ligand dimers. In the context of these models, we do not consider cis-activation ($k_5 = k_6 = 0$) because cis-activation is significantly weaker than trans-activation (31), such that, in this instance, its effects can be ignored. In Fig 6B, we simulated the steady-state levels of Notch activity (free Notch Intracellular domain) driven by the production rate of cis-ligand in the receiving cell (expressing Notch receptor) exposed to fixed levels of trans-ligand in a sending cell. Under these conditions, whether monomer- or dimer-induced cis-inhibition, increase in the production rate of cis ligand resulted in a corresponding inhibition of Notch receptor activity (Fig 6B). To further investigate the role of ligand monomers and dimers in cis-inhibition of Notch signalling, in Fig 6C, when the production rate of cis-ligand in the receiving cell is sufficient to inhibit Notch receptor activity, we simulated the effects of altering the dimerization rate of cis-ligand in the receiving cell on Notch receptor activity. Clearly, only Model C1, in which ligand dimers but not ligand monomers promote cis-inhibition, faithfully reproduced the experimental observations (Fig 4A), which show that dimer deficient ligands do not efficiently cis-inhibit Notch receptor activation. Therefore, simulations based upon Model C1 (a special case of our general model) match our conclusions based upon our experimental results, that Notch receptor cis inhibition is ligand dimer- and not ligand monomer-dependent.

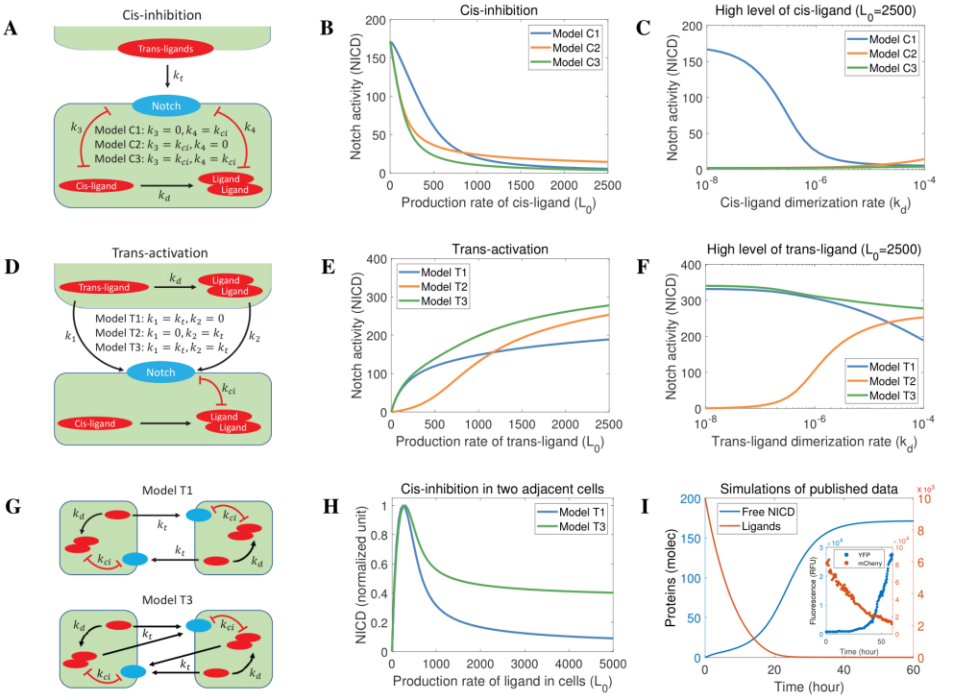

Figure 6. The role of Notch ligand monomers and dimers in Notch receptor cis-inhibition and trans activation. (A) The potential models governing cis-inhibition of Notch. The level of trans-ligand in sending cell is fixed whilst cis ligand levels in receiving cell vary as shown. (B) Notch activity in the receiving cell as a function of cis-ligand production rate for the different models shown in A. (C) Notch activity in the receiving cell as a function of cis-ligand dimerization rates for a high level of cis-ligand (the maximum production rate shown in B). (D) The potential models governing trans-activation of Notch. The production rate and dimerization rate of ligand in the receiving cell is fixed whilst trans ligand levels in sending cell vary as shown. (E) Notch activity in the receiving cell in response to increasing trans-ligand production rates for the different models shown in D. (F) Notch activity in the receiving cell in response to decreasing trans-ligand dimerization rates when the level of trans-ligand is high (the maximum production rate shown in E). (G) The potential roles of ligand monomer and ligand dimer governing Notch signaling in two identical cells. (H) Relative Notch activity in response to increasing Notch ligand production rates in two cells for the two cases shown in G. Notch activity is normalized against the maximum Notch activity. (I) *In silico* replication of published cis-inhibition dynamics (22). In common with their experimental conditions (22), the initial state of ligand levels is high (with a production rate of 0), whilst Notch receptor levels are low.

Having established the requirement of ligand dimerization for cis inhibition, we next addressed the role of ligand monomers and ligand dimers in trans activation. Fig 6D schematically depicts three alternative cases of trans-activation. In Model T1, ligand monomers mediate trans-activation. In Model T2, ligand dimers mediate trans-activation. In Model T3, both ligand monomers and

ligand dimers mediate trans-activation. In Fig 6E, we present the steady-state levels of Notch activity in the receiving cell driven by the production rate of trans-ligand in a sending cell. In common with the simulation described in Fig 6C, in Fig 6F, in the presence of a high production rate of trans-ligand in a sending cell, we measured Notch activity in the receiving cell driven by the dimerization rate of trans-ligand in the sending cell. These results (Fig 6E-6F) show that both Model T1 and T3 reproduce the Notch receptor trans-activation observed experimentally in Fig 4A, that is, dimer deficient ligands are capable of promoting Notch receptor trans-activation. To further test our model and investigate the potential roles of ligand monomers and dimers in cis-inhibition and trans-activation, we considered two adjacent (identical) cells. Based upon our earlier analyses, there are two cases (Model T1 and Model T3) governing Notch signalling in two adjacent cells (Fig 6G). In Fig 6H, we present Notch activity driven by increasing production rates of ligands in two cells. We see that Model T1 but not Model T3 shows that higher ligand expression levels elicit greater levels of cis-inhibition in two cells. Collectively, our results provide evidence in favour of a model in which Notch signalling is mediated by ligand monomer-dependent trans-activation and ligand dimer-dependent cis-inhibition.

To further test the general applicability of our model, we ran simulations of our ligand dimerization model to test if it could reproduce previously published experimental data. To measure cis-inhibition and trans-activation experimentally, Sprinzak et al. deployed elegant cell-based reporter assays enabling quantification of both cis-inhibition and trans-activation of Notch signalling (22). The experimental setting for trans-activation is similar to our model depicted schematically in Fig 6A, with fixed levels of trans Notch ligand. By comparing these simulations to the published data, we found that our ligand dimerization model successfully reproduces the reported experimental quantification of both cis-inhibition (Fig 6I) and trans-activation of Notch signalling (Fig SI 1).

Based on our experimental data and numerical simulations, we provide evidence in favour of a model in which Notch signalling is mediated by ligand monomers-dependent trans-activation and ligand dimers-dependent cis-inhibition. Mathematically, this model was derived from the general ligand dimerization model (Fig 5B) by setting $k_1 = k_t$, $k_2 = 0$, $k_3 = 0$, $k_4 = k_{ci}$, $k_5 = 0$ and $k_6 = 0$ in Eq. (1), that is

$$\begin{cases} \frac{dL}{dt} = L_0 - \beta L - 2k_d L^2 - k_t N_{ext} L, \\ \frac{dL^*}{dt} = k_d L^2 - \beta L^* - k_{ci} N L^*, \\ \frac{dN}{dt} = N_0 - \beta N - k_{ci} L^* N - k_t L_{ext} N, \\ \frac{dS}{dt} = k_t L_{ext} N - \beta_S S. \end{cases} \quad (7)$$

Eq. (7) can also be analytically solved in the steady state ($\bar{L}$, $\bar{L^*}$, $\bar{N}$, $\bar{S}$), leading to the following steady-state levels of Notch ligand monomer, ligand dimer and receptor:

$$\bar{L} = \sqrt{\left(\frac{\beta+k_t N_{ext}}{4k_d}\right)^2 + \frac{L_0}{2k_d}} - \frac{\beta+k_t N_{ext}}{4k_d}, \quad (8)$$

$$\bar{L^*} = \frac{k_d\bar{L}^2-N_0}{2\beta} - \frac{\beta_2}{2k_{ci}} + \sqrt{\left(\frac{k_d\bar{L}^2-N_0}{2\beta} - \frac{\beta_2}{2k_{ci}}\right)^2 + \frac{\beta_2 k_d\bar{L}^2}{\beta k_{ci}}}, \quad (9)$$

$$\bar{N} = \frac{\beta}{\beta_2}\bar{L^*} - \frac{k_d\bar{L}^2-N_0}{\beta_2}, \quad (10)$$

where $\beta_2 = \beta + k_t L_{ext}$. Similar to the analysis of Eq. (3-4), when the affinity of Notch for ligand dimers is high, Eq. (9-10) yields: $\bar{N} \approx 0$ if $N_0 < k_d\bar{L}^2$. This indicates that high production rates of Notch ligand could inhibit Notch receptor activity and reduce receptor availability in the same cell, which is consistent with the results (Eq. 5) of the mutual inactivation model. However, when the production rate of Notch is large ($N_0 > k_d\bar{L}^2$), we have:

$$\bar{N} \approx \frac{N_0-k_d\bar{L}^2}{\beta_2} \quad (11)$$

In contrast to the prediction (Eq. 6) of the mutual inactivation model with high Notch expression, here we find that the level of Notch ligand monomer (Eq. 8) is independent of the production rate of Notch. In other words, Notch receptor and Notch ligand monomer are not mutually exclusive in the same cell, which can co-express high levels of Notch receptor and ligand simultaneously (Eq. 8 and Eq. 11), an observation reported previously (53). The potential biological implications for the differences in the two models will be considered below.

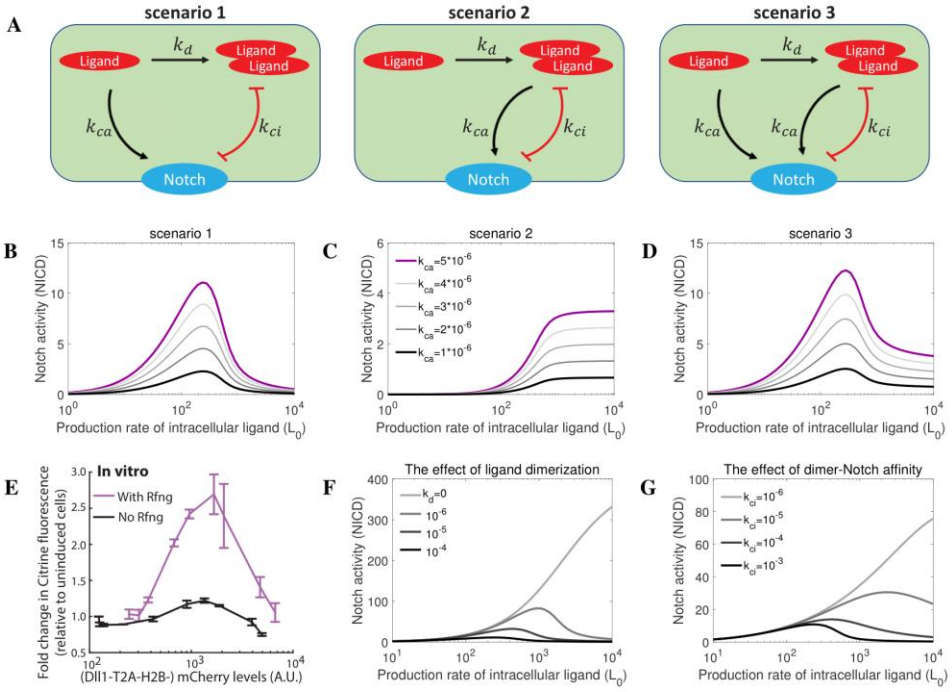

Figure 7. The role of Notch ligand monomers and dimers in cis-activation. (A) Schematic representation of different potential rules governing receptor/ligand interactions in Notch signaling. Scenario 1: monomer mediates cis-activation and dimer mediates cis-inhibition; scenario 2: dimer mediates cis-activation and cis-inhibition; scenario 3: monomer mediates cis-activation, dimer mediates both cis-activation and cis-inhibition. (B-D) Simulations of cis-activation for each of the scenarios. Different cis-activation rates are tested. (E) Published *in vitro* cis-activation experiments (31). The response of Notch to cis ligand level is non-monotonic. (F) The role of Notch ligand dimerization in cis-activation. Notch ligand dimer does not directly mediate cis-activation, but ligand dimerization is necessary to explain the experimental observations. (G) Lower affinity of Notch for ligand dimer promotes cis-activation and limits cis-inhibition of Notch signalling.

Modelling the role of ligand monomers and ligand dimers in cis-activation of Notch signalling

Elowitz and co-workers recently reported cis-activation as a novel, previously overlooked Notch signalling mechanism (31). In their cis-activation assay conditions, cell-cell contact was eliminated, that is, external ligands and receptors satisfy $L_{ext} = 0$, $L^*_{ext} = 0$ and $N_{ext} = 0$. We have shown that ligand dimers instead of ligand monomers mediate cis-inhibition of Notch, which means $k_3 = 0$ and $k_4 = k_{ci}$ in Eq. (1). Consequently, there are three possible scenarios (scenarios 1 to 3 in Fig 7A) for cis-activation of Notch, given mathematically by,

$$\begin{cases} \frac{dL}{dt} = L_0 - \beta L - 2k_d L^2 - k_5 NL, \\ \frac{dL^*}{dt} = k_d L^2 - \beta L^* - k_{ci} NL^* - k_6 NL^*, \\ \frac{dN}{dt} = N_0 - \beta N - k_{ci} L^* N - k_5 LN - k_6 L^* N, \\ \frac{dS}{dt} = k_5 LN + k_6 L^* N - \beta_S S, \end{cases} \quad (12)$$

with $k_5 = k_{ca}$ and $k_6 = 0$ for scenario 1; $k_5 = 0$ and $k_6 = k_{ca}$ for scenario 2; $k_5 = k_{ca}$ and $k_6 = k_{ca}$ for scenario 3. By running simulations using reference parameter values (Table 1), in Fig 7B-E we demonstrated that the experimental data (Fig 7E) is best explained by the ligand dimerization model with the parameters setting in scenario 1 (compare Fig 7B-7D and 7E), which assumes that ligand dimers mediate cis-inhibition whilst ligand monomers mediate cis-activation. In scenario 3, Notch signalling cannot be limited to a low level by high production rate of cis ligand because of ligand dimers-mediated cis-activation (Fig 7D). To explain the observed non-monotonic response of Notch receptor to cis ligand levels (Fig 7E), Nandagopal et al. (31) proposed a number of possible mechanisms, but did not include the explicit ligand dimerization step that our data suggest. Interestingly, the rate of ligand dimerization might modulate both the width and the amplitude of the Notch cis-activation peak, as well as the ligand concentration at which maximum cis-activation is reached (Fig 7F). Additional numerical simulations predict that a Notch receptor could show stronger cis-activation and weaker cis-inhibition if the affinity of Notch for ligand dimers is lower (Fig 7G), which is consistent with the reported experimental results (31). In summary, our simulations suggest that cis-activation is mediated by ligand monomers, but the non-monotonic response of Notch to cis ligand levels is dependent on ligand dimers-mediated cis-inhibition.

Modelling predictions are independent of ligand oligomer size and subcellular localization for ligand dimer-mediated cis-inhibition

It is currently not possible biochemically to quantitatively distinguish between ligand homo-oligomerization and homo-dimerization. To test if our modelling prediction would be affected by ligand oligomer size (n, the number of monomers composing an oligomer), we extended the ligand dimerization model to include ligand oligomerization, given mathematically by,

$$\begin{cases} \frac{dL}{dt} = L_0 - \beta L - P(L,n) - k_t N_{ext} L - k_{ca} N L, \\ \frac{dL^*}{dt} = Q(L,n) - \beta L^* - k_{ci} N L^*, \\ \frac{dN}{dt} = N_0 - \beta N - k_{ci} L^* N - k_t L_{ext} N - k_{ca} L N, \\ \frac{dS}{dt} = k_t L_{ext} N + k_{ca} L N - \beta_S S, \end{cases} \tag{13}$$

where $P(L,n) = nk_dL^n + (n-1)k_dL^{n-1} + \cdots + 2k_dL^2$ and $Q(L,n) = k_dL^n + k_dL^{n-1} + \cdots + k_dL^2$ represent the process of Notch ligand oligomerization. Here L^* is the quantity of ligand oligomers, of all possible sizes, in cells. To exclude the mixing effect of oligomers of different size, we only considered the homogeneous populations of oligomer of defined size in each simulation, which means $P(L,n) = nk_dL^n$ and $Q(L,n) = k_dL^n$ in numerical simulations. In Fig 8A-C, we present Notch activity (normalized) driven by the production rate of intracellular ligands in different experimental settings. These results clearly demonstrate that the Notch receptor activity is independent of oligomer size (dimer, trimer or tetramer). Thus, the predictions of the Notch ligand dimerization model are general and representative across a range of oligomer sizes.

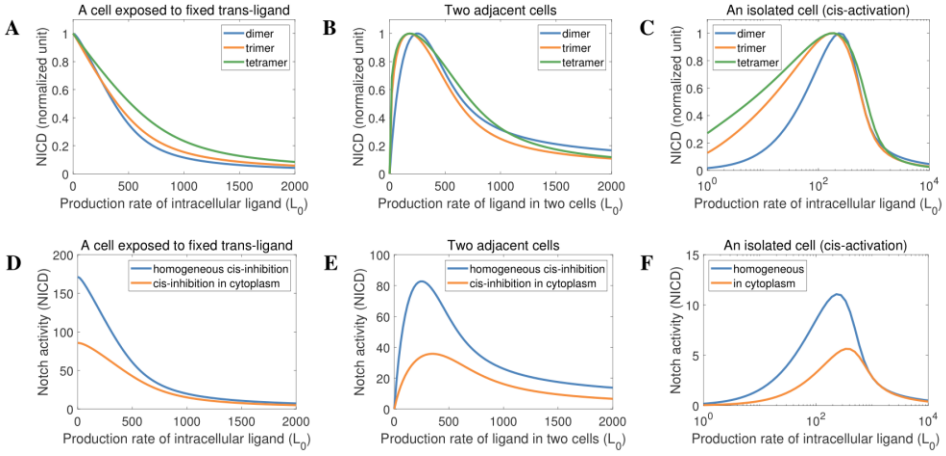

Figure 8. The effect of ligand oligomer size and subcellular localization on cis inhibition of Notch signalling. (A-C) The response of Notch to intracellular ligands of different oligomer size in a cell exposed to fixed levels of trans-ligand (A), in two identical cells (B), and in a single cell (C). Notch activity is normalized against the maximum Notch activity. (D-F) The response of Notch to the production rate of intracellular ligand. Here, we compared simulations of cis inhibition which can occur in all cell compartments (spatially homogeneous), with cis-inhibition occurring only in the cytoplasm.

Another interesting question relates to the subcellular compartment in which cis-inhibition occurs. To investigate the effect of the subcellular localization of ligand dimerization and dimer-mediated cis-inhibition on Notch signalling, we have developed a mathematical model which distinguishes the proteins found in the cytoplasm (with subscript c) and the proteins expressed on the cell membrane (with subscript m). Based on previous studies (31, 38), this model makes the following initial assumptions: ligand dimerization and ligand dimer-mediated cis-inhibition of Notch occurs in the cytoplasm; trans-activation and cis-activation happens at the membrane. This is expressed mathematically by,

$$\begin{cases} \frac{dL_c}{dt} = L_0 - \beta L_c - 2k_d {L_c}^2 - k_r L_c, \\ \frac{dL^*}{dt} = k_d {L_c}^2 - \beta L^* - k_{ci} N_c L^*, \\ \frac{dN_c}{dt} = N_0 - \beta N_c - k_{ci} L^* N_c - k_r N_c, \\ \frac{dL_m}{dt} = k_r L_c - \beta L_m - k_t N_{ext} L_m - k_{ca} N_m L_m, \\ \frac{dN_m}{dt} = k_r N_c - \beta N_m - k_t L_{ext} N_m - k_{ca} L_m N_m, \\ \frac{dS}{dt} = k_t L_{ext} N_m + k_{ca} L_m N_m - \beta_S S. \end{cases}$$

(14)

In this model, Notch ligands and receptors are produced in the cytoplasm, and are subsequently transported from the cytoplasm to the membrane with a transportation rate k_r. Other parameters are the same as those mentioned in Table 1. Based on Eq. (14), we simulated Notch activity driven by the production rate of cytoplasmic ligands in different experimental settings. In Fig 8D-F, we compared the response of Notch to increasing production rates of cytoplasmic ligands for the model where ligand dimerization and dimer-mediated cis-inhibition of Notch occurs in the cytoplasm (Eq. 14) and the model where cis inhibition is spatially homogeneous (Eq. 13). These simulations demonstrate that the modelling predictions do not depend on the subcellular localization of ligand dimerization and dimer-mediated cis-inhibition of Notch.

Modelling the role of dimer-dependent cis-inhibition in tissue patterning

The preceding analyses considered signalling mechanisms controlled by ligand dimer formation at the molecular and individual cell level. We next tested the validity of our model in the context of characterized tissue patterning processes. Whilst, it is established that the Notch pathway is indispensable for tissue development and maintenance in all known metazoans studied to date, historically, the fruit fly has proven to be an invaluable tool for delineating the basic components and modus operandi of the Notch network generally, and cis inhibition in particular. Indeed, the name Notch derives from the characteristic pattern of wing 'Notches' exhibited by the wings of Drosophila encoding Notch

mutations, first recorded a century ago. Notch signalling underpins two patterning processes occurring in two perpendicular planes during wing morphogenesis: anterior/posterior signalling required for the formation of wing veins (Fig 9A); and dorsal-ventral patterning needed to establish the wing margin (Fig 9A). To model the role of ligand dimers in wing vein patterning, we considered a gradient of Notch ligand, and a constant level of Notch receptor, across multiple cells yielding a central region of peak ligand concentrations, which delimited the site of vein formation through activation of Notch signalling in neighboring cells (expressing relatively lower levels of ligand, see Fig 9B). Our simulations show that the ligand gradient promoted two parallel bands of Notch signalling, which border, and thereby define the position of vein formation (Fig 9B). These results recapitulate observed *in vivo* patterning processes (59), which have also been successfully reproduced by other mathematical models, notably the Sprinzak model (22,25).

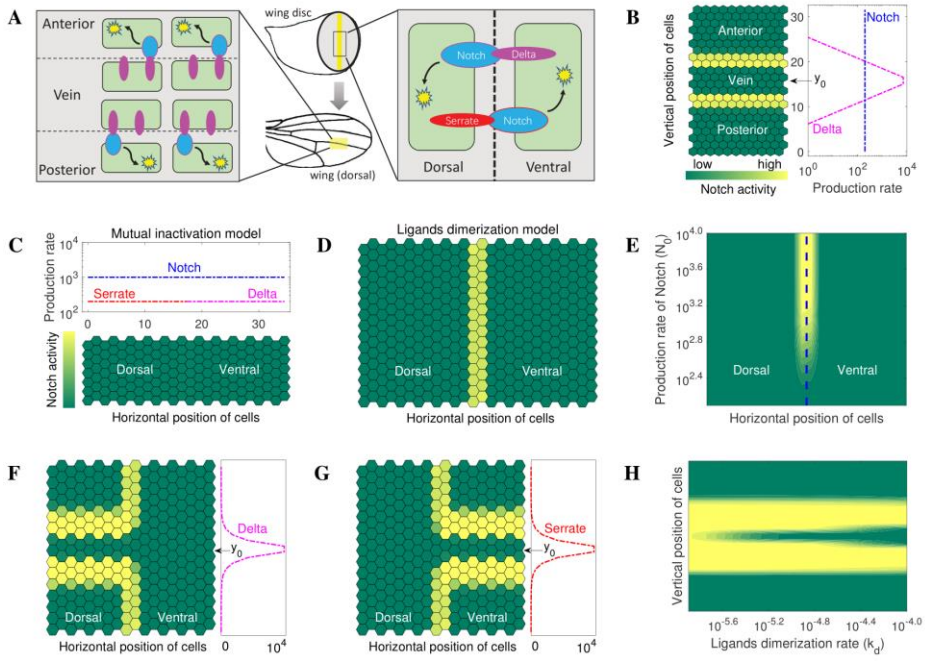

Figure 9. Modelling multicellular patterning. (A) Schematic representation of Notch signalling along the wing vein and along the dorsoventral boundary of the wing disc. Blue ovals represent Notch. Red ovals represent serrate. Purple ovals represent Delta. Notch activity is shown by yellow stars. (B) *In silico* replication of Notch signalling along the wing vein. The production rates of Delta decay exponentially from the center y_0, according to $L_0(y) = L_{max}/\exp(|y - y_0|)$. (C-H) *In silico* replication of Notch signalling around the dorsoventral boundary. (C-D) The ligand dimerization model, but not the mutual inactivation model, replicates the observed *in vivo* pattern of Notch signalling along the dorsal-ventral boundary in Drosophila wing discs.

< Figure 9 (continued). (E) Notch signaling at the dorsal-ventral boundary for different production rates of Notch show loss of the dorsal-ventral boundary as a function of decreasing Notch production rate, consistent with the results of *in vivo* experiments (60-61). (F-G) Ectopic expression of ligands induces Notch activity in dorsal cells (mediated by Delta) or ventral cells (mediated by Serrate) adjacent to the ectopic expression stripe where the production rates of ligands decay exponentially from the center y_0, similar to the profile described in B. (H) High production rates of Notch ligands stimulates ectopic Notch receptor activity when the ligands dimerization rate is low, consistent with previously published experimental data (55).

In contrast to wing vein formation, dorsal-ventral patterning of the Drosophila wing, in principle, presented a challenge to the mutual inactivation model since this model essentially precludes the co- availability of high levels of ligand monomers and Notch receptors in the same cells (see Eq. 5 and Eq. 6), an experimentally demonstrated prerequisite for this patterning (53). As mentioned previously (see Eq. 8 and Eq. 11), no such constraints exist in the dimerization model. During the early stages of wing development, a dorsal-ventral boundary (later the wing margin) divides wing cells into a dorsal compartment and a ventral compartment. Notch appears to be uniformly expressed in all cells whereas the Notch ligands are differentially expressed: Serrate expression is restricted to mainly dorsal cells, whilst Delta expression is chiefly localized to ventral cells (48, 49). To test if our model could reproduce wing dorsal-ventral patterning, we performed simulations in which Serrate and Delta were expressed in the dorsal and ventral compartments, respectively, whereas Notch was uniformly expressed throughout both compartments (Fig 9C). It has been established experimentally that the glycosyltransferase, Fringe, which is expressed dorsally, mediates the glycosylation of Notch and thus increases the affinity of Notch for Delta but reduces it for Serrate (50,51). Therefore, in our simulations, Notch in dorsal cells can only be trans-activated by Delta whereas Notch in ventral cells can only be trans-activated by Serrate, which is consistent with the experimental results induced by ectopic expression of Delta or Serrate in dorsal and ventral compartments (52-55).

Fig 9C, shows that a mutual inactivation model cannot generate a Notch-signalling-dependent dorsal-ventral boundary necessary for the establishment of a wing margin. As alluded to earlier, this is because Notch receptors and ligands are mutually exclusive within the same cell (Eq. 5-6). Consequently, there are insufficient levels of ligands in cells to trans-activate Notch signalling across the dorsal-ventral border. Strikingly, this not the case for the ligand dimerization model. Instead, we observe the robust dorsal-ventral patterning characteristic of normal wing morphogenesis observed *in vivo* (Fig 9D; 52-55). Several additional simulations further highlight the power of the ligand dimerization model (Fig 9E-9H). Decreasing the production rate of Notch results in the disappearance of Notch signaling at the dorsal-ventral border (Fig 9E), consistent with the classic Notch phenotype at the wing margin induced by a loss-of-function Notch

mutation *in vivo* (60,61). In Fig 9F-G, we replicated the experimental pattern of Notch signalling induced by ectopically expressed Delta or Serrate (52-55). Finally, our model simulations showed that high production rates of ligands, when the ligand dimerization rate is low, stimulated ectopic Notch receptor activity (Fig 9H). These results closely match the experimental findings of Flemming et al. (55). Interestingly, they showed, by means of expressing, during Drosophila wing disc development, serrate ligand mutants harbouring specific EGF domain deletions, that trans activation and cis inhibition could be uncoupled, that is, certain mutants could selectively promote Notch receptor trans activation but not execute cis inhibition.
Collectively, these results suggest that the ligand dimerization model can recapitulate *in vivo* tissue patterning processes.

DISCUSSION

In this study, we have taken a combined experimental and mathematical modelling approach to establish biochemically that Notch ligands can self-associate, and to dissect the potential role of this phenomenon in Notch signal transduction. Several lines of evidence are presented, centred chiefly on the Notch ligand, DLL4, which support the view that net signalling output from the Notch pathway is the product of ligand monomer-mediated trans activation (and cis-activation) counterposed by ligand oligomer-mediated cis inhibition of Notch receptor activity. Our new model is the first to propose a concrete molecular distinction, in terms of ligand configuration, between the two principal branches of Notch signalling, specifically that whereas ligand monomers promote Notch receptor transactivation, they are insufficient to account for cis inhibition which is induced via ligand dimers. Our model exhibits two features that are consistent with our molecular findings (see Figs 1-3). Firstly, cis inhibition is driven by ligand dimers, which can associate independently of receptor binding prior to receptor/ligand complex formation, that is, cis inhibition is not (strictly) a stepwise process of monomer to dimer transitions assembled on preformed receptor/ligand complexes at the cell membrane. Secondly, our modelling results do not depend on cis inhibition occurring at a particular subcellular compartment, such as the cell membrane. Rather, cis inhibition can also occur cytoplasmically (Fig 8D-F), in line with our observations that ligands lacking a transmembrane domain can efficiently self-associate and execute Notch receptor cis inhibition (see Fig 1 & Fig4; ZF & DAB unpublished data). These data are in agreement with earlier studies demonstrating cytoplasmic receptor/ligand binding (38) and raise the possibility that cytoplasmic ligand dimer-dependent cis inhibition of Notch activity could serve to block 'mis-firing' of the receptor prior to its expression at the plasma membrane. Related to this, whilst it is clear

that ligand dimers are necessary to drive cis inhibition, it not clear whether both ligand dimers and monomers are capable of stimulating receptor transactivation. To address this mathematically, we considered two cases: dimers promote cis inhibition/monomers promote transactivation; dimers promote cis inhibition/monomers and dimers can promote transactivation (Fig 6G). Our numerical simulations favour the former case (see Fig 6H). In further support of this idea is our finding that ligands harbouring mutations that abrogate self-association, stimulated Notch transactivation as efficiently as wild type ligands (see Fig 4A). The general applicability of our model in at both the cellular as well as the tissue level was demonstrated by the fact that it can recapitulate the results of previously published work (Fig 6I, Fig 9 and Fig SI 1).

Nandagopal et al. recently unveiled a previously overlooked dimension of Notch signalling, termed cis activation, which results from monomeric interactions between receptors and ligands expressed at the plasma membrane of the same cell (31). Our model could faithfully recapitulate the published experimental data (see Fig 7). Intriguingly, their mathematical model postulates that cis activation becomes cis inhibition, in a ligand concentration-dependent fashion, following binding of additional ligand monomers to ligand monomers complexed with Notch receptors at the cell membrane (presumably prior to receptor-bound monomer promoting cis activation). In light of this, and given the results of our own simulations, our model suggests that ligand dimerization may ensure a correct balance between cis inhibition and cis activation/trans activation (see Fig 7F).

To date, a major gap in Notch signalling knowledge is the precise nature of ligand, receptor and receptor/ligand complexes at a detailed molecular/structural level encompassing protein-protein interactions and the precise role of post-translation modifications such as glycosylation (39). In particular, it is unknown if trans receptor/ligand interactions differ conformationally from cis receptor/ligand interactions, and whether or not this could underlie or at least contribute to their distinct effects on receptor activity. Whilst such architectural details are currently lacking, a notable result of our mathematical modelling is that the size of ligand oligomers does not change the predictions of Notch receptor activity based on the ligand dimerization model (see Fig 8A-C). Additionally, Notch ligand oligomerization could have major implications for our understanding of the dynamics of the Notch pathway because regulation of dimer formation/dimer disassembly, might represent an extra point of Notch signalling strength control.

There are four mammalian Notch receptors and five mammalian Notch ligands, and the manifold potential receptor-ligand combinations will give rise to the different signalling outputs necessary for tissue patterning. It is established that different ligands can elicit unique cell fates. By example, JAG1 and DLL4 exert opposing effects on angiogenesis (40). Moreover, recent work has established

that ligands can stimulate either discrete pulses of Notch activity (in the case of DLL1) or a sustained period of signalling (in the case of DLL4) yielding distinct gene expression outcomes (24). In this context, two other potential facets of Notch signalling merit consideration. Whilst here we have uncovered a mechanistic role for ligand oligomerization, there is growing evidence that Notch receptors can also oligomerize/dimerize though the precise molecular consequences of this remains elusive (41,42). Moreover, since all Notch ligands share a common overall architecture, it could be of interest to investigate if there is a biological role for ligand hetero-oligomerization. Interestingly, simple biochemical experiments revealed that ligands can indeed hetero-oligomerize (see Fig SI 2 in S1 text). Such investigations coupled to refined mathematical models will help to fully disentangle this core signalling pathway.

In summary, we have delineated a previously unreported requirement for ligand dimerization in the cis inhibition of Notch receptor activity. This new mechanism could help determine the strength, the direction, the specificity and the nature of the output of the Notch signalling pathway. A novel mathematical model has been developed which successfully captures this process at the molecular and cellular level and, compellingly, can reproduce *in vivo* tissue patterning processes (50-55,59-61). It will be of interest to test if the same model can provide important insights into Notch-controlled physiological processes such as sprouting angiogenesis (43-45), and, given the global interest in the role of Notch signalling in human pathogenesis (46,47), to determine how these ideas will impact the design of novel therapeutic approaches to diseases.

METHODS

Parameters

The values of parameters in our model are determined based on previous works. The degradation rate of proteins is set $\beta = 0.1$ /hour, equivalent to a half-life of about 7 hours (56). The degradation of free Notch Intracellular Domain (S) is assumed to be $\beta_S = 0.5$ /hour because the signal in Notch signaling decays rapidly (57). Published data have suggested that Notch-related protein levels vary by up to a few hundred ng/ml (58), or a few thousand molecules per cell, thus the production rates of Notch ligands and receptors are assumed to be $L_0 = 200$ molecules/hour and $N_0 = 200$ molecules/hour, respectively. The trans-activation and cis-inhibition rate were derived from previous studies (26,27,28), the authors estimated their parameters by referring to relevant experimental reports. We assume that the ligand oligomerization rate $k_d = 10^{-4}/(\mathrm{molec}^{(n-1)} * \mathrm{hour})$, which is close to the order of magnitude of other parameters representing protein-protein interactions (Table 1).

TABLE 1. DESCRIPTION AND BASELINE VALUES OF PARAMETERS USED IN SIMULATIONS.

PARAMETER	Description	Values	Units	Source
L_0	Baseline production rate of Notch ligands	200	$\text{molec} * \text{hour}^{-1}$	Estimated from (58)
N_0	Baseline production rate of Notch receptors	200	$\text{molec} * \text{hour}^{-1}$	Estimated from (58)
k_d	Baseline oligomerization rate of ligand monomers (n=oligomer size)	$1 * 10^{-4}$	$\text{molec}^{-(n-1)} * \text{hour}^{-1}$	Assumed
k_t	Trans-activation rate	$5 * 10^{-5}$	$\text{molec}^{-1} * \text{hour}^{-1}$	(26,27,28)
k_{ci}	Cis-inhibition rate	$6 * 10^{-4}$	$\text{molec}^{-1} * \text{hour}^{-1}$	(26,27,28)
k_{ca}	Cis-activation rate	$5 * 10^{-6}$	$\text{molec}^{-1} * \text{hour}^{-1}$	Estimated from (31)
β	Degradation rate of typic proteins	0.1	hour^{-1}	Estimated from (56)
β_S	Degradation rate of free Notch Intracellular Domain	0.5	hour^{-1}	Estimated from (57)
k_r	Transportation rate of proteins from the cytoplasm to the membrane	0.1	hour^{-1}	Assumed

We performed parameter sensitivity analysis by quantifying the changes of Notch activity as function of the variations of all parameters (Fig SI 3). The results show that the sensitivity of most parameters is the same in three different experimental settings, thus showing a good consistency among the predictions of ligand dimerization model.

Numerical simulations

Numerical simulation, nonlinear curve-fitting and numerical analysis were performed on MATLAB R2021a. Runge–Kutta methods were used in all scenarios. In the simulations, the level of external ligand L_{ext} is context-dependent. For the single cell exposed to fixed level of trans-ligands in Fig 6B-C, Fig 6I, Fig 8A and Fig 8D, $L_{ext} = 1500$ molecules. For multiple interacting cells, the level of trans-ligand is the average of ligands in neighboring cells (Fig 9). Cis-activation of Notch is always ignored when external ligands-mediated trans-activation of Notch is present.

In Fig 6I, to mimic experimental conditions (22), the initial state of Notch ligand monomer, ligand dimer, Notch receptor and Notch activity in the cell is fixed at (500, 9500, 0, 0) molecules.
In Fig 9, the peak of gradient profile of Delta production rates in wing vein patterning (Fig 9B) and the peak of ectopic production rates of ligands in dorsal-ventral patterning (Fig 9F-G) is $L_{max} = 15000$ molecules/hour. The simulated cells are colored according to the level of Notch activity in each cell. Warmer color means higher Notch activity.

Cell culture, biochemistry and molecular biology
Human embryonic kidney 293T cells and U2OS osteosarcoma cells were cultured in DMEM (Gibco) supplemented with 10% fetal bovine serum (Gibco). Cell lines were typed using short tandem repeat analysis of the DNA and all cell lines were checked for mycoplasma with the MycoAlert kit (Lonza). Transfections, lentivirus production and cell infections, Western blotting and co-immunoprecipitations have been described previously (34,35). All lysis buffers contained a cocktail of protease inhibitors (phenylmethylsulfonyl fluoride, trypsin inhibitor, pepstatin A, leupeptin, aprotinin).

Recombinant protein production/ *in vitro* protein:protein interaction
Domains for recombinant protein production were cloned into the pET 28a vector in-frame to an N-terminal 6x HIS epitope. His epitope–tagged proteins were manufactured in Escherichia coli BL21(DE3). Following sonication (Misonix Sonicator 3000) in 3 mls ice-cold buffer / 50 ml bacterial culture (150 mM NaCl, 2.7 mM KCl, Na2HPO4, KH2PO4, 20 mM imidazole, 10 mM β-mercaptoethanol), proteins were purified onto 50 ul of Nickel- agarose beads (Qiagen) by 3 hours rolling at 4C. Beads were washed in 10 x 1 ml of the same buffer. Protein yields were determined by Bradford assay (Bio-Rad) and relative protein integrity and purity was determined by SDS-PAGE and Colloidal Blue staining (Invitrogen). Purified recombinant protein was incubated with 10 ul nickel beads in 1 ml of buffer for 2 hours at 4^{o}C with *in vitro* translated DLL4 proteins made using the TNT-coupled reticulocyte *in vitro* translation system (Promega). Beads were washed x10 with 1 ml of buffer. Proteins were separated by SDS-PAGE and associated proteins were detected by Western blot.

Plasmid construction
Unless otherwise stated, all cDNAs were fused in-frame with a Flag or an HA epitope tag and were cloned into the pLV lentiviral vector and pCS2 expression plasmid. Expression of these proteins was determined using antibodies directed against either epitope tag. Mutants were generated by site-directed mutagenesis using Phusion High-Fidelity DNA polymerase (Thermo fisher). All constructs were verified by Sanger sequencing (Macrogen).

Immunofluorescence
Immunostaining was performed as previously described (36,37) using Alexa Fluor 488 goat anti-mouse secondary antibodies (Thermo Fisher scientific). Imaging was performed with a Leica SP8 confocal microscope.

Luciferase reporter
Stable cell lines expressing epitope-tagged ligands and receptors were established via infection of cells with lentiviruses harbouring the appropriate ligand/receptor cDNA followed by selection with the encoded antibiotic (puromycin or neomycin). For 'cis inhibition' assays, cells co-expressing ligand, receptor and reporter were co-cultured with cells expressing ligand alone (to enable transactivation). Comparable results were obtained for co-culture ratios of 1:1, 1:2, 1:4. For transactivation analyses, cells stably expressing ligand alone were co-cultured with cells expressing receptor and reporter (1:1 ratio). For each experiment, cells were seeded in triplicate in 12-well plates. The Notch luciferase reporter harboured 10x RBPJ consensus binding sites, and was co-transfected with Renilla luciferase control plasmid. Transfection efficiencies (routinely >90%) were determined through visualization of co-transfected plasmid encoding the Tomato fluorescence reporter. Cells were lysed 36 hours post-plating, and luciferase activity was measured using a luciferase assay substrate (Promega). Luciferase activity was normalized by measuring Renilla luciferase activity (Promega). To confirm that luciferase activity was Notch-dependent, assays were performed in the presence or absence of 10 □M DAPT (Sigma). Receptor and ligand protein levels were determined by Western blotting. Experiments were performed three times.

Antibodies and drugs
Antibodies were obtained from the following sources: FLAG mouse M2 monoclonal (Sigma); anti-HA.11 mouse monoclonal (Covance); anti-HA rabbit polyclonal (Abcam); anti-FLAG rabbit (Sigma); anti-γ-tubulin (Sigma); anti-GFP (GeneTex); anti-His (Sigma). Anti- Calnexin (AbCam).

ACKNOWLEDGMENTS

We thank members of the Departments of Cell & Chemical Biology and the Leiden Institute of Biology for helpful discussions, technical advice and support, in particular Professor Peter ten Dijke, Jacob Visscher, Miguel Dickson and Yana van der Weegen.

CONFLICT OF INTERESTS

RMHM is associate editor of PLOS Computational Biology.

FUNDING

This work was supported by the Dutch Cancer Society (30861) to DAB, the Nederlandse Organisatie voor Wetenschappelijk Onderzoek grant NWO/ENW-VICI 865.17.004 to RMHM, the Cancer Genomics Centre Netherlands (CGC.NL) to XL. DC and HW were recipients of Chinese Scholarship Council (CSC) funding as part of the CSC Joint PhD Program on Artificial Intelligence and Bioscience between Leiden University and Xi'an Jiaotong University.

REFRENCES

1. Gazave E, Lapebie P, Richards GS, Brunet F, Ereskovsky AV, Degnan BM, et al. Origin and evolution of the Notch signalling pathway: an overview from eukaryotic genomes. BMC evolutionary biology. 2009;9(1):1--27.
2. Artavanis-Tsakonas S, Rand MD, Lake RJ. Notch signaling: cell fate control and signal integration in development. Science. 1999;284(5415):770--776.
3. Bray SJ. Notch signalling in context. Nature reviews Molecular cell biology. 2016;17(11):722--735.
4. Bray SJ. Notch signalling: a simple pathway becomes complex. Nature reviews Molecular cell biology. 2006;7(9):678--689.
5. Mumm JS, Kopan R. Notch signaling: from the outside in. Developmental biology. 2000;228(2):151--165.
6. Artavanis-Tsakonas S, Muskavitch MA. Notch: the past, the present, and the future. Current topics in developmental biology. 2010;92:1--29.
7. Koch U, Lehal R, Radtke F. Stem cells living with a Notch. Development. 2013;140(4):689--704.
8. Artavanis-Tsakonas S, Matsuno K, Fortini ME. Notch signaling. Science. 1995;268(5208):225--232.
9. Mašek J, Andersson ER. The developmental biology of genetic Notch disorders. Development. 2017;144(10):1743-1763.
10. Aster JC, Pear WS, Blacklow SC. The varied roles of notch in cancer. Annual Review of Pathology: Mechanisms of Disease. 2017;12:245--275.
11. Braune EB, Lendahl U. Notch—A goldilocks signaling pathway in disease and cancer therapy. Discovery medicine. 2016;21(115):189--196.
12. Ranganathan P, Weaver KL, Capobianco AJ. Notch signalling in solid tumours: a little bit of everything but not all the time. Nature Reviews Cancer. 2011;11(5):338--351.
13. Kopan R, Ilagan MXG. The canonical Notch signaling pathway: unfolding the activation mechanism. Cell. 2009;137(2):216--233.
14. D'Souza B, Meloty-Kapella L, Weinmaster G. Canonical and non-canonical Notch ligands. Current topics in developmental biology. 2010;92:73--129.
15. Henrique D, Schweisguth F. Mechanisms of Notch signaling: a simple logic deployed in time and space. Development. 2019;146(3):dev172148.
16. Sprinzak D, Blacklow SC. Biophysics of Notch signaling. Annual review of biophysics. 2021;50:157--189.
17. Fortini ME. γ-Secretase-mediated proteolysis in cell-surface-receptor signalling. Nature reviews Molecular cell biology. 2002;3(9):673--684.
18. Mumm JS, Schroeter EH, Saxena MT, Griesemer A, Tian X, Pan D, et al. A ligand-induced extracellular cleavage regulates γ-Secretase-like proteolytic activation of Notch1. Molecular cell. 2000;5(2):197--206.
19. Kitagawa M. Notch signalling in the nucleus: roles of Mastermind-like (MAML) transcriptional coactivators. The Journal of Biochemistry. 2016;159(3):287--294.
20. Guruharsha K, Kankel MW, Artavanis-Tsakonas S. The Notch signalling system: recent insights into the complexity of a conserved pathway. Nature Reviews Genetics. 2012;13(9):654--666.
21. del Álamo D, Rouault H, Schweisguth F. Mechanism and significance of cis-inhibition in Notch signalling. Current Biology. 2011;21(1):R40--R47.
22. Sprinzak D, Lakhanpal A, LeBon L, Santat LA, Fontes ME, Anderson GA, et al. Cis-interactions between Notch and Delta generate mutually exclusive signalling states. Nature. 2010;465(7294):86--90.
23. Collier JR, Monk NA, Maini PK, Lewis JH. Pattern formation by lateral inhibition with

feedback: a mathematical model of delta-notch intercellular signalling. Journal of theoretical Biology. 1996;183(4):429--446.

24. Nandagopal N, Santat LA, LeBon L, Sprinzak D, Bronner ME, Elowitz MB. Dynamic ligand discrimination in the notch signaling pathway. Cell. 2018;172(4):869--880.

25. Sprinzak D, Lakhanpal A, LeBon L, Garcia-Ojalvo J, Elowitz MB. Mutual inactivation of Notch receptors and ligands facilitates developmental patterning. PLoS computational biology. 2011;7(6):e1002069.

26. Stepanova D, Byrne HM, Maini PK, Alarcón T. A multiscale model of complex endothelial cell dynamics in early angiogenesis. PLoS Computational Biology. 2021;17(1):e1008055.

27. Boareto M, Jolly MK, Lu M, Onuchic JN, Clementi C, Ben-Jacob E. Jagged--Delta asymmetry in Notch signaling can give rise to a Sender/Receiver hybrid phenotype. Proceedings of the National Academy of Sciences. 2015;112(5):E402--E409.

28. Boareto M, Jolly MK, Ben-Jacob E, Onuchic JN. Jagged mediates differences in normal and tumor angiogenesis by affecting tip-stalk fate decision. Proceedings of the National Academy of Sciences. 2015;112(29):E3836--E3844.

29. Bentley K, Gerhardt H, Bates PA. Agent-based simulation of notch-mediated tip cell selection in angiogenic sprout initialisation. Journal of theoretical biology. 2008;250(1):25--36.

30. Boas SE, Merks RM. Tip cell overtaking occurs as a side effect of sprouting in computational models of angiogenesis. BMC systems biology. 2015;9(1):1--17.

31. Nandagopal N, Santat LA, Elowitz MB. Cis-activation in the Notch signaling pathway. Elife. 2019;8:e37880.

32. Luca VC, Jude KM, Pierce NW, Nachury MV, Fischer S, Garcia KC. Structural basis for Notch1 engagement of Delta-like 4. Science. 2015;347(6224):847--853.

33. Haltom AR, Jafar-Nejad H. The multiple roles of epidermal growth factor repeat *O*-glycans in animal development. Glycobiology 2015; 25(10): 1027-1042.

34. Roukens MG, Alloul-Ramdhani M, Moghadasi S, Op~den Brouw M, Baker DA. Downregulation of vertebrate Tel (ETV6) and Drosophila Yan is facilitated by an evolutionarily conserved mechanism of F-box-mediated ubiquitination. Molecular and cellular biology. 2008;28(13):4394--4406.

35. Roukens MG, Alloul-Ramdhani M, Vertegaal AC, Anvarian Z, Balog CI, Deelder AM, et al. Identification of a new site of sumoylation on Tel (ETV6) uncovers a PIAS-dependent mode of regulating Tel function. Molecular and cellular biology. 2008;28(7):2342--2357.

36. Roukens MG, Alloul-Ramdhani M, Baan B, Kobayashi K, Peterson-Maduro J, Van~Dam H, et al. Control of endothelial sprouting by a Tel--CtBP complex. Nature Cell Biology. 2010;12(10):933--942.

37. Forghany Z, Robertson F, Lundby A, Olsen JV, Baker DA. Control of endothelial cell tube formation by Notch ligand intracellular domain interactions with activator protein 1 (AP-1). Journal of Biological Chemistry. 2018;293(4):1229--1242.

38. Sakamoto K, Ohara O, Takagi M, Takeda S, KatsubeIntracellular K. Cell-Autonomous Association of Notch and Its Ligands: A Novel Mechanism of Notch Signal Modification. Developmental Biology 2000; 241(2):313-26.

39. Pandey A, Niknejad N, Jafar-Nejad H. Multifaceted regulation of Notch signaling by glycosylation. Glycobiology. 2021;31(1):8--28.

40. Benedito R, Roca C, Sörensen I, Adams S, Gossler A, Fruttiger M, Adams RH. The notch ligands Dll4 and Jagged1 have opposing effects on angiogenesis. Cell 2009;137(6):1124-35.

41. Kelly DF, Lake RJ, Middelkoop TC, Fan HY, Artavanis-Tsakonas S, Walz T. Molecular structure and dimeric organization of the Notch extracellular domain as revealed by electron microscopy. PloS one. 2010;5(5):e10532.

42. Zeronian MR, Klykov O, i~de Montserrat JP, Konijnenberg MJ, Gaur A, Scheltema RA, et al. Notch-Jagged signaling complex defined by an interaction mosaic. Proceedings of the National

Academy of Sciences. 2021;118(30).

43. Herbert SP, Stainier DY. Molecular control of endothelial cell behaviour during blood vessel morphogenesis. Nature reviews Molecular cell biology. 2011;12(9):551--564.

44. Carmeliet P, Jain RK. Molecular mechanisms and clinical applications of angiogenesis. Nature. 2011;473(7347):298--307.

45. Chung AS, Ferrara N. Developmental and pathological angiogenesis. Annual review of cell and developmental biology. 2011;27:563--584.

46. Andersson ER, Lendahl U. Therapeutic modulation of Notch signalling—are we there yet? Nature reviews Drug discovery. 2014;13(5):357--378.

47. Kuhnert F, Kirshner JR, Thurston G. Dll4-Notch signaling as a therapeutic target in tumor angiogenesis. Vascular cell. 2011;3(1):1--8.

48. Doherty, D., Feger, G., Younger-Shepherd, S., Jan, L.Y. and Jan, Y.N. Delta is a ventral to dorsal signal complementary to Serrate, another Notch ligand, in Drosophila wing formation. Genes & Development. 1996;10(4):421-434.

49. Lei, L., Xu, A., Panin, V.M. and Irvine, K.D. An O-fucose site in the ligand binding domain inhibits Notch activation. Development. 2003;130 (26): 6411–6421.

50. Irvine, K.D. Fringe, Notch, and making developmental boundaries. Current opinion in genetics & development. 1999; 9(4): 434-441.

51. Fortini, M.E. Notch signaling: the core pathway and its posttranslational regulation. Developmental cell. 2009; 16(5): 633-647.

52. Doherty, D., Feger, G., Younger-Shepherd, S., Jan, L.Y. and Jan, Y.N. Delta is a ventral to dorsal signal complementary to Serrate, another Notch ligand, in Drosophila wing formation. Genes & Development. 1996;10(4):421-434.

53. Celis de, J.F. and Bray, S. Feed-back mechanisms affecting Notch activation at the dorsoventral boundary in the Drosophila wing. Development. 1997; 124(17): 3241-3251.

54. Glittenberg, M., Pitsouli, C., Garvey, C., Delidakis, C. and Bray, S. Role of conserved intracellular motifs in Serrate signalling, cis‐inhibition and endocytosis. The EMBO journal. 2006; 25(20):4697-4706.

55. Fleming, R.J., Hori, K., Sen, A., Filloramo, G.V., Langer, J.M., Obar, R.A., Artavanis-Tsakonas, S. and Maharaj-Best, A.C. An extracellular region of Serrate is essential for ligand-induced cis-inhibition of Notch signaling. Development. 2013; 140(9): 2039-2049.

56. Eden, E., Geva-Zatorsky, N., Issaeva, I., Cohen, A., Dekel, E., Danon, T., et al. Proteome half-life dynamics in living human cells. Science. 2011; 331(6018): 764-768.

57. Wang, M. M. Notch signalling and Notch signalling modifiers. The international journal of biochemistry & cell biology. 2011; 43(11): 1550-1562.

58. Amsen, D., Blander, J.M., Lee, G.R., Tanigaki, K., Honjo, T., Flavell, R.A. Instruction of distinct CD4 T helper cell fates by different notch ligands on antigen-presenting cells. Cell. 2004; 117(4): 515-526.

59. Celis de, J.F., Bray, S. and Garcia-Bellido, A. Notch signalling regulates veinlet expression and establishes boundaries between veins and interveins in the Drosophila wing. Development. 1997; 124(10): 1919-1928.

60. Micchelli, Craig A., and Seth S. Blair. Dorsoventral lineage restriction in wing imaginal discs requires Notch. Nature. 1999; 401(6752): 473-476.

61. Diaz-Benjumea, Fernando J., and Stephen M. Cohen. Serrate signals through Notch to establish a Wingless-dependent organizer at the dorsal/ventral compartment boundary of the Drosophila wing. Development. 1995; 121(12): 4215-4225.

CHAPTER 4

Functional analyses of a human vascular tumor FOS variant identify a novel degradation mechanism and a link to tumorigenesis

J.Biol.Chem. (2018) 292 (52) 21282–21290

David G.P van Ijzendoorn[2]*, **Zary Forghany[1]*,** Frauke Liebelt[1], Alfred C. Vertegaal[1], Aart G. Jochemsen[1], Judith V.M.G Bovée[2], Karoly Szuhai[1], David A. Baker[1]

1. Leiden University Medical Center (LUMC), Department of Cell and Chemical Biology, Leiden
2. Leiden University Medical Center (LUMC), Department of Pathology, Leiden

***Joint first authors**

ABSTRACT

Epithelioid hemangioma is a locally aggressive vascular neoplasm, found in bones and soft tissue, whose cause is currently unknown, but may involve oncogene activation. FOS is one of the earliest viral oncogenes to be characterized, and normal cellular FOS forms part of the activator protein 1 (AP-1) transcription factor complex, which plays a pivotal role in cell growth, differentiation, and survival as well as the DNA damage response. Despite this, a causal link between aberrant FOS function and naturally occurring tumors has not yet been established. Here, we describe a thorough molecular and biochemical analysis of a mutant FOS protein we identified in these vascular tumors. The mutant protein lacks a highly conserved helix consisting of the C-terminal four amino acids of FOS, which we show is indispensable for fast, ubiquitin-independent FOS degradation via the 20S proteasome. Our work reveals that FOS stimulates endothelial sprouting and that perturbation of normal FOS degradation could account for the abnormal vessel growth typical of epithelioid hemangioma. To the best of our knowledge, this is the first functional characterization of mutant FOS proteins found in tumors.

INTRODUCTION

Epithelioid hemangioma is a neoplasm composed of cells that are phenotypically endothelial, which form vascular lumina or grow as solid sheets (see Fig. 1A) (1). Until now, the molecular underpinnings of this disease have yet to be deciphered. A recent cytogenetic and karyotypic survey of the disease, by us (2) and others (3), aimed at refining diagnoses and tumor classification, unearthed a significant number of FOS translocations raising the possibility that disruption of FOS function could promote tumorigenesis. The immediate-early FOS proto-oncogene is activated rapidly and transiently in response to a wide spectrum of cell stimuli (4–6), including serum, growth factors, cytokines, tumor-promoting agents, and DNA damage (7). The encoded FOS protein is a component of the crucial AP-1 transcription factor complex whose normal activity is regulated by controlled proteasome degradation (8, 9), and corruption of this process can lead to cell transformation (10–12). In this study, we have investigated the role of a novel mutant FOS protein we discovered in epithelioid hemangioma. We provide evidence that sustained expression of mutant FOS, due to loss of the C terminus, might drive the formation of vascular neoplasms by perturbing matrix metalloproteinase (MMP)4 production and the Notch signaling pathway that are known to facilitate both physiological and pathological angiogenesis. Operationally, we found that the extreme C terminus of FOS renders it intrinsically susceptible to ubiquitin-independent degradation by the 20S proteasome, an essential mechanism bypassed by tumor FOS proteins. This is the first report of a module that directly mediates ubiquitin independent proteasomal degradation (UIPD) and emphasizes the importance of UIPD in normal as well as tumor cells. Our work establishes the first demonstrable connection between mutations of FOS and the development of a naturally occurring tumor and unveils a potential, novel approach to treating epithelioid hemangioma by targeted inhibition of FOS or proteins whose expression is activated by FOS.

RESULTS AND DISCUSSION

C-terminally truncated FOS mutant is expressed in epithelioid Hemangioma

To determine whether mutations that disrupt the normal function of FOS might promote tumorigenesis, we investigated the role of a novel mutant FOS protein in epithelioid hemangioma (Fig. 1A). Fig. 1B depicts schematically a FOS deletion mutant (hereafter termed **FOSΔ**) that resulted from a FOSMBNL1 translocation (2). The mutant transcript is predicted to encode a FOS isoform lacking the C-terminal 95 amino acids but including the bZIP domain.

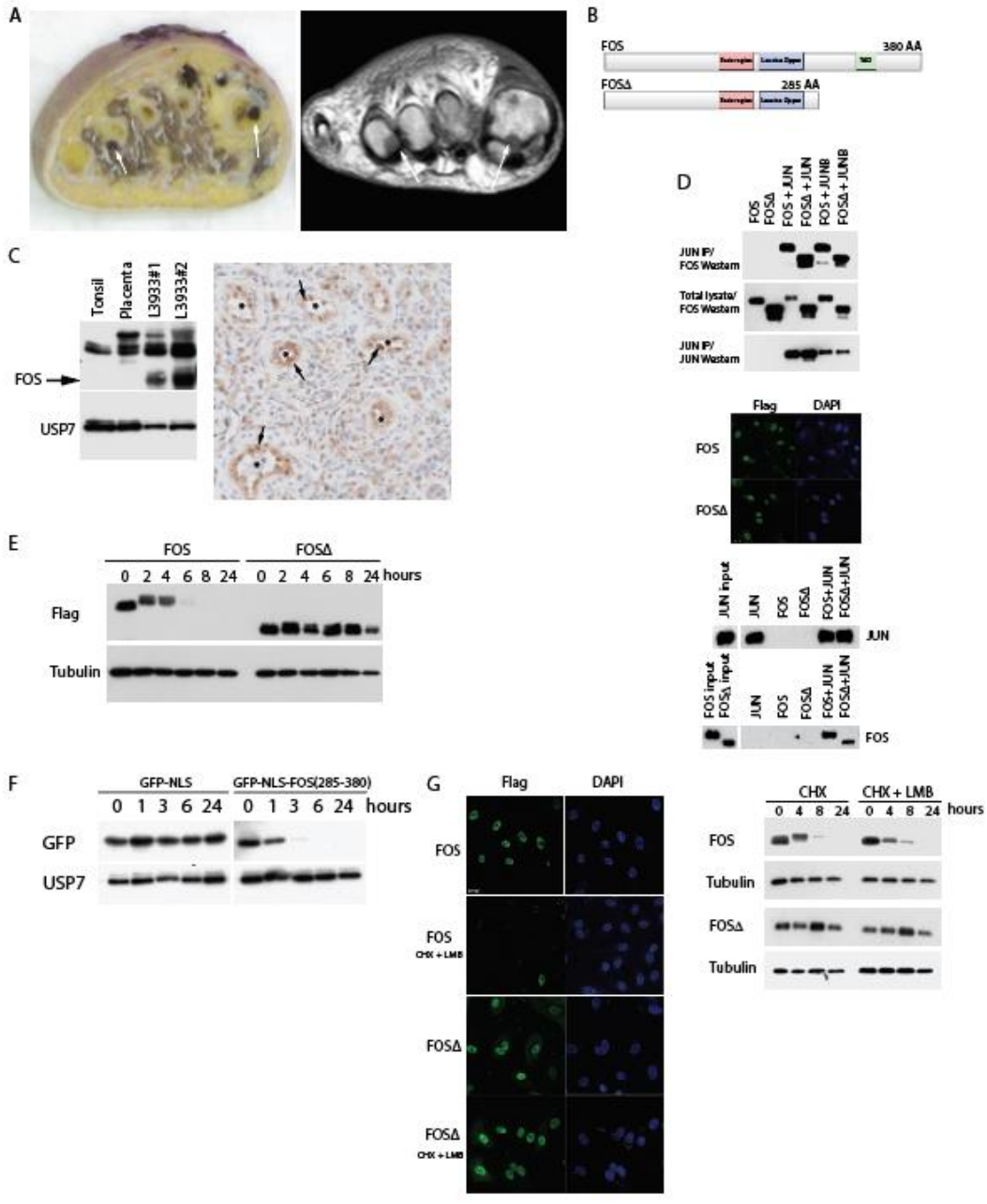

Figure 1. (A) epithelioid hemangioma case L3933. Left panel, gross specimen with polyostotic localization of a hemorrhagic tumor in the 1st and 4th metatarsal bones of the foot (arrows). Right panel, corresponding T1 weighted MR image. (B) tumor FOSΔ lacks the C-terminal 95 amino acids (including the C-terminal TAD). IP, immunoprecipitation.

< Figure 1 (continued). (C) left panel, Western blot of endogenous FOS proteins in control tonsil and placenta cell lysates compared with epithelioid hemangioma tumor cell lysates. Mutant FOSΔ protein is highlighted with an arrow. Right panel, high FOS expression (arrows) is indicated in the endothelial cells of epithelioid hemangioma tumor blood vessels (*). (D) AP-1 heterodimers were immunopurified from cells transfected with the indicated constructs (top panel). Immunofluorescence shows both FOS and FOSΔ localize to the nucleus (middle panel). FOS (and FOSΔ), JUN heterodimers bind to consensus AP-1 DNA-binding sites (bottom panel). (E) FOS stability assay on HUVECs stably expressing FOS or FOSΔ. (F) protein stability assay on HUVECs stably expressing either GFP or a GFP-FOS fusion (encompassing the C-terminal 95 amino acids of FOS). G, HUVECs expressing the indicated proteins were incubated with or without leptomycin B (LMB) in the presence of cycloheximide (CHX). Left panel, immunofluorescence. Right panel, Western blots.

Western blot analysis of lysates prepared from patient tumor tissue revealed a truncated FOS protein of the expected size demonstrating that the mutant FOS gene is translated *in vivo* (Fig. 1C). Moreover, immunohistochemistry of tumor sections showed a significant enrichment of FOS in tumor blood vessel endothelial cells (Fig. 1C). In common with wild-type FOS, FOSΔ is localized to the nucleus, can heterodimerize both with JUN and JUNB, and is efficiently associated with a consensus AP-1 DNA-binding site (Fig. 1D). However, FOSΔ protein levels appear to be significantly higher than wild-type FOS protein levels in patient cells (see Fig. 1C) suggesting that the mutant protein may be aberrantly stable. To elucidate the mechanistic consequences of this deletion, we first assessed FOS protein stability in primary endothelial cells. Fig. 1E shows that wild-type FOS, as expected, has a relatively short half-life of 1–2 h. By contrast, the deleted version of FOS is highly stable (half-life in excess of 8 h) suggesting that wild-type FOS harbors a destabilizing element in its C terminus, which is absent in the patient FOSΔ protein. In support of this view, tethering the FOS C terminus to a GFP reporter construct, led to a striking destabilization of the GFP protein (Fig. 1F), whereas a truncated FOS C terminus did not substantially alter the stability of the GFP reporter (see Fig. 3G). This observation is consistent with previous reports relating to FOS stability (8, 13, 14). Additionally, blocking nuclear export had no effect either on rapid FOS degradation or the stability of FOSΔ indicating that FOS is degraded in the nucleus and that FOΔS is resistant to this process (Fig. 1G). The above findings were confirmed in diploid HT1080 cell and HEK293T cells indicating that this mechanism is likely to be generic.

Mutant FOS is resistant to proteasomal degradation

To precisely delineate how FOS is degraded (and why FOSΔ is not), we monitored FOS protein degradation by the proteasome. Fig. 2Ashows that pharmacological inhibition of the proteasome, using either the specific inhibitor epoxomicin or MG132, markedly stabilized the wild-type FOS protein such that its half-life was comparable with that of the mutant FOSΔ protein. The half-life of FOSΔ was refractory to proteasome inhibition indicating that this deletion essentially lacks

the motif(s) responsible for this degradative process (Fig. 2A). It is established that degradation by the proteasome is either ubiquitin-dependent (15) or ubiquitin-independent (16–18), and multiple different mechanisms have been reported to regulate FOS stability (19–23).

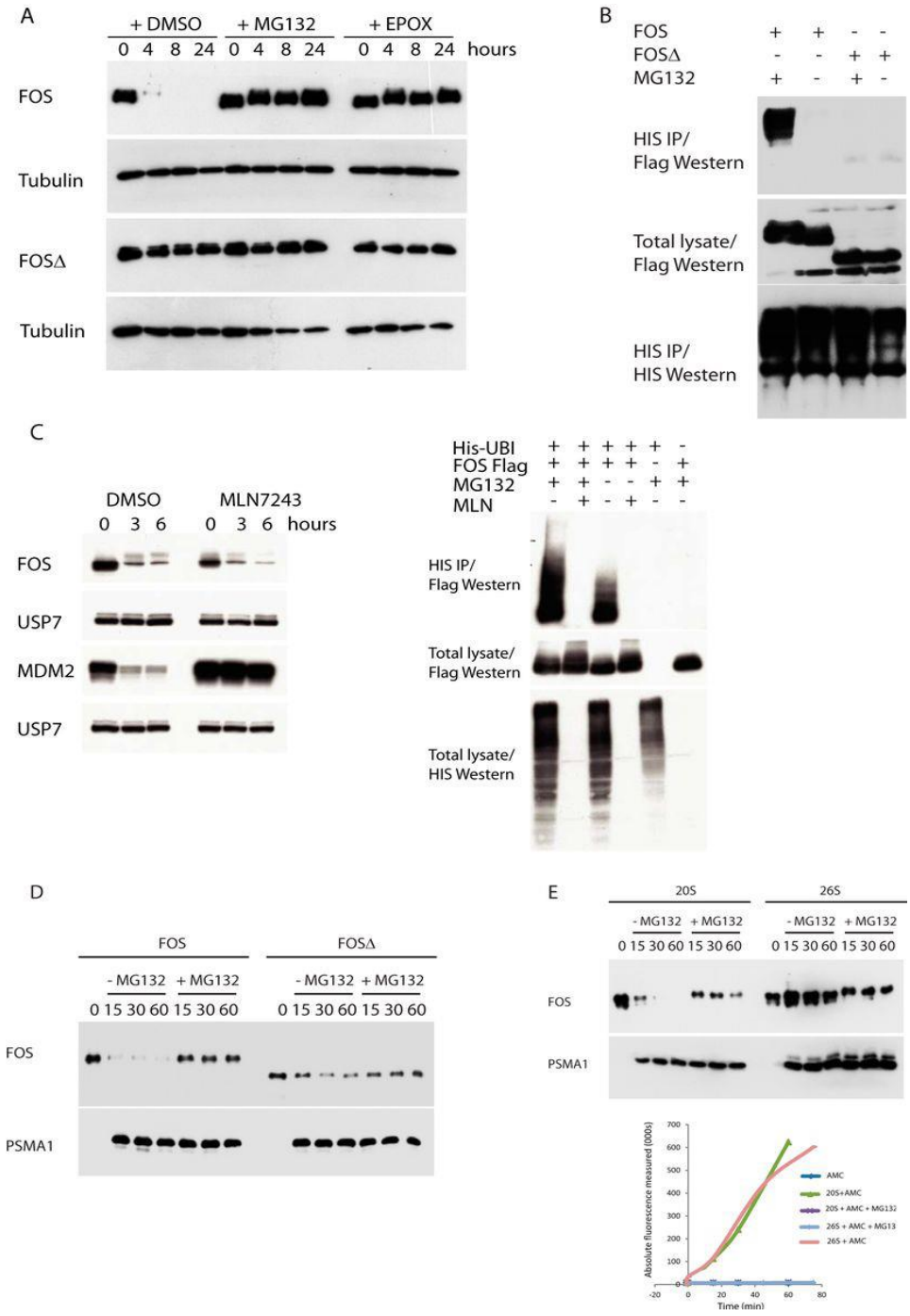

< Figure 2. (A) FOS stability assay on HUVECs stably expressing FOS or FOSΔ. (B) ubiquitin assay of cells transfected with the indicated constructs together with10x HIS epitope-tagged ubiquitin. (C) left

panel, FOS stability assay on HUVECs stably expressing FOS in the presence or absence of MLN7243. Right panel, ubiquitin assay of cells transfected with the indicated constructs and cultured in the presence or absence of MG132 and MLN7243. IP, immunoprecipitation. (D) *in vitro* translated FOS proteins were incubated with purified 20S proteasomes for the shown time course (minutes). 20S protein levels were determined by Western blotting using an antibody directed against PSMA1. 20S proteasome activity was independently quantified using the suc-Leu-Leu-Val-Tyr-AMC peptide (as shown in E). (E) experiment performed as in D.

In agreement with others (17, 18, 20), Fig. 2B shows that wild-type FOS can be ubiquitinated and subsequently processed by the 26S proteasome (see also Fig. 3C). We found that patient FOSΔ protein was not detectably ubiquitinated (Figs. 2B and 3C), and it fails to bind the E3 ligase, KDM2b, which has been demonstrated to stimulate FOS ubiquitination (see Fig. S1) (20). These observations could suggest that patient FOSΔ stabilization results from the absence of FOS ubiquitin-dependent degradation. However, several lines of evidence support the view that the tumor FOS protein is intrinsically resistant to ubiquitin-independent proteasome degradation and that this is the principal cause of its substantially increased stability. First, pharmacological inhibition of ubiquitin-activating enzymes ablated FOS ubiquitination but had no detectable impact on FOS degradation (Fig. 2C). In the same experiment, ubiquitin-dependent degradation of an established substrate of the proteasome, MDM2, was completely abrogated (see Fig. 2C). Second, wild-type non-ubiquitinated FOS but strikingly not FOSΔ was efficiently degraded by the 20S proteasome in a cell-free *in vitro* system (Fig. 2D). By contrast, FOS was completely resistant to degradation by the 26S proteasome under identical conditions (Fig. 2E). Consistent with these findings, selective inhibition of the 26S proteasome, but not the 20S proteasome (through shRNA-mediated abolition of the 19S subunits PSMD2 and PSMD14), stabilized the ubiquitinated fraction of FOS but failed to conspicuously inhibit FOS protein degradation, in sharp contrast to inhibiting both the 20S and 26S proteasomes (see Fig. 2A), indicating that degradation is principally via the 20S and not the 26S proteasome (Fig. S2). These results show that the FOS C terminus is vital for both ubiquitin-independent and ubiquitin-dependent proteasomal degradation and that both of these processes are lost by the mutant FOSΔ protein expressed in epithelioid hemangioma. These data show that the normal process of FOS degradation is severely corrupted in the tumor FOSΔ mutant protein and substantiate previous studies (21, 22) which suggest that FOS stability is governed chiefly by ubiquitin-independent proteasome degradation.

Mutant FOS lacks a conserved motif essential for ubiquitin-independent degradation by the 20S proteasome

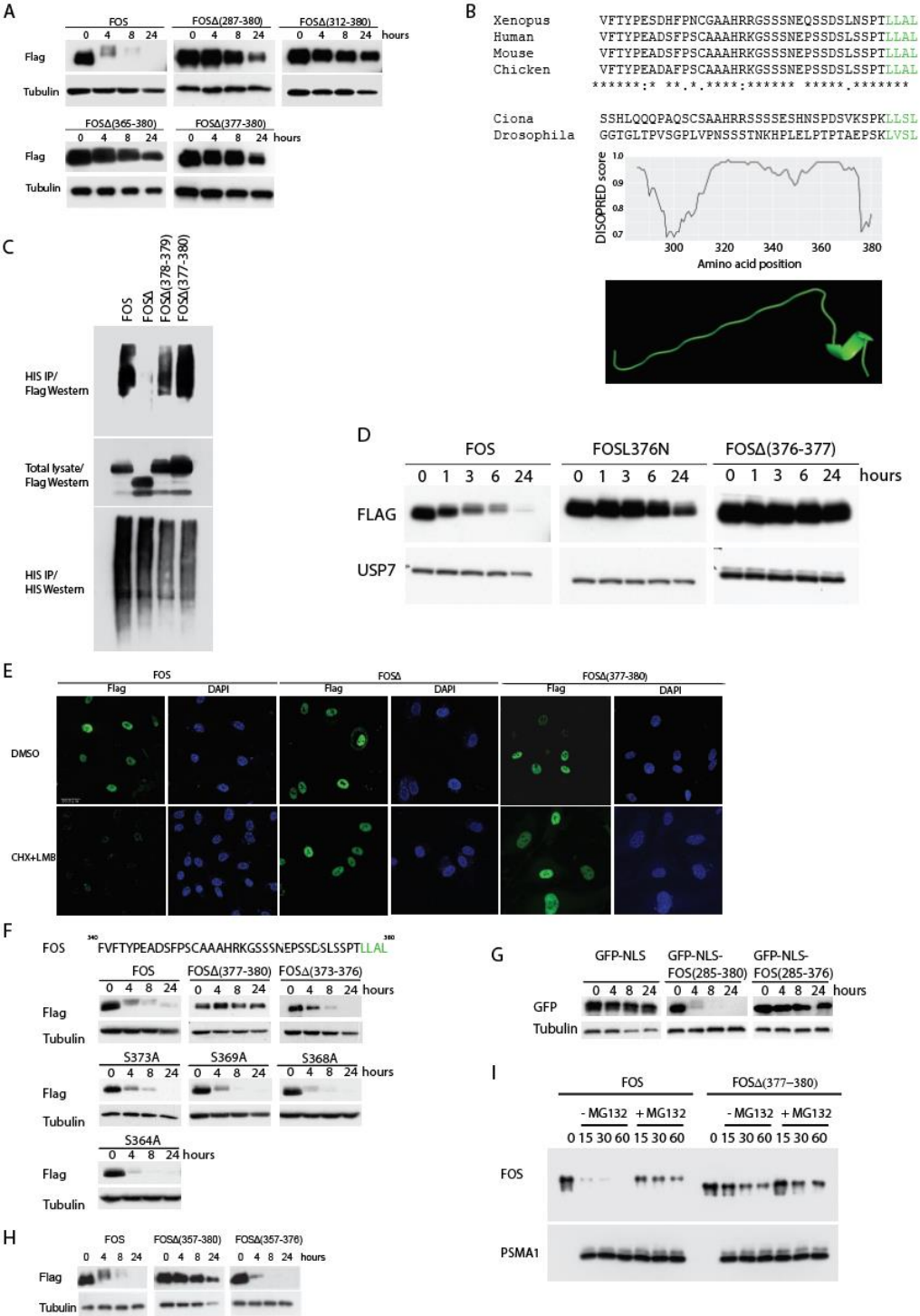
A
FOS
FOSΔ(287-380)
FOSΔ(312-380)
FOSΔ(365-380)
FOSΔ(377-380)
0 4 8 24 hours
Flag
Tubulin
B
Xenopus VFTYPESDHFPNCGAAHRRGSSSNEQSSDSLNSPTLLAL
Human VFTYPEADSFPSCAAAHRKGSSSNEPSSDSLSSPTLLAL
Mouse VFTYPEADSFPSCAAAHRKGSSSNEPSSDSLSSPTLLAL
Chicken VFTYPEADAFPSCAAAHRKGSSSNEPSSDSLSSPTLLAL
Ciona SSHLQQQPAQSCSAAHRRSSSSESHNSPDSVKSPKLLSL
Drosophila GGTGLTPVSGPLVPNSSSTNKHPLELPTPTAEPSKLVSL
DISOPRED score
Amino acid position
C
FOS
FOSΔ
FOSΔ(378-379)
FOSΔ(377-380)
HIS IP/ Flag Western
Total lysate/ Flag Western
HIS IP/ HIS Western
D
FOS
FOSL376N
FOSΔ(376-377)
0 1 3 6 24 hours
FLAG
USP7
E
FOS
FOSΔ
FOSΔ(377-380)
Flag
DAPI
DMSO
CHX+LMB
F
FOS 340 FVFTYPEADSFPSCAAAHRKGSSSNEPSSDSLSSPTLLAL 380
FOS
FOSΔ(377-380)
FOSΔ(373-376)
S373A
S369A
S368A
S364A
0 4 8 24 hours
Flag
Tubulin
G
GFP-NLS
GFP-NLS-FOS(285-380)
GFP-NLS-FOS(285-376)
0 4 8 24 hours
GFP
Tubulin
H
FOS
FOSΔ(357-380)
FOSΔ(357-376)
0 4 8 24 hours
Flag
Tubulin
I
FOS
FOSΔ(377–380)
- MG132 + MG132
0 15 30 60 15 30 60
FOS
PSMA1

< Figure 3. (A) FOS stability assay on HUVECs stably expressing the indicated FOS deletion mutants. (B) *ab initio* modeling of the FOS C terminus. (C) ubiquitin assay performed on cells transfected with the indicated constructs together with 10xHIS epitope-tagged ubiquitin. Cells were cultured in the presence of MG132. IP, immunoprecipitation. (D) FOS stability assay on HUVECs stably expressing the indicated FOS deletion mutants. (E) HUVECs expressing the indicated proteins were incubated with or without leptomycin B (*LMB*) in the presence of cycloheximide (*CHX*). FOS was visualized by immunofluorescence. (F) FOS stability assay on HUVECs stably expressing the indicated FOS deletion mutants. (G) protein stability assay on HUVECs stably expressing either GFP, a GFP-FOS fusion (encompassing the C-terminal 95 amino acids of FOS), or the same fusion lacking the last four amino acids of FOS. (H) FOS stability assay on HUVECs stably expressing the indicated FOS deletion mutants. FOSΔ _(357–380) lacks the C-terminal 23 amino acids (the IDR). FOSΔ (357–376) lacks the IDR but retains the C-terminal four amino acids. (I) *in vitro* FOS stability assay as described in Fig. 2, D and E.

To identify the motif(s) in the C terminus of FOS, which mediates FOS degradation (and is absent in FOSΔ), we performed a thorough mutational analysis of the FOS C terminus. Fig. 3A shows that deleting the C-terminal four amino acids was sufficient to strongly stabilize FOS and that lack of these amino acids might therefore cause the aberrant stability of the FOSΔ tumor protein. Ab initio modeling (24) of the FOS tail revealed that the C terminus is composed of an intrinsically unstructured region terminating in a helix composed of the C-terminal four amino acids (LLAL), which is conserved in all metazoans sequenced to date (Fig. 3B). Unlike FOSΔ, eliminating this helical region, either through point mutation or deletion, had no effect upon FOS ubiquitination (Fig. 3C). The same mutations did, however, efficiently block FOS degradation to the same degree as the tumor FOSΔ protein (see Fig. 3, D and E). The integrity of the four C-terminal amino acids, but not residues immediately adjacent to this motif, is absolutely required for priming FOS labileness (Fig. 3F). Deletions or point mutations of adjacent amino acids, which include consensus phosphorylation sites for ERK and GSK, failed to augment FOS stability. Indeed, a subset of these, in agreement with others (25), served to enhance FOS instability suggesting they play a role in stabilizing but not destabilizing the FOS protein (correspondingly, chemical inhibitors of MEK or deletion of the consensus ERK docking site had a comparable effect; data not shown). Three additional experiments further validated the importance of the C-terminal motif. One, deletion of the C-terminal four amino acids strongly attenuated the capacity of the FOS C terminus to destabilize GFP (Fig. 3G). Two, a deletion mutant lacking the intrinsically disordered region (IDR) (which is highly stable) but retaining the C-terminal four amino acids was as unstable as wild-type FOS (Fig. 3H). Three, in common with tumor FOSΔ, a mutant FOS lacking the C-terminal four amino acids, was highly resistant to 20S proteasomal degradation in a cell free *in vitro* assay (Fig. 3I). These data highlight a short helical region at the extreme C terminus of FOS as a crucial determinant of FOS stability and that perturbation of this motif leads to

pronounced FOS stabilization. A block in ubiquitin-independent degradation, due to loss of the extreme C terminus, is sufficient to explain mutant FOSΔ stability. Experiments in cell-free systems indicate that this motif can orchestrate direct proteasomal degradation of FOS independently of accessory proteins. IDRs have been reported to strongly influence proteasomal degradation (26), including the IDR found in the C terminus of FOS (27). Our data show that the FOS IDR, by itself, does not stimulate FOS degradation. Rather, a highly conserved helical motif at the extreme C terminus of FOS is essential for triggering ubiquitin-independent degradation.

FOS potently stimulates endothelial sprouting

Vascular neoplasms result from the dysregulated growth of endothelial cells or their precursors (1) and represent a unique model for gaining insights into pathological as well as normal angiogenesis. To recapitulate the cell biological consequences of the mutant FOS stabilization observed in epithelioid hemangioma, we ectopically expressed wild-type and mutant FOS proteins in primary HUVECs and assessed their ability to sprout. Fig. 4A shows that whereas loss of FOS abolished sprouting, sustained expression of FOS strongly promoted endothelial sprouting and the formation of stable endothelial cell networks. Similarly, expression of tumor FOSΔ or FOS lacking an intact C-terminal four amino acids strongly stimulated endothelial sprouting of HUVECs (Fig. 4B). This phenomenon was independent of marked changes in cell proliferation (Fig. 4B). Fig. S3 shows that FOS and FOSΔ also stimulated sprouting of human lung microvascular endothelial cells. The endothelial cell networks produced by cells expressing FOS and FOSΔ were stable and persistent. In this assay, ordinarily the sprouting network is relatively short-lived and collapses after 24 h. By contrast, endothelial cell networks expressing elevated levels of FOS and FOSΔ were sustained for at least 2 weeks of culture (sprouting networks expressing FOSΔ were noticeably more robust than the wild-type FOS-expressing networks), which resembles the illicit vessel growth observed in human epithelioid hemangioma.

Mutant FOS-driven sprouting is dependent on MMPs and Notch signaling

To understand the mechanistic basis of FOS-driven sprouting, we performed global transcriptome analyses of sprouts formed by FOS or patient FOS-Δ expressing primary endothelial cells. Fig. 4C shows a confirmatory qPCR of a selection of angiogenesis-control genes, which were up-regulated, including MMPs and components of the Notch-signaling pathway that are known to facilitate both physiological and pathological angiogenesis (28–33). ChIP analyses showed that endogenous FOS bound to these promoters (Fig. S4), and complementary ChIP studies showed that FOSΔ directly interacts with these promoters (see Fig. 4C).

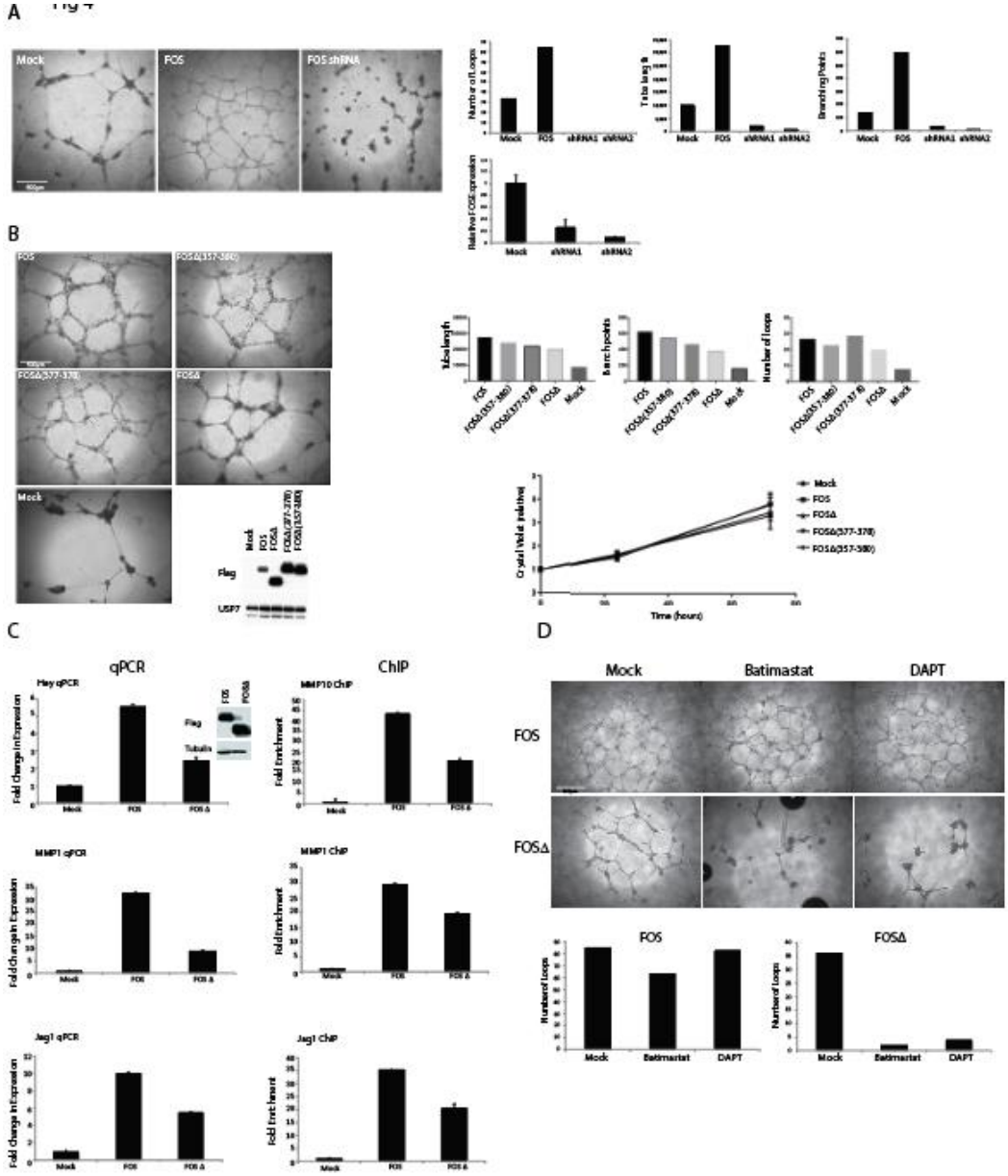

Figure 4. (A) HUVECs lacking endogenous FOS or ectopically expressing wild-type FOS were grown on Matrigel. A representative of several independent experiments is shown. Sprouting was quantified after 24 h using in-house computer software. Loss of FOS was determined by qPCR (lowermost graph). (B) Matrigel sprouting assay (see A) on HUVECs stably expressing the indicated FOS proteins. Lower graph, cell proliferation assay of the same HUVECs lines. Triplicate measurements were made at each time point. Values are means+/- S.E. of the mean.

< Figure 4 (continued). (C) left panel, expression levels of the indicated transcripts in HUVECs were determined by real-time qPCR. All values were averaged relative to TATA-binding protein (TBP), signal recognition particle receptor (SRPR), and calcium-activated neutral proteinase 1 (CAPNS1). Values were normalized against mock-treated cells. Values represent +/- S.D. (n = 3). Right panel, a ChIP analysis of FOS association with the indicated promoters in HUVECs stably expressing FOS or tumor FOSΔ. Three different primer sets were used for each promoter region. A single representative is shown (all three gave similar results). Results are presented as mean fold changes in recovery (as a fraction of input) relative to the Mock infected cells. Error bars represent the standard deviation (n = 3). Relative FOS and FOSΔ protein levels were determined by Western blotting. (D) HUVECs stably expressing the indicated FOS proteins were grown on Matrigel in the presence or absence of the MMP inhibitor, batimastat (10 μM), or the γ-secretase inhibitor, DAPT (10 μM). Sprouting was quantified after 48 h.

Our experiments uncover a previously unreported role for FOS as an activator of endothelial sprouting and show that patient FOSΔ could stimulate illicit endothelial sprouting by activating the Notch signaling pathway and increasing the production of MMPs. In this regard, it is notable that inhibitors of either MMPs or Notch signaling significantly inhibited the sprouting of FOSΔ-expressing endothelial cells (Fig. 4D). The same inhibitors had relatively little effect on cells expressing wild-type FOS under these assay conditions. This could reflect the fact that both MMP production and Notch signaling (as well as other FOS target pathways, see under "Transcriptome profiling) were significantly more augmented in cells expressing wild-type FOS compared with cells expressing FOSΔ (presumably because FOSΔ lacks the C-terminal TAD). Accordingly, a recently reported small molecule inhibitor of FOS (34), which has advanced to human Phase II clinical trials for the treatment of rheumatoid arthritis, efficiently inhibited FOS-driven endothelial sprouting (Fig. S5). In summary, our data have uncovered a previously unreported role for FOS in stimulating endothelial cell sprouting. We show that sustained expression of FOS, due to loss of the C terminus, could drive the formation of vascular neoplasms. By analyzing the C-terminal region of FOS, which is deleted in epithelioid hemangioma, we have discovered a highly conserved motif at the extreme C terminus of FOS that is critical for controlling its stability by rendering it intrinsically susceptible to ubiquitin-independent degradation by the 20S proteasome. Our work suggests that targeted inhibition of FOS or proteins whose expression is activated by FOS might represent a legitimate novel approach to treating these locally aggressive tumors.

EXPERIMENTAL PROCEDURES

Patient samples

Epithelioid hemangioma case L3933 was acquired from the archives of the Leiden University Medical Center (LUMC), Leiden, The Netherlands. The diagnosis of epithelioid hemangioma was established by a bone and soft tissue pathologist (J. V. M. G. B.). The study was approved by the LUMC Medical Ethical Commission under protocol B17006.

Cell culture, biochemistry, and molecular biology

Plasmid and shRNA construction Human FOS cDNAs fused in-frame with a FLAG or an HA epitope tag were cloned into the pLV lentiviral vector and pCS2expression plasmid. Gene-specific shRNA-expressing lentiviruses were generated using the TRC2-pLKO lentiviral vector system.

Transcriptome profiling

RNA was isolated from HUVECs stably expressing FOS or FOSΔ by treatment with TRIzol (Invitrogen) column purification (Direct-zol RNA isolation kit-Zymo Research). RNA quality was verified with a Bioanalyzer (Agilent), and sequencing was performed on the Illumina HiSeq 2500 (Genome Scan). HUVEC transcript sequencing data have been deposited under GenBankTM accession no. PRJNA390521.

Analysis of mRNA expression

RNA isolation, first strand cDNA synthesis, and analysis of expression of transcripts by quantitative PCR were performed as described previously (33).

Ubiquitination assay

293T cells were transfected with the appropriate plasmids. Proteasome degradation was blocked for 8 h with 10 M MG132 (Sigma). HIS pulldowns were performed as described previously (36).

HUVEC sprouting assay

96-well plates were coated with 60 l of Matrigel/well 30 min prior to seeding HUVECs. EGM-2 medium was supplemented with 50 ng/ml recombinant human VEGF 165 (R & D Systems). Images were taken at multiple time points. Analysis of the sprouting was performed with Stacks (in-house software, Department of Molecular Cell Biology, LUMC).

Immunohistochemistry/Immunofluorescence
Staining was performed on 4-m tissue sections. Paraffin was removed with xylene, and sections were rehydrated in a gradient of ethanol. Exogenous peroxidase was blocked using 0.3% H2O2. Microwave antigen retrieval was performed in TrisEDTA (pH 9.0). FOS antibody was used at a 1:400 concentration. Antibody was detected with (3,3'-diaminobenzidine), and counterstaining was performed with hematoxylin. Immunostaining was performed as described previously (37)

Proteasome purification and *in vitro* degradation assay
HT1080 cells, stably expressing GFP-PSMD12, were collected by trypsinization, washed 3x in phosphate buffered saline (PBS) and lysed in buffer containing 40mM Tris pH 7.5, 40mM NaCl, 2mM β-mercaptoethanol, 5mM MgCl2, 2mM ATP, 10% glycerol and 0.5 % NP40. Lysates were cleared by ultracentrifugation at 36000rpm for 45 min at 4˚C. Cleared lysates were incubated for 3 hours at 4˚C with prewashed Chromotek GFP-Trap® bead slurry. Beads were washed 4x in wash buffer containing 40mM Tris pH 7.5, 40 mM NaCl, 2mM β-mercapthoethanol, 5 mM MgCl2, 2 mM ATP and 10% glycerol. Activity of purified 26S proteasome and 20S proteasome (LifeSciences) was measured using 100µM suc-LLVY-AMC substrate (Bachem) in a buffer containing 50mM Tris pH 7.5, 40mM KCl, 5mM MgCl2, 1mM DTT (0.5mM ATP for the 26S proteasome) (Abs/Em= 353/442 nm). *In vitro*-translated FOS proteins were prepared using the TNT-coupled reticulocyte in vitro translation system (Promega). Cell-free degradation assays were performed as described previously (38).

Protein–DNA interaction assays
In vitro-translated protein was made as above. 50 pmol of biotinylated double-stranded oligonucleotides harboring three contiguous AP-1 DNA-binding sites were coupled to MyOne streptavidin C1 beads (Invitrogen). Reactions were incubated at 4 °C with vigorous shaking for 30 min in the presence of 1 g of poly(dI/dC), 4 mM spermidine, 50 mM KCl, 10 mM HEPES (pH 7.6), 5 mM MgCl2, 10 mM Tris (pH 8), 0.05 mM EDTA (pH 8), 0.1% Triton X-100, and 20% glycerol. Beads were successively washed three times with the aforementioned buffer. Associated proteins were eluted in Laemmli buffer, and protein–DNA interactions were determined by Western blotting.

ChIP
ChIP analyses were performed on confluent 10-cm tissue culture dishes of HUVECs as described previously (35).

Antibodies, growth factor, and drugs

Antibodies were obtained from the following sources: Flag mouse M2 monoclonal (Sigma-Aldrich); anti-HA.11 mouse monoclonal (Covance); anti- Ha rabbit polyclonal (Abcam); anti-FOS rabbit (Sigma); anti-Flag rabbit (Sigma); anti-USP7 rabbit (Bethyl); anti-γTubulin (Sigma); anti-GFP (GeneTex); anti-His (Sigma); anti-PSMA1 (Sigma). Drugs were used at the following concentrations: MG132 (Sigma), 10 μM; Cycloheximide (Sigma), 50 μg/ml; Epoxomicin (Sigma), 10μM; Leptomycin B (Sigma) 35 nM ; MLN-7243 (Active Biochem), 10 μM; Batimastat (Calbiochem), 10 μM; DAPT (Tocirs Bioscience), 10 μM.

Bioinformatics
Rosetta (RosettaCommons) was used for structure prediction of the FOS C terminus (24). Secondary structure was predicted using Psipred (version 4.01, UCL). Degree of disorder was predicted using Disopred (version 3.16, UCL).

ACKNOWLEDGMENTS

We thank members of the Departments of Molecular Cell Biology and Pathology for helpful discussions, technical advice and support in particular Hans van Dam and Professor Peter ten Dijke. We acknowledge Inge Briaire-de Bruijn for her technical assistance with the IHC. We are indebted to Dr. Hans Vrolik for designing computer software for quantifying sprouting assays. This work was supported by the Dutch Cancer Society to DAB (30861), an ERC grant to ACOV (310913).

AUTHOR CONTRIBUTIONS

ZF and DGP vI performed the majority of experiments. FL and ACV helped design and performed *in vitro* proteasome studies. JVMGB and AGJ offered expert advice. KS and DAB supervised the study. All authors read and approved the paper.

COMPETING FINANCIAL INTERESTS

The authors declare no competing financial interests.

REFERENCES

1. Rosenberg, A. E., and Bovée, J. V. (2013) in WHO Classification of Tumours of Soft Tissue and Bone (Fletcher, C. D., Bridge, J. A., Hogendoorn, P. C., and Mertens, F., eds) pp. 333–334, IARC Press, Lyon, France
2. van IJzendoorn, D. G., de Jong, D., Romagosa, C., Picci, P., Benassi, M. S., Gambarotti, M., Daugaard, S., van de Sande, M., Szuhai, K., and Bovée, J. V. (2015) Fusion events lead to truncation of FOS in epithelioid hemangioma of bone. Genes Chromosomes Cancer 54, 565–574
3. Huang, S. C., Zhang, L., Sung, Y. S., Chen, C. L., Krausz, T., Dickson, B. C., Kao, Y. C., Agaram, N. P., Fletcher, C. D., and Antonescu, C. R. (2015) Frequent FOS gene rearrangements in epithelioid hemangioma: A molecular study of 58 cases with morphological reappraisal. Am. J. Surg. Pathol. 39, 1313–1321
4. Wagner, E. F. (2001) AP-1 reviews. Oncogene 20, 2333–2497
5. Johnson, R. S., Spiegelman, B. M., and Papaioannou, V. (1992) Pleiotropic effects of a null mutation in the c-fos proto-oncogene. Cell 71, 577–586
6. Shaulian, E., and Karin, M. (2002) AP-1 as a regulator of cell life and death. Nat. Cell Biol. 4, E131–E136
7. Haas, S., and Kaina, B. (1995) c-Fos is involved in the cellular defence against the genotoxic effect of UV radiation. Carcinogenesis 16, 985–991
8. Wilson, T., and Treisman, R. (1988) Fos C-terminal mutations block down-regulation of c-fos transcription following serum stimulation. EMBO J. 7, 4193–4202
9. Gomard, T., Jariel-Encontre, I., Basbous, J., Bossis, G., Moquet-Torcy, G., Mocquet-Torcy, G., and Piechaczyk, M. (2008) Fos family protein degradation by the proteasome. Biochem. Soc. Trans. 36, 858–863
10. Van Beveren, C., van Straaten, F., Curran, T., Müller, R., and Verma, I. M. (1983) Analysis of FBJ-MuSV provirus and c-fos (mouse) gene reveals that viral and cellular fos gene products have different carboxy termini. Cell 32, 1241–1255
11. Eferl, R., and Wagner, E. F. (2003) AP-1: A double-edged sword in tumorigenesis. Nat. Rev. Cancer 3, 859–868
12. Monje, P., Marinissen, M. J., and Gutkind, S. (2003) Phosphorylation of the carboxyl-terminal transactivation domain of c-Fos by extracellular signalregulated kinase mediates the transcriptional activation of AP-1 and cellular transformation induced by platelet-derived growth factor. Mol. Cell. Biol. 23, 7030–7043
13. Ferrara, P., Andermarcher, E., Bossis, G., Acquaviva, C., Brockly, F., Jariel- Encontre, I., and Piechaczyk, M. (2003) The structural determinants responsible for c-Fos protein proteasomal degradation differ according to the conditions of expression. Oncogene 22, 1461–1474
14. Acquaviva, C., Brockly, F., Ferrara, P., Bossis, G., Salvat, C., Jariel-Encontre, I., and Piechaczyk, M. (2001) Identification of a tripeptide motif involved in the control of rapid proteasomal degradation of c-Fos protooncogene during the G0-to-S phase transition. Oncogene 20, 7563–7572
15. Collins, G. A., and Goldberg, A. L. (2017) The logic of the 26S proteasome. Cell 169, 792–806
16. Erales, J., and Coffino, P. (2014) Ubiquitin-independent proteasomal degradation. Biochem. Biophys. Acta 1843, 216–221
17. Jariel-Encontre, I., Bossis, G., and Piechaczyk, M. (2008) Ubiquitin-independent degradation of proteins by the proteasome. Biochem. Biophys. Acta 1786, 153–177
18. Ben-Nissan, G., and Sharon, M. (2014) Regulating the 20S proteasome ubiquitin-independent degradation pathway. Biomolecules 4, 862–884
19. Stancovski, I., Gonen, H., Orian, A., Schwartz, A. L., and Ciechanover, A. (1995) Degradation of the proto-oncogene product c-Fos by the ubiquitin proteolytic system in vivo and in vitro: identification and characterization of the conjugating enzymes. Mol. Cell. Biol. 15, 7106–7116
20. Han, X.-R., Zha, Z., Yuan, H. X., Feng, X., Xia, Y. K., Lei, Q. Y., Guan, K. L., and Xiong, Y. (2016)

KDM2B/FBXL10 targets c-Fos for ubiquitylation and degradation in response to mitogenic stimulation. Oncogene 35, 4179- 419
21. Adler, J., *et al.* (2010) c-Fos proteasomal degradation is activated by a default mechanism and its regulation by NAD(P)H:Quinone oxidoreductase 1 determines c-Fos serum response kinetics. *Mol. Cell. Biol.* 30, 3767–3778
22. Sasaki, T., Kojima, H., Kishimoto, R., Ikeda, A., Kunimoto, H., and Nakajima, K. (2006) Spatiotemporal regulation of c-Fos by ERK5 and the E3 ubiquitin ligase UBR1, and its biological role. *Mol. Cell* 24, 63–75
23. Bossis, G., Ferrara, P., Acquaviva, C., Jariel-Encontre, I., and Piechaczyk, M. (2003) c-Fos proto-oncogene is degraded by the proteasome independently of its own ubiquitinylation *in vivo*. *Mol. Cell. Biol.* 23, 7425–7436
24. Baker, D. (2014) Protein folding, structure prediction and design. *Biochem. Soc. Trans.* 42, 225–229
25. Okazaki, K., and Sagata, N. (1995) The Mos/MAP kinase pathway stabilizes c-Fos by phosphorylation and augments its transforming activity in NIH 3T3 cells. *EMBO J.* 14, 5048–5059
26. Prakashm S., Tian, L., Ratliff, K. S., Lehotzky, R. E., and Matouschek, A.(2004) An unstructured initiation site is required for efficient proteasome- mediated degradation. *Nat. Struct. Mol. Biol.* 11, 830–837
27. Campbell, K. M., Terrell, A. R., Laybourn, P. J., and Lumb, K. J. (2000) Intrinsic structural disorder of the C-terminal activation domain from the bZIP transcription factor Fos. *Biochemistry* 39, 2708–2713
28. Heo, S.-H., Choi, Y. J., Ryoo, H. M., and Cho, J. Y. (2010) Expression profiling of ETS and MMP factors in VEGF-activated endothelial cells: Role of MMP-10 in VEGF induced angiogenesis. *J. Cell. Physiol.* 224, 734–742
29. Lee, S., Jilani, S. M., Nikolova, G. V., Carpizo, D., and Iruela-Arispe, M. L. (2005) Processing of VEGF-A by matrix metalloproteinases regulates bioavailability and vascular patterning in tumors. *Cell Biol. J.* 169, 681–691
30. Juncker-Jensen, A., Deryugina, E. I., Rimann, I., Zajac, E., Kupriyanova, T. A., Engelholm, L. H., and Quigley, J. P (2013) Tumor MMP-1 activates endothelial PAR1 to facilitate vascular intravasation and metastatic dissemination. *Cancer Res*. 73, 4196–4211
31. Kopan, R., and Ilagan, M. X. (2009) The canonical Notch signaling pathway: unfolding the activation. *Cell* 137, 216–233
32. Herbert, S. P., and Stainier, D. Y. (2011) Molecular control of endothelial cell behavior during blood vessel morphogenesis. *Nat. Rev. Mol. Cell Biol.* 12, 551–564
33. Adams, R. H., and Alitalo, K. (2007) Molecular regulation of angiogenesis and lymphangiogenesis. *Nat. Rev. Mol. Cell Biol.* 8, 464–478
34. Ye, N., Ding, Y., Wild, C., Shen, Q., and Zhou, J. (2014) Small molecule inhibitors targeting activator protein 1 (AP-1). *J. Med. Chem.* 57, 6930–6948
35. Roukens, M. G., Alloul-Ramdhani, M., Baan, B., Kobayashi, K., Peterson- Maduro, J., van Dam, H., Schulte-Merker, S., and Baker, D. A. (2010) Control of endothelial sprouting by a Tel-CtBP complex. *Nat. Cell Biol.* 12, 933–942
36. Roukens, M. G., Alloul-Ramdhani, M., Moghadasi, S., Op den Brouw, M., and Baker, D. A. (2008) Downregulation of vertebrate Tel (ETV6) and *Drosophila* Yan is facilitated by an evolutionarily conserved mechanism of F-box-mediated ubiquitination. *Mol. Cell. Biol.* 28, 4394–4406
37. Roukens, M. G., Alloul-Ramdhani, M., Vertegaal, A. C., Anvarian ,Z., Balog, C. I., Deelder, A. M., Hensbergen, P. J., and Baker, D. A. (2008) Identification of a new site of sumoylation on Tel (ETV6) uncovers a PIAS-dependent mode of regulating Tel function. *Mol. Cell. Biol*. 28, 2342–2357
38. Asher, G., Tsvetkov, P., Kahana, C., and Shaul, Y. (2005) A mechanism of ubiquitin-independent proteasomal degradation of the tumor suppressors p53 and p73. *Genes Dev.* 19, 316–321

SUPPLEMENTARY FIGURES

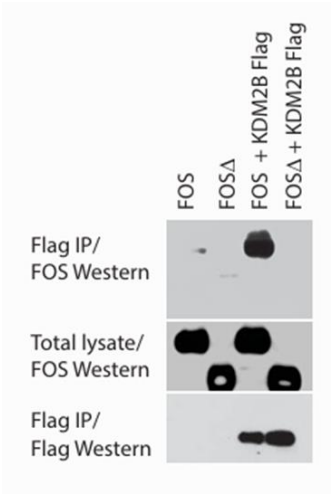

Supplementary Figure 1. FOSΔ does not interact with the E3 ligase KDM2B. Complexes were immunopurified from cells transfected with the indicated constructs. Western blots were performed as shown.

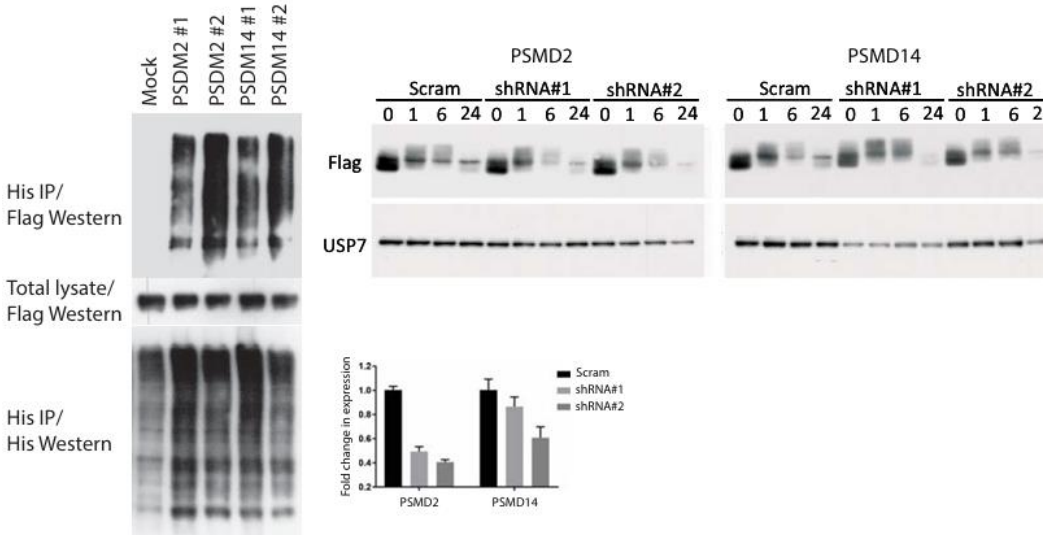

Supplementary Figure 2. Left Panel: A representative ubiquitin assay of cells transfected with the indicated constructs and cultured in the absence of MG132. Two different shRNA probes per gene were used. Upper right panel: FOS stability assay. Bottom right panel: Stable knockdown of PSMD2 and PSMD14 in HUVECs was determined by qPCR.

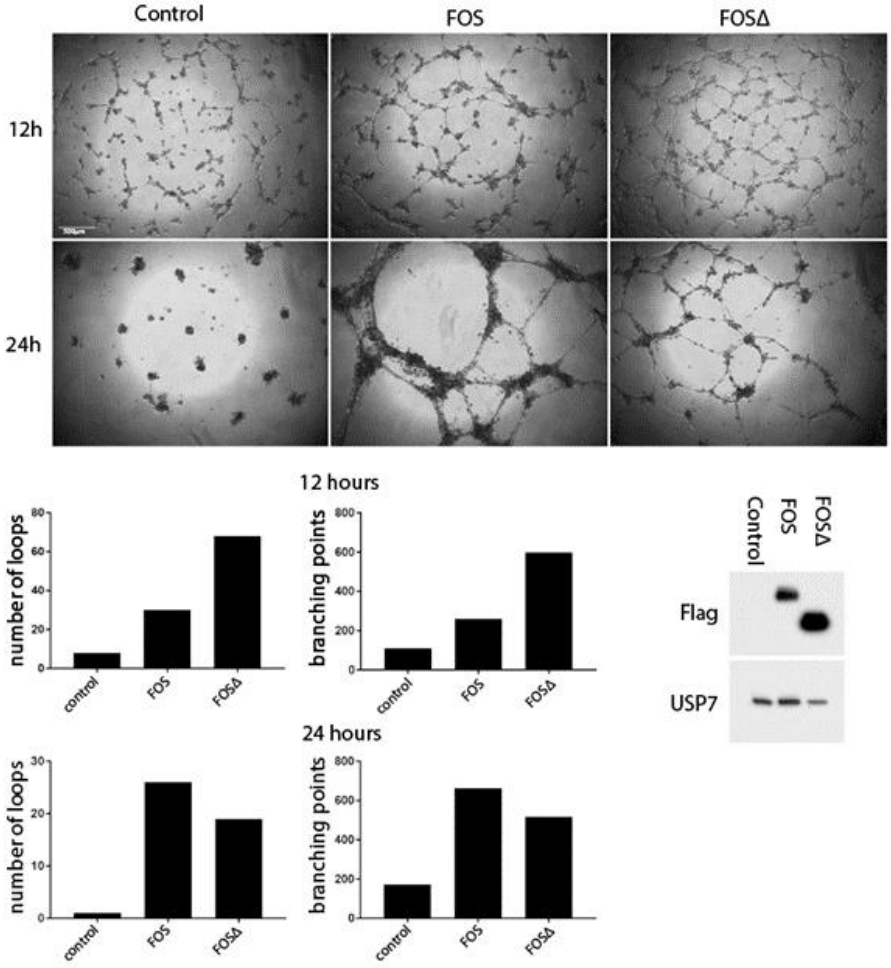

Supplementary Figure 3

HLMVECs ectopically expressing wild type FOS or FOSΔ were grown on Matrigel. A representative of several independent experiments is shown. Sprouting was quantified after 24 and 48 hours using in-house computer software. FOS expression levels were determined by Western blotting.

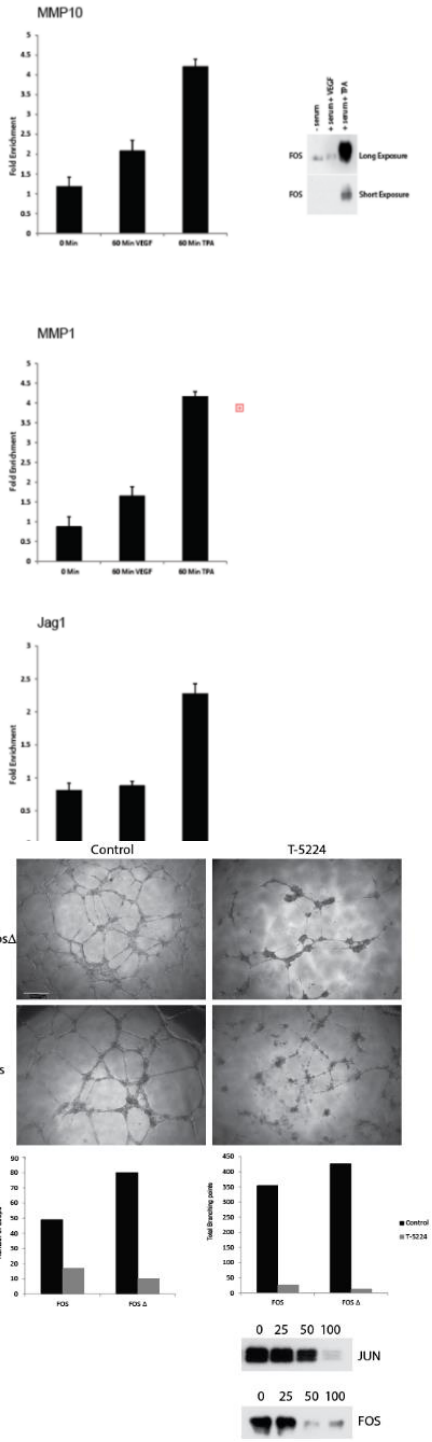

Supplementary Figure 4. A ChIP analysis of endogenous FOS association with the indicated promoters in HUVECs treated with or without 50 ng/ml VEGF or 1 µM 12-O-Tetradecanoylphorbol-13-acetate (TPA) for 1 hour. Three different primer sets were used for each promoter region. A single representative is shown (all three gave similar results). Results are presented as mean fold changes in recovery (as a fraction of input) relative to an IgG control antibody. Error bars represent the standard deviation (n = 3). Relative endogenous FOS protein levels were determined by Western blotting.

Supplementary Figure 5. HUVECs stably expressing the indicated FOS proteins were grown on Matrigel in the presence or absence of the AP-1 inhibitor, T5224 (20 µM). Sprouting was quantified after 24 hours. Lower right panel: T-5224 inhibits AP-1 DNA-binding *in vitro*. A double-stranded oligonucleotide harbouring three consensus AP-1 binding sites was incubated with a combination of FOS and JUN *in vitro* translated proteins in the presence or absence of the indicated concentrations of T-554 (µM). DNA-bound FOS and JUN was detected by Western blotting.

CHAPTER 5

Identification of Novel Small Molecule Inhibitors of ETS Transcription Factors

Zary Forghany[1], Shaima M. Abdalla[1], Jin Ma[1], Dipen M. Shah[2], Matteo Golo[3], Pancras Hogendoorn[1], David Baker[1]

1. Oncode Institute and Department of Cell and Chemical Biology, Leiden University Medical Center

2. Leiden Institute of Chemistry, Leiden University, Leiden the Netherlands

3. UNSW Medicine, UNSW Australia, Sydney, Australia

ABSTRACT

The **E**-**T**wenty-**S**ix_(ETS) family of transcription factors is a large and diverse protein family which regulates cellular development and differentiation. ETS factors have a substantial role in several disease states, particularly cancer, because many of these transcription factors are downstream of the major signal transduction pathways, which play critical roles in cell proliferation. Over the last two decades, multiple approaches have been developed to inhibit receptors and kinases with the aim of blocking tumor growth. However, most therapies have failed to deliver the anticipated clinical benefits due to drug resistance and toxicity. Consequently, there is an urgent need for new therapies. This study aims to identify potential small molecule inhibitors of ETS transcription factors binding to their consensus DNA binding site. The overall rationale is that this will limit overt toxicity and overcome the severe redundancy problems in cell signaling pathways and associated acquired resistance to therapy. To this end, we have performed proof-of-principal high throughput screens to find unique small molecules that inhibit the activity of ETS transcription factors by blocking their association with their DNA consensus sites. These screens and the characterization of resulting hit compounds suggest that targeting ETS activity could enable the identification of novel inhibitors of cancer cell proliferation, which exhibit relatively less toxicity than currently available treatments and may suffer less from problems of acquired drug resistance.

INTRODUCTION

In the past decade, oncology has witnessed a shift from traditional chemotherapies toward precision treatments that specifically target tumor cells to limit cytotoxicity in healthy tissues. While there have been some improvements in patient outcomes, the promised revolution has thus far failed to materialize. The two principal reasons for this are the acquisition of resistance to treatment and the fact that this class of inhibitors has, to date, been designed to block the activity of a relatively limited range of enzymes and receptors, e.g., kinases. Therefore, one ultimate goal is to design therapies that effectively treat the disease, do not cause off-target toxicity, and are not susceptible to resistance (Zhong, 2021; Manzari, 2021). In this light, there is a critical need to identify novel targets, particularly now that there is broader acceptance of the utility of searching beyond the historical constraints of the previously termed 'druggable genome. The druggable genome essentially encompasses enzymes and proteins expressed at the cell surface, thus making it accessible for treatment. However, such a restricted approach has proven not to be an unqualified success, and attention is now shifting to alternative targets previously considered to be 'non-druggable. Therefore, different novel targets, which have a demonstrable role in tumor development and evolution, need to be identified to develop more targeted treatments for tumors (Manzari, 2021; Hopkins, 2002; Zhong, 2021; Bushweller, 2019)

There are compelling reasons to think the ETS family of transcription factors (TFs) represents an excellent target (Sizemore, 2017). ETS factors were first discovered in 1983 as a fusion protein expressed by the avian retrovirus E26 (E-Twenty-Six). They are essential for normal cell proliferation, growth, and differentiation. Moreover, they sit downstream of the major MAP kinase signaling pathway and link it to other critical signaling networks, including the NOTCH system and the transforming growth factor beta (TGFβ) pathways (Hollenhorst, 2012; Wasylyk, 1998). In this way, they act as a central hub for translating extracellular stimuli into the changes in gene expression required to modulate cellular behavior. Mechanistically, these proteins function by binding to consensus DNA binding sites and thereby either activate or repress gene expression. Crucially, dysregulation of ETS factors often plays a role in tumor development by influencing cellular proliferation, invasion, migration, and evasion of apoptosis (Bazin, 2002; Butler, 2017; Fry & Inoue, 2018; Schober, 2005). Indeed, knock-down studies have demonstrated that loss of ETS activity blocks tumor cell growth (Fry & Inoue, 2018; Hsing, 2020). In addition to targeting tumor cells, there is good reason to assert that targeting ETS factors would also block other essential features of the tumor microenvironment (Li , 2010). For example, ETS

transcription factors are indispensable for angiogenesis (Lelièvre, 2001) , suggesting they could play an essential role in the angiogenic switch, a critical phase of tumorigenesis during which tumors stimulate the local vasculature to grow into the tumor, thereby enabling its growth and dissemination (Gu, 2020). Thus, because ETS factors underpin blood vessel growth, specific inhibitors could potentially accomplish two goals simultaneously: they could inhibit the proliferation of tumor cells and block tumor angiogenesis. (Oettgen, 2010).

Approaches for identifying ETS factor inhibitors

Targeting transcription factors is challenging owing to a lack of suitable targetable structural motifs due to their non-enzymatic mechanism of action (Chen, 2020). In this study, we apply novel methodologies for targeting ETS factors to identify (and characterize) small molecule inhibitors. For several reasons, small molecules are potentially the most effective means of targeting transcription factors compared to peptides or antibodies. Firstly, small molecules can generally penetrate cells more easily due to their size, allowing them to reach the transcription factor within the cell. Secondly, small molecules are unlikely to suffer the same problems of immunogenicity associated with therapeutic peptides and antibodies (Kuriakose, 2016; Jarvi,2021; Wei, 2021).

There are two main strategies for targeting transcription factors using small molecules. One involves selecting molecules that directly bind to the protein, such as DNA-encoded libraries or NMR-based assays (Goodnow, 2017). The second involves high-throughput screens (HTS) using multi-component functional assays in which the process of ETS DNA-binding is targeted. In this study targeted immobilization NMR screening (TINS) and HTS have been used to recover small molecule ETS factor inhibitors. The TINS approach uses small molecular scaffolds, which can sample significantly more chemical space (approximately 200 daltons) than bulkier small molecules (approximately 400 daltons). Thus, their small size enables a broader exploration of suitable chemical interfaces. The second screen was a multi-component high throughput functional screen yielding larger lead-like compounds capable of blocking ETS from associating with its consensus DNA site (Kim, 2015; Bon, 2022).

RESULTS

A fragment library screen (Targeted Immobilization NMR Screening (TINS)) to identify novel inhibitors of ETS transcription factors

To discover specific small molecule inhibitors of ETS factors, we aimed to screen for small molecule inhibitors that bind to the ETS DNA binding domain of ETS proteins. To that end, optimized purification protocols were developed to

produce milligram quantities of pure recombinant ETS DNA Binding Domain (DBD), initially of two ETS factors, TEL and FLI1. Figure 1A shows a Coomassie™ stain of FLI1 DBD, which has been double purified via two steps of column chromatography: nickel column chromatography followed by heparin column chromatography.

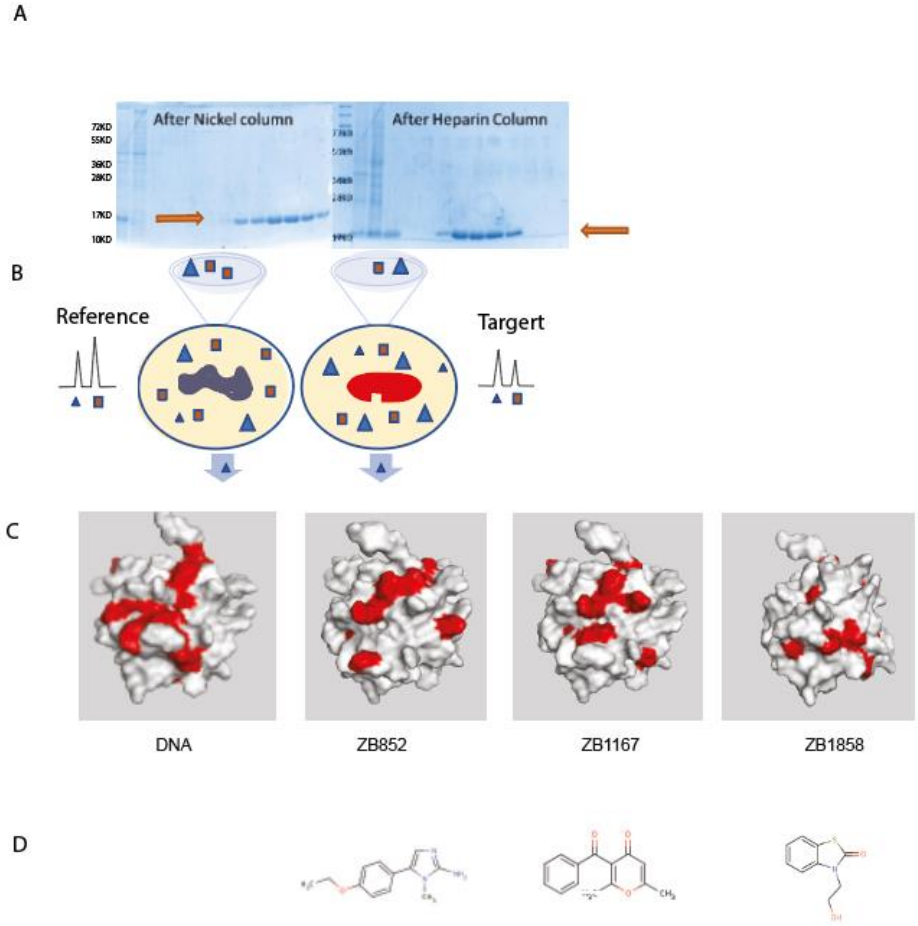

Figure 1. (A) Coomassie™ stain of FLI1 DBD. Two different columns (nickel column chromatography followed by heparin column chromatography) have been used for purifying the FLI1 DBD. Arrows indicated fractions were processed for further purification (B) Applying TINS method for Fragment-based drug discovery. A fragment library screen was done by simultaneously injecting a mix of fragments into a dual-cell sample holder with an immobilized TEL_{ETS} DNA-binding domain as a target and the reference protein. NMR spectroscopy detects peaks corresponding to fragments, as depicted by a reduced peak for the binder (red square) in the cartoon, while non-binders (blue triangle) exhibit unchanged peaks. Screening for a decrease in fragment peak intensity compared to a reference indicates binding. (C) Validation of the candidate fragments from the Targeted Immobilized TEL-DBD NMR Screen. NMR Chemical shift mapping of the TEL-DBD residues upon

fragment binding. The protein-DNA binding interface has been comparing to fragment binding to $TEL_{ETS.}$ (D) The chemical structure of fragment hits selected for follow-up studies.

Subsequently, the purified ETS DNA-binding domain was employed to screen a fragment library consisting of 1364 commercially available fragments using TINS (schematically represented in Figure 1B) in collaboration with the Chemistry department of Leiden University. This proof of principle screen, in which direct binding of molecular fragments to the TEL-DBD proteins of interest is assayed, identified multiple hits.
To validate these hit molecules, as the first step, NMR was deployed to map the site of binding of several 'top' hits to the DNA-binding domain. The structure of a protein-ligand complex was determined for three of the initial fragment hits obtained from the screen (Figure 1C). The chemical structures of the validated fragments are illustrated in Figure 1D. Notably, the pattern of contact between the ETS DNA binding domain (EDBD) and a consensus DNA site overlaps with the points of contact between the EDBD and a sub-set of hit compounds, suggesting that such molecules might disrupt ETS factor binding to DNA.

Fragments disrupt the binding of the ETS DNA binding domain to DNA, with low affinity.

To further validate the hit fragments, initially, we established an *in vitro* assay employing a biotinylated consensus ETS DNA-binding site and *in vitro* translated EDBDs to recapitulate the binding of ETS protein to DNA. This optimized assay has been used to assess the ability of fragments to block TEL binding to its DNA-binding site. Figure 2A illustrates at least two distinct classes of hits. For instance, one fragment (number 1838) displayed an enhancing DNA binding effect, while another fragment (number 852) exhibited the ability to inhibit DNA binding. The requirement for a high concentration (10 mM) due to the small size of the fragments indicates that these fragments exhibit low potency and low affinity for the target. This observation is not unexpected, as the fragment screen was anticipated to be a starting point for exploring bulkier novel analogues with superior affinities for the EDBD (Bon, 2022). Despite the direct interaction of fragments with the target protein, the affinities are far too low to elicit effects in cell-based assays because the fragments are not potent enough in practice. Broadly, there are two ways to address this issue: 1) with medicinal chemistry, which specifically modifies fragment side chains; 2) screen computationally for analogues that share common structural features with the original fragment candidates identified in the initial screen.

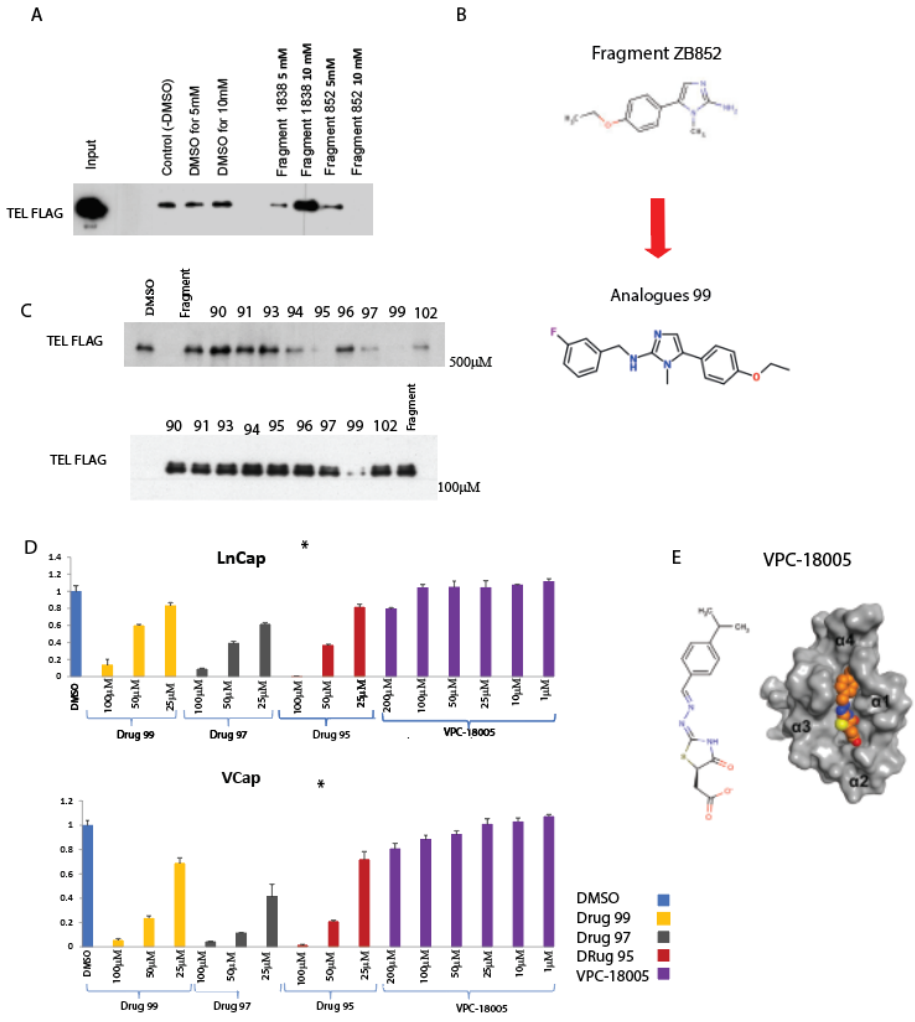

Figure 2. (A) Shown is hit validation using *in vitro* binding assay. A biotinylated consensus ETS DNA-binding site and *in vitro* translated proteins were used to validate the ability of binding to (TEL). DNA-bound proteins were detected by Western blotting using a FLAG mouse monoclonal antibody. Fragments disrupt binding with low affinity. **(B)** A chemical compound database (CHEMDOC) has been used to identify analogues. **(C)** Analogues disrupt TEL binding to a consensus DNA site at lower concentrations in *in vitro* binding assays. **(D)** Cell viability assay have been done using analogues versus VPC-18005 on prostate cancer cell proliferation. The indicated cell lines were incubated in the presence or absence of a range of analogues 95, 97, and 99 concentrations in LnCap (upper panels) and VCap (lower panels). Proliferation was assessed using the Cell Titer-Blue cell reagent. Each data point is the mean of triplicate measurements. Error bars represent the standard deviation of the mean. **(E)** The chemical structure of VPC-18005 and a space-filling representation of the predicted VPC-18005 binding pocket within the ERG-ETS domain. VPC-18005, as an anti-ERG drug, has been developed recently and targets the DNA-binding domain of ERG protein (Butler, 2017).

In general, analogues are identical to the original fragment except for additional chemical side chains (Figure 2B). Since medicinal chemistry is time-consuming and high-risk (modifying the fragment may make it less potent), we initially implemented the second strategy. Consequently, over 100 fragment analogues were selected through computational screening of selected hits. For example, Figure 2B shows a typical analogue of fragment 852. These analogues were chosen for further characterization in biochemical and biological assays.
Figure 2C demonstrates an improved effect of the analogues (500-100 µM), upwards of 100-fold in terms of potency, in a functional *in vitro* binding assay. Subsequently, we investigated whether the proliferation of tumor cells could be influenced when they are exposed to the analogues. This was examined on two prostate cancer cell lines: the TMPRSS2-ERG mutant line (VCaP cells) and the TMPRSS2 wild-type tumor line (LnCaP cells). The analogues efficiently inhibited cell proliferation of both lines, with IC50 values within the range of 25-100 µM (Figure 2D). By contrast, a recently reported putative ETS factor inhibitor discovered by computational chemistry methods, VPC-18005 (Figure 2E), failed to inhibit tumor cell proliferation at comparable drug concentrations (Figure 2D). Collectively, these data suggest that fragment-based screening could potentially identify molecular scaffolds that bind to the EDBD, and subsequent selection of the analogues might generate clinically valuable compounds. Such an approach has been routinely adopted by the industry as a proof-of-principle test of the suitability of targets for larger-scale screens (Kirsch, 2019). In this context, we next performed an ultra-high-throughput screen of a substantial small molecule library.

Ultra-high Throughput Screen (HTS) to identify novel ETS factor inhibitors

The second screen was conducted in collaboration with the European Lead Factory (ELF). This type of screening is only feasible when the assay is rapid, scalable, and automated. For this purpose, HTRF (Homogeneous Time-Resolved Fluorescence) has been applied by using the His-epitope tagged ETS DNA-binding domains (of TEL or FLI1) and a biotinylated oligonucleotide harboring three ETS binding sites (Figure 3A). It should be emphasized that HTRF is the most frequently used generic assay technology, which is widely used in drug target studies involving high-throughput screening (Degorce, 2009). This technology is based on a combination of fluorescence resonance energy transfer technology (FRET) with time-resolved measurement (TR). This energy transfer occurs between two Fluorophore conjugated antibodies (donor and acceptor) when they come close (Bazin, 2002; Mathis, 1999). In the case of the ETS screen, one fluorophore was attached to the antibody, which binds to the His tag of the protein. Another fluorophore was coupled to the antibody, which recognizes the

biotinylated DNA site. When two fluorophores are in close proximity, upon excitation of the donor by a light source, energy is conveyed from the donor to the acceptor. Subsequently, the activated acceptor emits fluorescence at a specified wave length. Compounds that could disrupt the binding of the ETS protein to the DNA site lead to a loss of the fluorescence signal. Figure 3A schematically represents the mode of action of the HTRF biomarker assay.
Using this assay, 450000 small molecules have been screened to identify lead-like compounds capable of blocking ETS from associating with DNA (a so-called functional screen). This screen led to the identification of five compounds. For simplicity, ELF compounds have the designations A-E in the following experiments. The chemical structures of the small molecule inhibitors are depicted in Figure 3B.
As mentioned, a structural comparison of fragments and small molecule inhibitors showed that these molecules contain more drug-like molecular features, whereas the fragment molecules are smaller and less potent.

Biochemical validation of small molecule inhibitors in functional *in vitro* binding assays

Using *in vitro* assays shown earlier for the fragments and analogues (Figure 2A and 2C), we showed that the hits clearly inhibit TEL DNA binding, particularly drugs A and D (Figure 3C and 3D). It should be noted that unlike the fragment assay, in which fragments were used at a concentration of 10 mM, here only 50 µM concentrations were sufficient to observe an inhibitory effect. A critical issue to address is whether the drugs function by specifically blocking TEL binding to DNA or by intercalating into the oligonucleotide (what we would call non-specific inhibition). To address this, we tested the ability of the drugs to block the binding of the unrelated JUN protein to its consensus Activator Protein (AP)-1 transcription factor binding site (Figure 3E). Our evidence suggests that JUN binding is not obviously affected by drugs A, B, C, and D but is inhibited by drug E. These experiments are consistent with the idea that drugs A, B, C, and D might inhibit ETS DNA binding by targeting the ETS protein rather than the DNA. By contrast, drug E inhibited the binding of full-length TEL, FLI1, and JUN binding to the AP-1 consensus site. Therefore, the binding is likely non-specific, and this molecule was subsequently excluded from further studies.

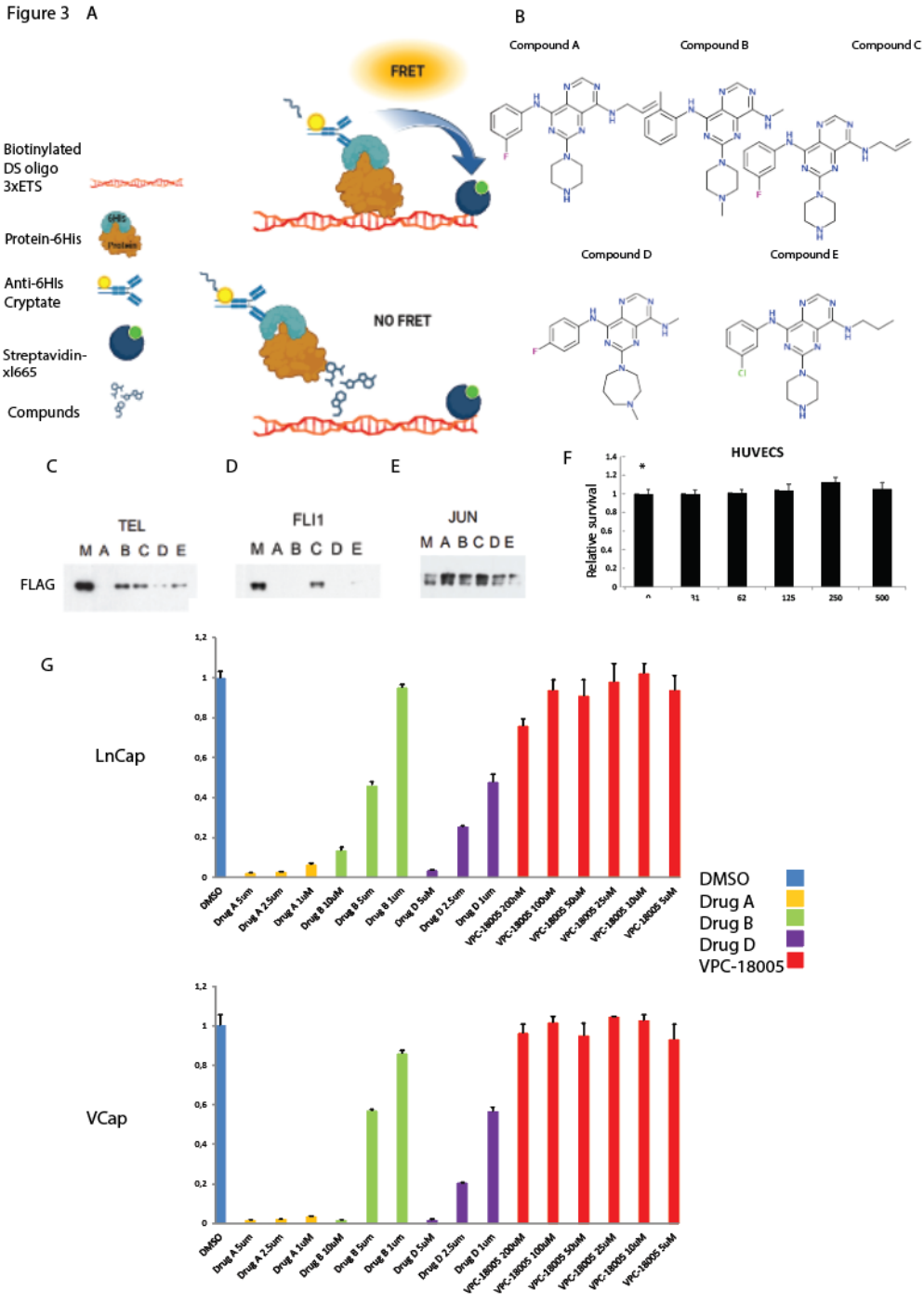

Figure 3. (A) Schematic representation of disruption of Protein-DNA binding through Ultra-high throughput screen.

< Figure 3 (continued). (B) Chemical structures of the small molecule inhibitors (ELF drugs, A, B, C, D, E). **(C)** ELF compounds inhibit ETS protein binding to DNA (*In vitro* DNA-binding assay). Double-stranded oligonucleotides harboring either three consensus ETS binding sites for TEL **(C),** FLI1 **(D)**, or three AP-1 binding sites for JUN **(E)** were incubated with *in vitro* translated TEL, FLI1 and JUN respectively. All constructs were FLAG epitope-tagged to enable a formal comparison. ELF drugs were added to a final concentration of 50 µM. DNA-bound proteins were detected by Western blotting using a FLAG mouse monoclonal antibody. **(F)** The impact of ELF drugs on HUVECs' cell viability is illustrated. Unaffected growth of 'normal' HUVECs was observed upon treatment with the shown concentration of drug A. **(G)** The treatment effects of drugs on the proliferation of prostate cancer cells (VCaP and LnCaP) compared to VPC-18005 are depicted. Cell proliferation reduction due to treatment with ELF Drugs A, B, and D on prostate cancer cells is compared to an in silico developed ETS inhibitor, VPC-18005. ELF compounds inhibit the proliferation of cancer cells harboring ETS fusion proteins. The indicated cell lines were incubated in the presence or absence of a range of concentrations of compounds A, B, and D (both left and right-side panels) compared to VPC-18005. Error bars represent the standard deviation of the mean.

Candidate-hit compounds significantly inhibit tumor cell proliferation

ETS transcription factors play critical roles in normal cell growth and proliferation, and cancer cells often exhibit aberrant ETS protein activity. In this section, initially, we have compared the growth of 'normal' primary cells (human umbilical vein endothelial cells (HUVECs) with the growth of 2 prostate cancer lines: VCaP (which contain a chromosomal translocation resulting in sharply elevated ERG protein levels) and LnCaP cells.

Figure 3F clearly illustrates that the growth of 'normal' HUVECs was relatively unaffected by the presence of the most potent compound, drug A, across all tested concentrations (31 nM – 500 nM). However, the proliferation of the two cancer cell lines was significantly suppressed by drugs A, B, and D, each showing half-maximal inhibitory concentration (IC50) values in the 1-10 µM range (Figure 3G). This evidence strongly suggests that the ELF drugs might exhibit tumor-specific effects, given their lack of impact on the growth of normal cells. In addition, as it has been shown, cell proliferation was not significantly inhibited by treatments with VPC-18005 (Butler, 2017).

Candidate hit compounds inhibit angiogenic sprouting

Considering the data obtained from our functional studies and the established role of ETS transcription factors in sprouting angiogenesis, we sought to elucidate the effect of the ETS inhibitors on angiogenesis. Three different angiogenesis assays were deployed.

- ***In vivo* analyses using the zebrafish embryo model**

The fli1a:gfp transgenic line (Lawson, 2002) produces embryos in which all of the endothelial cells are marked by GFP. Coupled to their optical transparency, this enables direct visualization of angiogenesis. During the first 2 days of development, the reiterated pattern of intersegmental trunk vessels (ISV) are formed by angiogenic sprouts from dorsal aorta endothelial cells that grow to

the dorsal side of the trunk where they interconnect to form the dorsal longitudinal anastomotic vessel (DLAV). Interestingly, incubation of zebrafish embryos with 10µM of ELF compound for 16 hours resulted in clear disruption of angiogenesis, manifested by a reduction in the number of vessels, aberrant vessel trajectories, and the premature stalling of dorsal aorta sprouts (Figure 4A). Effects were most obvious for drugs A, B, and D. Incubation with drug C resulted in less disruption vessels that have been visualized using confocal microscopy.

- **Primary cell angiogenic tube formation assay**

To further characterize the inhibitory effect of the small molecules, they were added to three-dimensional (3D) cultures of primary HUVECs. HUVECs were grown on Matrigel in the presence or absence of resynthesized drugs (10 µM). Sprouting was quantified after 24 hours using in-house computer software. Figure 4B demonstrates that all drugs inhibited sprouting, with drugs A and D showing the most apparent effects. Together, these findings suggest that the ELF drugs (most notably drugs A, B, and D) might exert specific inhibitory effects on angiogenesis by targeting ETS.

- ***Ex vivo* fetal bone metatarsal explant assay**

Mouse fetal metatarsals allow the analysis of blood vessel growth in a dish and recapitulate critical features of angiogenesis observed *in vivo* (Song, 2015). Fetuses at embryonic stages E15.5–18.5 can be used for metatarsal preparation, as they exhibit similar vessel outgrowth.

For this study, metatarsals were isolated from fetuses at embryonic stages E17.5 and incubated in a defined medium containing vascular endothelial growth factor (VEGF) in the presence or absence of 1 µM ELF compounds. The assay has been performed according to the protocol provided in the Methods section. Vessel formation was monitored by phase-contrast light microscopy from day 2. Compounds A, B, and D each inhibited ectopic angiogenesis of metatarsals isolated from fetal mice. Immunofluorescence staining with PECAM-1 (CD31 antibody) was performed to visualize metatarsal vessel outgrowth. Confocal images of microvessel are shown (Figure 4C). A quantitative analysis of vessel branching was determined based on the number of pixels in the vessel area. Taken together, these data demonstrate the potential anti-angiogenic inhibitory effect of the hit compounds.

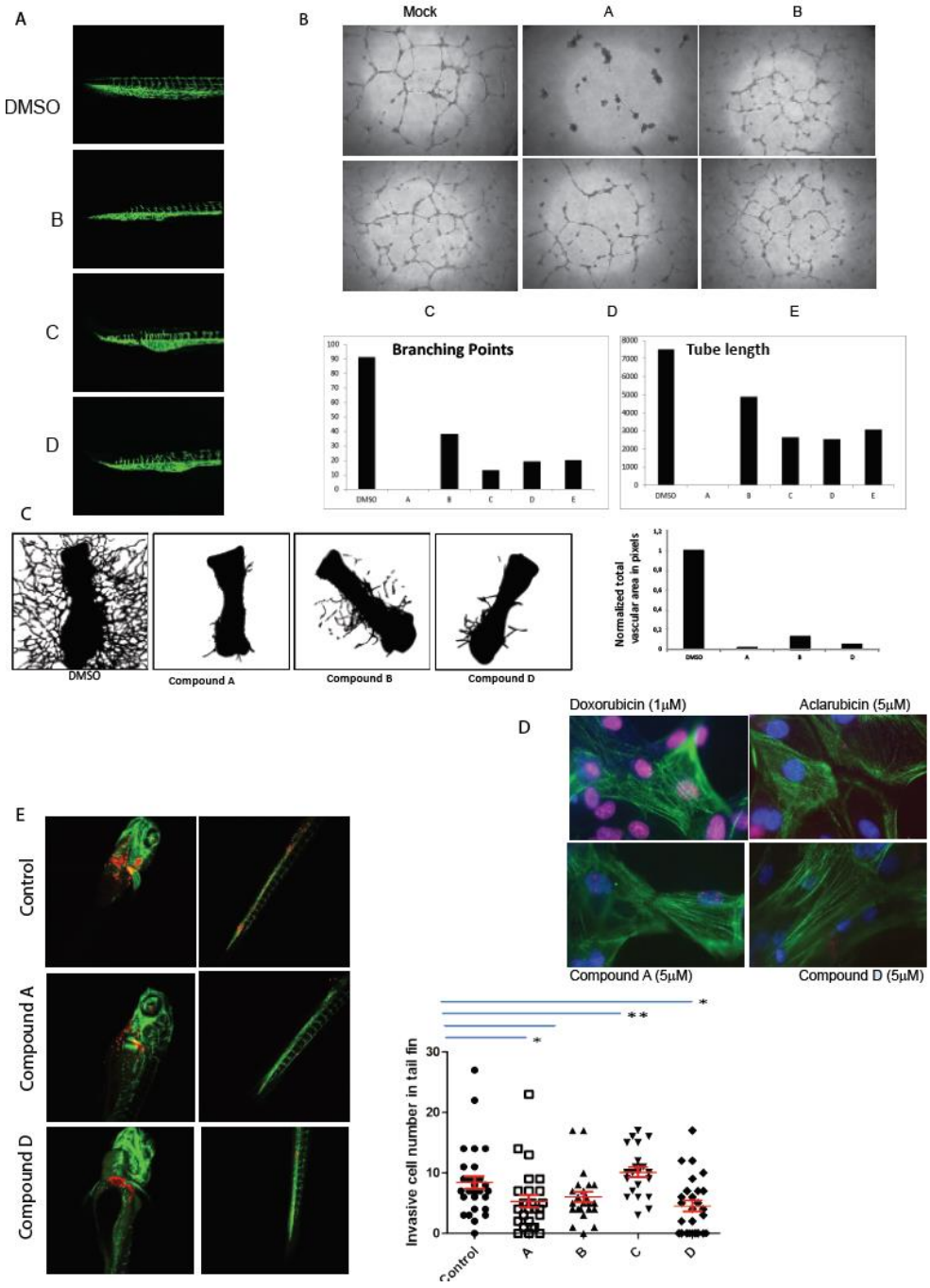

Figure 4. (A) The *fli1*a:gfp transgenic zebrafish embryos were treated with 10 μM of ELF compounds for 16 hours. Blood vessels were imaged by confocal microscopy.

< Figure 4 (continued). (B) Effect of ELF compound on human primary endothelial cell tube formation. HUVECs were grown on Matrigel in the presence or absence of ELF drugs (10 µM). Sprouting was quantified after 24 hours using in-house computer software. **(C)** Mouse metatarsal assay. Metatarsals isolated from fetal mice were incubated ex-vivo in a defined VEGF medium in the presence or absence of 1 µM ELF compounds. Blood vessels were visualized using a CD31 antibody. Ten metatarsals were scored per condition. The scale bar represents 500 µm. **(D)** Evaluating DNA Damage in hPSC-derived cardiomyocytes and HUVECs. Assessing cardiotoxicity in hPSC-derived cardiomyocytes that were cultured overnight in the indicated conditions. Shown are confocal images of cells stained for Troponin I (TNNI3; green) and phospho-histone H2A.X (red- to visualize DNA damage). All nuclei were stained with DAPI (blue). **(E)** ELF compounds inhibit breast cancer cell invasion in xenotransplanted zebrafish embryos. Fluorescently labeled breast cancer cells were microinjected into the duct of Cuvier of 3-day-old zebrafish embryos. Tumor cell invasion was measured 3 days later.

Evaluation of hit compound cardiotoxicity

Toxicity is a fundamental problem associated with chemotherapy treatments, in particular treatments that damage DNA. In the case of doxorubicin, which is a widely used chemotherapy reagent, the main problem is cardiotoxicity, which leads to damage to cardiac tissue and heart failure. Therefore, cardiotoxicity is one of the most important considerations when developing novel therapies that improve current treatments. Doxorubicin acts by inhibiting topoisomerase II, leading to double-stand DNA breaks, which activate the DNA-damage response machinery, ultimately resulting in apoptosis. While this is an efficient means of killing cancer cells, doxorubicin and similar chemotherapy reagents also target 'normal' cells, leading to serious side effects of toxicity.

As the primary activity of ETS inhibitors takes place within the nucleus, genotoxic testing was conducted by assessing γ-H2AX levels in human iPSC-derived cardiomyocytes (hiPSC-CM). Phosphorylation of histone H2AX is a standard measure of DNA-damage response activation, which can be visualized using a specific antibody (Kuo, 2008). Cardiotoxicity was evaluated in both the presence and absence of the specified drugs, utilizing an antibody targeting phosphorylated histone H2AX. The ETS inhibitors exhibited relatively minimal levels of damage when compared to the conventional chemotherapy drug, doxorubicin (Figure 4D).

In vivo inhibition of migration and invasion of tumor cells in zebrafish

The importance of ETS factors in cellular migration and invasion has often been observed within aggressive tumors. Therefore, an effective ETS inhibitor might suppress cellular migration (Buchwalter, 2005; Schober, 2005). We employed zebrafish xenotransplantation to investigate cell extravasation and intravasation. Approximately 400 human breast cancer MDA-MB-231 cells were injected into

the duct of Cuvier (Doc) 48h after fertilization. Injected zebrafish embryos were treated with compounds in their water. The embryos also remained viable when cultured in the presence of up to 25 µM of the compounds for five days. EGFP-labeled vasculature of Tg (*fli1:gfp*) and mCherry-labeled tumor cells enabled visualization of cancer cell invasion and dissemination in the living zebrafish. The Figure 4E shows, that the dissemination of the breast cancer cell lines toward the head and tail was significantly reduced in the presence of compounds A, B and D (10 uM).
Taken together, these data suggest that, in addition to directly inhibiting proliferation of tumour cells, selected hit compounds exert an inhibitory effect on angiogenic sprouting.

DISCUSSION AND FUTURE PERSPECTIVES

While the past two decades witnessed considerable efforts to target receptors and kinases to impede tumor growth, the clinical success of such therapies has often been hampered by drug resistance and toxicity issues. In response to this pressing challenge, our study has tested an innovative approach to inhibiting cancer proliferation by focusing on inhibiting ETS transcription factors. Although targeting transcription factors was historically disregarded due to structural complexities and intrinsically disordered regions, recent progress in drug discovery and modern chemistry has reignited interest in targeting such proteins. Here, we explored the possibility of targeting the ETS family, knowing that such an approach holds the promise of effectively targeting tumor growth and angiogenesis. This introduces a multidimensional strategy for cancer treatment. Our main approach aims to mitigate overt toxicity and address prevalent redundancy issues in cell signaling pathways, ultimately combating acquired resistance to therapy. As compared to other signaling pathways, TFs are the most downstream component, so there are fewer parallel pathways to bypass. Therefore, in principle, targeting ETS should be less prone to therapy resistance.
Here, we presented the discovery of novel small-molecule inhibitors targeting the ETS DNA binding domain of transcription factors (TEL and FLI1). Initially, two types of screens have been done for hit identification. Firstly, fragment-based screening selects molecules that directly bind to the DBD. Secondly, HTS of lead-like small molecules, which are multi-component functional assays, have been used to discover compounds capable of blocking ETS DBD binding to DNA. We have initiated a hit-to-lead characterization of these molecules through a variety of biochemical and cell-based experiments to select the most promising candidates.
As tumor proliferation and migration are the primary drivers of tumorigenesis, assessing the suppression of these two events is a satisfactory starting point for

testing the inhibitors (Erkizan, 2009; Butler, 2017). We showed that the inhibitors reduced the proliferation of cancer cell lines and also blocked angiogenesis and vessel growth in different assays. Furthermore, a zebrafish xenotransplantation study suggests that the compounds may block cancer cell invasiveness (see Figure 4E). The results of our *in vitro* biochemistry assays also verified the mode of action of these compounds, which includes the inhibition of ETS protein DNA binding. These data provided proof-of-principle evidence that targeting ETS factors might represent a novel approach to inhibiting tumor growth. Follow-up studies will be required to validate this idea by using mouse models and organoids.

Concerning toxicity, testing DNA damage in cultured cardiomyocytes showed significantly lower damage levels in the cells that had been treated with the ETS inhibitors compared to doxorubicin. There was an increase of γ-H2AX caused by compound A (Figure 4D), but this was much lower than the effect of doxorubicin at comparable drug concentrations. This suggests that the novel compounds cause less damage than the conventional chemotherapy treatment. Regarding toxicity, it is noteworthy that zebrafish embryos tolerated low µM quantities of the compound. However, it will also be essential to conduct toxicology and pharmacokinetic studies in mammalian model systems. Minimizing on-target toxicity is indeed also a significant challenge in drug development, particularly as ETS transcription factors have an important role in normal cell proliferation and differentiation. One might expect on-target toxicity of these compounds when given systemically. In order to balance therapeutic efficacy, we could use specific ETS inhibitors selectively acting on specific ETS factors associated with. In addition, combination therapies might help in optimizing drug dosage and minimizing toxicity.

There are clearly potential specificity issues because of the number of ETS factors that have a common core binding motif. There are potential differences in their mode of action and the specific sequence of the DNA binding sites that could be explored, but due to this overall conservation, we may end up with inhibitors which inhibit more than one ETS factor. One way to limit specificity problems is by using different ETS sites and also purifying and screening full-length ETS proteins. This has proven to be very challenging technically, but once overcome, it opens up the possibility of selecting even more targeted compounds. Furthermore, the purification of full-length ETS protein will offer us the possibility of obtaining a deeper understanding of these factors, their function, and their involvement in the pathology of disease. With a complementary effort to characterize the nature of ETS-controlled gene networks, we can more dissect the effects of the novel compounds at the molecular level through transcriptome analyses and proteome analyses.

MATHERIALS AND METHODS

Cell culture, biochemistry

The prostate cells, LnCaP, and VCaP were cultured in Iscove's Modified Dulbecco's Medium (IMDM) from Gibco, supplemented with 15% Fetal Bovine Serum (FBS). The primary HUVECs (Lonza) were cultured in EGM-2 (Lonza) medium supplemented with the Bullet kit (Lonza) and 10% fetal bovine serum (Gibco).. The culture dishes were coated for 30 minutes with 0.2% gelatin at 37℃. All cell lines were maintained in a 5% CO_2, 37 °C humidified incubator, tested monthly for mycoplasma contamination and checked for authenticity by short tandem repeat (STR) profiling. Cardiomyocytes generously provided by Dr. Richard Davis (Anatomy & Embryology, LUMC).

Proliferation assays

The cells were seeded in triplicate in appropriate concentrations; 30,000 cells/mL LnCaP and VCaP/60,000 cells/ml into 96-well white plates with a clear flat bottom in 100µl of regular medium. The next day, the medium was supplemented with the different concentrations of compounds. The number of viable cells was determined using a Cell Titer-Blue reagent (Promega, Madison) at 0, 3, and 5 days after treatment. The analysis was done by removing the excess medium and adding 85µl of regular media with 15µl of the Cell Titer-Blue Reactions were left at 37°C for 2 hours, and absorbance readings were taken at 544 nm/590 nm (RFU) using the Victor X3 multi-label plate reader from Perkin Elmer.

Protein Expression and purification

Phage-resistant BL21 E. coli were transformed with pETHIS-Fli1DBD constructs, followed by selection of colonies on LB + kanamycin. Subsequently, the selected colonies were grown in 200 ml LB media + kanamycin at 30°C and induced with 1 mM Isopropyl β-D-1-thiogalactopyranoside (IPTG) at OD600. Protein expression was carried out for four hours. After induction, cells were centrifuged at 5,000 rpm at 4°C, and the resulting pellets were snap-frozen in liquid nitrogen and stored at -80°C.

Frozen cells pellets were lysed in 3ml of N.1 buffer (Imidazole 16.6 mM, NaCl 500 mM, Dithiothreitol (DTT) 2mM, 5% glycerol. pH 7.4) and sonicated at 60% amplitude, with a 10-second on and 15-second off cycle for 10 minutes, until the lysate cleared. The sonicated lysates were centrifuged at 17,000 rpm at 4°C for 10 minutes, and the resulting pellets and supernatant were subjected to 12% SDS

gel. Protein release into the supernatant was confirmed by staining with Instant Blue™ Protein Stain. The FLI-1 binding domain was purified by passing the sample diluted in N.1 buffer through a 1 ml nickel column, eluting fractions with N.2 buffer (Imidazole 332 mM, NaCl 500 mM, Dithiothreitol (DTT) 2 mM, 5% glycerol, pH 7.4). Subsequently, the cleanest fractions were diluted in H.1 Buffer (Hepes 20 mM, EDTA 0.5 mM, DTT 2 mM, 5% glycerol, pH 7.4) and run through a 1 ml heparin column, eluting fractions with H.2 buffer (NaCl 1 M, Hepes 20 mM, EDTA 0.5 mM, DTT 2 mM, 5% glycerol, pH 7.4). The clean fractions were then pooled and snap-frozen in liquid nitrogen for storage at -80°C. All fractions were assessed by running on a 12% SDS gel and staining with Instant Blue™ Protein Stain.

***In vitro* DNA binding assay**

In vitro translated protein was made using the TNT-coupled reticulocyte *in vitro* translation system (transcription and translation-Promega). Subsequently, 50 pmol of biotinylated double-stranded oligonucleotides harboring either three consensus ETS binding sites (for TEL and FLI1) or three AP-1 binding sites (for JUN) were coupled to MyOne streptavidin C1 beads (Invitrogen). Double-stranded oligonucleotides were incubated with *in vitro* translated TEL, FLI1, or JUN. It is important that all constructs were FLAG epitope tagged to enable a formal comparison with monoclonal antibodies. ELF drugs were also added to the reaction with the final concentration of 50 µM. Reactions were incubated at 4 °C with vigorous shaking for 30 min in the presence of 1 µg of poly (dI/dC), 4 mm spermidine. Beads were successively washed three times with the Binding buffer (50 mm KCl, 10 mm HEPES (pH 7.6), 5 mm MgCl2, 10 mm Tris (pH 8), 0.05 mm EDTA (pH 8), 0.05 mm, 0.1% Triton X-100, 20% glycerol). Associated proteins were eluted in Laemmli buffer, and protein-DNA interactions were determined by western blotting, which has been described previously (Forghany, 2018) using a FLAG mouse monoclonal antibody (Sigma).

HUVEC tube formation/sprouting assay

96-well plates were coated with 60 µl of Matrigel/well 30 min prior to seeding 25000 HUVECs/well. Cells were grown on Matrigel in the presence or absence of ELF drugs (10 µM). EGM-2 medium was supplemented with 50 ng/ml recombinant human VEGF 165 (R & D Systems) EGM2 medium(Endothelial Cell Growth Medium-2 with Bullet Kit/Lonza) was supplemented with 50 ng/ml recombinant human VEGF 165 (R&D Systems). Images were taken at multiple time points. After 24 hours, sprouting was analyzed with Stacks (in-house software; Department of Cell and Chemical Biology, Leiden University Medical Center). The analysis of sprouting was done after 24 using in-house computer software developed by the Department of Chemical and Cell Biology at LUMC

(van IJzendoorn,2017). Each individual space bounded by connected tubes constitutes a loop. Branches are the intersections made by connected tubes, and total length is the combined length of all tubes (not all the data shown here).

Zebrafish assay

The toxicity of ELF drugs has been explored using the fli1a:gfp transgenic line (Lawson, 2002). Zebrafish care, maintenance, and handling in the Laboratory have been done according to the international guidelines (Avdesh , 2012). All animal experiments were approved by the local institutional committee for animal welfare (Dier Ethische Commissie "DEC" of the Leiden University Medical Center).

For the experiments described here embryos were kept in egg water (60 µg/mL sea salts; ~60 embryos/dish) at incubate at 28 c. Chorions were removed mechanically using two forceps before 24hp. As a popular solvent, Dimethyl sulfoxide (DMSO) has been used to deliver compounds. Drug administration has been done with titration and final concentrations of 5, 10, 20, and 50 µM. Embryos were anesthetized using tricaine methane sulfonate (Sigma-Aldrich) with the final 40 mg/ml concentration in egg water, approximately 10 minutes before imaging. Imaging of vessels was carried out by using a Leica SP2 confocal microscope (Leica Microsystems) using a ×10 or ×20 objective. Vessel characteristics of 20 embryos per condition were scored.

Metatarsal assay

This protocol comprises multiple steps, including dissecting, seeding the metatarsals, staining, imaging, and quantifying. It is important to isolate the embryos from the uterus for the metatarsal assay and keep them in phosphate buffered saline (PBS) with calcium and magnesium on ice until the metatarsals are isolated. The metatarsal dissection procedure was done according to nature protocol (Song, 2015) from a mouse embryo at day 17 of gestation. In the whole experimental procedure, it is essential to prevent the isolated metatarsals from drying, which compromises the sprouting step. We used DPBS (Dulbecco's PBS) with calcium and magnesium to isolate the metatarsals. The medium for culturing the metatarsals was MEM Alpha Medium (Thermo Scientific) and GlutaMAX (Gibco™), which contained FBS and penicillin-streptomycin. This medium was then supplemented with 50 ng/ml recombinant human VEGF 165. The metatarsal should be placed in the middle of a 0.1 % gelatin-coated plate. The plates were kept in the back of the incubator, especially for the first 2–3 days, without any movement to avoid floating the bones. From day 2, the culture medium needs to be changed. Then, approximately every other day until the experiment ends, the medium should be refreshed and supplemented with 10µm small molecule inhibitors. In addition, fibroblast migration from

metatarsals begins to grow underneath on day 2. The vessel sprouting was visible with phase-contract microscopy on day 7, and the treated metatarsal indicates significant differences compared to the control.
To visualize vessel outgrowth from metatarsals immunofluorescence, staining was done after removing the culture medium on day 5. Metatarsals were washed with DPBS (Dulbecco's PBS; Gibco, with calcium and magnesium), and metatarsals were fixed in Zink Macrodex Formalin (PFA; Sigma-Aldrich) for 15 min. Staining on the metatarsals was performed using the CD31 antibody (BD Pharmingen™) as previously described (Forghany, 2018). For a detailed analysis of vessel formation, images were processed in Photoshop. After thresholding, vessel configurations were converted into black-and-white binary images. Vascular area (Black) in pixels was quantified using in-house computer software developed by the Department of Cell and Chemical Biology at LUMC. In all the treatments, the total vascular area or tube length in pixels has been normalized against the pixel of the metatarsal bones (Song, 2015). All animal experiments were approved by the local animal ethics committee.

Cardiomyocytes

The hiPSC-CM (stem cell-derived cardiomyocytes) were grown on 5mm coverslips in 100µl Matrigel™(BD Matrigel™ Basement Membrane Matrix) and 1ml culture medium. The culture medium for the hiPSC-CM was DMEM 10% FBS with Supplement 100x) stock from Gibco, 450 µM α-MTG, 0.05 mg/ mL L-Ascorbic acid 2-phosphate from Sigma-Aldrich, 2 mM GlutaMAX supplement 100x stock from Gibco, 0.5 % Penicillin/ streptomycin (Thermo Scientific). Matrigel™ Matrix Growth Factor Reduced (BD) was diluted with 0.5 mg Matrigel in a 6 mL cold culture medium.
Cells were treated with ETS inhibitors, Aclarubicin, and doxorubicin. Following 16 hours of treatment, the cells were fixed with 4% paraformaldehyde-phosphate buffered saline (PBS) for 15 min and permeabilized in 0.2% Triton X-100-PBS for 5 min. Subsequently, the cells were washed with PBS 0.5% Tween and blocked with a solution containing PBS 0.5% Tween and 5% bovine serum albumin for 30 min. Primary antibodies Troponin I and anti phospho-histone H2A.X (Ser139) (Cell signaling) were then added to the blocking buffer and incubated with the cells for 1 hour, followed by washing and incubation with secondary antibodies in the blocking buffer for 30 min. After another round of washing, the cells were mounted with a DAPI mounting solution (10 µg/ml) and sealed with nail varnish. All immunostaining procedures were performed at room temperature and were visualized using a Leica SP8 confocal microscope.

Antibodies and drugs

The following primary antibodies were used: FLAG mouse M2 monoclonal (Sigma-Aldrich), anti-HA.11 mouse monoclonal (Covance), anti-HA rabbit polyclonal (Abcam), Secondary antibodies; anti-Rabbit Alexa Fluor® 488 and anti-Mouse Alexa Fluor® 594 (Thermo Fisher scientific), anti-JUN rabbit (Cell Signaling Technology), anti-JUN mouse (Santa Cruz Biotechnology), anti-FLAG rabbit (Sigma), anti-γ-tubulin (Sigma), Rat Anti-Mouse CD31 (BD Pharmingen), anti-TroponinI (Santa Cruz), anti-phospho-histone H2A.X (Ser139)(Cell signaling), Aclarubicin (Sigma Aldrich), doxorubicin (Sigma Aldrich), Triton (Merck), Puromycin (Sigma-Aldrich).

Statistical analysis

Statistical analysis was performed using GraphPad Prism 9. The unpaired Student's t-test was used for most analyses, and $P < 0.05$ was considered statistically significant. All measurements in this study were taken from distinct samples.

ACKNOWLEDGMENTS

We thank Miguel Dickson for outstanding technical assistance. Annelies van der Laan for help with the confocal microscopy, and Dr. Hans Vrolijk for designing computer software for quantifying sprouting data. We Thank Dr. Richard Davis for providing Cardiomyocytes. The authors gratefully acknowledge the financial support by the Dutch Cancer Society (30861) to DAB and the Oncode Institute (to PtD). The small molecule HTS was performed within the European Lead Factory and received support from the Innovative Medicines Initiative Joint Undertaking under grant agreement n°115489, resources of which are composed of financial contribution from the European Union's Seventh Framework Programme (FP7) and EFPIA companies' in-kind contribution.

REFERENCES

1. Avdesh A, Chen M, Martin-Iverson MT, Mondal A, Ong D, Rainey-Smith S, Taddei K, Lardelli M, Groth DM, Verdile G, Martins RN. Regular care and maintenance of a zebrafish (Danio rerio) laboratory: an introduction. J Vis Exp. 2012 https://doi.org/10.3791%2F4196
2. Bazin, H., Trinquet, E., & Mathis, G. (2002). Time-resolved amplification of cryptate emission: a versatile technology to trace biomolecular interactions. J Biotechnol, 82(3), 233-250. https://doi.org/10.1016/s1389-0352(01)00040-x
3. Bon M, Bilsland A, Bower J, McAulay K. Fragment-based drug discovery-the importance of high-quality molecule libraries. Mol Oncol. 2022 Nov;16(21):3761-3777. https://doi.org/10.1002/1878-0261.13277
4. Buchwalter, G., Gross, C., & Wasylyk, B. (2005). The ternary complex factor Net regulates cell migration through inhibition of PAI-1 expression. Mol Cell Biol, 25(24), 10853-10862.
https://doi.org/10.1128/MCB.25.24.10853-10862.2005
5. Bult, C. J., Eppig, J. T., Kadin, J. A., Richardson, J. E., Blake, J. A., & Mouse Genome Database, G. (2008). The Mouse Genome Database (MGD): mouse biology and model systems. Nucleic Acids Res, 36(Database issue), D724-728. https://doi.org/10.1093/nar/gkm961
6. Bushweller, J. H. (2019). Targeting transcription factors in cancer - from undruggable to reality. Nat Rev Cancer, 19(11), 611-624. https://doi.org/10.1038/s41568-019-0196-7
7. Butler, M. S., Roshan-Moniri, M., Hsing, M., Lau, D., Kim, A., Yen, P., Mroczek, M., Nouri, M., Lien, S., Axerio-Cilies, P., Dalal, K., Yau, C., Ghaidi, F., Guo, Y., Yamazaki, T., Lawn, S., Gleave, M. E., Gregory-Evans, C. Y., McIntosh, L. P., Cherkasov, A. (2017). Discovery and characterization of small molecules targeting the DNA-binding ETS domain of ERG in prostate cancer. Oncotarget, 8(26), 42438-42454. https://doi.org/10.18632/oncotarget.17124
8. Chen, A., & Koehler, A. N. (2020). Transcription factor inhibition: lessons learned and emerging targETS-1. Trends in molecular medicine, 26(5), 508-518. https://doi.org/10.1016/j.molmed.2020.01.004
9. Degorce, F., Card, A., Soh, S., Trinquet, E., Knapik, G. P., & Xie, B. (2009). HTRF: A technology tailored for drug discovery - a review of theoretical aspects and recent applications. Curr Chem Genomics, 3, 22-32. https://doi.org/10.2174/1875397300903010022
10. Erkizan, H. V., Kong, Y., Merchant, M., Schlottmann, S., Barber-Rotenberg, J. S., Yuan, L., Abaan, O. D., Chou, T. H., Dakshanamurthy, S., Brown, M. L., Uren, A., & Toretsky, J. A. (2009). A small molecule blocking oncogenic protein EWS-FLI1 interaction with RNA helicase A inhibits growth of Ewing's sarcoma. Nat Med, 15(7), 750-756. https://doi.org/10.1038/nm.1983
11. Feng, F. Y., Brenner, J. C., Hussain, M., & Chinnaiyan, A. M. (2014). Molecular pathways: targeting ETS gene fusions in cancer. Clin Cancer Res, 20(17), 4442-4448. https://doi.org/10.1158/1078-0432.ccr-13-0275
12. Findlay, V. J., LaRue, A. C., Turner, D. P., Watson, P. M., & Watson, D. K. (2013). Understanding the role of ETS-mediated gene regulation in complex biological processes. Adv Cancer Res, 119, 1-61. https://doi.org/10.1016/B978-0-12-407190-2.00001-0
13. Forghany, Z., Robertson, F., Lundby, A., Olsen, J., & DA, B. (2018). Control of endothelial cell tube formation by Notch ligand intracellular domain interactions with activator protein 1 (AP-1). J Biol Chem, 293(4), https://doi.org/10.1074/jbc.M117.819045
14. Fry, E. A., & Inoue, K. (2018). Aberrant expression of ETS1 and ETS2 proteins in cancer. Cancer Rep Rev, 2(3). https://doi.org/10.15761/crr.1000151
15. Fu Li, Julie A. Wallace, Michael C. Ostrowski (2010) ETS Transcription Factors in the Tumor Microenvironmen, The Open Cancer Journal, 2010, 3: 49-54
16. https://doi.org/10.2174/1874079001003010049
17. Goodnow Jr, R. A., & Davie, C. P. (2017). DNA-encoded library technology: a brief guide

to its evolution and impact on drug discovery. Annual Reports in Medicinal Chemistry, 50, 1-15. https://doi.org/10.1016/bs.armc.2017.09.002

18. Gu, T. L., Goetz, T. L., Graves, B. J., & Speck, N. A. (2000). Auto-inhibition and partner proteins, core-binding factor beta (CBFbeta) and Ets-1, modulate DNA binding by CBFalpha2 (AML1). Mol Cell Biol, 20(1), 91-103. https://doi.org/10.1128/MCB.20.1.91-103.2000

19. Gu,A., Wang, J,. O Madu,C., (2020) Yi LuThe Role of Transcription Factors in Cancer Angiogenesis and Metastasis https://doi..org/10.31031/NACS.2020.05.000609

20. Hollenhorst, P. C. (2012). RAS/ERK pathway transcriptional regulation through ETS/AP-1 binding sites. Small GTPases, 3(Jul). https://doi.org/10.4161%2Fsgtp.19630

21. Hsing, M. (2020). ETS transcription factors as emerging drug targets in cancer. Medical Research Review, 40(1). https://doi.org/10.1002/med.21575

22. Jarvi, N.L., Balu-Iyer, S.V. Immunogenicity Challenges Associated with Subcutaneous Delivery of Therapeutic Proteins. BioDrugs 35, 125–146 (2021). https://doi.org/10.1007/s40259-020-00465-4

23. Kim, H. Y., & Wyss, D. F. (2015). NMR screening in fragment-based drug design: a practical guide. Methods in molecular biology (Clifton, N.J.), 1263, 197–208. https://doi.org/10.1007/978-1-4939-2269-7_16

24. Kirsch P, Hartman AM, Hirsch AKH, Empting M. Concepts and Core Principles of Fragment-Based Drug Design. Molecules. 2019 Nov 26;24(23):4309. https://doi.org/10.3390/molecules24234309.

25. Kuo, L. J., & Yang, L. X. (2008). Gamma-H2AX - a novel biomarker for DNA double-strand breaks. In vivo (Athens, Greece), 22(3), 305–309.

26. Kuriakose A, Chirmule N, Nair P. Immunogenicity of Biotherapeutics: Causes and Association with Posttranslational Modifications. J Immunol Res. 2016;2016:1298473. https://doi.org/10.1155/2016/1298473

27. Lelievre, E., et al., The Ets family contains transcriptional activators and repressors involved in angiogenesis. Int J Biochem Cell Biol, 2001. 33(4): p. 391-407. https://doi.org/10.1016/s1357-2725(01)00025-5

28. Lawson, Nathan D. M. Weinstein(2002) In Vivo Imaging of Embryonic Vascular Development Using Transgenic Zebrafish, Developmental Biology, ISSN 0012-1606,

29. https://doi.org/10.1006/dbio.2002.0711.

30. Li, C., Wang, Z., Chen, Y., Zhou, M., Zhang, H., Chen, R., Shi, F., Wang, C., & Rui, Z. (2015). Transcriptional silencing of ETS-1 abrogates epithelial-mesenchymal transition, resulting in reduced motility of pancreatic cancer cells. Oncol Rep, 33(2), 559-565. https://doi.org/10.3892/or.2014.3613

31. Ma J, Ren J, Thorikay M, van Dinther M, Sanchez-Duffhues G, Caradec J, Benderitter P, Hoflack J, Ten Dijke P. Inhibiting Endothelial Cell Function in Normal and Tumor Angiogenesis Using BMP Type I Receptor Macrocyclic Kinase Inhibitors. Cancers (Basel). 2021 Jun 12;13(12):2951. https://doi.org/10.3390/cancers13122951.

32. Manzari MT, Shamay Y, Kiguchi H, Rosen N, Scaltriti M, Heller DA. Targeted drug delivery strategies for precision medicines. Nat Rev Mater. 2021 Apr;6(4):351-370.https://doi.org/10.1038/s41578-020-00269-6.

33. Mathis, G. (1999). HTRF(R) Technology. J Biomol Screen, 4(6), 309-314. https://doi.org/10.1177/108705719900400605

34. Oettgen P. The role of ets factors in tumor angiogenesis. J Oncol. 2010;2010:767384. https://doi.org/10.1155/2010/7673844

35. Roukens, M. G., Alloul-Ramdhani, M., Baan, B., Kobayashi, K., Peterson-Maduro, J., van Dam, H., Schulte-Merker, S., & Baker, D. A. (2010). Control of endothelial sprouting by a Tel-CtBP complex. Nat Cell Biol, 12(10), 933-942. https://doi.org/10.1038/ncb2096

36. Schober, M., Rebay, I., & Perrimon, N. (2005). Function of the ETS transcription factor Yan in border cell migration. 132(15), 3493-3504. https://doi.org/10.1242/dev.01911 %J Development

37. Siegal, G., Ab, E., & Schultz, J. (2007). Integration of fragment screening and library design. Drug Discov Today, 12(23-24), 1032-1039. https://doi.org/10.1016/j.drudis.2007.08.005

38. Sizemore, G. M., Pitarresi, J. R., Balakrishnan, S., & Ostrowski, M. C. (2017). The ETS family of oncogenic transcription factors in solid tumors. Nat Rev Cancer, 17(6), 337-351. https://doi.org/10.1038/nrc.2017.20

39. Song, W., Fhu, C. W., Ang, K. H., Liu, C. H., Johari, N. A., Lio, D., Abraham, S., Hong, W., Moss, S. E., Greenwood, J., & Wang, X. (2015). The fetal mouse metatarsal bone explant as a model of angiogenesis. Nat Protoc, 10(10), 1459-1473. https://doi.org/10.1038/nprot.2015.097

40. Wasylyk, B., Hagman, J., & Gutierrez-Hartmann, A. (1998). Ets transcription factors: nuclear effectors of the Ras-MAP-kinase signaling pathway. Trends Biochem Sci, 23(6), 213-216.

41. https://doi.org/10.1016/s0968-0004(98)01211-0

42. Wei F, Wang S, Gou X. A review for cell-based screening methods in drug discovery. Biophys Rep. 2021 Dec 31;7(6):504-516.

43. https://doi.org/10.52601/bpr.2021.210042

44. Ye, W., Qian, T., Liu, H., Luo, R., & Chen, H. F. (2017). Allosteric Autoinhibition Pathway in Transcription Factor ERG: Dynamics Network and Mutant Experimental Evaluations. J Chem Inf Model, 57(5), 1153-1165. https://doi.org/10.1021/acs.jcim.7b00073

45. Zhong, L., Li, Y., Xiong, L. et al. Small molecules in targeted cancer therapy: advances, challenges, and future perspectives. Sig Transduct Target Ther 6, 201 (2021). https://doi.org/10.1038/s41392-021-00572-w

46. Zhou, X., Zhou, R., Zhou, H., Li, Q., Hong, J., Meng, R., Zhu, F., Zhang, S., Dai, X., Peng, G., Wu, G., & Li, Z. (2018). ETS-1 Induces Endothelial-Like Differentiation and Promotes Metastasis in Non-Small Cell Lung Cancer. Cell Physiol Biochem, 45(5), 1827-1839. https://doi.org/10.1159/000487874

.

CHAPTER 6

General Discussion

This thesis focuses on angiogenesis, the formation of new blood vessels from pre-existing ones. It plays a crucial role in various physiological processes, such as wound healing, tissue repair, tumor growth, invasion, and metastasis (Liu et al., 2023; Bielenberg and Zetter, 2015; Lugano et al., 2020). 2023; Bielenberg and Zetter 2015; Lugano, Ramachandran, and Dimberg 2020). While angiogenesis is mediated by a variety of signaling pathways such as cytokines and extracellular matrix molecules, it is orchestrated mainly by two principal pathways: one comprises intracellular signaling through vascular endothelial growth factor (VEGF) receptors (VEGFR), and the other includes intercellular signaling via the NOTCH/DLL4 pathway. Understanding the mechanisms of this process is crucial for developing therapies for diseases associated with abnormal angiogenesis such as cancer and diabetic retinopathy.

Intriguingly, within the scope of this thesis, we have uncovered new fundamental aspects of NOTCH/DLL4 signaling. This has introduced a new dimension for understanding the molecular mechanisms governing angiogenesis. Interestingly, we have also identified mutant FOS protein in human vascular tumors and conducted functional analyses of this FOS variant. Although, concerning angiogenesis, the NOTCH pathway in general, and DLL4 in particular, have emerged as potential and promising targets for novel therapeutic interventions in cancer. However, the work presented in this thesis provides an excellent methodology for drug screening and has led to the characterization of a novel ETS transcription factor inhibitors.

In the scope of this thesis, we have uncovered new basic features of NOTCH signalling that might strongly influence basic angiogenesis mechanisms. This understanding has the potential to greatly benefit drug discovery efforts aimed at inhibiting angiogenic signaling pathways.

CHAPTER 2

The NOTCH signaling pathway plays a critical role in cell differentiation, tissue growth, tissue remodeling, and apoptosis of most metazoan cell types. However, accumulating evidence suggests that there are multiple, less well-defined layers of regulation in the NOTCH signaling pathway. The work in chapter 2 has provided strong insight into how NOTCH ligands control endothelial cell (EC) tube formation. Until now, little was known about the cleavage of the intracellular domain (ICD) of the NOTCH ligand, DLL4 (DLL4INTRA). The experiments reported in chapter 2 provide a new insight into the potential relationship between the intracellular domain of DLL4 and specific components of the AP-1 transcription factor complex. This study suggested that DLL4INTRA, a component of the NOTCH signaling pathway, can play a direct role in gene regulation and signaling by inhibiting the activity of the JUN transcription factor.

While previous research has focused on the canonical NOTCH signaling pathway (Zhu et al., 2019; Schober et al., 2005), our results demonstrate the possible existence of multiple layers of regulation, which to date are not well-defined. These results build on existing evidence of the effects of ligand ICDs at the cellular level. It has been shown that ectopic expression of the DLL1 ICD causes growth arrest of primary ECs (Fortini, 2009). In addition, inhibition of NOTCH1 signaling by the JAGGED1 ICD can modulate cardiac homeostasis in the postnatal heart (Metrich et al., 2015). However, in this study our results strikingly highlight a potential link between untethered NOTCH ligand ICDs and the immediate-early gene AP-1 transcription factor complex. Our findings provide additional information about the potential role of DLL4INTRA in endothelial cell response through cross-talk with the bZIP domain of JUN. Furthermore, our study suggests that corruption of this mechanisms might play a role in disease processes such as tumor angiogenesis and developmental disorders. This important finding may further highlight the NOTCH pathway as a primary target to inhibit tumor growth therapeutically, and it has also been linked to rare congenital disorders and diseases.

Interestingly, our present data also indicates that DLL4 ICD is required for normal DLL4 subcellular localization. The experiments revealed that JUN does not appear to interact with the full-length version of DLL4, which contains an intracellular domain. This suggests that the overall structure of DLL4 may impede the occurrence of this interaction. Additionally, it is possible that DLL4 forms oligomers or dimers (Consistent with our discovery discussed in Chapter 3), which may have impact on DLL4 interactions and which could make the C terminus inaccessible for interactions with JUN These findings indicate that the intracellular domain of DLL4 may have a dual role, interacting with the bZIP domain of JUN and also encoding a PDZ-binding domain that enables a functional association with multi-PDZ domain protein MUPP1, which is required for normal ligand trafficking, as well as the cAMP responsive element binding protein CREB3. Notably, our results provide evidence for the importance of the JUN bZIP domain in the stimulation of sprouting of ECs. In line with our finding that DLL4INTRA inhibits JUN-driven EC sprouting, it can be concluded that this occurs by inhibiting JUN binding to a consensus AP-1 DNA site and thereby controlling the expression of JUN target genes, including DLL4. This finding suggested that JUN-DLL4INTRA interactions, could form part of a feedback loop in regulating DLL4 expression. This result ties in well with previous studies wherein genome-wide screens have shown cooperation between AP-1 and ETS transcription factor via neighboring AP-1 and ETS DNA-binding sites (Plotnik et al., 2014).

Furthermore it has been reported that ETS transcription factors regulate angiogenesis (Craig and Sumana,s 2016; Randi et al., 2009; Roukens et al., 2010) via control of DLL4 expression (Shah et al., 2017; Roukns et al., 2010).Overall, our

results suggest that upon VEGF stimulation, DLL4INTRA, in association with ETS/AP-1 factors could potentially regulate DLL4 expression.
Our results shed new light on the intracellular domain of the NOTCH ligand DLL4, which might participate in signaling and downstream transcription. These results may lead to a better understanding of the potential bidirectional signaling of NOTCH/DLL4. Furthermore, our key findings highlight the untethered NOTCH ligand ICDs as a point of cross-talk between the NOTCH pathway and other pathways, such as receptor tyrosine kinase (RTK) signaling. It will be of great importance to explore the specific mechanisms of DLL4INTRA cleavage and turnover, as well as determining the possible similar functionality of other NOTCH ligand ICD domains. Further studies should investigate the function and regulation of NOTCH signaling through the DLL4 ICD, which could lead to a better understanding of the pathway and uncover new, potential therapeutic targets.

CHAPTER 3

The NOTCH receptor has been intensely studied since its initial description by Thomas Hunt Morgan in 1917 (Andersson et al., 2011). Although, experimentally and theoretically, numerous research efforts have been directed toward a comprehensive understanding of NOTCH signaling, several gaps in the field still need to be addressed. In Chapter 3, we aimed to provide a new perspective on understanding the mechanism of the NOTCH pathway. The NOTCH signaling pathway is a critical signaling system that plays a role in the development and differentiation of cells. It involves the interaction between NOTCH receptors and ligands expressed on neighboring cells (trans signalling) and within the same cell (cis inhibition).
Different molecules and force requirements are needed to initiate NOTCH signaling. An important open question in the field is how specific output is generated from the combination of Cis and Trans interactions of the various NOTCH ligands and receptors. In this chapter, we embarked on a series of experimental and mathematical modeling studies to understand the mechanism of the NOTCH pathway and answer these questions.
It is assumed that the DLL4 ligand functions as a monomer, but surprisingly, in this study, we have presented evidence that NOTCH ligands can efficiently homo- and heterodimerize. NOTCH ligand dimerization/oligomerization could have a crucial impact on our understanding of the dynamics of NOTCH signaling, as the regulation of dimer formation and its disassembly may serve as an additional point of control for the strength of NOTCH signaling.
Specifically, in Chapter 3, we demonstrated that NOTCH ligands can self-associate and that this dimerization is required explicitly for cis-inhibition of NOTCH receptor activity but not NOTCH receptor transactivation. In light of this, we developed a mathematical model to take into account the role of ligand

dimerization in cis-inhibition and found that the model accurately reproduced previously published experimental data and could improve the predictions. Interestingly, our results suggest that the net output of NOTCH signalling is determined by a balance between ligand monomer-driven transactivation and ligand dimer-mediated cis-inhibition. A new general model adapted from the mutual inactivation model has been developed to explore the potential role of ligand monomers and dimers in net signaling output from the NOTCH pathway.
Importantly, our results shed new light on the cellular mechanism underlying the formation of boundaries in the development of the Drosophila wing's discs, which historically has been an essential model system for understanding NOTCH signalling. Our dimerization model's validity has also been verified in the context of tissue patterning processes. We also analyzed a further extension of our dimerization model, in which we showed that the ligand dimerization mechanism of NOTCH enables veins and inter-vein formation in the Drosophila wing.
The four mammalian NOTCH receptors and the five mammalian NOTCH ligands give rise to at least 20 different receptor-ligand combinations. The finding of ligand dimerization potentially increases the range of possible receptor-ligand combinations and resulting signaling outputs. Additionally, our biochemical experiments showed that ligands can also hetero-oligomerize. Therefore, ligand oligomerization may offer additional complexity in NOTCH signaling and yield diverse signaling outputs (see Fig C in S1 Text chapter 3).
Besides our previous discovery regarding NOTCH/DLL4 bidirectional signaling, understanding the biological function and mechanism of the DLL4 dimerization might be integral to designing robust treatments. In this regard, a more complete understanding of the mechanism of binding different interactions between NOTCH ligands and receptors will require additional analysis. However, from an experimental aspect, several technical hurdles still had to be overcome, including the size and complexity of the extracellular domains of ligands and receptors, which make some experiments more challenging. For instance, NOTCH receptors and ligands are single-pass transmembrane proteins of about 150-300 kDa in size. Hence, the technical challenges associated with purifying sufficient quantities of receptors and ligands have precluded biochemical studies with full-length proteins.
Further work is certainly required to disentangle these complexities. Under these circumstances, recent technological advances such as Cryo-EM might enable a deeper structural understanding of the dimerization process and its role in NOTCH signalling.
Collectively, uncovering this novel dimension of NOTCH signaling opens up entirely new perspectives for understanding the dynamics of the NOTCH pathway and, accordingly, of angiogenesis. It would be interesting to examine

whether the NOTCH receptors themselves can also oligomerize/dimerize and, if so, to delineate the mechanistic consequences. This also has potential implications for understanding the role of NOTCH in disease.

CHAPTER 4

The research in Chapter 4 presented the first functional characterization of mutant FOS proteins discovered in a human tumor, specifically, an epithelioid hemangioma tumor. In order to elucidate the underlying cause of this bone tumor, we analyzed three previously characterized translocations (van et al. 2015). We analyzed human epithelioid cell Lysate and revealed a truncated FOS protein lacking a C-terminal disordered region. Although the involvement of a FOS gene in this type of cancer was established before (Antonescu et al., FOS-MBNL1 translocation), this is the first study to functionally characterize mutant FOS proteins discovered in a human tumor.

To the best of our knowledge, this was the first report that indicates sustained expression of FOS due to deletion of the four C-terminal amino acids of FOS, which could initiate the formation of vascular neoplasms. By taking a mutagenesis approach, we discovered that the terminal short helical region of C terminal FOS can orchestrate the ubiquitin-independent degradation of FOS. The fact that ubiquitination is not a prerequisite for FOS proteasomal degradation and that truncated FOS appears to be resistant to this process, coupled with the fact that FOSΔ protein levels appear to be substantially higher than wild-type FOS protein levels in patient cells, suggests that the highly conserved helical motif is critical for controlling FOS stability. Our data reveals a novel mechanism by which aberrant FOS protein can drive the formation of vascular neoplasms.

Our global transcriptome analyses clarified the mechanistic basis of FOS-driven sprouting. Importantly, we found that both wild-type and mutant FOS control the expression of angiogenesis-related genes, including MMPs and components of the NOTCH-signaling pathway. These findings were among the first to highlight FOS as an activator of endothelial sprouting by direct interaction with the FOS promoter. Our work presented in Chapter 3 has uncovered a new role for FOS in stimulating endothelial cell sprouting. We also demonstrated that a recently reported small molecule inhibitor of FOS (Makino et al., 2017) can inhibit FOS-driven endothelial sprouting (Figure. S5). This finding might help the development of novel treatments for rheumatoid arthritis and open a new dimension for understanding tumor angiogenesis.

CHAPTER 5

Angiogenesis can be controlled through various mechanisms like inhibition of angiogenic signaling pathways, suppression of critical transcriptional regulators, and targeting specific angiogenic molecules (Liu et al., 2023). While anti-

angiogenic therapies have shown promise in treating cancer with combination therapy, there are growing appeals for new targets due to a growing concern about the development of drug resistance and tumor recurrence, among other limitations (Liu et al., 2023). Although these challenges are also evident in anti-angiogenic therapy and chemotherapy, consuming anti-angiogenic combination therapy to its full potential is urgently needed to treat various clinical conditions where treatment options are lacking (Nandagopal et al., 2019; Fleming et al., 2013). For example, maximizing the clinical efficacy of treatment for non-small cell lung cancer (NSCLC) has been achieved through a combination of angiogenesis inhibitors, immune system regulators, and chemotherapy. This combination overcome the resistance issue regarding the treatment of EGFR-mutant NSCLC (Sun et al., 2022). Therefore, the angiogenesis process has been widely observed, and several approaches to inhibit the angiogenic signaling pathways have been considered through the last decades.

Through the use of new technologies, the pool of potential drug targets is expanding. Rather than targeting the upstream components of cell signalling networks (presumed to be druggable), we developed methodologies for identifying small molecule inhibitors of transcription factors downstream of these pathways (previously regarded as undruggable). It is likely that the action of transcription factors, which are downstream of signalling systems, ultimately drive the illicit behaviors of tumor cells. This makes them attractive targets for rational anticancer drug design.

The research presented in Chapter 5 builds on existing evidence of the central role of ETS transcription factors in regulating angiogenesis. To the best of our knowledge, this is the first report of identifying small molecule inhibitors that block the activity of these transcription factors and their association with specific DNA binding sites. As stated in Chapter 5, ETS transcription factors are frequently dysregulated in cancers. Additionally, certain ETS factors are also crucial in angiogenic development. Therefore, blocking the angiogenesis process by targeting ETS proteins could represent a novel approach to cancer treatment.

Through fragment-based screening, we identified potential fragment hits, which were screened by NMR. We selected the fragment hits as an ETS/DNA binding inhibitor, followed by a high-throughput screen to obtain lead-like compounds. Thus, this project aimed to identify potential ETS inhibitors and validate them through various cell-based and biochemical approaches. To investigate the anti-tumor activity of our inhibitors, several cancer types, in particular prostate cancer and Ewing's sarcoma, were studied.

As it has been established that the promotion of cellular proliferation is probably the most important function of ETS factors within cancer, and also ETS mutations are the primary drivers of cellular proliferation, one would expect to see cancer cell proliferation reduction with the treatment of effective ETS inhibitors (Zhu et

al., 2019). Here, we observed that the ETS inhibitors strongly inhibited cellular proliferation and movement of cancer cell lines. Additionally, it has been demonstrated that the treatment with our compounds reduced sprouting vessels in Metatarsal angiogenesis assays, thereby highlighting an additional potential benefit of this anti-angiogenic treatment. The validity of this data can be validated through the use of Xenograft mouse cancer models, which would allow us to determine the impact of our drugs on *in vivo* tumorigenesis. This is the next essential step in our study.

Targeting specific transcription factors could help overcome problems such as drug resistance and toxicity. One way to potentially enhance specificity would be to perform screens with full-length protein and not simply the ETS DBD. With a complimentary effort of characterizing and determining the nature of gene networks, we will address the influence of the novel compounds at the molecular level through transcriptome analyses, proteome analyses, and genome-wide ChIP studies and by examination of the expression of ETS and ERG-regulated genes, such as SOX9, which has been earlier shown to stimulate PCa invasion (Cai et al., 2013; Wang et al., 2008).

Resistance to treatment is a significant problem in oncology. In future studies, we will investigate the potential of cancer cells to develop resistance to the ETS inhibitors THIS. Testing potential synergistic interactions between our ETS inhibitors and other inhibitors, such as the BCL2 inhibitor venetoclax, will be important.

While it was outside the scope of this study to thoroughly examine all possible avenues for further investigation, future research will greatly benefit from incorporating the additional experiments mentioned. The concept that ETS proteins can serve as viable targets for drug development could represent a significant advancement in the field of oncology, as these previously considered undruggable targets are now considered potential options for future treatments.

REFERENCES

1. Andersson, E. R., R. Sandberg, and U. Lendahl. 2011. 'Notch signaling: simplicity in design, versatility in function', Development, 138: 3593-612.
2. Bielenberg, D. R., and B. R. Zetter. 2015. 'The Contribution of Angiogenesis to the Process of Metastasis', Cancer J, 21: 267-73.
3. Craig, M. P., and S. Sumanas. 2016. 'ETS transcription factors in embryonic vascular development', Angiogenesis, 19: 275-85.
4. de Celis, J. F., and S. Bray. 1997. 'Feed-back mechanisms affecting Notch activation at the dorsoventral boundary in the Drosophila wing', Development, 124: 3241-51.
5. Doherty, D., G. Feger, S. Younger-Shepherd, L. Y. Jan, and Y. N. Jan. 1996. 'Delta is a ventral to dorsal signal complementary to Serrate, another Notch ligand, in Drosophila wing formation', Genes Dev, 10: 421-34.
6. Fleming, R. J., K. Hori, A. Sen, G. V. Filloramo, J. M. Langer, R. A. Obar, S. Artavanis-Tsakonas, and A. C. Maharaj-Best. 2013. 'An extracellular region of Serrate is essential for ligand-induced cis-inhibition of Notch signaling', Development, 140: 2039-49.
7. Folkman, J. 2003. 'Angiogenesis inhibitors: a new class of drugs', Cancer Biol Ther, 2: S127-33.
8. Fortini, M. E. 2009. 'Notch signaling: the core pathway and its posttranslational regulation', Dev Cell, 16: 633-47.
9. Glittenberg, M., C. Pitsouli, C. Garvey, C. Delidakis, and S. Bray. 2006. 'Role of conserved intracellular motifs in Serrate signalling, cis-inhibition and endocytosis', EMBO J, 25: 4697-706.
10. Kelly, D. F., R. J. Lake, T. C. Middelkoop, H. Y. Fan, S. Artavanis-Tsakonas, and T. Walz. 2010. 'Molecular structure and dimeric organization of the Notch extracellular domain as revealed by electron microscopy', PLoS One, 5: e10532.
11. Liu, Z. L., H. H. Chen, L. L. Zheng, L. P. Sun, and L. Shi. 2023. 'Angiogenic signaling pathways and anti-angiogenic therapy for cancer', Signal Transduct Target Ther, 8: 198.
12. Lugano, R., M. Ramachandran, and A. Dimberg. 2020. 'Tumor angiogenesis: causes, consequences, challenges and opportunities', Cell Mol Life Sci, 77: 1745-70.
13. Makino, H., S. Seki, Y. Yahara, S. Shiozawa, Y. Aikawa, H. Motomura, M. Nogami, K. Watanabe, T. Sainoh, H. Ito, N. Tsumaki, Y. Kawaguchi, M. Yamazaki, and T. Kimura. 2017. 'A selective inhibition of c-Fos/activator protein-1 as a potential therapeutic target for intervertebral disc degeneration and associated pain', Sci Rep, 7: 16983.
14. Metrich, M., A. Bezdek Pomey, C. Berthonneche, A. Sarre, M. Nemir, and T. Pedrazzini. 2015. 'Jagged1 intracellular domain-mediated inhibition of Notch1 signalling regulates cardiac homeostasis in the postnatal heart', Cardiovasc Res, 108: 74-86.
15. Nandagopal, N., L. A. Santat, and M. B. Elowitz. 2019. 'Cis-activation in the Notch signaling pathway', Elife, 8.
16. Nandagopal, N., L. A. Santat, L. LeBon, D. Sprinzak, M. E. Bronner, and M. B. Elowitz. 2018. 'Dynamic Ligand Discrimination in the Notch Signaling Pathway', Cell, 172: 869-80 e19.
17. Plotnik, J. P., J. A. Budka, M. W. Ferris, and P. C. Hollenhorst. 2014. 'ETS1 is a genome-wide effector of RAS/ERK signaling in epithelial cells', Nucleic Acids Res, 42: 11928-40.
18. Randi, A. M., A. Sperone, N. H. Dryden, and G. M. Birdsey. 2009. 'Regulation of angiogenesis by ETS transcription factors', Biochem Soc Trans, 37: 1248-53.
19. Roukens, MG, M Alloul-Ramdhani, B Baan, K Kobayashi, J Peterson-Maduro, H van Dam, S Schulte-Merker, and DA Baker. 2010b. 'Control of endothelial sprouting by a Tel-CtBP complex', Nat Cell Biol, 12: 933-42.
20. Schober, M., I. Rebay, and N. Perrimon. 2005. 'Function of the ETS transcription factor Yan in border cell migration', Development, 132: 3493-504.
21. Shah, A. V., G. M. Birdsey, C. Peghaire, M. E. Pitulescu, N. P. Dufton, Y. Yang, I. Weinberg,

L. Osuna Almagro, L. Payne, J. C. Mason, H. Gerhardt, R. H. Adams, and A. M. Randi. 2017. 'The endothelial transcription factor ERG mediates Angiopoietin-1-dependent control of Notch signalling and vascular stability', Nat Commun, 8: 16002.

22. Sprinzak, D., A. Lakhanpal, L. Lebon, L. A. Santat, M. E. Fontes, G. A. Anderson, J. Garcia-Ojalvo, and M. B. Elowitz. 2010. 'Cis-interactions between Notch and Delta generate mutually exclusive signalling states', Nature, 465: 86-90.

23. Sun, R., Z. Hou, Y. Zhang, and B. Jiang. 2022. 'Drug resistance mechanisms and progress in the treatment of EGFR-mutated lung adenocarcinoma', Oncol Lett, 24: 408.

24. Teleanu, R. I., C. Chircov, A. M. Grumezescu, and D. M. Teleanu. 2019. 'Tumor Angiogenesis and Anti-Angiogenic Strategies for Cancer Treatment', J Clin Med, 9.

25. van, IJzendoorn D. G., D. de Jong, C. Romagosa, P. Picci, M. S. Benassi, M. Gambarotti, S. Daugaard, M. van de Sande, K. Szuhai, and J. V. Bovee. 2015. 'Fusion events lead to truncation of FOS in epithelioid hemangioma of bone', Genes Chromosomes Cancer, 54: 565-74.

26. Zeronian, M. R., O. Klykov, I. de Montserrat J. Portell, M. J. Konijnenberg, A. Gaur, R. A. Scheltema, and B. J. C. Janssen. 2021. 'Notch-Jagged signaling complex defined by an interaction mosaic', Proc Natl Acad Sci U S A, 118.

27. Zhu, N., L. Gu, J. Jia, X. Wang, L. Wang, M. Yang, and W. Yuan. 2019. 'Endothelin-1 triggers human peritoneal mesothelial cells' proliferation via ERK1/2-Ets-1 signaling pathway and contributes to endothelial cell angiogenesis', J Cell Biochem, 120: 3539-46.

28. Benedito R, Roca C, Sörensen I, Adams S, Gossler A, Fruttiger M, Adams RH. The notch ligands Dll4 and Jagged1 have opposing effects on angiogenesis. Cell 2009;137(6): 1124–1135. doi: 10.1016/j.cell.2009.03.025

29. Cai C, Wang H, He HH, Chen S, He L, Ma F, Mucci L, Wang Q, Fiore C, Sowalsky AG, Loda M, Liu XS, Brown M, et al. ERG induces androgen receptor-mediated regulation of SOX9 in prostate cancer. J Clin Invest. 2013;123:1109–22.

30. Wang H, Leav I, Ibaragi S, Wegner M, Hu GF, Lu ML, Balk SP, Yuan X. SOX9 is expressed in human fetal prostate epithelium and enhances prostate cancer invasion. Cancer Res. 2008;68:1625–30.

A

Appendix

Summary in English

Nederlandse Samenvatting

List of Abbreviation

Publications

Acknowledgments

Curriculum Vitae

SUMMARY IN ENGLISH

Angiogenesis, the process of new blood vessel formation from existing blood vessels, is essential for wound healing, embryonic development, as well as organ function regulation. Vascular Endothelial Growth Factor Receptor (VEGFR) and NOTCH signaling are among the main pathways that work in coordination to orchestrate the complex process of angiogenesis. Understanding the underlying molecular and cellular mechanisms is crucial for developing angiogenesis-based therapies for treating diseases like cancer and cardiovascular disease. Approaches to control angiogenesis encompass targeting specific angiogenic signalling molecules and suppressing their key intracellular transcriptional effectors. Within the scope of this thesis I investigated the precise control of angiogenesis and the potential effects of pharmacological intervention of signaling pathways involved in angiogenesis. The obtained insights have shed new light on the basic mechanism underlying angiogenesis and may aid drug discovery endeavors focused on manipulating angiogenic signaling pathways for therapeutic gain.

The NOTCH receptor is a transmembrane receptor that consists of NOTCH extracellular domain (NECD), the transmembrane (TM) domain, and (the NOTCH intracellular domain (NICD). In mammals four NOTCH receptors are found that are highly conserved. NOTCH signaling is initiated when DELL or JAGGED ligands, which are also transmembrane proteins, engage with Notch receptors and thereby induce a proteolytic cleave resulting in the release of the intracellular domain, which translocate to the nucleus and directs specific transcriptional responses. This pathway is regulated in multiple ways and new mechanisms continue to be discovered. Besides, the aforementioned control of angiogenesis, NOTCH signaling also plays a pivotal role in cell differentiation, tissue growth, tissue remodeling, and apoptosis in various cell types, including neuronal and also cancer cells.

The research in chapter 2 has shed light on how NOTCH ligands influence the formation of endothelial cell tubes. Previously, the cleavage of the intracellular domain (ICD) of the NOTCH ligand (DLL4) was poorly understood. We provided evidence that DLL4 ICD which is highly conserved throughout vertebrate is proteolytically cleaved. In addition to that, our data highlights two previously unreported roles for DLL4 ICD. Firstly, it is required for normal DLL4 subcellular localization. Secondly, the untethered ICD interacts with JUN transcription factor and can prevent Jun from binding to DNA, which, in turn, regulates the activation of JUN target genes, including DLL4 itself. Our research also revealed that JUN plays a significant role in promoting the formation of endothelial cell tubes, while DLL4 acts to restrain this process. These findings suggest the intriguing possibility of bidirectional signaling of NOTCH/DLL4 pathway and propose that the DLL4 ICD

may serve as a crucial point of interaction between NOTCH and receptor tyrosine kinase (RTK) signaling.

Previous studies have shown that NOTCH receptors are regulated by two primary mechanisms. One is by direct cell-cell contact, during which NOTCH ligands from one cell interact with NOTCH receptor in another cell, leading to intercellular (trans) NOTCH activation. The second mechanism involves inhibition of receptor function by ligand-receptor interactions within a single cell, known as cis inhibition. Moreover, recent findings have also indicated the occurrence of cis activation upon ligand-receptor interaction within one cell. In Chapter 3 our research demonstrates that NOTCH ligands, such as DLL4 can self-associate effectively, in both biochemical assays and *in vitro* cell culture studies. We show that the specific region responsible for this binding is the membrane proximal epidermal growth factor (EGF)-like repeat of DLL4. Our findings suggest that DLL4 ligand dimerization is crucial for inhibiting NOTCH receptor activity within the same cell (cis inhibition). Our results of NOTCH ligand dimerization/oligomerization are of great importance for understanding the dynamics of the NOTCH signaling, as the regulation of dimer formation and its disassembly may serve as an additional point of control for the strength and specificity of NOTCH signaling.

To strengthen these findings, we have employed powerful mathematical modelling approaches to extended existing models of NOTCH signaling, centered on the use of regular differential equations. The generated computational simulations were greatly supportive of the idea of dimerization-dependent cis inhibition of NOTCH signalling, as revealed in our biochemical and cell biological based study. Importantly, our refined mathematical model recapitulates published experimental data, and improves predictions based upon published mechanisms of NOTCH-driven tissue development. Our model introduces a new perspective for the understanding of the biological processes, which are controlled by NOTCH, underpinning embryo development and angiogenesis.

In chapter 4 we explore the connection between aberrant function of the transcription factor FOS and vascular tumors such as epithelioid hemangioma, which is an aggressive tumor characterized by vascular neoplasms in bones and soft tissue. Recent research has highlighted FOS translocations as a potential contributor to tumorigenesis, though to date no such mutations had been identified as causal mutations in human cancer. Through analysis of human epithelioid hemangioma tumor cell lysates, we revealed a truncated FOS (mutant FOS) protein *in vivo*, which resulted from a FOS-MBNL1 translocation. The finding led us to investigate the molecular underpinnings of a possible role of FOS translocations in vascular tumor evolution and also tumor angiogenesis. Our study represents the first comprehensive molecular and biochemical evaluation of a mutant FOS protein identified within this human vascular tumor. We

provided evidence that the mutant FOS protein was much more stable, due to a C-terminus truncation, and this could drive the emergence of vascular neoplasms. We found that the mutant FOS protein potently stimulated endothelial sprouting, and stimulated vascular tumor formation by disturbing matrix metalloproteinase (MMP) production and the NOTCH signaling pathway, which are key players of angiogenesis. Our study also introduced the concept of ubiquitin-independent proteasomal degradation (UIPD), and revealed the role of the unstructured FOS C-terminus in mediating protein degradation. This is the first link between FOS mutations and natural tumor development. Moreover, our results provide therapeutic avenues for the treatment of epithelioid hemangiomas with mutant FOS proteins by targeting mutant FOS or proteins whose expression is triggered by FOS.

Malfunction of multiple ETS transcription factors have been implicated in contributing to the emergence of various tumors, including Ewing's sarcoma (ES) and prostate cancer. This research described in chapter 5 demonstrates the feasibility of developing molecular inhibitors to reduce ETS factor transcriptional activity through the disruption of ETS protein-DNA interactions. Our unique approach involved obtaining pure protein preparations of ETS factors and conducting functional -high throughput screens to identify novel small molecules inhibitors of ETS function. Selection of the molecules that inhibit ETS-DNA interaction may enable generation of drug-like molecules that will be able to target specific ETS proteins. Initially an HTRF assay was performed which measured the ability of compounds to disrupt binding of a purified ETS DNA-binding domain to its specific consensus DNA binding site resulting in the identification of five novel compounds. Subsequently, we interrogated the inhibitors in different biochemical/biological assays (such as cell proliferation, cytotoxicity and endothelial sprouting assay using primary human endothelial cells as well as, zebrafish and mouse Metatarsal). Our present results offer promising initial indications that these compounds have the potential to impede tumor cell growth, inhibit angiogenesis and that the observed effects could result from inhibition of the activity of ETS transcription factors. This ongoing study has the potential to provide novel therapeutic agents that target ETS proteins.

NEDERLANDSE SAMENVATTING

Angiogenese, het proces waarbij nieuwe bloedvaten zich vormen uit bestaande bloedvaten, is essentieel voor wondgenezing, embryonale ontwikkeling en de regulatie van orgaanfuncties. Vascular Endothelial Growth Factor Receptor (VEGFR)- en NOTCH-signaleringswegen behoren tot de belangrijkste paden die samenwerken om het complexe proces van angiogenese te coördineren. Het begrijpen van de onderliggende moleculaire en cellulaire mechanismen is cruciaal voor de ontwikkeling van op angiogenese gebaseerde therapieën voor de behandeling van ziekten zoals kanker en hart- en vaatziekten. Benaderingen om angiogenese te beheersen omvatten het richten op specifieke angiogene signaalmoleculen en het onderdrukken van hun belangrijke intracellulaire transcriptiefactoren. In het kader van dit proefschrift heb ik het precieze beheer van angiogenese en de potentiële effecten van farmacologische interventies in de signaleringswegen die betrokken zijn bij angiogenese onderzocht. De verkregen inzichten werpen nieuw licht op het basismechanisme dat ten grondslag ligt aan angiogenese en kunnen helpen bij ontdekkingsinspanningen voor geneesmiddelen die gericht zijn op het manipuleren van angiogene signaleringswegen voor therapeutisch gewin. De NOTCH-receptor is een transmembraanreceptor die bestaat uit het NOTCH-extracellulaire domein (NECD), het transmembraandomein (TM) en het NOTCH-intracellulaire domein (NICD). Bij zoogdieren worden vier NOTCH-receptoren aangetroffen die sterk geconserveerd zijn. NOTCH-signalisatie wordt geïnitieerd wanneer DELL- of JAGGED-liganden, die ook transmembraaneiwitten zijn, zich binden aan NOTCH-receptoren en daardoor een proteolytische splitsing veroorzaken. Dit resulteert in de afgifte van het intracellulaire domein, dat naar de kern transloceert en specifieke transcriptionele reacties aanstuurt. Deze route wordt op verschillende manieren gereguleerd en nieuwe mechanismen worden voortdurend ontdekt. Naast de bovengenoemde beheersing van angiogenese speelt NOTCH-signalisatie ook een cruciale rol in cel differentiatie, weefselgroei, weefselremodellering en apoptose in verschillende celtypen, waaronder neurale- en kankercellen.

Het onderzoek in hoofdstuk 2 heeft licht geworpen op hoe NOTCH-liganden de vorming van endotheelcelbuizen beïnvloeden. Voorheen was de splitsing van het intracellulaire domein (ICD) van de NOTCH-ligand (DLL4) slecht begrepen. We hebben aangetoond dat DLL4 ICD, dat sterk geconserveerd is bij gewervelde dieren, proteolytisch wordt gesplitst. Daarnaast benadrukken onze gegevens twee eerder niet-gerapporteerde rollen voor DLL4 ICD. Ten eerste is het vereist voor de normale subcellulaire lokalisatie van DLL4. Ten tweede, het ongebonden ICD interageert met de JUN-transcriptiefactor en kan voorkomen dat JUN zich bindt aan DNA, wat op zijn beurt de activering van JUN-doelgenen, waaronder

DLL4 zelf, reguleert. Ons onderzoek toonde ook aan dat JUN een significante rol speelt bij het bevorderen van de vorming van endotheelcelbuizen, terwijl DLL4 dit proces beperkt. Deze bevindingen suggereren de intrigerende mogelijkheid van bidirectionele signalisatie van de NOTCH/DLL4-route en stellen voor dat de DLL4 ICD kan dienen als een cruciaal interactiepunt tussen NOTCH- en receptor-tyrosinekinase (RTK)-signaaltransductie.
Eerdere studies hebben aangetoond dat NOTCH-receptoren worden gereguleerd door twee primaire mechanismen. Eén is door direct cel-celcontact, waarbij NOTCH-liganden van de ene cel interageren met de NOTCH-receptor in een andere cel, wat leidt tot intercellulaire (trans) NOTCH-activering. Het tweede mechanisme betreft de remming van receptorfunctie door ligand-receptorinteracties binnen één cel, bekend als cis-remming. Bovendien hebben recente bevindingen ook de aanwezigheid van cis-activering bij ligand-receptorinteracties binnen één cel aangetoond. In hoofdstuk 3 toont ons onderzoek aan dat NOTCH-liganden, zoals DLL4, effectief kunnen samenvoegen, zowel in biochemische assays als in vitro celkweekstudies. We hebben aangetoond dat het specifieke gebied dat verantwoordelijk is voor deze binding, de membraan proximale epidermale groeifactor (EGF)-achtige herhaling van DLL4 is. Onze bevindingen suggereren dat dimerisatie van DLL4-ligand cruciaal is voor het remmen van NOTCH-receptoractiviteit binnen dezelfde cel (cis-remming). Onze resultaten over NOTCH-ligand dimerisatie/oligomerisatie zijn van groot belang voor het begrijpen van de dynamiek van de NOTCH-signalisatie, aangezien de regulatie van dimer formatie en de afbraak daarvan kan dienen als een extra controlepunt voor de kracht en specificiteit van de NOTCH-signalisatie. Om deze bevindingen te versterken, hebben we krachtige wiskundige modelleringsbenaderingen gebruikt om bestaande modellen van NOTCH-signalisatie uit te breiden, gericht op het gebruik van gewone differentiaalvergelijkingen. De gegenereerde computer gesimuleerde gegevens ondersteunden sterk het idee van dimerisatie-afhankelijke cis-remming van NOTCH-signalisatie, zoals onthuld in ons biochemische en celbiologische onderzoek. Belangrijk is dat ons verfijnde wiskundige model gepubliceerde experimentele gegevens recapituleert en voorspellingen verbetert op basis van gepubliceerde mechanismen van door NOTCH aangedreven weefselontwikkeling. Ons model introduceert een nieuw perspectief voor het begrijpen van de biologische processen die worden gecontroleerd door NOTCH, waarbij embryonale ontwikkeling en angiogenese worden onderbouwd.
In hoofdstuk 4 verkennen we de connectie tussen abnormale functie van de transcriptiefactor FOS en vasculaire tumoren zoals epithelioïde hemangioom, een agressieve tumor gekenmerkt door vasculaire neoplasmen in botten en weke delen. Recent onderzoek heeft FOS-translocaties benadrukt als een potentiële bijdrage aan tumorigenese, hoewel tot op heden geen dergelijke

mutaties als causale mutaties in menselijke kanker zijn geïdentificeerd. Door analyse van menselijke epithelioïde hemangioom tumorcellysaten onthulden we een ingekort FOS (mutant FOS) eiwit in vivo, resulterend uit een FOS-MBNL1-translocatie. Deze vondst leidde ons tot het onderzoeken van de moleculaire basis van een mogelijke rol van FOS-translocaties in vasculaire tumorevolutie en ook tumorangiogenese. Onze studie vertegenwoordigt de eerste uitgebreide moleculaire en biochemische evaluatie van een mutant FOS-eiwit geïdentificeerd in deze menselijke vasculaire tumor. We hebben aangetoond dat het mutant FOS-eiwit veel stabieler was vanwege een carboxy (C)-terminus truncatie, wat de opkomst van vasculaire neoplasmen zou kunnen veroorzaken. We ontdekten dat het mutant FOS-eiwit krachtig endotheliale uitlopers stimuleerde en vasculaire tumorvorming stimuleerde door de productie van matrix metalloproteïnases (MMP) en de NOTCH-signalisatieweg te verstoren, die sleutelspelers zijn in angiogenese. Onze studie introduceerde ook het concept van ubiquitine-onafhankelijke proteasomale afbraak (UIPD) en onthulde de rol van de ongestructureerde FOS C-terminus bij het bemiddelen van eiwitafbraak. Dit is de eerste link tussen FOS-mutaties en natuurlijke tumorgroei. Bovendien bieden onze resultaten therapeutische mogelijkheden voor de behandeling van epithelioïde hemangiomen met mutant FOS-eiwitten door het richten op mutant FOS of eiwitten waarvan de expressie wordt getriggerd door FOS.

De disfunctie van meerdere ETS-transcriptiefactoren is in verband gebracht met het ontstaan van verschillende tumoren, waaronder Ewing-sarcoom (ES) en prostaatkanker. Het onderzoek beschreven in hoofdstuk 5 toont de haalbaarheid aan van het ontwikkelen van moleculaire remmers om de transcriptionele activiteit van ETS-factoren te verminderen door de verstoring van ETS-eiwit-DNA-interacties. Onze unieke benadering omvatte het verkrijgen van zuivere eiwitpreparaten van ETS-factoren en het uitvoeren van functionele high-throughput screens om nieuwe kleine moleculen remmers van ETS-functie te identificeren. Selectie van de moleculen die ETS-DNA-interactie remmen kan de generatie van geneesmiddelachtige moleculen mogelijk maken die in staat zijn specifieke ETS-eiwitten te targeten. Aanvankelijk werd een “Homogeneous Time Resolved Fluorescence” (HTRF)-assay uitgevoerd die het vermogen van verbindingen mat om de binding van een gezuiverd ETS-DNA-bindingsdomein aan zijn specifieke consensus-DNA-bindingsplaats te verstoren, wat resulteerde in de identificatie van vijf nieuwe verbindingen. Vervolgens hebben we de remmers in verschillende biochemische/biologische assays onderzocht (zoals celproliferatie, cytotoxiciteit en endotheliale uitlopers assay met behulp van primaire menselijke endotheelcellen, evenals zebravissen en muismetatarsalen). Deze lopende studie heeft het potentieel om nieuwe therapeutische middelen te leveren die gericht zijn op ETS-eiwitten.

LIST OF ABBREVIATION

AMC Amido-4-methylcoumarin
AP-1 Activator protein 1
CAPNS1 Calcium-activated neutral proteinase 1
CHX Cycloheximide
CHIP Chromatin Immunoprecipitation
DBD DNA binding domain
DLL Delta-Like DLL Delta-Like
DLL1 Delta-Like 1 (Notch ligand)
DLL4 Delta-Like 4 (Notch ligand)
INTRA Intracellular domain of DLL4
IMDM Iscove's Modified Dulbecco's Medium
ECs Endothelial cells
EDBD ETS DNA binding domain
EGFP Enhanced Green Fluorescent Protein
EGF Epidermal growth factor
ETS E26 Transformation-Specific
FOS Proto-oncogene FOS
GFP Green fluorescent protein
hiPSC-CM Human iPSC-derived cardiomyocytes
HUVEC Human umbilical vein endothelial cell
HTS High Throughput Screen
ICD Intracellular domain
IDR Intrinsically disordered region
JAG Jagged
JAK Janus kinase
MAPK Mitogen-Activated Protein Kinase
MMP Matrix metalloproteinase
MNNL Module N-terminus of Notch Ligands
NICD Notch intracellular domain
NECD Notch extracellular domain
NMR Nuclear Magnetic Resonance
NSCLC Non-small cell lung cancer
PLA Proximity Ligation Assay
PECAM-1 Platelet endothelial cell adhesion molecule-1
qPCR Quantitative PCR
RTK Receptor tyrosine kinase / Matrix metalloproteinase\
shRNA Short hairpin RNA
siRNA Small interfering RNA
SRPR Signal recognition particle receptor
TAD Transactivation domain

TBP	TATA binding protein
TINS	Targeted Immobilization NMR Screening
Tg(fli1)	Transgenic zebrafish expressing GFP under the fli1 promoter
TGFβ	Transforming growth factor β
TINS	Targeted Immobilization NMR Screening
TME	Tumor microenvironment
TPA	Tetradecanoylphorbol-13-acetate
UIPD	Ubiquitin-independent proteasomal degradation
VEGF	Vascular endothelial growth factor
VEGFR	Vascular Endothelial Growth Factor Receptor

PUBLICATIONS

• A new model of Notch signaling: Control of Notch receptor cis-inhibition via Notch ligand dimers; **Zary Forghany***, Daipeng Chen*, Xinxin Liu, Roeland M.H. Merks, David A. Baker; PLoS Comput Biol 19, Jan 2023: e1010169; doi: https://doi.org/10.1371/journal.pcbi.1010169.

• Control of endothelial cell tube formation by Notch ligand intracellular domain interactions with activator protein 1 (AP-1); **Zary Forghany***, Francesca Robertson*, Alicia Lundby, Jesper V. Olsen, David A. Baker; J Biol Chem Jan 2018 1;293(4):1229-1242; https://doi.org/10.1074/jbc.M117.819045.

• Functional analyses of a human vascular tumor FOS variant identify a novel degradation mechanism and a link to tumorigenesis; **Zary Forghany***, David G.P van Ijzendoorn*, Frauke Liebelt, Alfred C. Vertegaal, Aart G. Jochemsen, Judith V.M.G Bovée, Karoly Szuhai, David A. Baker; J Biol Chem Nov 2017 292(52):21282-21290; doi: analyzing samples

• Identification of Novel Small Molecule Inhibitors of ETS Transcription Factors by Disrupting Protein: DNA Interactions; **Zary Forghany**, Shaima Abdalla , Xinxin Liu, David A. Baker (Under preparation 2025)

OTHER PUBLICATIONS

• Gene regulatory network model identification using artificial bee colony and swarm intelligence; **Zary Forghany**, Mohsen Davarynejad, B. Ewa Snaar-Jagalska, 2012 IEEE Congress on Evolutionary Computation; doi: https://doi.org/10.1109/CEC.2012.6256461.

• Mass-Dispersed Gravitational Search Algorithm for Gene Regulatory Network Model Parameter Identification; Mohsen Davarynejad, **Zary Forghany**, Jan van Den Berg; 2012 Lecture Notes in Computer Science; doi: https://doi.org/10.1007/978-3-642-34859-4_7.

• Characterization and expression analysis of two novel zebrafish P38 isoforms; Hanan Rian, **Zary Forghany**, S. Krens, Herman Spaink, E. Snaar-Jagalska Published 2014 Biology Corpus ID: 215752152

• Predicting the Impact of Supplemental Phytase, Wheat and Phosphorus on the Performance of Laying Hen;
Zary Forghany, Leila Zartash, Mohsen Davarynejad; World Congress on Computers in Agriculture and Natural Resources –2009, Michigan, US

ACKNOWLEDGMENT

Despite the numerous challenges I have faced in my life, I remained motivated to continue, progressing slowly but steadily, and ultimately completing this significant chapter of my life. This achievement would not have been possible without the support and encouragement of those around me.

David, from the moment I began my master's internship in your lab, I had the opportunity to experience real science alongside you. You were always open to my questions and encouraged me to explore new avenues. I appreciate your enormous knowledge; you taught me how to be brave, dive into unknown fields, and find confidence. I am sincerely grateful.

I want to express my deepest gratitude to my promoter, Peter, for your exceptional guidance and unwavering support. Your advice has been invaluable, not only in the scientific aspects of this work but also in providing emotional encouragement throughout this journey. Your mentorship has contributed significantly to my personal and academic growth, and I am genuinely thankful for that.

To my dear friends Eka, Matty, Amina, Maaike, Joost, Karo, Ivo, Igno, Chen, Jin, Sija, Francesca, Sumit, Roman, Gelila, Catalina, Jing, Thilo—with you, I felt at home in the CCB department at LUMC. Julia, many thanks for being there for educational help, wise advice, and being such a good listener. Willem, Joop, Hans, and Annelies, thank you for your technical support in the facilities.

Thanks to all the students I had the privilege of supervising—Helen, Miguel, Yana, Siger, Sten, Camiel, Dieuwke. Working with each of you has been a rewarding experience. Manuel and Harald, thank you for adding valuable discussions to my PhD evaluation. How lucky I am to deserve your friendship, Kseniya and Frauke. I'm happy to celebrate years of friendship with you, while you continue supporting me as my paranymphs in this memorable ceremony. Maarten, thanks for helping me with the Dutch translation. I would like to acknowledge all the members of the CCB department—Alfred, AG, Karoly, Lenard, Pauline—and everyone whose names I cannot fit into this acknowledgment.

A huge thanks to my best friends outside of LUMC, Vincenzo, for all the discussion time and brainstorming; Fatemeh, for your unconditional help and great friendship; Leila, for all the incredible thoughts. Reza and Shiva, thank you for incredible help and support even till the last minute. Hamidreza, thank you for always being enthusiastic and happy to answer my questions. Sara, Shima, Behroz—without your help, I couldn't have faced so many problems during the pandemic. Zahra, Maryam, Fariba, Samaneh, Zeinab, Hanieh, Sobhan, Ehsan, Nazi, Simin, Vahideh, and Azadeh— thanks for being present whenever was needed outside the lab. Helma, I always remember your generous offer to take

care of Manelie when I had to meet my deadlines. Thanks to Robert, Marlindeh, and Henk for all the great thoughts and brainstorming.
I want to say a heartfelt thank you to my dad and my little angel Nazanin, who were both so excited to celebrate the end of my PhD with me. Although that day never came, I know they are watching over me now, and I received your spiritual support whenever I needed it. I always regret not spending enough time with you until it was too late. You are in my heart forever. Mom, you were always there encouraging me through this difficult time. Thank you a thousand times for your genuine interest in every task I have ever undertaken since birth. My dearest sister, you are my big hero. I've never seen a person with your patience, Soroor and Mohammad, you are a significant lesson for me for the rest of my life.
Huge thanks to Baba Hossein and Maman Talat, I am happy to have you on board. Whenever the whole family was stressed, you came to the Netherlands to help us. Thank you for understanding and encouraging us to stay faithful to our destiny. I wish you could stand next to me when I receive my doctoral diploma.
Thanks to all members of my fabulous family, especially Danial, Yasaman, Soodeh, and Malihe, for your emotional support.
To Mikael, the treasure of my life, who spent 9 months in the lab with me during my pregnancy—you were with me through it all. Despite the many challenges we faced, your love gave me the strength to keep going. And to Manelie, my little princess, you bring true meaning to my life. You arrived during one of the most chaotic times in the world, the pandemic, and while it may have been hard on you, I couldn't have made it through without you.
And finally, my beloved Mohsen! Thank you for your true love, for always being there, sharing in my happiness, and standing by me through every challenge, both the tears and the triumphs. I will never forget your unconditional love when I felt disappointed and depressed, which happened often. You are the warmth and light of my life. Your support made this achievement possible.

CURRICULUM VITAE

Zary Forghany was born on May 4th, 1983, in Tehran, Iran. She obtained her high school diploma cum laude with a specialization in Science. After completing her bachelor's degree in Animal Science (2008), she began working as a Research Assistant at a poultry supply chain company.

In 2010, Zary moved to Leiden to study Master in Molecular Biology at Leiden University, within the Institute of Biology Leiden (IBL) department. She had the opportunity to work with zebrafish under the supervision of Prof. Dr. Ewa Snaar-Jagalska. She performed her second internship in the laboratory of Dr. Baker at the Department of Molecular Cell Biology (LUMC), and upon completing that she earned her master's degree cum laude in 2013.

She continued her research on angiogenesis signaling as a PhD student under the supervision of Dr. Baker, focusing on novel mechanisms and signaling pathways in angiogenesis. In 2017, she worked in the same lab on a drug discovery project, in collaboration with the European Lead Factory and funded by Prof. Dr. Pancras Hogendoorn, aimed at identifying and validating novel small molecule inhibitors of ETS transcription factors. This ongoing project is one of the key focus of her thesis. Currently, she is involved as a researcher on the cultivated meat projects at DSM-Firmenich company, in Delft.